1991

RAPID CRYOGENIC FIXATION OF BIOLOGICAL SPECIMENS FOR ELECTRON MICROSCOPY

RYAN, KEITH PATRICK

RAPID CRYOGENIC FIXATION OF BIOLOGICAL SPECIMENS FOR ELECTRON MICROSCOPY

KEITH PATRICK RYAN

A thesis submitted in partial fulfilment of the requirements
of the Council for National Academic Awards
for the degree of Doctor of Philosophy

September 1991

Polytechnic South West in collaboration with the
Marine Biological Association of the United Kingdom
and Plymouth Marine Laboratory

COPYRIGHT

CONTENTS

List of Figures

List of Tables

RAPID CRYOGENIC FIXATION OF BIOLOGICAL SPECIMENS FOR ELECTRON MICROSCOPY

KEITH PATRICK RYAN

Abstract

This thesis describes investigations into cryofixation by the plunge-cooling technique, at ambient pressure. The objective was to characterise coolants which are commonly used for cryofixation, so that the structure and chemistry of biological specimens may be preserved in a more life-like state. The work began with the design of a suitable cooling device. This was developed further into a large test-bed apparatus which was used in both biological and methodological experiments. The large cooling apparatus demonstrated for the first time that ethane was a superior coolant under forced convection, compared to propane or Freon 22, for bare thermocouples, for exposed hydrated specimens and for metal-sandwiched hydrated specimens. Ice crystal formation was monitored in sandwiched specimens and found to correspond closely to modelling predictions. A biological application was the X-ray microanalysis of body fluids in "indicator" species of Chaetognaths, where results obtained from cryo-scanning electron microscopy revealed ecophysiological differences. The use of low thermal mass supports demonstrated that good freezing can occur in the centre of specimens. A new cryomounting method was developed to load well-frozen specimens into the microscope. The effect of post-freeze processing temperature was investigated by monitoring ice crystals in red blood cells. Exposure to 213 K (-60°C) over a 48 hour period did not induce crystal growth and exposure to 233 K (-40°C) for 8 days showed minimal ice crystal damage. The progress of cryosubstitution was monitored over 48 h at 193 K (-80°C), this showed that uranium ingressed to a depth of 320 μm which could be doubled when shrinkage was allowed for. The conclusion was that observed ice crystal damage originated during the initial freezing and not during subsequent cryoprocessing.

Acknowledgements

I wish to express my thanks to Dr. Quentin Bone FRS, my local supervisor, particularly for helping me to set up my first rapid cooling experiments in 1984. At the same time, Dr. Vic Howarth of the Marine Biological Association introduced me to the art of making sensitive thermocouples, with wires that were half the diameter of a human hair. Many thanks are also owed to Prof. James Lovelock FRS who persuaded me to venture into a new scientific discipline.

It is a particular pleasure to acknowledge the Austrian connections regarding this work. Prof. Hans Adam, Zoology Institute, University of Salzburg, was a constant source of encouragement as was Prof. Hellmuth Sitte, Department of Medical Biology, University of Homburg-Saar, Germany, who first introduced me to the world of "cryo" in 1983. He later invited me to speak at several of his cryo-workshops at Seefeld, in his native Tirol.

I wish also to thank Dr. Brian Grout, my supervisor at Polytechnic South West, for his guidance and help in easing my progress through the thesis procedure and my colleagues, Dr Ann Pulsford, who provided flounder blood for experiments, and Dr. Jim Nott, who read the manuscript. I also thank other colleagues who contributed to this work; Mr. David Purse, Mr. John Wood, Mr. David Nicholson, Dr. Bill Bald (University of York), Dr. Klaus Neumann (University of Homburg) and Dr. Peter Simonsberger (University of Salzburg). Their contributions are listed in Appendix 1.

Finally, I must thank my wife, Bernadette, and my children, Matthew and Lucinda, for their patience and understanding during the many long evenings and weekends when I worked in the Laboratory.

1 *Introduction*

Biological specimens which are destined for examination in electron microscopes need to be preserved, because living material is incompatible with the environment which is found within these instruments. A high vacuum is required to maintain the electron beam and this will quickly dessicate fresh specimens. Further, the electron beam will induce radiation damage in the specimens due to molecular excitation, ionisation and subsequent chemical reactions (Glaeser, 1975; Reimer, 1975).

In order for specimens to withstand these conditions, they can be preserved by a chemical fixative such as glutaraldehyde (Sabatini *et al.*, 1963). They can then be dehydrated and either embedded in resin and sectioned for transmission electron microscopy (TEM) as described by Pease (1964) and Kay (1965), or critical point dried for scanning electron microscopy (SEM) as described by Boyde & Wood (1969).

Alternatively, the specimens can be frozen and then processed for TEM by freeze-drying (Richards *et al.*, 1943), freeze-substitution (Fernández-Morán, 1957), freeze-fracture replication (Steere, 1957), cryosectioning (Bernhard & Leduc, 1967) or direct viewing (Taylor & Glaeser, 1976). Frozen specimens can also be examined directly by cryoSEM or after freeze-fracturing, freeze-drying, freeze-substitution or cryosectioning (Echlin, 1973; Moreton *et al.*, 1974, Saubermann & Echlin, 1975).

The purpose of the work described in this thesis was to investigate aspects of the plunge-cooling method of cryofixation. "Cryofixation" describes the preservation of biological specimens by freezing them very rapidly and "plunge-cooling" describes the method of achieving this,

namely, by plunging into a liquid coolant (Richards *et al.*, 1943; Stephenson, 1956; Rhebun, 1972). Alternative methods are the jetting of coolant onto specimens (Moor *et al.*, 1976; Mueller *et al.*, 1980) and the freezing of specimens on a cold metal block (Van Harreveld & Crowell, 1964).

When cryofixation is performed successfully, the specimen is preserved in a more life-like state than when it is preserved by chemical fixatives. This is important when the specimen is destined for examination by electron microscopy and also when its chemical composition is to be analysed.

After freezing, the specimen may be examined in the frozen state or subjected to other low temperature processing steps which return it to ambient temperature. These can involve cryosectioning, freeze-fracture, freeze-etching, surface replication, freeze-drying, cryosubstitution and low temperature resin embedment.

It should be borne in mind throughout that cryofixation is not a permanent "fixation" of the specimen as is defined in histological usage (Sjöstrand, 1990). It is an initial preservation, after which the specimen can undergo alterations during subsequent processing steps. These alterations include secondary ice crystal growth when the specimen is rewarmed, loss of ions and soluble components during cryosubstitution in organic solvents, radiation damage if specimens are examined in the electron microscope in the frozen state, artefacts due to decoration of fractured surfaces by coating materials during the replication of frozen surfaces and structural shrinkage during freeze-drying.

The advantage of cryofixation is that the specimen is preserved by a physical process in a short time interval, which is measured in milliseconds, compared to the time interval associated with preservation by chemical fixatives, which is measured in minutes. Thus, the speed of preservation is enhanced by several orders of magnitude (Robards, 1984). Ideally, this should be matched by an increase in the speed of specimen sampling and delivery to the coolant (Sitte *et al.*, 1977).

The potential of cryofixation is realised when it is used in conjunction with physiological or biochemical experiments. Transitory membrane phenomena such as synaptic exocytotic events can be captured (Heuser *et al.*, 1979), muscle fibres can be frozen at known points in the physiologically recorded time-course of a single twitch (Padron *et al.*, 1988) and intermediate macromolecular moities can be visualised in biochemical reactions with millisecond time-resolution, for example, myosin heads on actin filaments after a reaction time of 50 ms (Pollard *et al.*, 1990). Cryofixation also captures dynamic ionic fluxes for investigation by X-ray microanalysis (Zierold, 1991).

The importance of near-instantaneous preservation by rapid freezing is that specimens do not suffer the undesireable effects that are associated with chemical processing methods. When cells are fixed with solutions containing formaldehyde, glutaraldehyde and osmic acid, they undergo changes in oxygen tension, acidity and osmotic pressure (Hayat, 1981). Enzymatic processes are affected and cause autolytic changes which perturb the physiology of the cell. These continue until its life processes are finally arrested and fixed by chemical bonding with the fixing agents. The result is that the preserved structure is changed from its native state (Van Harraveld & Crowell, 1964). Dissolution and loss of some ions,

sugars, amino acids and proteins occurs during fixation (Coetzee & Merwe, 1984). Further loss ensues during dehydration with solvents such as alcohol and acetone, so that the chemical integrity of the specimen is not preserved (Morgan, 1980).

Cryofixation should transform a specimen into one which, ideally, differs only from the *in vivo* state by the solidification of its water. This should occur without the formation of ice crystals and thus achieve the truly vitrified state. This is achieveable and can be demonstrated in the cryo-electron microscope with frozen thin film specimens by means of their electron diffraction patterns. The characteristic pattern shows only diffuse rings and not the sharply defined patterns associated with different forms of ice crystal (Dubochet *et al.*, 1982).

The rate of cooling is critically important. When a specimen is frozen by slow cooling, its water forms large ice crystals (Stephenson, 1956). These distort and rupture cell membranes and organelles to the point of rendering structural features unrecogniseable. In other words, the structure of the specimen is destroyed (Meryman, 1957). Since ice crystals consist purely of water molecules, large ionic shifts occur during their growth. This process greatly alters the distribution of chemical elements, the distribution of which may be required to be investigated using X-ray microanalysis. Gross translocation of these elements can therefore render X-ray microanalytical results meaningless (Elder *et al.*, 1982).

Essentially, the faster a specimen is cooled, the smaller are the resulting ice crystals (Stephenson, 1956). The vitrified water films of Dubochet *et al.* (1982) were approximately 1 μm thick and the cooling rate that was necessary to achieve vitrification in these has been calculated to

be at least three million degrees per second (Bald, 1987). Tissue samples are inevitably much thicker than this and, consequently, because of their thermophysical characteristics, they are much more difficult to cool ultrarapidly. Herein lies the reason for wanting to characterise coolants, in order to find which has the greatest cooling efficiency, that is, produces the fastest cooling in a specimen.

This work had several objectives and the principal questions addressed were:

(1) measurement of cooling rates in coolants by plunging bare thermocouples into them under controlled conditions, in order to compare the results with previously published work

(2) measurement of cooling in exposed hydrated gel specimens, which mimic exposed tissue specimens

(3) measurement of cooling in metal-sandwiched gel specimens, which mimic freeze-fracture specimens enclosed in metal holders

(4) to correlate the cooling experiments with ice crystal damage in hydrated specimens.

Concommitant objectives addressed were:

(5) the effect of long exposure to the freeze-substitution temperature of 193 K (-80°C)

(6) the speed of freeze-substitution

(7) an application of the techniques.

The first question addresses the cooling efficiency of liquid coolants. These are used not only in the plunge-cooling method, where specimens are rapidly immersed into coolants, but also in jet-freezing, where coolants

are jetted onto specimens, and in droplet-spray-freezing, where specimens are sprayed as small droplets into coolants.

Coolant characterisation is relevant to a wide range of applications in specimen cryopreparation technique for biological electron microscopy: namely freeze-fracture, freeze-etching, freeze-drying, freeze-substitution, low temperature embedding, cryo-sectioning, thin-layer and bare-grid technique, cryo-scanning electron microscopy and cryo-transmission electron microscopy. These techniques are applied to the study of the fine ultrastructure of tissues, cells, organelles and macromolecules, also to the investigation of their chemistry by histochemical, cytochemical and immunological methods and analysis of chemical elements by X-ray microanalytical and electron energy loss methods.

The investigation was prompted by several factors. The results of Silvester *et al.* (1982), who measured cooling in 1.8 mm diameter water droplets plunged into different coolants, were modelled by Bald (1984) who concluded that, while ethane gave faster cooling than the more commonly used propane, their experiments were not performed under forced convection, which is the most effective cooling mode in liquid coolants. In other words, they did not detect the real potential for cryofixation. This coincided with the intention of building an improved plunge-cooling device, following the finding that hydrated specimens 0.5 mm^3 plunged 90 mm into coolants also did not cool under forced convection conditions (Ryan & Purse, 1985a).

The problem is approached in terms of cooling efficiency as measured by thermocouples and by ice crystal damage produced by freezing similar specimens under controlled conditions. The coolants

investigated were propane and Freon 22, which have been used for many years (Bell, 1952a, 1952b; Stephenson, 1956; Gersch *et al.*, 1957a), and ethane which is a more recent introduction to electron microscopy (Dubochet & McDowall, 1981; Silvester *et al.*, 1982).

The first step was to increase the coolant depth in the original device by about 50%, to 130 mm, in order to prolong the initial period during which the specimen surface could be maintained at the initial temperature of the coolant. This contrasted with an earlier much-cited model which was only 30 mm deep (Costello & Corless, 1978). Other improvements were the addition of a heater to maintain coolant temperatures and improvement of the infra-red sensor which monitored plunge motion. The resulting plunger was described by Ryan & Purse (1985b). It was used to test several coolants with a bare thermocouple and the results were reported by Ryan *et al.* (1987).

The apparatus was developed further and a much larger version was built in which the coolant was 600 mm deep. An improved electronic system was assembled to record the cooling curves and motion signals using a transient store, an XY plotter and a double oscillosope arrangement. This system revealed (1) the ultimate cooling efficiencies of propane and ethane, which related to predictions made by Bald (1984); (2) that epoxy resin cannot model cooling in hydrated specimens where latent heat release is a factor; and (3) that the effects of the vapour film around bare thermocouples may be suppressed at high plunge velocities. These results were also reported by Ryan *et al.* (1987).

During this phase of the work, the plungers were used to freeze Arrowworm specimens (*Sagitta*: Chaetognatha) in a study of coelomic

fluids. The frozen specimens were cryomounted onto supports for cryo-scanning electron microscopy, where the hydrated coelomic fluid was examined by X-ray microanalysis. Quantitative results were produced which were corroborated by colleagues who used other methods. The results were reported by Bone *et al.* (1987).

An interesting phenomenon noted in freeze-substituted Arrowworm specimens was that cryofixation in the centre of the animals could be very good. This resulted from the use of low-thermal mass supports which enabled increased central cooling through the convergence of cooling fronts from different directions.

The final stage of the main investigation involved plunging metal-sandwiched hydrated gelatin or blood specimens into the coolants at different plunge velocities, to compare with results from bare thermocouples and exposed hydrated specimens. Motion records showed whether cooling was accomplished under forced convection. A simple experiment illustrated the difference between cooling by simple immersion and cooling by forced convection. Cooling curves were successfully obtained from one gelatin specimen over a wide range of experimental conditions. All the sandwiched specimens had the same dimensions which meant that ice crystal formation in red blood cells could be meaningfully analysed after freeze-substitution. These experiments were modelled by W.B. Bald, so as to predict ice crystal size. The results were reported by Ryan & Bald (1990) and Ryan *et al.* (1990).

Finally, two further projects were undertaken which were designed to test the validity of the ice crystal results. The question arises as to whether the ice crystal spaces which are seen after freeze-substitution are

formed during freezing or during subsequent processing? In other words, can they grow after the specimen is frozen? To test this, frozen specimens were exposed to temperatures of 193, 213, 233, 253 and 263 K (-80, -60, -40, -20 and -10°C), over periods of 45 min to 8 days. They were then freeze-substituted and embedded for sectioning. The results have significant implications for freeze-substitution, freeze-drying and cryosectioning techniques.

The second experiment was designed to test whether the ice crystals develop as a result of rewarming after freeze-substitution? It can be envisaged that freeze-substitution is a limiting step, in that perhaps only a surface layer is properly substituted in 48 h. To test this, specimens were freeze-substituted for various times, arrested, fractured and examined by cryo-SEM with a controllable cryostage (Ryan *et al.*, 1985a, 1985b). The intention was to monitor the ingress of heavy metal fixing agents, by X-ray microanalysis and backscattered electron imaging, and the progress of solvent penetration by differential etching. This method proved unsatisfactory for reasons stated later. Results were obtained by freeze-drying specimens after different time intervals in freeze-substitution. They were then embedded in resin, planed and examined by back-scattered electron imaging.

In summary, this thesis presents data from experiments in which various rapid cooling parameters are defined. By this means, modellers can progress towards a clearer understanding of the freezing process. The thesis characterises the coolants from experiments under optimised plunge-cooling conditions which resolve their order of cooling efficiency. It correlates plunge velocity and cooling rates in various coolants; it correlates plunge velocity and ice crystal size in coolants; it correlates

experimental and predicted ice crystal size (the predicted sizes were calculated by W.B. Bald); it describes results from application of the plunging technique to an analytical problem using cryo-SEM, revealing an ecophysiological difference between two species of Chaetognath; it describes a new cryomounting technique for attaching frozen specimens to cryo-SEM supports; it describes the effect of processing specimens at different subzero temperatures; and it reports on the effect of time on fixing agent penetration during freeze-substitution.

The thesis presents conclusions regarding the origins of ice crystal damage and comments on the possibility of using higher post-freeze cryoprocessing temperatures than hitherto normally used. The latter point does not apply to cryoprotected specimens or to those destined for observation in the hydrated vitreous state.

2. *Literature Review*

Sections 2.1-2.5 consider background aspects of cryotechnique, Sections 2.6-2.14 consider physical aspects of water relevant to freezing specimens for electron microscopy, and Sections 2.15-2.22 consider the methodological approaches to rapid cooling.

2.1 Background to specimen preservation for electron microscopy

Golgi (1878), Flemming (1884) and Bouin (1897), among others, realised that biological specimens destined for microscopy must be preserved, otherwise they deteriorate. To this end, they formulated preserving fluids using acetic acid, osmium tetroxide or formaldehyde, with other compounds which coagulate and precipitate proteins.

Baker (1966) noted that electron microscopy demands finer, non-coagulative fixatives. Osmium tetroxide and formaldehyde are still suitable and widely used for structural studies. Sabatini *et al.* (1963) introduced other aldehydes including glutaraldehyde for histochemical use. These mixtures are normally buffered (Hayat, 1981) and aldehyde fixatives should incorporate osmotic control (Young, 1935; Bone & Ryan, 1971; Glauert 1975).

2.2 Problems of chemical processing for electron microscopy

While much descriptive work in biology has used chemical methods and Pearse (1980) noted that these are important in histochemical studies, there are serious reservations.

There are two problem areas: Boyde *et al.* (1977) reported that from a structural viewpoint there can be marked shrinkage during dehydration with solvents. This can be 15% linear (40% volume), and after critical point

drying for scanning electron microscopy as much as 24% linear (62% volume) shrinkage. This is reduced to 4.6% linear (or 13% volume) shrinkage if identical specimens are freeze-dried. Van Harraveld *et al.* (1965) have shown a pronounced loss of extracellular space, which is retained by using freeze-substitution. Zierold *et al.* (1989) reported that there are also serious problems with regard to the capture of rapid cellular events due to the delay of fixative penetration times.

From a compositional and microanalytical viewpoint, chemical fixatives cause substantial loss of cellular components. Morgan (1980) showed that diffusible ions can suffer 95% loss, while Coetzee & Merwe (1984) showed that sugars, amino acids and proteins are also lost.

Clearly, chemically fixed specimens are affected to the detriment of both their structural and their chemical integrity.

2.3 Introduction of cryotechniques into microscopy methods

Altmann (1890) realised the problems referred to above and introduced a physical approach to preservation. He froze fresh, native specimens (now termed *cryofixation*) and then removed the frozen water by sublimation in a vacuum (now termed *freeze-drying*).

Gersch (1932) reintroduced the technique for light microscopy and Richards *et al.* (1943) used it in electron microscopy, on smears of squid giant axon. Gersch *et al.* (1957a, 1957b) first used it successfully with tissue blocks for electron microscopy.

2.4 The potential of cryofixation

Woolley (1974) noted that cryofixation can effect preservation almost instantaneously and arrest transitory and labile phenomena. Robards (1984) calculated that cryofixation could immobilise *Abutilon* (Malvaceae) trichome tip cells with a diameter of 15 μm in less than a millisecond, which is 1 million times faster than the 10 minutes necessary for glutaraldehyde fixation. Finely controlled timing of stimulation and reaction of cellular events is also possible, as shown by Van Harreveld *et al.* (1974), Heuser *et al.* (1979), Sjöström (1980), Gupta & Hall (1984), Padron *et al.* (1988), Edelmann (1989), Zierold *et al.* (1989), Wendt-Gallitelli & Isenberg (1989), Knoll & Plattner (1990), Pollard *et al.* (1990) and Lepault *et al.* (1991). Van Venetie *et al.* (1981) used the technique to preserve different temperature-dependent phases of lipids. Monaghan & Robertson (1990) reported the preservation of fixative-resistant and fixative-labile antigens by freeze-substitution without fixatives.

After freezing, the specimen is ready for subsequent cryo-processing by a variety of methods, namely freeze-fracture, freeze-etching, freeze-drying, freeze-substitution, low temperature embedding or cryosectioning. These were reviewed by Robards & Sleytr (1985).

2.5 The problems of cryofixation

Sitte *et al.* (1977) noted that specimen perturbation and the time-lag during sampling are important problems. Trinick & Cooper (1990) demonstrated that thin hydrated layers undergo rapid evaporation, leading to artifacts in specimens prepared for cryo-electron microscopy unless preventative measures are taken. Stephenson (1956) highlighted the commonest problem of cryofixation, however, which is ice crystal damage. This occurs when cooling is too slow. It distorts structure and

alters elemental distribution. Many factors can contribute to this, which are either specimen-related or technique-related (Elder *et al.*, 1982).

Specimen-related factors include the size, shape and nature of the specimen, also how it is supported. If it is on a metal support then this is not an efficient approach to rapid freezing. Some of these factors were noted by Ryan & Purse (1984, 1985a) in studies published before the work described in this thesis was undertaken. Technique-related factors include the chosen cooling method, the particular coolant and how it is used (this thesis addresses questions in this area).

2.6 Water, cooling and crystal nucleation

Water comprises the bulk of most biological specimens. The molecules consist of one oxygen atom bonded to two hydrogen atoms, forming a V-shaped dipole. Eisenberg & Kauzmann (1969) described the O-H distance as approximately 0.1 nm and the bond angle of the free molecule being 104.5°. This confers a molecular shape which is ideal for participation in four hydrogen bonds, so that fully bonded water molecules form a lattice of tetrahedrons.

Angell & Choi (1986) described the liquid phase of water as being very dynamic, with highly mobile molecules constantly and randomly bonding and unbonding. The exchange, relaxation, or rotation time at room temperature is in the order of 10^{-12} s. At any one instant, many bonds are strained, distorted, or broken. At the same time, some molecules will be locally clustered into a transitory lattice structure. Dubochet *et al.* (1988) compared the latent heats of fusion (333 J/g or 80 cal/g) and vaporisation (2255 J/g or 540 cal/g) of water and suggested that only 15% of the H-bonds are broken at any one moment.

Franks (1982) noted that as water cools to its freezing point at 273 K, nucleation theory predicts that molecular fluctuations produce localised clusters which act as seed crystals and which nucleate freezing. Bachmann & Mayer (1987) suggested that as the temperature falls, water molecules lose energy and clusters grow by monomer addition. When a critical size is reached, the increase in surface energy (which drives dissolution) is overcome by the decrease in volume free energy (which drives crystallisation). Thus, a nucleus, or "embryo crystal", is formed.

Bachmann & Mayer (1987) further suggested that, at this point, the water molecules constitute a small crystal in which they are more stable. Simultaneously, the instability of the solid-liquid interface increases so that the crystal dissolves again. In *pure* water this process can continue down to the *homogeneous*, or *spontaneous*, nucleation temperature, below which freezing is unavoidable. Rasmussen (1982) pointed out that this nucleation temperature is kinetic in nature and is dependent partly on the cooling rate and partly on specimen size. The energetics of the process are such that the nucleation of ice cannot be avoided. Angell (1983) showed that the minimum homogeneous nucleation temperature is 232 K (-41°C), at ambient pressure.

Dubochet *et al.* (1988) noted that in most rapid freezing situations, crystallisation is initiated by *heterogeneous* nucleation that occurs at some intermediate temperature. This is triggered by an insoluble component in the system, which enhances the stability of the nucleus when it forms against the surface of such a component.

Bachmann & Mayer (1987) discussed *vitrification,* as this is the prime objective of cryofixation. It is the rapid cooling of water into a glass,

rather than a crystallised state. It depends on two factors: (1) the cooling rate and (2) crystallisation kinetics. The latter involves nucleation frequency and crystal growth rate, which both have their own time scales.

τ_{in} is the time scale for molecular relaxation in supercooled water. It relates to nucleation and scales with viscosity. At room temperature, water viscosity is about 10^{-2} poise which corresponds to τ_{in} of 10^{-12} s. Both values increase as temperature falls. At the glass transition temperature, viscosity is 10^{13} poise and τ_{in} is 10^{3} s.

τ_{out} is the escape time, which is the time scale for crystallisation of a given volume fraction (normally 50%) of the liquid. It is a complicated combination of nucleation and crystal growth rates. When cooling from melting point, τ_{out} decreases initially as the thermodynamic driving force for crystallisation (G_{cryst}-G_{liquid}) increases. At about 240 K (-33°C) for heterogeneous nucleation and 190 K (-83°C) for homogeneous nucleation, there is a minimum value or "nose" in each curve which approximates to 10^{-3} s for homogeneous and 10^{-7} s for heterogeneous nucleation. This results from competition between the driving force and molecular mobility. The latter falls with decreasing temperature.

$\tau_{"nose"}$ indicates the least time for the given volume to crystallise. It is necessary, therefore, to "bypass the nose" to avoid crystallisation. This can be done by modifying the specimen with cryoprotectants (see Section 2.13), although these are not recommended for cryofixation purposes. The alternative is to use a sufficiently fast cooling rate, which can be limited by the method and/or the nature of the specimen. A short-cut for bypassing "the nose" is to lower the nucleation temperature closer to the glass transition temperature, so that the critical temperature range to be cooled

is reduced. This can be achieved under high pressure conditions and is described in Section 2.19.

2.7 Cell water

Dubochet *et al.* (1988) noted the high dielectric constant of the water molecule ($\varepsilon = 80$) and its relatively high dipole moment (1.8 Debye), which explain its polarity and enables it to act as a solvent. These factors also cause it to align in the electric fields which surround ions.

Kellenberger (1987) pointed out that biomolecules are generally hydrophilic; they include polysaccharides, nucleic acids, lipid bilayers and most proteins. These macromolecules bind water strongly, as part of their structure. This "structural" water is an important concept, as it is ordered in a different manner to the free water within the cell. It constitutes the hydration shell of the macromolecules and probably consists of several layers of water molecules which decrease in ordered orientation away from the macromolecule.

Robards & Sleytr (1985) noted that up to 15% of the water in the cell is bound and is not incorporated into ice crystals when freezing occurs. This "unfreezeable" water removes a large proportion of the potential heterogeneous nucleation sites. Kistler (1936) discussed the measurement of "bound" water, citing work from 1906 onwards. He suggested that the amount of unfrozen water in a frozen specimen depends partly on the cooling mode.

2.8 Crystallisation and latent heat release

Stephenson (1956) stated that once freezing is triggered, crystallisation proceeds rapidly. As water molecules are recruited into a

crystal they give up the latent heat of fusion of ice, 334 J/g at 273 K (0°C). This is equivalent to 80 calories and tends to rewarm the specimen back towards its melting point. Complete crystallisation equates potentially to a local temperature rise of 80 degrees.

When a biological specimen is frozen rapidly, crystallisation is initiated by heterogeneous nucleation in the extracellular medium near the specimen surface (Dubochet *et al.*, 1988). The crystal grows into the specimen, with its surface temperature remaining close to 273 K. The crystal dendrites increase in diameter as they progress deeper into the specimen, because the effective cooling becomes less and the water molecules have more time to migrate to the growing lattice (which is at a lower energy state). When this process terminates, the cells cool and freeze by homogeneous nucleation, with crystal growth following a similar pattern. This explains the results of Handley *et al.* (1981) which showed this pattern and the pattern is depicted in Fig. 5.3 of Roos & Morgan (1990).

Dubochet & McDowall (1984) showed electron diffraction evidence that only a few crystals exist in a frozen cell. The fields of view show many ice profiles but there may actually be only one highly branched crystal in each membrane-limited compartment of the cell.

2.9 Phase separation and eutectic temperature

Roos & Morgan (1990) reiterated that when ice crystals appear, they consist only of water molecules. This means that the solid phase of the water (ice) is separated from the dissolved salts and other cell constituents. The salts are concentrated into the remaining aqueous phase, which constitutes the "eutectic" or grain boundary between ice crystals. The salt

concentration increases as crystallisation proceeds, thereby causing large ion shifts, with severe osmotic and pH changes. Rey (1960) noted that as the temperature falls, a point is reached at which the concentrated salts freeze. This is the *eutectic temperature* and when the specimen is rewarmed to this temperature the eutectic will melt before the ice melts.

2.10 Types of ice

There are currently 10 known polymorphs of frozen water (Polian & Grimsditch, 1984), most of these occur at high pressures which cause various distortions of the hydrogen-bond network. Dubochet *et al.* (1982) highlighted that in the electron microscope only 3 types of ice occur. They are identified by characteristic electron diffraction patterns. The commonest form is *hexagonal* ice, which is characterised by 6-membered lattice paths from and returning to any one molecule. It is formed when water is frozen naturally and by inadequate rapid freezing for electron microscopy. The ice consists of branching crystals which can be many micrometers in diameter. Water in this phase is in a more open lattice than in the liquid phase. The density falls to 933 kgm^{-3} and a linear expansion of 2-3% occurs; this implies that there is a volume expansion of up to 9%.

Faster freezing may form *cubic* ice, a finer polymorph, which has crystals that range in size from 30-100 nm (Dubochet *et al.*, 1988). It differs structurally from hexagonal ice in that neighbouring water molecules are rotated 180° with respect to each other along the hydrogen bond. Dubochet *et al.* (1982) have achieved the ultimate goal of cryofixation which is to produce *vitreous* ice. This is amorphously solidified water, analogous to a glass, which has cooled so rapidly that the random molecular fluctuations are captured and nucleation which leads to crystal

lattice formation is avoided. The density is the same as that of cubic and hexagonal ice (Dubochet *et al.*, 1983). The necessary cooling rate is extremely high and was calculated by Bald (1987) to be 3×10^6 Ks^{-1}. Heide & Zeitler (1984, 1985) reported that vitreous ice may be polymorphous and that it may have a high density form.

Amorphous vitreous ice was first reported by Burton & Oliver (1935), who used X-ray diffraction to study water sublimed onto a copper plate at 118 K (-155°C). They reported that crystallisation occurred at 163 K (-110°C).

Lepault *et al.* (1983) showed that amorphous solid water can be formed in the electron microscope by irradiating hexagonal or cubic ice at temperatures below 70 K (-203°C). The electron diffraction pattern is indistinguishable from that of vitreous ice produced by rapid freezing. Devitrification of this anomalous "vitrified ice" reveals a peculiarity; when derived from hexagonal ice it devitrifies back to that form and not to the usual cubic ice.

2.11 Phase transitions

Roos & Morgan (1990) emphasised that after a specimen is frozen it is not stable, unless kept at a very low temperature. Vitreous ice converts to cubic ice in the electron microscope at between 140 K and 156 K (-133 and -117°C). This is the *devitrification temperature.* The variation depends on the time of exposure to the elevated temperature. Exposure to the electron beam in a microscope also contributes energy to devitrification. Pryde & Jones (1952) demonstrated that the transition was reproducible in pure water during calorimetry experiments and that it occurred always at 144 K (-129°C). Dowell & Rinfret (1960), using X-ray diffraction data, cited

a lower extreme of 113 K (-160°C). Hallbrucker & Mayer (1987) used differential scanning calorimetry, with heating at 10 $Kmin^{-1}$ and showed this conversion at 163 K (-110°C).

Dowell & Rinfret (1960) showed that cubic ice made by condensing water vapour converts to hexagonal ice after about 100 min at 183 K (-90°C). It converts at a lower extreme of 153 K (-120°C) after 6.9 days. Mayer & Hallbrucker (1987) showed the transition beginning slowly at 203 K (-70°C) in cubic ice made by condensing 3 μm diameter liquid water droplets. It is not observable in the electron microscope because at these high temperatures sublimation occurs in the vacuum.

Bachmann & Mayer (1987) noted that below the devitrification temperature is the *glass transition temperature.* This is often obtained by extrapolation from experiments using concentrated binary solutions and denotes the transition from the viscous, supercooled phase to the noncrystalline rigid phase. It is characterised by a sudden increase in specific heat while slowly heating, but without crystallisation occurring. Pryde & Jones (1952) reported glass transition in vitreous water at 126 K (-147°C), but they were unable to confirm it. Angell (1970) reported that this is dependent on cooling rate and is therefore kinetic in origin. Boutron (1984) noted that while this transition has been characterised for concentrated cryoprotectants, little is known regarding biologically-relevant low concentration solutions, because the applied method of thermal analysis does not give satisfactory results. Bachmann & Mayer (1987) implied that only below this very low temperature can molecular mobility, and hence structural change and ionic migration, be totally inhibited.

Mayer (1988) reviewed previous work and reported new findings from differential scanning calorimetry. His samples were prepared by accelerating aerosol droplets through a 200 μm aperture with nitrogen carrier gas at supersonic speed through high vacuum onto a cryo-plate. This results after 1 h in a 1-2 mm thick disk of hyperquenched glassy water, with up to 5% cubic ice. Warming at 30 $Kmin^{-1}$ produced the first signs of change in thermal behaviour at 136 K (-137°C). This was a weak exotherm and it was interpreted as relaxation enthalpy, which marked the beginning of the *glass transition temperature.* It signified that there is a high degree of mobility far below the glass transition temperature. It led to structural relaxation and produced a denser glass. This mobility occurs on a molecular scale and does not extend to long range diffusion. The midpoint of the transition was 142 K (-131°C) and the end temperature was 150 K (-123°C) at which point conversion to cubic ice began. Warming at 10 $Kmin^{-1}$ is a slower process and induces the start of exotherm at 123 K (-150°C). This underlines the thermodynamic and kinetic nature of these phenomena.

2.12 Ice crystal growth in frozen specimens after freezing

It is clear from the consideration of phase changes in Section 2.11 that frozen water is metastable. Metastability can be defined for the purpose of this work as "an apparent stability in the state of solidifed water which is maintained under certain temperature conditions at ambient pressure". Even hexagonal ice is not stable. It has long been thought that ice crystals can increase in size during storage or during subzero processing methods and this has been termed "secondary" damage by Pease (1973). Rapatz & Luyet (1959) and MacKenzie & Luyet (1967) rewarmed specimens to very high subzero temperatures, *e.g.* 263 K (-10°C). These seem, at first sight, perhaps unhelpful regarding modern electron

microscopical cryomethodology, where most processing is carried out at about 193 K (-80°C).

Meryman (1957) used shadowed replicas of vacuum-deposited amorphous ice films which were warmed to low temperatures and they produced alarming results. They suggested that exposure to 203 K (-70°C) for 0.5 min could produce 1.0 μm-sized crystals from structureless controls and that 5.5 min at 193 K (-80°C) produced 0.5 μm crystals. This is at variance with more recent results and may have resulted from heat input during the shadowing and replication steps.

Luyet (1960) used polarised light cryomicroscopy and defined two terms for describing ice crystal growth in frozen specimens. *"Irruptive recrystallisation"* was applied when apparently crystal-free films were warmed until they became opaque due to crystal formation. This occurred over a wide range of temperatures which related to the molecular weight of the solute. Extremes of solute concentration only alter this temperature by 1 or 2 degrees. Examples given were 193 K (-80°C) for formaldehyde solutions, 208 K (-65°C) for glycerol, 242 K (-31°C) for sucrose solutions, 261 K (-12°C) for gelatin, and 267 K (-6°C) for soluble starch solutions. The implication given to this was that:

> *"to free water molecules from their partly amorphous, disordered surroundings and make them available to join growing ice crystals would require a rise in temperature to only -129°C if the surrounding consists of pure water, to some -90°C if it consists of a solution of very small molecules, and to near zero if it consists of a solution of very large molecules".*

"Migratory recrystallisation" was applied to the growth of larger crystals at the expense of smaller ones by migration of water molecules when frozen solutions containing a range of crystal sizes were rewarmed. A frozen solution of 10% glycerol showed this phenomenon after 15 min at 253 K (-20°C). No difference was seen in frozen 10% gelatin, even after 36 h at 253 K (-20°C). This supported the concept of irruptive recrystallisation.

Van Harreveld & Crowell (1964) freeze-substituted some specimens at 223 K (-50°C) for 72 h. Compared to those processed at 188 K (-85°C), they stated that *"reasonable preparations were still obtained"*. None were obtained after processing at 248 K (-25°C).

Nei (1971) suspended erythrocytes in saline and froze some rapidly and some slowly. The cells showed small ice profiles and when they were rewarmed to 243 K (-30°C) for 30 min the appearance did not change. In a second study, Nei (1973) repeated this result and compared it with those from cells which contained 30% glycerol. When *glycerinated* cells were rewarmed to 193 K (-80°C) for 30 min crystal growth occurred in the extracellular medium; while at 203 K (-70°C) for 30 min small crystals were produced in the blood cells; specimens kept at 213 K (-60°C) for 30 min produced crystal profiles of 100 nm. Long term storage for 14 days at 193 K (-80°C) produced similar results. He concluded that the cryoprotectant lowered the recrystallisation temperature.

Steinbrecht (1985) rewarmed cryofixed sensory hairs on the antennae of a moth to 233 K (-43°C) for 10 min without inducing observable change. The specimens needed exposure to 253 K (-23°C) to produce obvious crystal growth. Woolley (1974) freeze-substituted sperm at

223 K (-50°C), without sign of ice crystal damage and Barlow & Sleigh (1979) freeze-substituted for scanning electron microscopy at 203 K (-70°C) and 223 K (-50°C) and observed no difference in the appearance of ciliary bands.

Gupta *et al.* (1977) commented on phase transitions and crystal growth and noted that the transitions are slow. Also, if the microcrystals are separated by an organic matrix, such as occurs in cells, then the thermotropic conversion to larger crystals may be substantially slowed or even prevented. They stipulated that for X-ray microanalysis, crystal size must be smaller than the spatial resolution of the microprobe.

The results of Luyet, Nei, Steinbrecht and Woolley relate well to those of MacKenzie (1980), who modelled cooling/rewarming in a wide range of gels by differential thermal analysis. This study showed that, during slow rewarming at about 2 $Kmin^{-1}$, specimens were thermally stable up to high subzero temperatures. At between 238 and 263 K (-35 and -10°C) they acquired new translational motion (termed "antemelting") and between 243 and 267 K (-30 and -6°C) they exhibited exotherms from migratory recrystallisation, or grain growth. This denotes the growth of already-frozen ice crystals.

2.13 Cryoprotection against ice crystal damage

Skaer (1982) reviewed the protection of specimens against ice crystal damage by using cryoprotective chemicals. These serve variously to lower the equilibrium freezing point, lower the homogeneous nucleation temperature (thus increasing the supercooling capacity), lower the eutectic point, raise the recrystallisation point (thus reducing the critical cooling range and the critical cooling rate) and bind free water (thus reducing the

water available for nucleation and crystallisation). The agents in common use are glycerol, dimethylsulphoxide and ethylene glycol which all penetrate cells, and polyvinylpyrollidone, hydroxyethylstarch and dextran, which do not penetrate cells.

Lovelock (1953) noted that cryoprotectants are used mainly in cryobiology, where the goal is to revive specimens after freezing. Stolinski (1977) noted that, for electron microscopy purposes, they were much used in freeze-fracture for ultrastructural studies but now it is recognised that they produce their own artifacts. They can be toxic (Mathes & Hackenseller, 1981), induce endocytosis (Barnard, 1980) or exert pronounced osmotic effect (Wilson & Robards, 1982). Tokuyasu (1970, 1980) introduced sucrose for cryosectioning in immunocytochemistry studies.

Franks (1977) noted that cryoprotectants often induce cellular dehydration, with marked shrinkage. For electron microscopy purposes, this distorts both structure and ionic concentrations and should be avoided. The use of sucrose in the Tokuyasu method necessitates chemical prefixation which, for cryofixation *per se*, must be avoided.

2.14 Modelling the cooling process

The accumulation of physical data allows theoretical consideration of the cooling process. Stephenson (1956) modelled rapid cooling with the aid of experimental results described in the same report. He showed that if a specimen were cooled inefficiently, it could cool to below the freezing point and then rewarm to the melting point due to the amount of latent heat released within the specimen during crystallisation. Based on experimental cooling curves, he derived an all-or-none crystallisation

theory, in which a critical cooling rate, which, if achieved, would result in complete vitrification of the specimen. He also introduced the *proviso* that the specimen surface be maintained at the initial temperature of the coolant throughout the cooling process. Stephenson (1960) considered cooling kinetics and nucleation and recognised the tendency of specimens to rewarm while crystallising.

Riehle (1968) and Riehle & Hoechli (1973) in conjunction with practical experiments, reported on high pressure effects on the nucleation of water and the freezing of 5% glycerin. They postulated that the critical cooling rate occurs over a reduced temperature range between the homogeneous nucleation temperature and the devitrification temperature. Their experimental results showed a rapid increase in crystal size below a critical cooling rate which agreed with Stephenson's prediction. A pressure of 2100 bar reduces the freezing point of water to 251 K (-22°C) and the homogeneous nucleation temperature to 183 K (-90°C). This reduces the critical cooling rate for vitrification of pure water to 2×10^4 Ks^{-1}. The cooling rate for biological specimens is reduced to approximately 100 Ks^{-1}.

Van Harreveld *et al.* (1974) modelled cooling at 5 and 10 μm from the surface of a specimen based on experimental results, which were obtained by measuring the changing electrical resistance of agar blocks as they froze on a cold copper block. The freezing times were 4.1 and 8.3 ms respectively although these were remodelled with more optimistic results by Jones (1984), see below in this Section. The experiments are reviewed in Section 2.21.

Rosenkranz (1975) considered cooling rates in a water droplet of radius 0.6 mm by applying the thermophysical characteristics of Frigens

(Freons) 22 and 13, propane and melting nitrogen. The results were cooling rates of 2060 Ks^{-1} in melting nitrogen, 1410 Ks^{-1} in propane, 460 Ks^{-1} in Freon 13, and 110 Ks^{-1} in Freon 22. A real droplet specimen in Freon 22 cooled at 110 Ks^{-1} and in Freon 13 at 470 Ks^{-1}. Propane was not tried and nitrogen was ignored because of the metal specimen holder and its Leidenfrost effect.

Toscano *et al.* (1975) modelled the thermodynamics of ice nucleation in red blood cells. Numerical solutions were obtained for both homogeneous and heterogeneous nucleation which incorporated an allowance for intracellular water loss during freezing. For cooling rates below 10^4 K $\underline{min}^{-1}$ the homogeneous nucleation temperature was 210 to 212 K (-63 to -61°C). At faster cooling rates, it was 233 K (-40°C). As a comparison, the homogeneous nucleation temperature of a modelled blood cell composed of pure water was found to be 234 K (-39°C) at a cooling rate of 100 K min^{-1} to 233 K (-40°C) at 10^5 K min^{-1}. At the higher cooling rates these curves are separated by a small amount, due to presence or absence of electrolytes in the models. For modelling heterogeneous nucleation, particles of radius 3.2 nm were assumed to be present at a density of 32 x 10^7 per cell, these being characteristics typical of intracellular proteins. Further assumptions were necessary to consider the contact angle between the embryo crystal and the impurity; cosines between -1.0 and +1.0 were used. For cooling rates below 10^3 $Kmin^{-1}$, the nucleation temperature was 220 K to 241 K (-53 to -32°C). For faster cooling rates, it was 239 to 262 K (-34 to -11°C).

Venrooij (1975) and Van Venrooij *et al.* (1975) considered position in a cylindrical specimen and related crystal size to cooling rate. They used a model which was based on finite differences in which choices could be

made regarding boundary and initial conditions. The conclusion was that crystal size was smaller in the centre and at the surface than halfway between the two.

Heuser *et al.* (1979) treated muscle between an aluminium support and a copper cryoblock as the dielectric between the plates of a capacitor. A battery-powered circuit was completed when the specimen made contact with the cryoblock. As soon as the surface layer froze the resistance became so high that the circuit was effectively broken, within 1 ms. After this, the capacitive current was monitored. With liquid helium, it reached a final plateau within 2 ms, and with liquid nitrogen it took 4 ms, which indicated that liquid helium-cooled blocks cool twice as fast as those cooled by liquid nitrogen. During modelling, they noted that copper at liquid helium temperature had an extremely low specific heat, which if *maintained* would give very *poor* cooling. They surmised that on initial contact with the specimen, the block temperature rose to approximately 223 K (-250°C), at which point it became a good heat transfer medium. For reasons of this nature, they decided that silver possessed no special advantage as a cryoblock material. The final experimental result was that the surface 10 μm of specimen froze after 2 ms.

Van Harreveld & Trubatch (1979) studied the progressive fusion of water into ice in gelatin and tissue slices by essentially the same impedance method of Heuser *et al.* (1979) reviewed above. They used the large difference in dielectric constants of ice and water to calculate the position of the freezing front at given times and concluded that the surface 10-15 μm fused in about 5 ms.

Elder *et al.* (1982) used two models to analyse cooling in slices of tissue mounted on brass stubs. One model assumed a constant initial boundary temperature which allowed the coolant thermal diffusivity to tend to infinity. This model illustrated maximum cooling rates achievable at different depths in the specimen. The second model allowed the coolant temperature across the boundary to rise and was based on conduction alone. Thus, cooling was limited by the properties of the coolant and highlighted the poor thermal properties of the liquid coolants compared to a cold copper block. The models were tested with both thermocouple experiments and ice crystal measurements. The work concluded that the maximum relative movement of the specimen and liquid coolant must be maintained and that sufficient depth of coolant must be provided for this process.

Kopstad & Elgsaeter (1982) modelled cooling with a copper block and in copper-sandwiched, freeze-fracture specimens cooled in a liquid propane jet. The conclusions were that a helium-cooled copper block would cool specimens 30-40% faster (ideally) than a liquid nitrogen-cooled block. At liquid nitrogen temperature, both copper and liquid coolant produced the same cooling rates.

Silvester *et al.* (1982) briefly considered heat loss into a low-temperature fluid. Their main point concerned the Biot modulus, a dimensionless number, $B = (l \times h)/\lambda$ (where l is specimen radius or half thickness, h is the convective heat transfer coefficient and lambda is the thermal conductivity of the sample). B is less than unity when highly conductive specimens are cooled in poor coolants, when coolant properties limit cooling. B is more than unity when poorly conductive specimens are cooled in efficient coolants, where the specimen properties limit cooling. In

their 1.8 mm diameter water droplets, B was approximately 0.1. They indicated that it was worth seeking improved coolants.

Jones (1984) modelled freezing times at a 10 μm depth in the specimen and found that cooling rates of 4×10^4 Ks^{-1} occurred with times of less than 0.5 ms. The model* was applied to published experimental times so as to extrapolate the time taken to freeze at 10 μm deep in the specimen. Times of 0.1 to 0.6 ms were derived for liquid coolants and 0.1 ms for a copper block. Fig. 3a from Jones (1984) shows fits of Van Harrevelds (1974) results to Jones' equations with a comparison to the original curve. Jones calculated a 0.1 ms freezing time for Van Harrevelds results compared to the original calculation of 8.3 ms, although Jones allows that the theory may not hold for the thin tissue slices used by Van Harreveld. A source of possible error in Van Harreveld's calculation was the application of factors "a" and "b" which gave best curve fits when both were equal to 1.1. Also, there is imprecision in modelling which arises from the time taken for specimens to make complete contact with a cold block. This applies likewise to liquid coolants and can produce an error in the region of ±0.5 ms. The time during which freezing occurs at any one point is up to 250 μs, this being the ultimate limit for time resolution in cryofixation.

Bald (1983) has used finite element numerical techniques to compare different metals for cryoblock cooling (slamming) and has concluded that silver at 15.6 K (-257.4°C) is the most efficient metal. Other conclusions are that at liquid nitrogen temperatures copper blocks need not be ultra-pure and that when metals are cooled to liquid helium temperatures their cooling potentials are inhibited; they should be used at specific optimal initial temperatures.

* The model explicitly assumed that the surface of the specimen was instantly lowered to and maintained at the temperatures of the different coolants.

Bald (1984) has analysed the thermophysical characteristics of liquid coolants and concludes that nitrogen above its critical pressure is the most effective for rapid cooling. Other conclusions are that cryofixation should be completed during the active plunge phase (ie. under forced convection) and that at ambient pressure, ethane is a more efficient coolant than propane and Freon 22.

Bald (1985) has compared the various cooling methods mathematically. He concludes that cooling by a metal block produces the maximum freeze penetration depth and that plunging is sufficient for specimens less than 50 μm thick. Other conclusions are that thin flat specimens in metal holders are best cooled by the plunging method and that supercritical nitrogen would be superior to other liquids.

Bald (1986) proposed a theoretical model to correlate the critical cooling rate and average ice crystal size at depths throughout the specimen; the vitrification of pure water was found to occur at cooling rates which exceed 3×10^6 Ks^{-1}. This, together with other previous work, is correlated into a book which quantifies cryofixation with many worked examples which employ the various cooling methods (Bald, 1987).

Bald (1988) has also considered the importance of the Biot modulus, the Stefan number and the Jakob number in the basic field equations which define the rapid freezing problem. The Biot modulus determines the type of solution that is valid for rapid freezing. The Jacob number is the ratio of heat absorbed by the solid phase to the latent heat of fusion at any instant during rapid freezing. The Stephan number is the dimensionless relationship of latent heat, divided by the product of the specific heat of the solid phase and the difference between the specimen freezing temperature

and coolant temperature. If the Jacob number is greater than unity, the heat stored in the solid phase is high compared to the latent heat of fusion and the specimen cools as a homogeneous solid, with negligible freezing effects. If the number is less than unity, as is common in cryofixation, the latent heat effects predominate and the pseudo steady state is valid.

Zasadinski (1988) proposes a convection-limited model, instead of the usual conduction-limited type, for when the Biot modulus is less than unity (the modulus measures the ratio of convective to conductive heat transfer). The model predicts that cooling is limited by the surface area to volume ratio and is independent of the specimen thermal conductivity and inversely proportional to the thermal density (this being the product of specimen density and heat capacity). Many results from the literature fit the model. It is suggested (Zasadinsky, 1988) that the ideal specimen carrier should be very thin and of high tensile strength, such as the 4 μm thick titanium foils used by Handley *et al.* (1981). The thinnest possible specimen and the best available coolant near its freezing point should be used. In this situation, a further improvement in the heat transfer coefficient can only be achieved by increasing the velocity of the cryogen relative to the specimen.

2.15 Cooling methods

There are essentially three cooling methods: *plunging* the specimen into a liquid coolant, *jetting* coolant onto a specimen and bringing the specimen into contact with a cold metal block (or "metal mirror"), often referred to as *slamming, impact* or *cryoblock* cooling.

There are specialisations within these methods. For instance, the plunging method includes the spraying of small specimens into coolant as

microdroplets. Also there is "reverse plunging" where the coolant bath is raised up to immerse a suspended specimen (Wendt-Gallitelli & Isenberg, 1989) and hyperbaric plunging in supercritical nitrogen at 33 bar. The jet approach includes the high pressure method with liquid nitrogen at 2100 bar and the propane "shower", which captures movement in *Amoeba* which is perturbed by movement (Karl Zierold, *pers. comm.*). The metal mirror method includes the clamping of specimens in copper-jawed pliers which are precooled (Gersch, 1932; Eränkö, 1954; Hagler & Buja, 1984; Hagler *et al.*, 1989) and falling cryoblocks (Edelmann, 1989).

The various cooling and cryo-methods are reviewed by Costello & Corless (1978), Sitte (1979), Plattner & Bachmann (1981), Plattner & Knoll, 1984), Robards & Sleytr (1985), Gilkey & Staehelin (1986), Menco (1986), Sitte *et al.* (1986) and Elder & Robards (1988). Menco's review is remarkable for its 572 citations, many of which are applications of cryofixation.

2.16 Coolants (liquid)

A wide range of liquid coolants have been introduced for rapid freezing and these are set out in Table 1 (see next page).

2.17 Coolants (solid)

Specimens can be frozen by contact with the cold surfaces of metals, namely copper and silver. Gersch (1932) cooled a copper plate in liquid air and then placed it on the tissue to be frozen, another report of the technique was by Simpson (1941). Eränkö (1954) used copper plates in a similar fashion, except that they were paired and mounted on forceps. They were forerunners of the modern cryo-pliers and "Cryo-snapper" (Hagler & Buja, 1984; Hagler *et al.*, 1989). Copper was used in

Coolant	Reference
liquid air	Gersch, 1932;Richards*et al.*, 1943
ethanol	Scott, 1933; Marchese-Ragona, 1984
isopentane	Hoerr, 1936
propane	Bell, 1952a; Stephenson, 1956
liquid helium II	Fernández-Morán, 1960
nitrogen-	
as a boiling liquid	Bernhard & Leduc, 1967
as a subcooled liquid	Umrath, 1974
as a melting slush	MacKenzie, 1969
in supercritical phase (at 33 bar)	Bald & Robards, 1978
under high pressure (at 2100 bar)	Rhiele, 1968; Rhiele & Hoechli, 1973
isopentane-propane mixtures	Bell, 1952a; Jehl *et al.*, 1981
hexane-butane mixture	Harvey *et al.*, 1976
ethylene glycol	Pease, 1967a, 1967b, 1973
chlorodifluoromethane (Freon 22)	Bell, 1952b
fluorotrichloromethane (Freon 11)	Echlin & Moreton, 1976
difluorodichloromethane (Freon 12)	Echlin & Moreton, 1976
dichlorofluoromethane (Freon 21)	Echlin & Moreton, 1976
acetone	Echlin & Moreton, 1976
ethane	Dubochet & McDowall, 1981
89% propane-11% ethane	Hoch, 1986

Other fluorocarbons and hydrocarbons, including ethane, butane, butene, ethylene and propylene were tested by Rhebun (1972).

Table 1. Liquid coolants introduced for rapid freezing.

sophisticated devices by Heuser *et al.* (1979) and Escaig (1977, 1982) with liquid helium as the coolant for the metal block. Silver was used by Van Harreveld & Crowell (1964), who cooled with liquid nitrogen, with the block later being purged with cooled *helium* gas (Van Harreveld *et al.* 1974). Synthetic sapphire was used by Meisner & Hagins (1978), solid

mercury by Schwabe & Teraccio (1980), and solid Freon by Somlyo *et al.* (1985).

2.18 Plunge cooling methods

including microdroplet-spray-freezing and hyperbaric plunging.

Plunge-cooling is also known as immersion-cooling, quench-cooling, cryo-quenching and snap-freezing. The adjectives snap, fast, rapid and ultra-rapid have been variously applied.

There have been many published designs of equipment for plunge-cooling biological specimens. One of the most impressive approaches is the ballistic cryofixation method published by Monroe et *al.* (1968). In this method a rifle fired a hypodermic needle, at about 400 ms^{-1}, through muscle undergoing physiological stimulation. The needle shot into a flask, hitting the end wall which buckled the needle and extruded the tissue sample into liquid propane.

Rhebun (1972) illustrated a simple rubber-band powered injector which shot specimens on coated grids about 25 mm into Freon 22, ejected them and automatically withdrew the injector rod. An early spring-powered device was described by Glover & Garvitch (1974); this had a piston which formed a built-in shock absorber.

Umrath (1974) described a double-walled liquid nitrogen (LN_2) device. A central LN_2 well with a magnetic stirrer was surrounded by an outer LN_2 container. This outer area was evacuated by a rotary pump, so that the LN_2 boiled under reduced pressure, gave up heat and cooled to its freezing point at 63 K (-210°). This was controlled by a leak valve. The

outer nitrogen cooled the inner nitrogen by conduction, so that it was well below its boiling point at 77 K (-196°C).

Echlin & Moreton (1976) illustrated a mechanical injector which was based on the device of Glover & Garvitch (1974). The device was connected to an oscillosope via a phototransistor which monitored plunge velocity through a cardboard mask.

Somlyo *et al.* (1977) illustrated a compressed air-operated piston which injected specimens into a 50 mm depth of Freon 22 at 0.66 ms^{-1}.

Costello & Corless (1978) described perhaps the best documented device. This was a guillotine, the name adopted originally by Luyet & Gonzales (1951, see Section 2.21). It consisted essentially of a gantry which supported the plunge-rod mechanism. This was a rod with a T-piece at the top, to the ends of which were attached rubber bands for driving the rod downwards into the coolant. In the original device, plunge velocity was timed by means of two thermocouples, one mounted 6.3 mm above the other. The responses of the thermocouples on entering the coolant were recorded by an oscilloscope and the velocity was calculated from the distance and times of response. Costello (1980) replaced this system with a linear potentiometer. The specimens penetrated 15 mm into the coolant (a factor commented on later by Bald (1985) as not allowing completion of forced convection cooling).

Handley *et al.* (1981) described a spring-powered device which injected specimens into a 30 mm depth of Freon at a calculated velocity of 10 ms^{-1}. They used thin specimens sandwiched between 4 μm thick titanium foil.

Escaig (1982) described an electric solenoid-operated device which plunged specimens 15 mm into propane at up to 3.0 ms^{-1}.

Robards & Crosby (1983) described another spring-powered device which injected specimens 30 mm into a 100 mm depth of propane at velocities of up to 8.0 ms^{-1}.

Ryan & Purse (1985a,b) reported a device which features in this thesis. It was an elastic-powered plunger with an original depth of 90 mm (1985a) which was increased to 130 mm (1985b). It had a heater to maintain coolant temperatures and an infra-red sensor to record the plunge-motion. This allowed velocities to be calculated and thermal events to be compared with the motion and position in the coolant column. This device was based on experience from a training course which featured a prototype of the now commercially available Reichert KF80 device.

A recent introduction is *countercurrent plunge cooling* by Murray *et al.* (1989). This is a 100 mm deep device with a basal impeller which causes the coolant to well upwards constantly in the coolant container. The device has a thermocouple-heater system to maintain coolant temperatures and was available as the CQ6000 from Oxford Instruments Ltd.

Bald & Robards (1978) introduced a new concept in plunge-cooling: the use of liquid nitrogen above its critical pressure so that it cannot form an insulating gas layer around the cooling specimen. The device operates at above the critical pressure of 33.5 bar for nitrogen and has a coolant depth of approximately 0.5 m. It is currently available as the CS5000 Cryospeed from Oxford Instruments Ltd.

Another specialisation in plunge freezing is the injection of specimens in microdroplet form into a coolant, whereby the droplets are effectively plunge cooled. This is *spray-freezing*. An early application for electron microscopy was the use of a nebuliser and spray-gun for the freeze-drying of viruses (Williams, 1954). The technique was refined for freeze-fracture use by Bachmann & Schmitt (1971), Bachmann & Schmitt-Fumian (1973a,b) and Plattner *et al.* (1973) using artists airbrushes. An advantage of the technique is that it exploits the high surface area/volume ratio of the specimen which enhances efficient cooling. A commercial unit for spraying was the SFU 020 from Balzers Union, Liechtenstein.

Mengold *et al.* (1974, 1979) used a variation on the droplet specimen approach. A large droplet sample was positioned between two wires which were just touching and which were fractured after plunging for freeze-etch purposes.

2.19 Jet cooling methods

including the high pressure liquid nitrogen jet method
and the liquid paraffin method.

Moor *et al.* (1976) introduced the jetting of propane coolant onto the specimen. Improvements were made by Mueller *et al.* (1980), which appeared as the commercially available QFD 020 Cryo-Jet from Balzers Union, Liechtenstein. Recent improvements were suggested by Haggis (1986). Also available is the MF7200 Gilkey-Staehelin Propane Jet device from RMC Inc., Tuscon, Arizona.

There are several variations of the technique. Pscheid *et al.* (1981) and Knoll *et al.* (1982) used a single-sided jet, whereas Hippe (1984) used

the double-sided jet arrangement. There is also variety in the specimen sandwich arrangement; it can have high-conductivity material (normally copper planchettes) on both sides or have an insulator on one side such as Thermanox, bearing cultured cells (Pscheid *et al.*, 1981; Espevik & Elgsaeter, 1981).

Burstein & Maurice (1978) applied jet-cooling to the surface of bulk specimens but normally it is applied to thin metal-sandwiched specimens for freeze-fracture purposes. The thin metal sandwich foils were introduced by Gulik-Krzywicki & Costello (1978) originally for plunge-cooling, they possess a high surface area/volume ratio and thus cool efficiently.

Van Venetie *et al.* (1981) described an application of jet-cooling to the freezing of temperature-dependent liquid-crystal/solid phases and hexagonal II/lamellar phases of different lipids. They held specimens in a temperature-controlled metal block and then ejected them out of it past a sensor which triggered the cooling.

A sophisticated specialisation of the jet-cooling method is the high pressure liquid nitrogen double jet device introduced by Moor & Riehle (1968), with the principle described by Riehle (1968) and Riehle & Hoechli (1973). The technique has been applied to a number of problems, with reviews given by Mueller & Moor (1984) and Moor (1987). The application of 2.1 kbar at the moment of cooling not only prevents the formation of any nitrogen vapour phase, thus optimising thermal efficiency, but also introduces physical changes into the process in that it reduces the freezing point of water to 251 K (-22°C), with supercooling possible down to 181 K (-92°C). Kanno *et al.* (1975) showed this in their classic pressure/ temperature phase diagram for water. This situation reduces the critical

cooling rate for the vitrification of pure water to 2 x 10^4 Ks^{-1} and of specimen water to only 100 Ks^{-1}. Specimens are inserted into the device in metal sandwiches, as in other jet devices and the sandwich is opened after freezing. Studer *et al.* (1989) and Mueller (1990) report an improvement in the technique with the use of 1-hexadecene. This replaces extraspecimen water and solidifies prior to the specimen water. It reduces the likelihood of extraspecimen ice nucleation and prevents the reduction of cooling by not releasing any latent heat of fusion. It also maintains good thermal contact between the specimen and the holders. Kaeser *et al.* (1989) found the method to be particularly effective with fresh plant material, which normally freezes very poorly. The device is commercially available as the HPM 020 from Balzers Union, Liechtenstein.

The *liquid paraffin method* can be mentioned in association with the high pressure method. Buchheim (1972, 1977) and Buchheim & Welsch (1978) described the emulsification of small specimens into globules in a viscous liquid paraffin, using a homogeniser. These are frozen in freeze-fracture specimen holders by standard methods. As Plattner & Bachmann (1982) point out, extraction of hydrophobic substances may occur and, also, the effect of homogenisation on cellular integrity cannot be ignored. The principle involved is that as the specimen water cools to freezing point, its anomalous expansion is inhibited by the paraffin matrix. This probably leads to a pressure rise in the droplets with effects similar to those described for the high pressure jet method. This relates to the improvement reported by Mueller (1990) in high pressure freezing through the use of a paraffin (1-hexadecene) to fill interstitial spaces in specimens.

including cryo-guns and the Freon popsicle method.

The first use of a cold metal surface for freezing in microscopy appears to be by Gersch (1932), who cooled a copper plate in liquid air and then placed it on the tissue to be frozen. This approach was repeated by Simpson (1941) who used a brass block, as well as isopentane or liquid nitrogen. Simpson re-examined the freeze-drying approach of Altmann (1890) and Gersch (1932). In order to compare freezing damage with vacuum damage he introduced another cryodehydration technique - that of etching away frozen specimen water with solvents. This, he called "freezing-substitution". One of the criteria he used to measure good freezing was *"the homogeneity of the nuclear juice"*, a criterion known today as "the uniformity of the nuclear heterochromatin". Eränkö (1954) used cooled copper plates mounted on forceps. These were predecessors of the cryopliers described by Hagler & Buja (1984) and Tvedt *et al.* (1988). Commercial versions are the Cryoplier from Pelco Inc., Tustin, California, and the "Cryo-snapper" described by Hagler *et al.* (1989), from Gatan, Houston, Texas.

Van Harreveld & Crowell (1964) described the first sophisticated cryoblock device. This consisted of a silver rod, 25 mm long and 27 mm in diameter, which had its lower end in liquid nitrogen. In the improved version reported by Van Harreveld *et al.* (1974) the rod was 130 mm long and 27 mm in diameter and the freezing surface was located at the bottom of a 20 mm deep well (previously this was 140 mm deep). The well was flushed with dry *helium* gas from a coil immersed in the liquid nitrogen. This served to keep the block surface free of frost contamination by condensed water and gases from the air. The specimen was mounted on a

vertical rod which was applied to the cryoblock by a falling piston arrangement. The loss of air from the piston/cylinder was regulated by a needle valve and so controlled the rate of fall. This was measured by suitably placed contacts which triggered an oscilloscope. The specimen was held against the block by a spring, while the falling piston travelled a further 30 mm.

Coulter & Terracio (1977) used a simple arrangement of a massive copper bar (200 mm high by 80 mm diameter) in a styrofoam container. Tissue was sliced by hand, placed on the end of an aluminium foil covered cork, blotted, and applied by hand to the freezing surface. The published results, after freeze-drying and osmium vapour fixation, appeared to be unperturbed by visible ice crystal damage.

Escaig *et al.* (1977) introduced a liquid helium-cooled copper block with various electronic controls. The cryoblock, about 20 mm diameter by 20 mm deep, was housed in a vacuum chamber. At the appropriate moment (when block temperature was 4 K/-269°C) the evacuated space above the block was flushed with exhaust helium gas and a vacuum shutter valve pulled back to allow passage of the descending specimen. This arrangement prevented frost formation on the freezing surface. There was provision for optical switching of an electrical stimulator for physiological procedures. This latter aspect was described by Escaig (1982, 1984). The device was marketed by Reichert-Jung (France) as the "Cryoblock".

Heuser *et al.* (1979) used a copper block cooled by a liquid helium spray. It was flushed with the exhausting helium gas. The specimen was attached to a falling rod and was held against the freezing surface by a magnet. An important aspect of this device was that it was designed as

part of a physiological experiment to freeze frog neuromuscular junctions at known times after electrical stimulation, which was induced during the fall of the specimen to the cryoblock. The results showed the release of synaptic vesicles captured in different states of discharge, and, importantly, proved the potential of cryofixation. The device was marketed by Polaron Equipment Ltd. as the E7200 "Slammer" and currently by Med-Vac Inc., St. Louis, U.S.A. as the "Cryopress".

Akahori *et al.* (1980) described a liquid helium-cooled pure copper block contained in a vacuum chamber. Evacuation produces LHe II, at 2.2 K (-270.8°C), which cools the block prior to freezing the specimen. This apparatus was marketed as the RF-2 (for liquid nitrogen) and the RF20 (for liquid helium) devices by Eiko Engineering, Mito, Japan.

Boyne (1980) described a cryoblock device which had a very gentle action. It prevented bounce or recoil of the specimen from the cryoblock after impact, thereby ensuring optimal thermal contact during the cooling process. It used a pure copper anvil cooled by liquid nitrogen. Its special feature was the design of the striker and damping mechanism. When the specimen stopped moving, a weighted damper continued downward, inhibiting the initial bounce reaction. In doing so, glycerin was forced up into side chambers, compressing air pockets. These then re-expanded and pushed the damper up to maintain pressure downwards on the specimen. This effect was monitored by an oscilloscope and found to suppress bounce for up to 50 ms. This is long enough for the critical freezing period with suitable specimens. This device was marketed as the Model 39000 "Gentleman Jim" by Ted Pella Inc., California.

Sjöström (1974) described a double falling hammer system which had two pneumatically-driven cooled metal blocks. These were cooled to different temperatures by liquid nitrogen in order to facilitate the preparation of ready-mounted specimens for cryoultramicrotomy. One hammer was cooled to liquid nitrogen temperature and the other was cooled to 198-203K (-75 to -70°C). The latter gave the best attachment of specimens to cryo-ultramicrotomy specimen supports which were housed in the second hammer. The system was used to freeze muscle fibres of physiologically defined length and functional state. The specimens were maintained in a bath containing oxygenated Ringer saline solution. At the appropriate moment with regard to electrical stimulation, the bath was lowered by the same pneumatic system that drove the cold hammers. The specimen was then exposed to air for 5-10 ms before freezing between the hammers; the entire process was monitored with an oscilloscope (cited by Sjöström, 1980, p.288).

Verna (1983) described a simple liquid nitrogen-cooled copper block device which was essentially a hand-operated hinge mechanism. The specimen was mounted onto a support which was on an arm which was then lifted over and clamped down onto the cryoblock. The block was self-flushed by exhaust nitrogen gas and the clamping movement was dampened by a rubber stopper.

Elgsaeter *et al.* (1984) illustrated a device for use with liquid helium or liquid nitrogen, but gave no operational details. It was stated, however, that impact was observed through a long working distance stereo microscope. The specimens were dilute solutions of macromolecules. They were seen to contact the cryoblock, freeze at their surface, then recoil from the block, melt and recontact the block rather slowly. It was stated that

"this strongly non-ideal behaviour was much less pronounced or not observed for highly viscous specimens".

Heath (1984) described in detail how to make a liquid helium-cooled copper block device. It followed the Heuser principle of cooling and was notable for its simple, but firm, hand operated plunge-rod which delivered the specimen onto the cooling surface. It was novel in that vacuum was used to retain the specimen holder on the plunge rod.

Allison *et al.* (1987) reported a simple liquid nitrogen-cooled copper block cooling apparatus, consisting of a falling rod in a guide tube which was trapped by a magnet as an anti-bounce measure.

Edelmann (1989) illustrated a falling hollow copper block system which was filled with liquid nitrogen. Muscle specimens were prepared in Ringer saline for stimulation and then maintained in a humidity chamber. At an appropriate moment, an anti-frost plate was removed and the falling block triggered electrical stimulation of the muscle.

Livesey *et al.* (1989) described briefly a gold-plated copper block cooled by liquid nitrogen. It was maintained in a vacuum under a shutter mechanism similar to that described earlier by Escaig (1977, 1982). The plunge mechanism was pneumatic and all functions were microprocessor controlled, including reheating to defrost the block under vacuum between specimen runs. The device is currently marketed by LifeCell Corporation, Texas, as the CF 100.

Chang *et al.* (1980) described a cryogun device that sampled and froze specimens rapidly. Basically, a biopsy needle was housed in a

cylinder chamber where it was cooled by a stream of liquid nitrogen. The positive pressure of escaping gas served to prevent frosting. The cutting action of the needle was assisted by its rotating at 1200 rpm while it entered the specimen to be sampled. Release of the trigger mechanism caused withdrawal of the frozen sample.

Von Zglinicki *et al.* (1986) described a simple device which consisted of a spring-loaded biopsy needle in a small housing. The whole device was cooled in cryogen and then manually stabbed into the specimen for sampling. The sample was then ejected with a spring-loaded piston. The novel feature was the suggested use of propane as the cryogen, because some was carried over to the specimen and enhanced measured cooling rates. Freezing is effected by a suggested combination of liquid coolant and metal mirror cooling.

Another solid coolant, at least initially, is frozen Freon. This is used in the so-called "popsicle" method, where a specimen is frozen between 2 chunks of solid coolant which form the jaws of clamping pliers (Somlyo *et al.*, 1985).

2.21 Rapid cooling experiments

The first paper that recorded ultra-rapid changes in temperature during cooling was that of Luyet & Gonzales (1951), where an apparatus described as a "guillotine" was used to immerse 1, 2 & 3 mil (1 mil = 25.4 μm) diameter wire thermocouples (chamfered 45° and soldered end-to-end), falling under gravity into isopentane. Cooling rates at the moment of immersion were 300000, 200000, & 100000 Ks^{-1}. The recording system was an early oscillograph which overcame the inertia of the string galvanometers used up to that time. The sensitivity of the system was such

that it detected prechilling of the finest thermocouple in the cold gas layer above the coolant. Next, to ensure that the normal freezing course in water could be reproduced with fine thermocouples, a 76 μm thermocouple was sandwiched with water (100 μm thick) between thin sheets of mica. They noted that when a large mass of water (eg. 1 kg) is cooled it shows (1) a descending curve to a few degrees below freezing point (2) a vertical rise to freezing point when crystallisation of the supercooled water begins (3) a plateau while congelation proceeds and (4) a descending curve to the bath temperature. This thermal history was repeated when the test specimen was plunged into liquid nitrogen, so the events could be reproduced on a very fine scale. They also wrapped muscle around a 3 mil thermocouple to form a small ball, 1.6 mm diameter. Cooling curves were recorded with the muscle fresh and after it had dried. It cooled considerably faster when dried. The paper concluded that:

> *"In the last analysis, the cooling velocity depends essentially on the bulk of the material and its heat capacity (for a given heat dissipation area and bath temperature)".*

Stephenson (1956) recorded cooling curves from thin copper specimens (0.3 x 10 mm) with fine thermocouples attached and found that propane was more efficient than isopentane and that liquid nitrogen was very inefficient. He also embedded thermocouples in small tissue specimens and recorded cooling curves. The specimens were then examined by electron microscopy, with the finding that the specimen which produced the faster cooling curve, of the two illustrated, also possessed the smallest ice crystals. Thus, ice crystal size was shown to be linked to cooling rate.

Luyet & Kroener (1960) plunged a bare 25 μm diameter wire thermocouple into various coolants and measured cooling rates of 100000, 78000, 39000, and 2700 Ks^{-1} in melting nitrogen, isopentane, boiling nitrogen, and liquid helium II respectively. When the thermocouple was sandwiched between 2 layers of Scotch tape (each 70 μm thick) cooling rates of 2560, 2200, & 1685 Ks^{-1} were obtained from propane, Freon 22 and isopentane respectively (cited by Costello & Corless, 1978, p.20).

Cowley *et al.* (1961) found that cooling rates in liquid nitrogen could be improved if the specimen was coated with an insulator (cited by Rebhun, 1977, p.24 *et seq.*). This apparent anomaly operates by increasing nucleate boiling sites on the specimen surface which promote faster cooling because film boiling is overcome. Film boiling occurs in liquid nitrogen, which is already a boiling liquid at ambient pressure, by rapid initial cooling leading to the formation of an vapour layer around the specimen. This then insulates the specimen from the coolant (Westwater, 1959).

Bullivant (1965) tested liquid helium I and liquid helium II with a 3 mm solder sphere/thermocouple specimen and confirmed earlier suggestions that LHeII was a better coolant than LHeI (Fernández-Morán, 1960). However, propane was shown to be better than both forms of liquid helium.

MacKenzie (1969) measured cooling rates in melting and boiling nitrogen and found that cooling measured by a bare thermocouple (250 μm diameter wires) over 273-223 K was over 4 times faster in melting nitrogen. With a thermocouple (75 μm diameter wires) sandwiched between two 200 μm thick Vibratome slices of rat kidney the ratio over 273-263 K was 3.0, and over 263-223 K it was 2.0.

Rebhun (1965, 1972) plunged a thermocouple which was soldered into a 17-gauge (=1.4 mm diameter) 2.75 mm long section of steel tube into propane, propylene, ethane, ethylene, isopentane, isobutane, Freons 12, 13, 13-B-1, 14 and 22, Genetron 23 and other coolants. The specimen was also coated with various nucleating agents, after Cowley *et al.* (1961). Insulators such as vaseline, oils, glycerol, dibutyl phthalate and Formvar were tried, and powders such as copper, carbon, silicas, rosins, aluminas and pollen grains. The conclusions were that propane or propylene were the most efficient and that they were matched by ethane and ethylene if nucleating agents were used.

Van Harreveld *et al.* (1974) measured the thermal conductivity of specimens during cooling. The first experiment investigated the cooling rate of the surface of the specimen as it fell towards a silver cryoblock. The change in resistance of a constantan wire was monitored over 8 trials, with a mean chilling of 6.7 K (SE 0.35). The thermophysical parameters were analysed and compared to those of brain tissue, with the conclusion that the surface of brain would chill by 8.4 K before slamming. Next, the freezing time at the surface of an agar specimen was measured, based on its non-conducting property when frozen, compared to its finite resistance when not frozen. On contacting the cryoblock a circuit was made between the silver block and an aluminium electrode at the base of the specimen. Freezing of the specimen surface produced an open circuit condition in a mean time of 0.28 ms (SE 0.03, n = 6). Finally, the freezing times of specimens of different thicknesses were measured with 2 separated electrodes at the base of the specimens. The results were plotted and used to derive freezing times for the surface layers. It was found that freezing 5 and 10 μm from the surface took 4.1 and 8.3 ms respectively. The thickness

of a specimen which froze in about 0.3 ms (from the previous experiment) was found to be 0.36 μm.

Glover & Garvitch (1974) used a spring-powered injector to plunge specimens at about 2 ms^{-1}, as determined by a high speed camera, into a 5 ml coolant bath. The specimens were a thermocouple (details not reported) with or without a copper disc bearing 0.25-5.0 μl volumes of water. Essentially this work showed that melting nitrogen cooled faster than Freon 22 or Freon 12 and that these give faster cooling than boiling liquid nitrogen.

Umrath (1975) reported two simple cooling rates from a subcooled nitrogen device. A thermocouple embedded in Aradite within a 3.0 mm long x 1.5 mm diameter tube cooled at 311 Ks^{-1} in propane and at 365 Ks^{-1} in subcooled nitrogen.

Venrooij (1975) and Van Venrooij *et al.* (1975) modelled (see Section 2.14) and measured cooling in glycerol solutions at different locations across a 2 mm long x 2 mm diameter silver tube (with 100 μm-thick walls). They illustrated 3 recorded cooling curves which showed that cooling was fastest at the centre and slowest near the surface. This agreed with modelled results which showed that cooling was fastest at the centre, where cooling fronts converge radially. The predicted cooling rates reflected measured ice crystal sizes which were smallest in the centre and at the surface. It was concluded that specimens under 0.3 mm diameter could be vitrified and that in specimens 0.3-1.0 mm diameter there could be central vitrification.

Clark *et al.* (1976) tested three thin film thermocouples which were made for use in low temperature SEM. One was made specifically for testing cryogens by hand plunging, although the bulk of epoxy glue that was necessary for suport inhibited rapid cooling. Acetone, natural gas of unknown composition, Freon 22, Freon 11 and liquid nitrogen were tested. Interestingly, the fastest cooling was in the natural gas which presumably contained a high proportion of methane. Thin wire thermocouples were also made for comparison, from 71 μm diameter copper and 41 μm diameter constantan wires. These were more sensitive than the thin film thermocouples and recorded the fastest cooling in Freon 22 (the natural gas was not tested).

Echlin & Moreton (1976) reported that mechanical injection of a 0.5 mm long thermocouple junction made from 81 μm diameter wires into coolants gave cooling rates 2-7 times better than by hand-dipping. However, when the thermocouple was buried in 1 mm cubes of fresh pea root or fixed liver, the cooling rates were 5-50 times lower.

Costello & Corless (1978) produced a valuable contribution from a hydraulically damped guillotine device which housed a 28 mm deep coolant well and with thermocouple output to a storage oscilloscope. The thermocouples were made from 25 μm wires, with bead diameters of 40-80 μm. Specimens penetrated about 15 mm into coolant normally at 0.49 ms^{-1}, although mean entry velocities of 0.39-0.74 ms^{-1} were available through the use of rubber bands. Freons 12, 13, and 22, isopentane and propane and also various mixtures of coolants were tested. One of the important results of this work was the finding that heat conduction along fine thermocouples was negligible during *rapid* cooling, so that insulation of the leads is not necessary. Bare thermocouple results showed the order of

coolant efficiency to be: propane, closely followed by a propane-isopentane-methylcyclohexane mixture, Freon 13, Freon 22, Freon 12, isopentane, subcooled liquid nitrogen and boiling liquid nitrogen. A large part of the project was the investigation of the various types of specimen holder available for freeze-fracture specimens. These were tested by embedding a standard thermocouple in egg lecithin/35% water in the holders. The holders were plunged into Freon 22 and propane baths. The propane produced consistently faster cooling and the fastest cooling was obtained with the lowest mass holders, namely the copper sandwich.

Barlow & Sleigh (1979) performed "reverse-plunging" experiments with both bare thermocouples and thermocouples in 10 μl water droplets. A 460 μm diameter bead on 190 μm copper/constantan wires was used with the specimen clamped on a support to minimise mechanical disturbance. Rapid immersion was achieved by raising the coolant up around the specimen. A mixture of propane/α-butylene appeared to cool faster to 233 K (-40°C) at the centre of the water droplet than propane alone, followed by α-butylene and Freon 12 which were similar, followed by isopentane and, lastly, liquid nitrogen.

Heuser *et al.* (1979) performed perhaps the most elegant cooling experiment to date. The cooling of a muscle specimen on a cryoblock was monitored simultaneously by thermocouple and by both resistive and capacitive methods. The simplest aspect was the thermocouple, which was in contact with the muscle sample. However, no thermocouple could monitor cooling in the surface 10-20 μm of the sample contacting the cryoblock, where the cooling rate is fastest. To augment this, the muscle between the aluminium support and the copper block was treated as the dielectric between the plates of a capacitor, with a circuit being completed

when the specimen touched the cryoblock. This circuit was monitored by 2 further circuits, one measured voltage through a resistance in series with a 1.5 V battery and the other measured capacitance by applying a 100 kHz signal to the specimen support which went to a virtual earth through the copper block. When the surface layer froze, within 1 ms, the resistance became so high that the circuit was effectively broken. During this 1 ms a current flowed and a voltage decaying from 1.5 V to zero was measured, but afterwards capacitance was measured. This altered as specimen water (dielectric constant of 80) converted to ice (dielectric constant of 2). The signal appeared, after 1 ms, as about 600 mV and declined to a final plateau value of about 150 mV as freezing progressed. Using liquid helium, this occurred in 2 ms and with liquid nitrogen it took 4 ms. The final result was that the surface 10 μm of specimen froze after 2 ms.

Van Harreveld *et al.* (1979) studied the progressive fusion of water into ice in gelatin and tissue slices by the impedance method of Heuser *et al.* (1979). The large difference in dielectric constants of ice and water were used to calculate the position of the freezing front at given times. The work concluded that the surface 10-15 μm fused in about 5 ms.

Schwabe & Teraccio (1980) evaluated rapid freezing techniques by both thermocouple and ultrastructural methods. Specimens fell 30 mm under gravity into coolants. The thermocouple results showed that propane produced the fastest cooling rate, followed in order by Freon 22, Freon 12, isopentane, a flowing stream of liquid helium, a flowing stream of liquid nitrogen and unstirred liquid nitrogen. A significant finding was that all the coolants performed better when vigorously stirred. Cooling on solid mercury was also performed and found, by extrapolation of the measured cooling rate compared with the thermocouple bead area contacting the

mercury surface, to be better than propane. The same procedure showed copper to be better again. The tissue results showed that ice crystal size was correlated with measured cooling rates. The two are only relative because the measured cooling rates cannot be applied directly to the tissue specimens, only to the order of efficiency.

Costello (1980) systematically investigated parameters which are related to the plunge cooling of thin, sandwiched specimens. Typically, the specimens were 10-20 μm thick, with a thermocouple bead 20 μm thick, enclosed between 50 μm thick copper sheets. The apparatus used was the guillotine described in 1978, but a 40 mm linear potentiometer was added to monitor plunge motion. The main results of this work showed that (1) cooling was related to plunge velocity into the coolant, (2) cooling reflected the thickness of a shell of epoxy formed around the thermocouple bead and (3) that each coolant performed best near its own freezing point (Costello, 1980, Fig. 9). Low temperature X-ray diffraction patterns showed that typical hexagonal ice peaks (at 3.90, 3.67, and 3.44 Å) occurred in 1 mm^3 globular, aqueous specimens which contained up to 20% glycerol. When smaller samples were used or the glycerol was raised to 30%, the typical single peak at 3.7 Å for cubic ice was seen. Thin, sandwiched, aqueous specimens showed the diffuse scatter seen only from amorphous ice, or from microcrystalline ice in which crystallites are poorly formed. Attempts at vitrifying pure water with this method were not successful.

Mueller *et al.* (1980) froze thin sandwiched layers, about 12 μm thick, between 2 conventional freeze-fracture copper sheets using a double-sided propane jet. The thermocouple experiment was very simple: a specimen simply dipped into Freon 12 cooled some 30 times slower than that cooled by the propane jet.

Pscheid *et al.* (1981) compared the cryofixation in real specimens with the cooling of a bare thermocouple by various methods: dipping into nitrogen slush, Freon 22 and propane and by cooling with a single-sided propane jet. The specimens consisted of a Thermanox layer bearing cultured hepatocytes, a 15 μm-thick copper spacer and a 100 μm thick copper freeze-fracture sheet. The jet was applied onto the copper sheet of the specimen assembly. The jet produced the fastest cooling, followed by dipping into propane and then by dipping into the Freon. The details of the method for dipping were not described.

Robards & Severs (1981) investigated cooling rates with a thermocouple sandwiched between two copper planchettes, each 100 μm thick. The thermocouple took the form of a 75 μm diameter bead on 25 μm copper and constantan wires. The specimen was cooled by hand-plunging into liquid propane and by the Balzers QFD 101 Cryo-Jet. The cooling rates between 273 and 173 K (0 and -100°C) from the jet device were 6079 ± 1096 Ks^{-1} and from hand-plunging were 7910 ± 350 Ks^{-1}. The report discussed the wide variation in cooling rates obtained from the jet, and also the illustration of Mueller *et al.* (1980) where the line thickness, time scale, and galvanometric recorder all served to mask the variations in recorded cooldowns. The factors suggested in the report include spurious emfs and possibly static effects. In the light of a paper by Haggis (1986) on improvements to the device, it would seem that the device itself was at fault.

Van Venetie *et al.* (1981) used cryofixation by a double-sided propane jet to preserve lipid phases which occur at above 313 K (40°C), which implies ultrarapid cooling without the opportunity for phase

transition in the lipids. Simple thermocouple experiments showed faster cooling in the jet device compared to dipping in propane.

Escaig (1982) described in more detail an improved slamming device first described by Escaig *et al.* (1977) and included a plunging device which plunged specimens some 15 mm into liquid propane at up to 3 ms^{-1}. Very thin thermocouples were made by sputter-coating 100 nm of constantan onto 6 or 12 μm thick polyimide film; then 100 nm of chromel was deposited, partially overlapping the constantan so as to form the junction. When applied onto the copper cryoblock the thermocouples could register cooling rates of 200000 to 300000 Ks^{-1}. The important results came from cryostat slices of tissue which were thawed onto the thermocouple and then rapidly frozen within 15 s, to avoid drying. The slices were 20, 40, 80 and 120 μm thick. The results showed that cooling on the copper block was about 4 times faster than plunging into propane.

Costello *et al.* (1982) measured some simple cooling rates in sandwiched specimens, by double-sided propane jet, plunging into liquid propane and on a copper block cooled by liquid helium (after Heuser *et al.*, 1979). They found rates from 273/173 K (0/-100°C) were 13000 Ks^{-1} (jet), 12000 Ks^{-1} (plunger) and 6000 Ks^{-1} (cryoblock) which indicated that the jet was more efficient. However, if the cooling slope at 273 K (0°C) was measured, the rates were 32000 Ks^{-1} (jet), 10000 Ks^{-1} (plunger) and 17000 Ks^{-1} (cryoblock). This study placed emphasis on cryofixation results on dilauryllecithin-water systems. When frozen fast enough, these specimens retain the disordered arrangement of lipid in the lamellar (L-α) phase, which gives smooth freeze-fracture faces. When cooling is done less effectively, a worm-like texture is seen in freeze-fracture images which signifies molecular ordering which is typical of the P-β phase. The

transition (with 30% water present) occurs at 273 K (0°C). All 3 cooling methods gave satisfactory results, with each having its own advantages.

Elder *et al.* (1982) plunged a 305 μm thermocouple into propane, Freon 22, Freon 12, nitrogen slush and liquid nitrogen at a calculated entry velocity of 1.4 ms^{-1}. The cooling rates (Ks^{-1}) were 19100 (propane), 9000 (Freon 22), 6500 (Freon 12), 1700 (nitrogen slush) and 800 (liquid nitrogen). The experiments also tested the effect of coolant temperature, from 173 K (-100°C) to the coolant melting points and showed that there was a considerable advantage in using the lowest possible temperatures. Another important result was that thermal gradients in excess of 100 K could form in the surface layers of unstirred coolants.

Knoll *et al.* (1982) performed experiments with both single and double-sided propane jets. The normal procedure was to use cultured cells on a Thermanox support, separated by a 10 μm thick spacer from a copper support which formed a "roof" over the cells. The jet was applied onto this roof, with the specimen held in forceps about 1 cm from the horizontal jet; this was termed "frontal" cooling. Other approaches were (1) to cool specimens "tangentially", which means holding the specimen edge-on to the jet in a manner that is analagous to plunging, in that both sides are cooled simultaneously (2) single jet frontal cooling using a commercial device with one of its 2 jets blocked off and (3) double-sided jet cooling. Cooling was monitored by thermocouples with 50 μm-diameter beads made from chromel/alumel wires 12.5 μm thick. Several experiments were performed with double copper sandwiched samples of glycerol. With these specimens, tangential cooling was always faster, especially when a spacer was used. Under these conditions, cooling was generally twice as fast (with one experimental exception) compared to frontal cooling with the single jet.

The commercial device, used with only one jet, was normally less efficient than the home-made device and when used with both jets it tended to be worse than the home-made device used tangentially (which is equivalent to double-sided cooling). With the Thermanox/copper specimens, the double-sided jet was always less efficient than the frontal approach using the home-made single jet device.

Silvester *et al.* (1982) examined cooling in water droplets (volume 3 µl, with diameter 1.8 mm) plunged manually into various coolants. The results showed that ethane cooled about twice as fast as propane at 660 compared to 358 Ks^{-1}, over 273/173 K (0/-100°C). Much slower were methane, 2-methylpentane, Freon 12, ethanediol, methanol, propanol and acetone. Interestingly, ethanol closely matched the ethane cooling curve down to 223 K (-50°C) and was the third fastest of the coolants tested. A report on its successful use for freeze-substitution appeared later (Marchese-Ragona, 1984). Subsequent analysis of the cooling experiments by Bald (1984) indicated that they revealed the cooling effects of the transient and natural convection stages at the bottom of the plunge motion. This is due possibly to the size of the specimen, the assumed plunge depth and the potential for error through plunging by hand. A further source of error might be differential deformation of the water droplet as it is forced through the coolant. The potential for forced convective cooling had not been realised.

Robards & Crosby (1983) discovered a linear relationship between cooling rate and entry velocity into liquid propane. The specimen was a 60 µm thermocouple bead clamped between two 50 µm-thick copper sheets. Entry velocities ranged from 2.3 to 6.35 ms^{-1} and the specimen was plunged 30 mm into a 100 mm depth of coolant. It was noted that the

cooling rate increased after the specimen came to rest and Bald (1987) pointed out that this illustrated the peak heat flux, or so-called Leidenfrost phenomenon, which obtains when metal specimens are brought to rest at different temperatures in a coolant. In the experiment, the faster plunged specimen cooled at a similar rate by forced convection to the more slowly plunged specimen; however the former came to rest at a higher temperature and then cooled at a higher rate by natural convection than the slower plunged specimen which came to rest later and at a somewhat lower temperature. This lower temperature did not promote such a high heat flux by natural convection and the specimen cooled more slowly. This situation is confined to specimens with high thermal diffusivities and occurs too late in the process for cryofixation purposes. However, it does highlight important aspects of metal specimens (or specimen holders).

Costello *et al.* (1984) illustrated the improved guillotine device which had been described in 1982 and showed similar cooling curves from a 30 μm diameter thermocouple sandwiched in dilauryllecithin/50% water and sandwiched in epoxy resin between two 75 μm-thick copper foils, indicating vitrification without ice crystal formation and consequent latent heat release in the hydrated specimen. There was no increase in cooling rate when the specimens were plunged at above 2 ms^{-1} into coolant which was about to 30 mm deep. Ryan & Purse (1985a) reported that larger specimens could even cool more slowly with increasingly faster plunging, because they reached plunge bottom at increasingly higher temperatures, without then manifesting the high heat fluxes enabled by natural convection which are seen seen with metal specimens (Robards & Crosby, 1983).

Plattner & Knoll (1984) published cooling curves from similar experiments reported by Knoll *et al.* (1982), which compared Thermanox/copper sandwiched specimens cooled by a single jet and double copper sandwiches cooled by a commercial double-sided jet device. They repeated the results of the earlier work and showed that the slower cooling by the double-jet device which could be attributable to various design features. Among these are: primarily a lack of synchrony of jet arrival at the 2 specimen surfaces which may be due to internal differences in jet construction and to the precise positioning of the specimen between the 2 jets; long delivery tubes to the jets and partial blocking in the lines. Cooling was compared in two different specimens which were cooled differently.

Murray *et al.* (1989) introduced the principle of countercurrent plunging, in which specimens were plunge-cooled into an upwelling 100 mm column of coolant. Bare thermocouple experiments showed that cooling was faster in ethane than in a propane/ iso-pentane mixture and that Freon 22 gave the slowest cooling. Comparison was made with a horizontally stirred coolant, in which a thermal gradient existed where the surface was 22-24 K warmer. The upwelling coolant performed about 9-times more efficiently.

Padron *et al.* (1990) used a modified a Heuser-type apparatus to freeze muscle fibres at precisely measured points in the tension- time course of single twitches or during tetanus. The goal was to study intermediate stages in the cross-bridge cycle. Figure 12 of Padron *et al.* (1990) shows 15 records of measured tension forces during stimulation-induced twitches, some of which were frozen at clearly different stages in the twitch state.

2.22 Specimen rewarming during handling after freezing

Knoll *et al.* (1982) showed the importance of rapid handling of low mass sandwiched specimens after jet-freezing. Approximately 0.5 s after jet-cooling, the temperature of the specimen rises to about 133 K (-140°C) during transfer to liquid nitrogen for storage. This is close to the devitrification temperature. Pscheid *et al.* (1981) showed that a sandwiched specimen in a brass freeze-fracture table (*i.e.* sandwich holder) begins to rewarm after 10 s towards the freeze-fracture device preset temperature of 123 K (-150°C), which it reaches in 1 min. Silvester *et al.* (1982) exposed a frozen 3 µl water droplet (1.8 mm diameter) to the atmosphere from liquid nitrogen and in 2 s it reached 173 K (-100°C), thawing after 20 s. These observations should be considered with regard to phase transitions (Section 2.11) and ice crystal growth (Section 2.12).

2.23 Conclusions

It is evident from this review that cryofixation is a complicated process and that a variety of coolants have been used in a variety of methods. All of the methods have a degree of success.

It is also clear that when the choice of coolant, the mode of use and the type of specimen are all suitably optimised, limitations occur. Some are due to the efficiencies of the coolants but they mostly produce similar results. The major limitation is usually the specimen itself.

Progress can be made by modifying the specimen, as by using chemical cryoprotectants, but these produce unwanted side-effects. A useful approach for cryofixation is to change the characteristics of water by applying high pressure at the moment of freezing.

There is a large literature concerned with the physical characteristics of water. A variety of methods are available for study: these range from simple calorimetry and differential thermal analysis, to differential scanning calorimetry, nuclear magnetic resonance spectroscopy, X-ray diffraction, cryo-electron microscopy and electron diffraction. These are specialised fields and beyond the remit of this thesis.

This review has attempted to illustrate the scope of the problem and to demonstrate the various aspects which are relevant to rapid freezing for cryofixation purposes. However, despite the volume of published work, there are still many problems. This thesis addresses a fundamental question: which of the many coolants introduced for plunge cooling is the most efficient? A corollary to this is whether the same coolant is most efficient for metal specimens, namely bare thermocouples; exposed hydrated specimens, which mimic tissue specimens; and compound metal-sandwiched hydrated specimens, which mimic freeze-fracture specimens?

It is clear from the thirty-four experimental reports reviewed in Section 2.21 that propane and Freon 22 are particularly efficient coolants and these will be further tested in this work. Ethane has been introduced as a coolant and this will also be tested. Its main attribute is its high vapour pressure for faster evaporation in the cryo-electron microscope (Dubochet & McDowall, 1981; Dubochet *et al.*, 1988), although Silvester *et al.* (1982) have found that it cools water droplets faster than propane.

Bald (1984) concludes that forced convection is the most efficient mode of cooling in a liquid coolant, so that the specimen surface temperature is maintained close to the coolant temperature, thus promoting the fastest transfer of heat into the coolant. He concludes also

that Silvester's experiments were not performed under forced convective cooling and that they did not show the real cooling efficiency of ethane. He further proposes that, due to the difference between the melting and boiling points of coolants, propane is a more efficient coolant for metal specimens than ethane (Bald, 1985). This is because ethane, with a lower boiling point than propane, will vapourise more readily when cooling metal specimens.

The work described in this thesis will address these questions by monitoring specimen motion and cooling simultaneously, so as to ensure that forced convection is maintained during cooling in different coolants. Continuous forced convection will be maintained by the use of deeper coolant baths than used hitherto.

Another question to be addressed is whether the coolant efficiencies, as evaluated by thermocouple experiments, relate to ice crystal size in hydrated specimens? This will be investigated using specimens frozen in freeze-fracture planchettes because these will ensure uniform-sized specimen; this is important for the production of comparable results.

An excursion from the main line of investigations outlined above will be the investigation of real biological specimens by cryofixation and X-ray microanalysis using cryoSEM. The use of low thermal mass specimen holders for improved cooling efficiency will also be described. These holders require a new method of remounting optimally frozen specimens onto standard supports for the cryoSEM and this will be described.

A question addressed towards the end of the thesis touches on another area of uncertainty in cryotechnique which, it could be argued,

throws doubt on the validity of ice crystal analysis. This asks if the processing of specimens at 193 K (-80°C) during freeze-substitution can induce secondary ice crystal growth further to that which occurs during the initial freezing of the specimen? This will be investigated using specimens stored at temperatures between 193 K (-80°C) to 263 K (-10°C) for periods of between 45 minutes and 8 days. The question of cryoprocessing temperature, be it for freeze-substitution, freeze-fracturing, freeze-etching, freeze-drying or cryosectioning, is fraught with uncertainty, with there being little information in the literature for electron microscopy purposes and some of that which there is fails to distinguish between the handling of fresh material and cryoprotected material.

The final question to be addressed will concern the rate of cryosubstitution. This is one of several techniques named above which are commonly performed at 193 K (-80°C), although, since its introduction by Fernández-Morán (1960), there have been remarkably few studies of the technique in the literature. It is possible that only the surface areas of specimens have frozen water replaced by solvent at 193 K (-80°C) and that completion occurs on returning to ambient temperature, during which process there could be further growth of ice crystals. This question will be addressed by arresting the process at known time intervals and then examining the penetration of a heavy metal fixing agent, namely, uranyl acetate.

3 *Materials and Methods*

This Section describes the routine materials and methods used in the work. The design and use of cooling devices and specialised methods are described in the relevant Sections.

3.1 Coolants

The coolants used in these experiments were: ethane CP grade (99.0% minimum purity C_2H_6) and propane CP grade (95% min. purity C_3H_8) later renamed Grade N.1 (Tech), both from British Oxygen Company, Special Gases Division, Deer Park, London SW19 3UF; Propane (Domestic Grade) and Freon 22 (99.7% purity $CHClF_2$ in vapour phase, monochlorodifluoromethane) from British Oxygen Company, Industrial Gases Division, Plymouth branch; iso-Pentane (99% purity C_5H_{12}, renamed 2-methylbutane) from BDH Chemicals Ltd., Poole, Dorset; and liquid nitrogen (LN_2) from CryoServices Ltd, Worcester.

3.2 Safety

Two important areas of safety had to be considered in this work. Firstly, the use of liquid nitrogen and other liquefied gases demanded caution regarding the handling of cryogenic fluids. Secondly, the use of ethane, propane and iso-pentane demanded precautions for the use of flammable gases.

Use of cryogens. Information was obtained from CryoService Ltd. as a leaflet entitled *"Recommended safety precautions for handling cryogenic liquids"* and from B.O.C. as a leaflet entitled *"Care with cryogenics: the safe use of low temperature liquefied gases"*. Also, the relevant chapters in Robards & Sleytr (1985) and Steinbrecht & Zierold (1987) were consulted. The main concerns were protection of the face by means of a full face-

shield and adequate ventilation to prevent asphyxiation. Asphyxiation is a serious possibility in small rooms. Liquid nitrogen boils to give nearly 700 times its volume in the gas phase. Air contains about 21% oxygen and when this falls below 18% then unconciousness ensues; this would be terminal if not quickly remedied (Sitte *et al.*, 1987). For example, a 4 x 3 x 3 m room has a volume of 36 m^3; displacing 3% of this requires 1.08 m^3, which is the volume of gas derived from only 1.54 l of LN_2. Large volumes of LN_2 used in an unventilated small room could easily induce a danger situation. Other precautions, such as thick leather gloves to enable sure and safe handling and trousers worn over shoes to prevent LN_2 ingress, were taken.

Use of flammable gases. Data sheets were obtained from B.O.C. The main concern was the avoidance of flammable conditions. At ambient temperature this was ensured by (1) the use of a recommended Spectrol SP507 regulator with a needle valve (2) checks that cylinders and valves were in good condition and did not leak (3) checks that cylinder main valves were closed when gas was not being demanded (4) the provision of good ventilation (5) the removal of cylinders of flammable gas to outside stores when finished with and (6) the avoidance of all sources of possible ignition. These gases are also asphyxiants in high concentrations.

The flammable coolants were maintained in a safe condition at low temperatures by (1) ensuring they remained below their flashpoints (propane 169 K/-104°C, ethane 143 K/-130°C) and (2) maintaining the level of LN_2 in the cooling chamber, this both cooled the coolants to very low temperatures and constantly flushed the cooling chamber with inert gaseous nitrogen. Thus, there was no oxygen available for combustion and insufficient flammable gas concentration above the coolant for ignition.

The continual flushing was important because otherwise oxygen would have condensed into coolants at temperatures below 90 K (-183°C); this is the boiling point of oxygen (Stephenson, 1954).

During the period of this work, a safety audit was conducted in 1986 by Inspectors of the Health and Safety Executive, Bristol. This audit queried the quantities of explosive gases which could be produced from the coolants. Explosive volumes derived from the evaporation of 1.0 ml of each coolant after dilution to the limits of flammability were calculated. These, together with other safety information, were published in the Journal of Microscopy (Ryan & Liddicoat, 1987).

3.3 Liquefaction of gases

Initially, the gas to be liquefied was condensed while passing through a small-bore coiled copper tube, immersed in liquid nitrogen. The delivery end was positioned over a plastic Tripour beaker, which was sitting on a large brass block cooled by liquid nitrogen within a polystyrene Igloo box. This proved difficult in use because the gas liquefied quickly and then froze, blocking the tube.

A second method was used routinely for some time. Plastic tubing was connected to the gas supply, coiled at room temperature, held in shape with long forceps and immersed in liquid nitrogen in the particular cooling device. This proved very satisfactory. An important safety precaution necessary with this method was that the end of the delivery tube was *not* immersed under the surface of collected coolant (see Figure 1). The reason for this was that if the gas supply was turned off then coolant was quickly sucked back up the delivery tube. It then vapourised violently and expelled the collected coolant out of the cooling device.

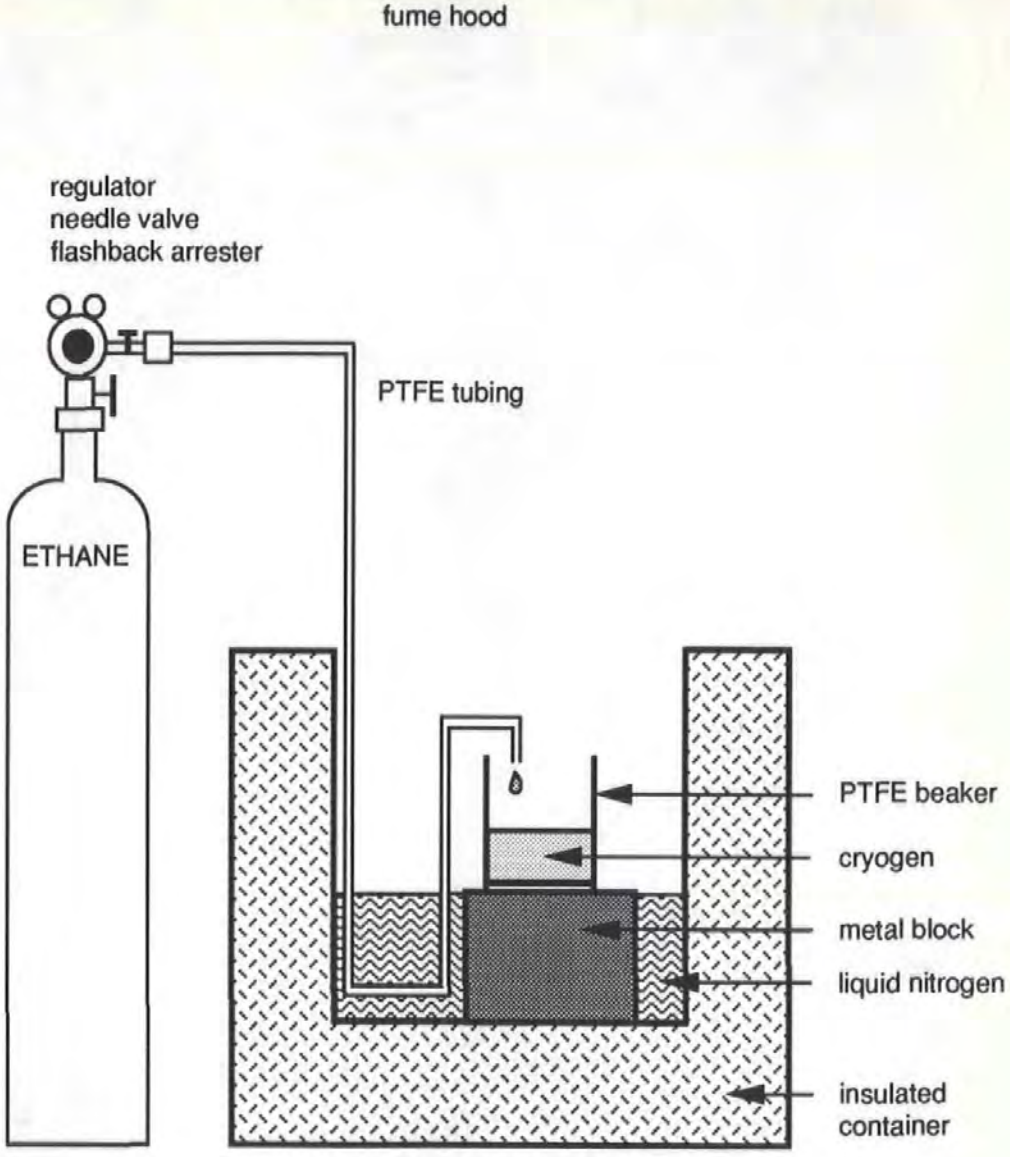

Figure 1. Liquefaction of gases

The gaseous phase of the cryogen is condensed in plastic tubing which is cooled by liquid nitrogen. Note that the end of the delivery tube is not immersed under the meniscus of the condensed cryogen (described in Section 3.3).

A third method used what was essentially a modified glass bottle of 200 ml capacity. The bottle top was converted into a pouring spout, behind which arose a vertical handle, about 100 mm high, with a right-angle bend and a horizontal section, about 100 mm long. A glass delivery tube ran down the side of the bottle and entered through a welding at the base. The bottle was held in liquid nitrogen and when the coolant gas was passed down the tube it condensed and collected inside. This system proved very easy to use and was adopted as routine. The device was presented by Dr Peter Simonsberger, University of Salzburg.

After collection, it was important to maintain the coolant at a low temperature by cooling it with liquid nitrogen. Spare coolant for topping up purposes was often allowed to solidify until needed.

3.4 Temperature control of coolants

This was not effected in early experiments, where 1 part of iso-pentane was mixed with 3 parts of propane (after Feder & Sidman, 1958). This mixture can be cooled to liquid nitrogen temperature without solidifying and was later tested against the other coolants.

A development, used for most experiments, involved the use of a 100 W cartridge heater. This was located near the base of the cryogen container and supplied with a variable voltage either from a Variac control unit (ac) or, later, a specially made simple dc supply. Temperatures were very stable and control was effected manually with reference to a separate thermocouple which read the coolant temperature. Little adjustment was necessary once a power input level was ascertained for a particular temperature.

The final development was to use a thermocouple-feedback system, where a set-temperature was maintained via a Eurotherm control module.

3.5 Thermocouples

Thermocouple thermometry exploits the Seebeck Effect. This is the phenomenon whereby a change in temperature at the junction of two dissimilar metals in a circuit induces an electromotive force (emf) or voltage. This signal is dependent on the metals involved, the direction of temperature change and its magnitude. This is the opposite to the Peltier Effect, where heat is absorbed or evolved when a current is passed through a junction of two dissimilar metals.

Two types of thermocouple were used, type E and type T. Type E was made from 25 μm diameter wires of chromel (90% nickel + 10% chromium) and constantan (55% copper + 45% nickel). The wires were obtained from Goodfellow Metals Ltd., Cambridge. Type T was made from copper and constantan wires, 0.3 mm in diameter, which were obtained as a PVC-coated twisted pair of solid conductors from Oxford Instruments Ltd., Oxford. The fine chromel/constantan thermocouples were used primarily for reasons of economy because 25 μm diameter copper wire cost 4 times as much as the alloys. An extra advantage was that chromel/constantan gave 9.793 mV total signal over the range 291 to 77 K (18 to -196°C), compared to 6.248 mV from copper/constantan.

Thermocouple junctions were made by soldering with Eutecrod 157 stainless steel low temperature welding alloy (1/16th inch coil) and 157 BN Eutector flux, both from Eutectic Co. Ltd., Feltham, Middlesex. These components are recommended for the strength with which they join alloys containing chromium and nickel. They readily form a very thin, stable,

oxide film which is transparent and which protects against further corrosion.

3.6 Thermocouple construction

The fine thermocouples were made as follows. One wire, 0.5 m long, was laid over a glass microscope slide on a piece of stiff card, under a stereo microscope. It was fixed by Scotch tape which was applied a short distance from its ends. The free ends were then bent away from where the second wire was to lay. The second wire was then laid parallel to and touching the first wire, being adjusted and fixed down by means of Scotch tape at its ends. The central area under the microscope was then flooded with flux and a section up to 10 mm in length was soldered. This was then washed with distilled water to remove traces of flux and blotted dry (see Figure 2).

The soldered section was then anchored to the slide with a small piece of adhesive tape. The ends of the wires were then freed and fine forceps used to manipulate them. First, the wires were bent apart at right angles to the soldered junction. Then, about 5 mm from the junction they were bent at right angles again so as to run parallel to each other. A piece of adhesive tape was positioned below the wires so that they lay on the adhesive, a second piece was placed over the wires so that they were sandwiched. This arrangement allowed easy handling of the assembly. The junction was then cut with a fresh scalpel blade, using a calibrated graticule in the microscope eyepiece to give a final junction length of 50-75 μm (Figure 3).

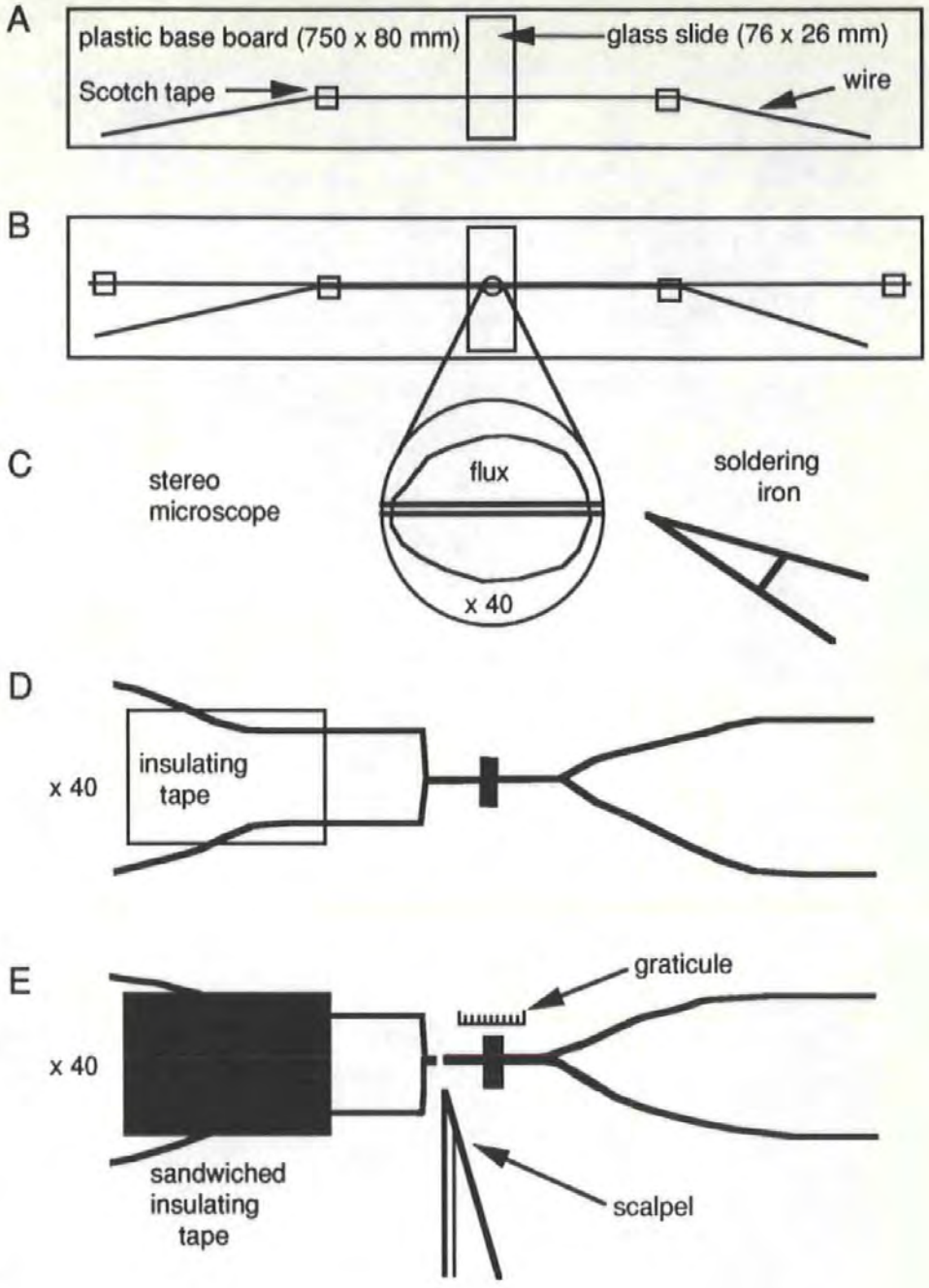

Figure 2. Thermocouple construction

25 μm diameter constantan and chromel wires are fixed to a board, soldered together, washed with water, dried, anchored centrally, the wires arranged and sandwiched between insulating tape and the junction cut to a length of 50-75 μm (described in Section 3.6).

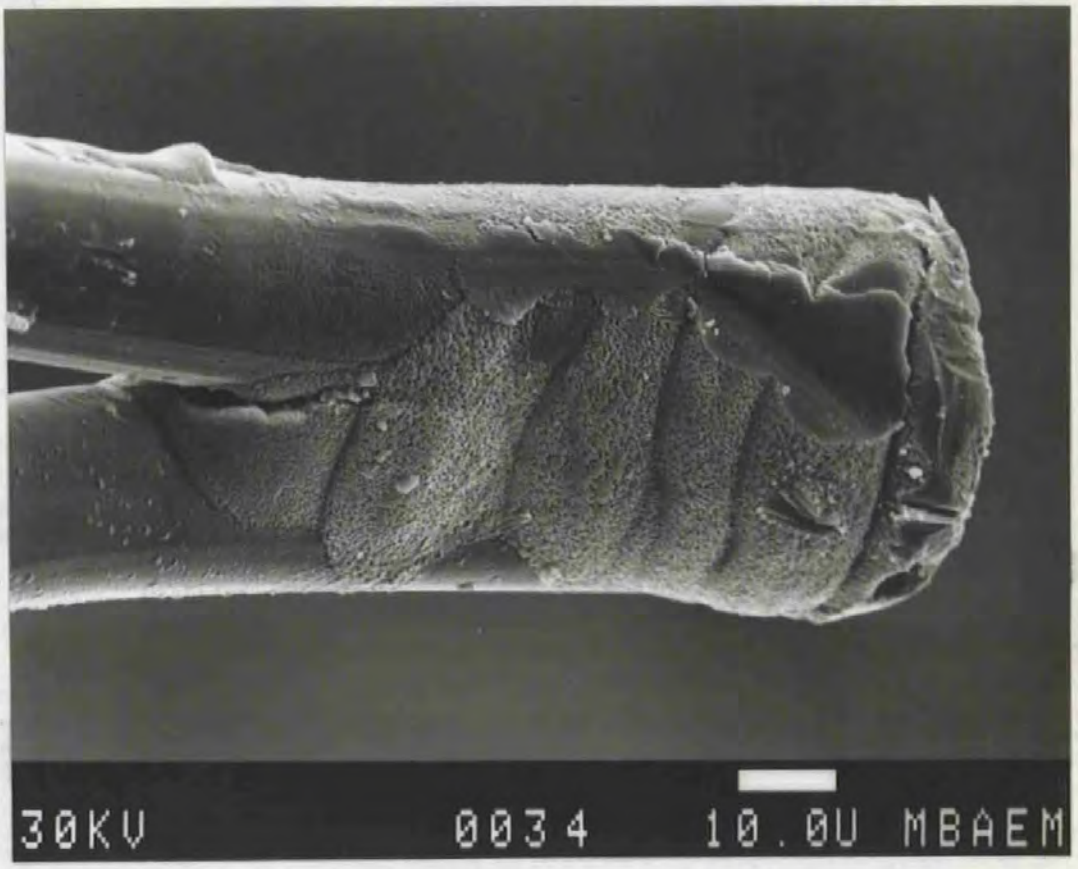

Figure 3. Scanning electron micrograph of a fine thermocouple

This figure shows a thermocouple constructed by joining 25 μm diameter chromel (90% nickel-10% chromium) and constantan (55% copper-45% nickel) wires with stainless steel solder, as described in Section 3.6 and illustrated in Figure 2. The soldered junction is 77 μm long. This ensures high sensitivity combined with sufficient mechanical strength to withstand the physical shock of plunging into coolants at high velocities. Scale bar: 10 μm.

This method was used with the bench-top cooling device, where the thermocouple leads were about 200 mm long. It had the advantage also of yielding two thermocouples from each soldering. The thermocouple tails were soldered to 1.0 mm jack plugs which connected onto a coaxial lead to the recording system. For use with the big plunger, thermocouples with 1.25 m long tails were necessary. These were made on a 2 m length of melamine-faced board, with only one junction being made from a soldering (the short ends were discarded).

The thermocouple leads were very delicate and were sometimes insulated for use with the bench-top plunger and always insulated for use with the deep plunger. This was accomplished by soldering the ends to lengths of 150 μm diameter stainless steel wires which were passed through polythene catheter tubes. The tubing was obtained in a 30 m length, inner diameter 0.58 mm and outer diameter 0.96 mm, from Portex Ltd., Hythe, Kent. The steel wires were then pulled so as to draw the thermocouple tails through the plastic tubes. For use with the deep plunger, the catheters were previously passed along the 1.0 m long hollow tube that held the specimen for plunging into the coolants.

The larger thermocouples were made by removing a length of insulation from the wires, trimming the ends with a sharp scalpel and butt-soldering them together. For streamlined bare thermocouple experiments, the ends were trimmed at 45° which produced an arrow-like tip. For hydrated gel specimens, they were trimmed at right angles. The same solder was used as before (Figure 4).

Figure 4. Photograph of the 300 μm diameter thermocouples

These thermocouples were constructed from 0.3 mm diameter copper and constantan (55% copper-45% nickel) wires by soldering together with stainless steel solder as described in Section 3.6. The thermocouple at the left was used in bare thermocouple experiments in Section 4. The others were used to test cooling in exposed, hydrated gelatin specimens in Section 5. The thermocouple at the right shows the dimensions of the gel specimen. The shell thickness of gelatin around the wires was 125 μm, this gave a 0.25 mm diameter specimen. The thermocouple at the right was an epoxy resin specimen which was used for comparison purposes.

3.7 Thermocouple sensitivity

The sensitivity, "lag", or "response time" of thermocouples was defined by Baker *et al.* (1961) as the time taken for a degree of approach to equilibrium after a sudden imposed change. This is the time required to come to within 1/e of equilibrium, that is 1-1/e or 63.2% of full response, where e = 2.71828 as the base for natural logarithms. This was measured for a fine thermocouple as 0.48 ms, while recording a cooling rate of 258772 Ks^{-1} in ethane. To a large extent, measuring this response depends on the coolant and other experimental factors that this thesis addresses. The measured response relates well to that given by Costello (1984) of "*about 0.5 ms*". His figure was obtained from a commercially purchased finer thermocouple (12.5 μm wire diameter with a 30 μm bead diameter).

3.8 Plunge velocity sensor

This device was an integral part of the experiments and was constructed to be transferred between the plunging devices. It enabled measurement of the velocity at which specimens plunged in the coolant. The signal it produced was recorded and displayed simultaneously to the thermal record from the thermocouple. Thus, it was easy to see at what stage of each plunge the various thermal events occurred.

The device was a reflective opto-switch which consisted of a combined infra-red light emitting diode and a phototransistor (part number 307-913, from RS Components Ltd., Corby, Northants). The phototransistor responds to radiation from the diode when a reflective surface is placed within the field of view. A simple circuit was constructed and is shown in Figure 5. The device can be seen in later photographs of the equipment (Figures 13 & 16). Plunge motion was monitored by

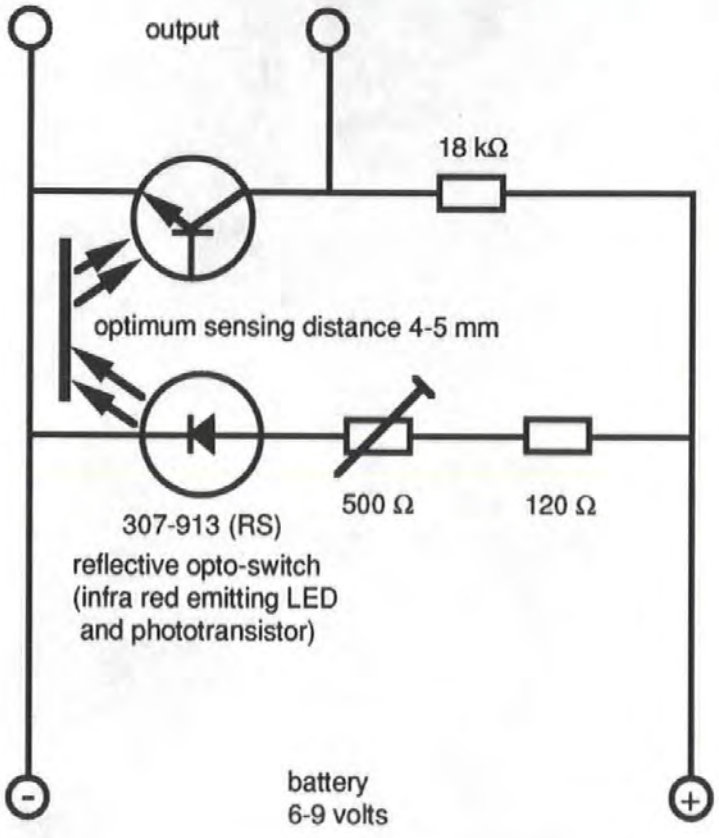

Figure 5. Plunge velocity sensor

The velocity sensor is seen in the photograph above with its circuit diagram below. The sensor is adjusted adjacent to a white surface to give a diode output between 0.2 and 0.4 V, the diode current is then 20-30 mA. Any increase on this will shorten battery life and reduce black/white differential (described in Section 3.8).

scanning a scale of 5 mm high black and white bands which was attached to a vertical side-arm of the plunging rod, thus producing a cyclical waveform.

3.9 Recording and display electronics

In early experiments, a Tektronix Type 5103N dual beam storage oscilloscope was used. It was triggered by the signal from the plunge velocity sensor so that the plunge motion and the thermocouple signals were displayed together on the screen. These could then be photographed with a Polaroid camera and the prints photocopied for drawing and measuring purposes. It quickly became apparent that the photographic approach would be too expensive to maintain (a total of 2009 paper traces were made later).

A more sophisticated recording system was arranged, by Mr John Wood of the laboratory's electronics workshop (Figure 6). It was based around a Datalab 902 transient waveform recorder (Data Laboratories Ltd., Mitcham, Surrey). This had two independent recording channels with 2048 channels each, a switched timebase, a window trigger, split memory recording and other features, including digital output for plotting purposes. This system was triggered by the thermocouple signal, with a switchable delay which was chosen to optimise the stored waveform with regard to the start and finish of recording and the displayed format on the screen. The entry point into the coolant could be marked by a 1.0 mm high black strip which was positioned on the scale scanned by the sensor to be opposite the sensor's window as the specimen contacted the coolant.

The thermocouple signal had to be amplified by a 5103N oscilloscope before passing to the transient store. The motion sensor

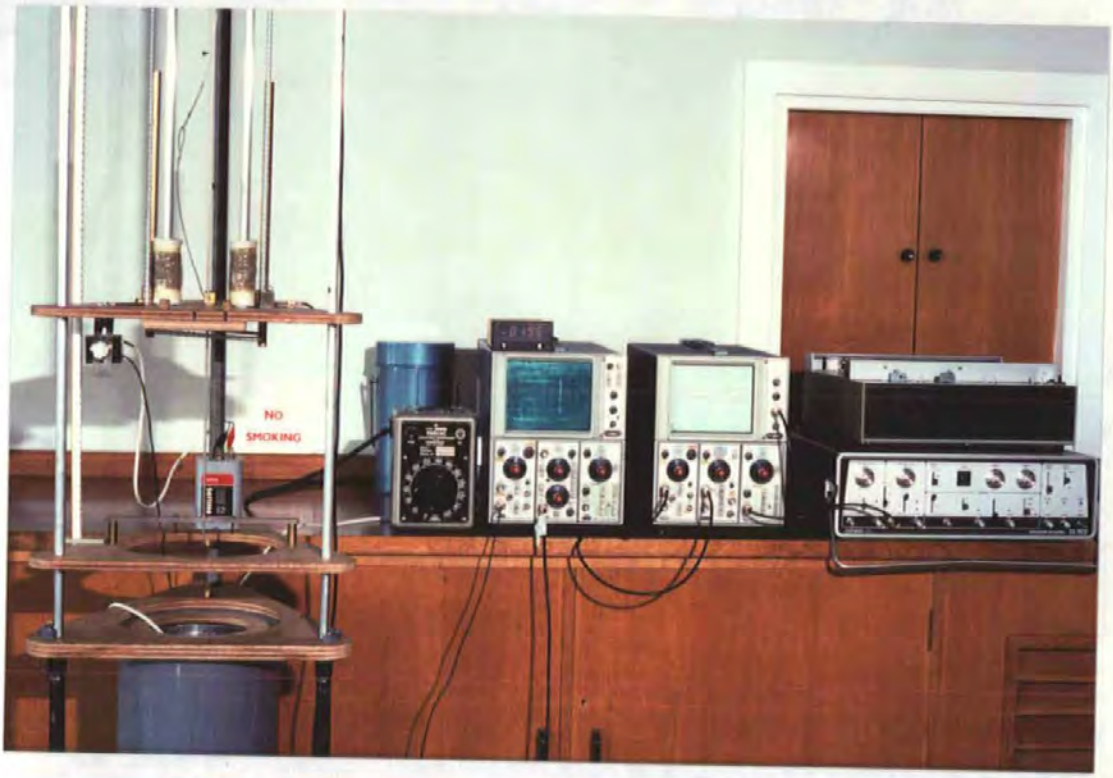

Figure 6. Recording and display electronics

The thermocouple signal was applied to the left amplifier of the left oscilloscope and thence to the transient recorder (at right, bottom). The motion record was applied directly to the transient recorder. The stored signals were displayed on the second oscilloscope. Permanent records were made by amplifying the signals through the centre amplifier of the left oscilloscope and thence on to the XY plotter which is seen above the transient recorder. The Variac unit provided power to the coolant cartridge heater and the battery provided power for the motion sensor (see Figure 5).

signal was plugged straight into the store. The stored signals were displayed simultaneously on a second oscilloscope. They could be recorded as high quality hard copy on graph paper using an XY plotter. For this purpose, the signals were passed through the second channel of the first oscilloscope for suitable amplification. The stored signals could have been transferred to floppy disk for permanent storage and later analysis via a simple interface to a BBC microcomputer if funding had been available.

The time constant or response time of the recording system was tested by simulating a sudden change by short-circuiting the thermocouple signal input, as described by Silvester *et al* (1981). Their time was "*approximately 2 ms*". The best time for this system was 0.15 ms. The same test with the transient recorder on its own gave 0.03 ms.

3.10 Calculation of cooling rates

Cooling rates were normally calculated over the range from 273-173 K (0 to -100°C), although cooling rates over several ranges were analysed in the final cooling experiment (Section 6). The time taken to cool this 100 K was measured against the set time-base of the system and converted to a *pro rata* figure for a whole second, as shown in Figure 7. The method used was that of Costello & Corless (1978), which used recorded ambient and coolant temperatures as reference points. This procedure avoided the use of separate ice-point thermocouples, which would have have been tedious to maintain over the long experimental sessions, or the use of an ice-point reference box for which there was no funding. The connections onto the recording system constituted ambient temperature reference thermocouples.

Standard thermocouple tables were used (supplied by TC Ltd, Uxbridge, Middlesex) in the calculations. As these are produced with 273 K (0°C) reference thermocouples, it was deemed adviseable to check them against the system used. The tables give a measurement of 9.793 mV from 291-77 K (18 to -196°C, which is liquid nitrogen temperature). A Polaroid record of cooling in LN_2 is shown in Figure 8, where it is difficult to see any deviation from this value. The signal can only be measured as 10 mV on this size of display where the width of the trace masks about 0.2 mV.

3.11 Calculation of plunge velocity

The plunge motion sensor produced an oscillating signal as the alternate 5 mm high black and white bands fell past the window of the sensor. One complete cycle of the signal represented 10 mm of downward motion. In bare thermocouple experiments it was sufficient to measure the time taken for only 1 cycle and to convert that to ms^{-1}. Cooling of the fine thermocouples took place over fractions of a millimeter. Larger hydrated specimens cooled over plunge distances in excess of 400 mm. In this situation, it was evident that acceleration occurred during the course of the plunge. Plunge velocity was then measured over the cooling range (normally 273 to 173 K or 0 to -100°C), converted to a rate per second and expressed as a mean plunge velocity (see Figure 7).

3.12 Hydrated gelatin-thermocouple specimens

The gelatin used in these experiments was the standard powdered product from BDH Ltd., Poole, Dorset. It was made up as a 20% concentration in distilled water by standing overnight in a 308 K (35°C) oven and then used in the preparation of hydrated specimens which were constructed around thermocouples. The thermocouple was normally

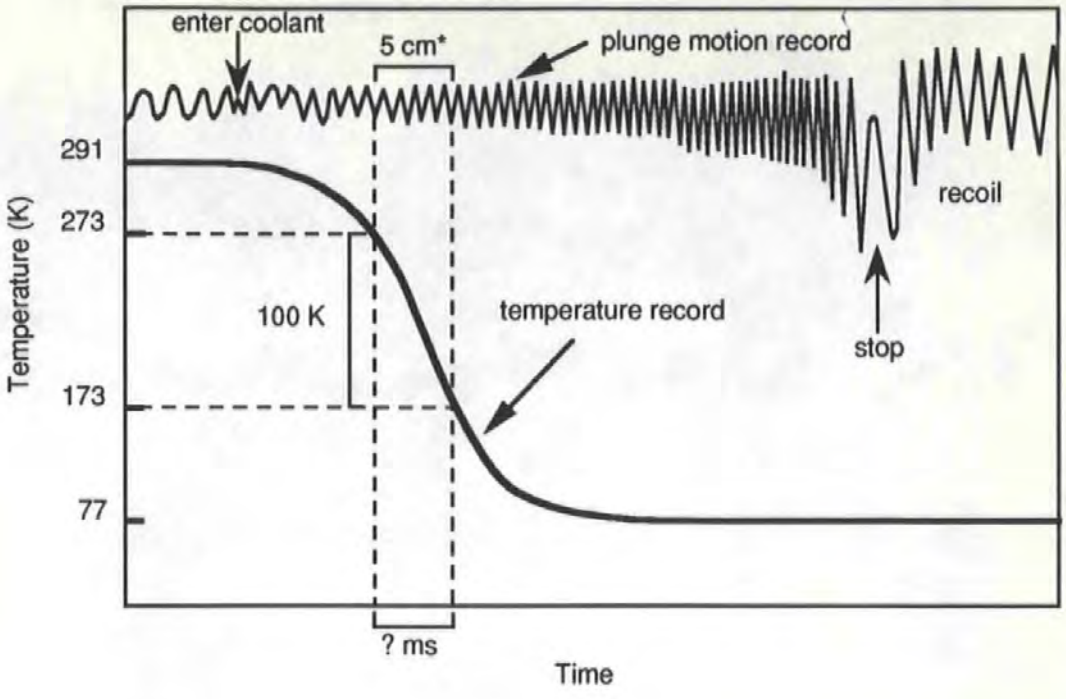

Plunge velocity: $\frac{\text{? ms}}{\text{5*}}$ = y ms/cm

$\frac{\text{1000 ms}}{\text{y}}$ = cm/s

$\frac{\text{cm/s}}{\text{100}}$ = metres per second

Cooling rate: $\frac{\text{1000 ms}}{\text{? ms}}$ x 100 K = degrees per second

Figure 7. Calculation of plunge velocity and cooling rate

Plunge velocity is calculated by timing the plunge against the preset time-base over the distance taken to cool from 273 to 173 K. Cooling rate over the 100 K is measured and extrapolated to a rate per second (described in Sections 3.10 and 3.11).

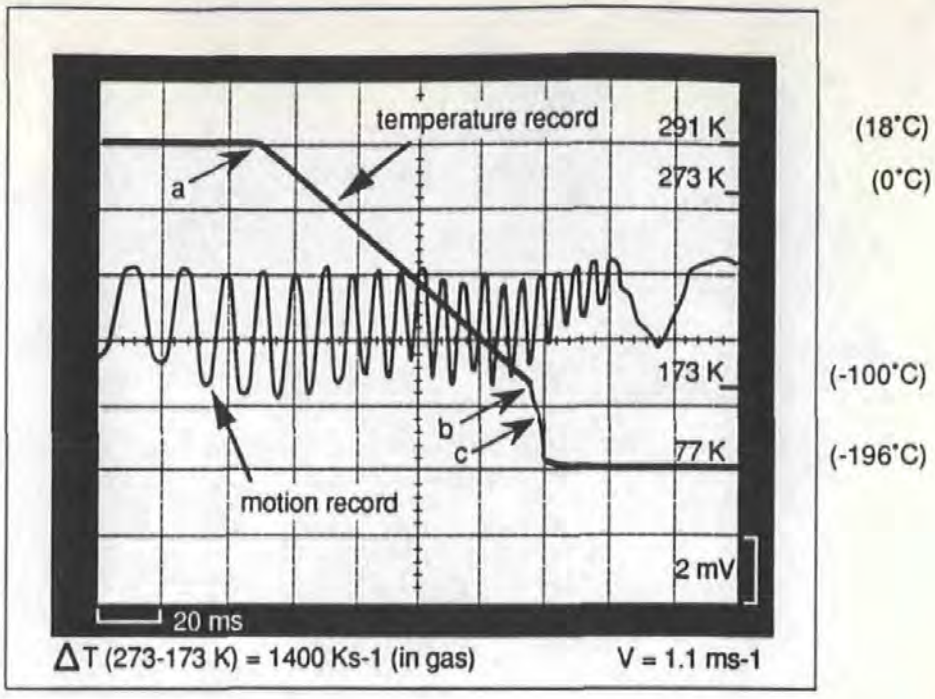

Figure 8. Thermocouple response in liquid nitrogen

This figure was prepared by scanning Polaroid photographs of the record and the oscilloscope screen into a Macintosh computer, copying the traces and the screen graticule and then combining them into a composite image with reversed contrast of the record for improved clarity. It is shown at its normal size and shows the response of a fine chromel/constantan thermocouple* entering the cooling chamber at "a" and plunging 12 cm in cold gas before entering LN_2 at "b". The transition from film to nucleate boiling, sometimes termed the "Leidenfrost point", is seen at "c". The total signal registers as 10 mV. The thickness of the trace is equivalent to 0.215 mV which represents 14.5 K at ambient and 10 K at liquid nitrogen temperature. The response is non-linear and this and the thickness of the trace contribute to imprecision in measurements on records from the oscilloscope screen. The experimental arrangement is shown in Figure 24 (inset). This record can be compared to Figure 14 which is from the double oscilloscope/transient store/XY plotter method which was normally used throughout this work (see Section 3.10).

(* as shown in Figure 3)

attached to a matchbox by means of the sandwiching adhesive tape. It could then be easily examined from most directions by turning/upending the box. This was done under an long-arm mounted stereo dissecting microscope. The gelatin was maintained fluid in a hot water bath and kept capped to avoid water loss or uptake. A *fine* sewing needle was warmed in the hot water bath, dipped carefully in the gel and moved to the thermocouple (Figure 9). A shell of hydrated gelatin was built around the thermocouple with a thickness of one-half the nominal specimen "diameter". In other words, a 0.25 mm diameter specimen would have a shell thickness of 0.125 mm all around the somewhat asymmetrical junction, including the area behind the junction where the tail leads joined it.

The construction was carried out over the lid from a freshly boiled kettle, which was a useful hotplate. Normally a small amount of gel was applied, spread and allowed to gel. It was then immediately swamped with cold water from a standard mounted dissecting needle. This maintained hydration and allowed examination of the specimen within the water droplet. To add further gelatin, the kettle lid was reheated, the water was drained with filter paper and more hot gel applied, followed again by cold water. When the desired size was achieved the specimen was immersed in 5% glutaraldehyde to fix it. The desired size was normally a fraction smaller than the nominal size because the specimen would swell slightly with fixing and storage in water until needed.

The final gel concentration probably remained close to 20%, because water loss resulted in surface drying and the rapid appearance of first a dull and then a wrinkled surface. The use of cold water did not appear to lead to marked swelling which would give a decrease in gel

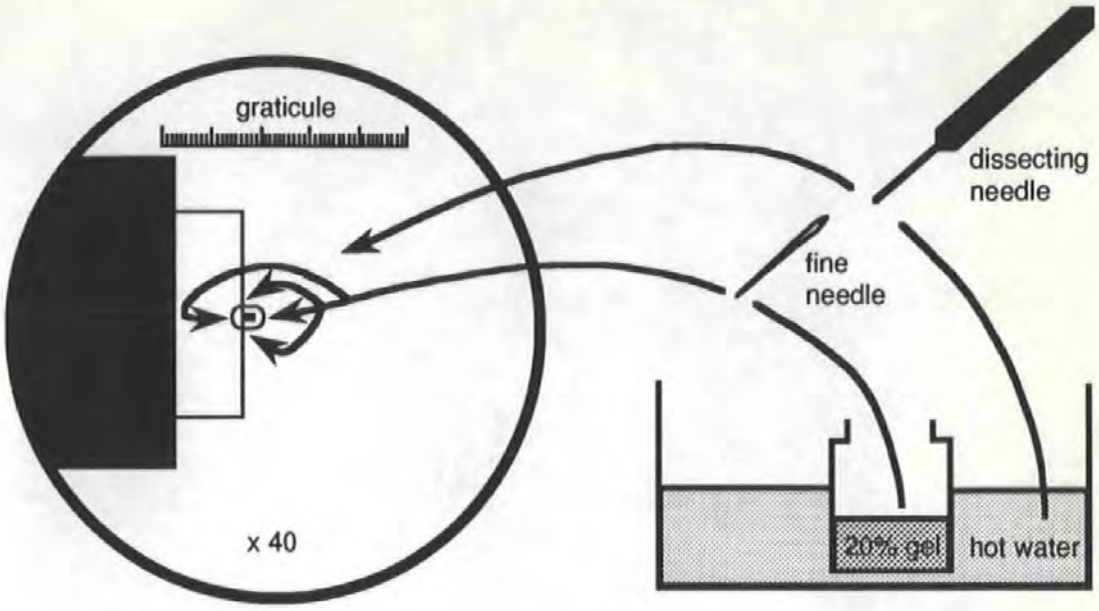

Figure 9. Construction of hydrated gel specimens

A thermocouple is mounted above a hotplate so that it can be examined from all directions under a stereomicroscope. A hot water bath maintains 20% gelatin in distilled water in a fluid state and small amounts are quickly applied to the thermocouple with a fine needle which is previously warmed in the hot water. When shrinkage is observed, by the evaporation of water from the gelatin, a small amount of hot water is added with a larger needle to maintain specimen size. After the desired size is attained with reference to an ocular graticule, the specimen is stored under 5% glutaraldehyde in water until required for experiments (described in Section 3.12).

concentration. Some specimens were monitored and found to swell by approximately 5% in overall diameter.

3.13 Metal-sandwiched gelatin-thermocouple specimens

In the final cooling experiment (Sections 6 & 7), specimens were supported between copper sheets, or planchettes, as used in the freeze-fracture technique. These ensured consistently sized specimens. The planchettes used were Balzers BUO 12 057, 110 μm thick. A special holder was made (Figure 10) so that the thermocouple could be positioned centrally and then surrounded with 20% gelatin. It was a 2-part brass device, the larger part of which grub-screwed onto the end of the plunge-rod. A wire "V" was soldered into it with one planchette soldered onto the ends of the wires. A fine thermocouple was made, with its leads drawn up through plastic catheters in the plunge-rod and carefully positioned to lay centrally over the depression (1250 x 1650 μm x 200 μm deep) in the planchette. The thermocouple was fixed by a thin film of Araldite epoxy adhesive and allowed to set overnight. The film was 50-60 μm thick. This approximated to the thickness of Scotch tape, small pieces of which were positioned around the other edges of the planchette so that even spacing was achieved between planchettes. The planchette was then positioned over the hot kettle-lid and fluid gelatin added so as to slightly overfill it. Simultaneously, gelatin was added to the other planchette. The second planchette was mounted on the ends of a V-wire which was soldered into a brass piece which, in turn, screwed onto the first block. The planchettes were immediately brought together, so that the gelatin flowed into one mass and the assembly clamped by screws. The plunge-rod was then up-ended and clamped so that the specimen was maintained under water, until needed for experiment.

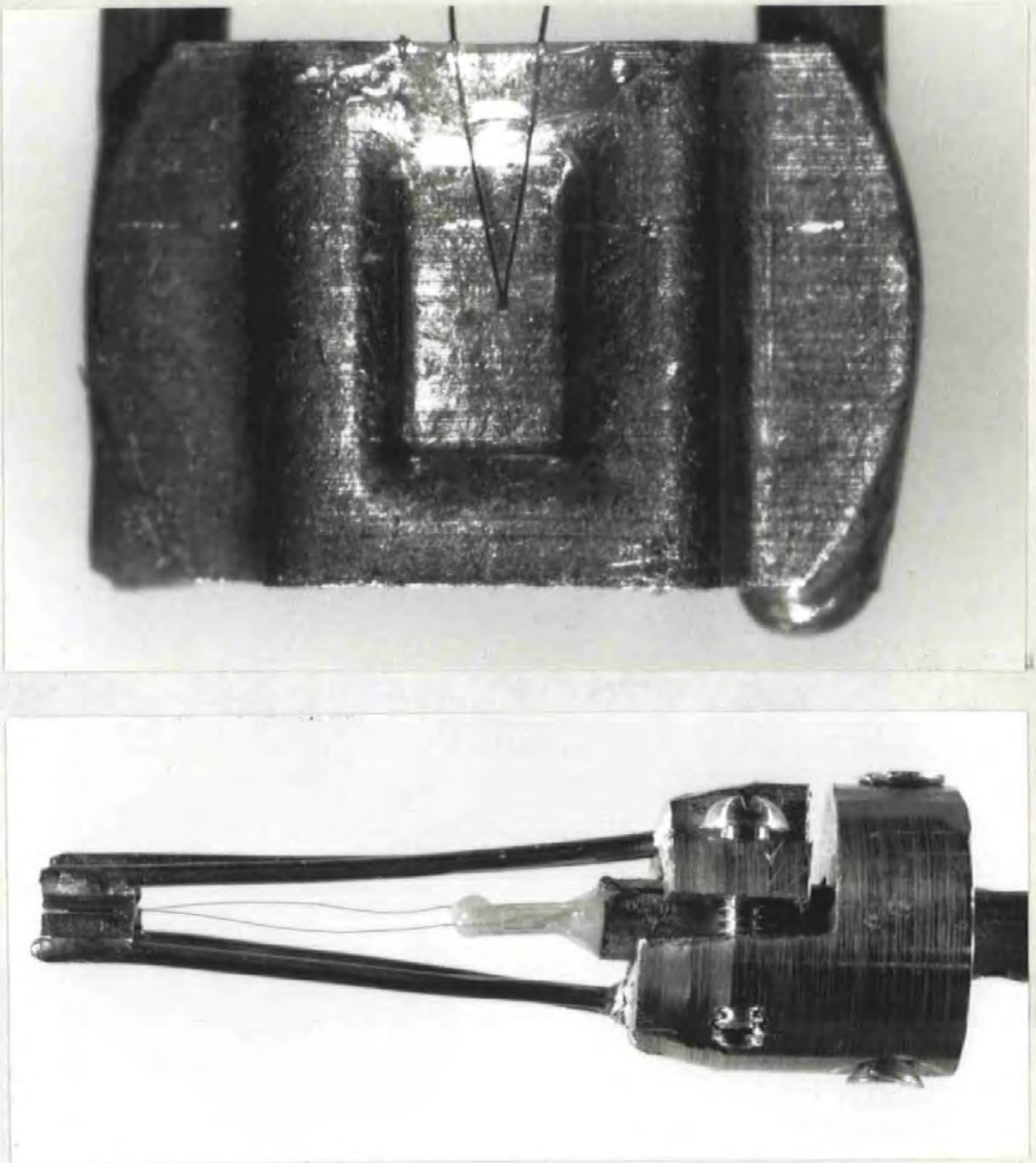

Figure 10. Metal-sandwiched hydrated gel/thermocouple specimen

Above: face view of a copper planchette with a fine thermocouple attached (at top) by a thin film of epoxy adhesive. The planchette is soldered onto support wires.

Below: side view of the clamping device which carries the copper planchettes (at left) on the ends of support wires. The device is grub-screwed onto the plunge rod and the thermocouple wires are seen running from the planchettes into plastic tubes in the plunge rod.

3.14 Metal-sandwiched hydrated gel and blood specimens

These two types of specimen were used in the appraisal of ice crystal damage in cryofixed samples. They were sandwiched between the same type of freeze-fracture planchettes described above. The main difference here being that the planchettes were loaded and clamped tightly together under a stereo microscope in a specially-made holder, subsequently this could be inserted into the deep plunging device. The reason for using these specimens was that they were uniformly-sized. The planchettes were clamped together without spacers as above (which were necessary to allow passage of the thermocouple wires) to prevent seepage of blood. The gelatin was 20% in distilled water and loaded as described above. The blood was collected in heparinised 1 ml syringes from flounders, *Platichthys flesus*, which were kept in circulating seawater.

3.15 Freeze-substitution

Specimens which were destined for analysis of residual ice crystal "ghosts" by electron microscopy were freeze-substituted, embedded in resin and ultrathin sectioned. Freeze-substitution was performed at 193 K (-80°C) over 48 h in pure methanol which contained 1% osmium tetroxide. Before substitution, the planchettes were opened under LN_2 in order to allow access of the substituting medium. This is the process of freeze-fracture and entailed loss of the top layer of the surface which split in this process. The thickness of the lost layer was minimal and its loss was scarcely detectable in later measurements. This fracture plane must have passed through the best frozen (*i.e.* surface) layer, as illustrated by Escaig (1984). Substitution was done in 1.5 ml Nunc cryotubes. These were suspended in a brass gauze basket in the neck of a one-third full 25 l LN_2 dewar. Temperature was monitored with a thermocouple connected to a Comark digital thermometer. At the end of the process, the specimen basket was

raised by a long mechanical thread, to room temperature. This process took place gradually over 3-4 hours. The solvent was replaced with several changes of acetone and embedded in epoxy resin (Spurr, 1969). The final freeze-substitution, to check on the progress of substitution, was performed with 4% uranyl acetate in methanol. This was done because it was intended to examine refrozen specimens taken at timed intervals during the substitution process by cryo-scanning electron microscopy.

3.16 Transmission electron microscopy (TEM)

The resin blocks were sectioned on Reichert OmU3 or Ultracut ultramicrotomes. Silver sections, 60-80 nm thick, were collected on Formvar-coated 2 x 1 mm slot copper grids and stained with lead citrate (Fahmy, 1967). They were examined in a Philips EM300 transmission electron microscope and photographs were taken on Kodak 35 mm Fine Grain Positive Release film and later Kodak SO-281 film. This was developed in Kodak Dektol developer diluted 1 in 10 for 3 minutes at 20°C. The films were fixed in Ilford Ilfospeed diluted 1 in 4 for 5 minutes, washed for 30 minutes in running water and then dried. Photographic prints were made on Ilford Multigrade paper.

3.17 Arrowworm (Sagitta) specimens

Specimens of *Sagitta setosa* and *S. elegans* (Chaetognatha), 15 mm long, were caught from the plankton off-shore from Plymouth by the specimen supply department of the Marine Biological Association and Plymouth Marine Laboratory. They were brought to the laboratory in fresh condition and cryofixed immediately, normally on low thermal mass supports. This was part of a collaborative study to investigate differences between the 2 species which act as "indicator" species for different water

masses. The results were published in the Journal of the Marine Biological Association of the U.K. by Bone *et al* (1987).

3.18 Low thermal mass specimen supports

Sagitta specimens were normally mounted on specially made supports for cryofixation (Figure 11). These reduced specimen contact with the thermal mass of the support and thus enabled more efficient cooling. The support design used mostly in this study was an aluminium V-wire. The base was soldered into a specimen pin as used in the Reichert FC4 cryoultramicrotome. The arms were approximately 5 mm long and bore small squares of aluminium foil, fixed with epoxy glue. These served as specimen contact areas. The specimen was thus suspended between the arms of the "V" and plunged down into coolant which could flow freely around it. The frozen specimens could then be processed on through freeze-substitution or detached and remounted for cold-stage scanning electron microscopy (see below, Section 3.20). Some specimens were mounted on the original FC4 pin design which had been modified as described by Ryan & Purse (1984). This type bore a streamlined arch of aluminium foil on which specimens were positioned for freezing. A final type was designed with a shape which was similar to a table-tennis bat. It consisted of an aluminium wire bent into a Y-shape. Aluminium foil was fixed between the arms with epoxy. This design was used to freeze thin, flat specimens (Section 10).

3.19 Specimens for monitoring crystal growth in frozen specimens

Thin, flat specimens of fixed flounder spleen were prepared by Mr Michael Wombwell of Bio-Rad Microscience Ltd., Hemel Hempstead, Herts., using a Bio-Rad H1200 vibrating microtome. These were cut to a thickness of 100 μm and used as described later in Section 10. Small

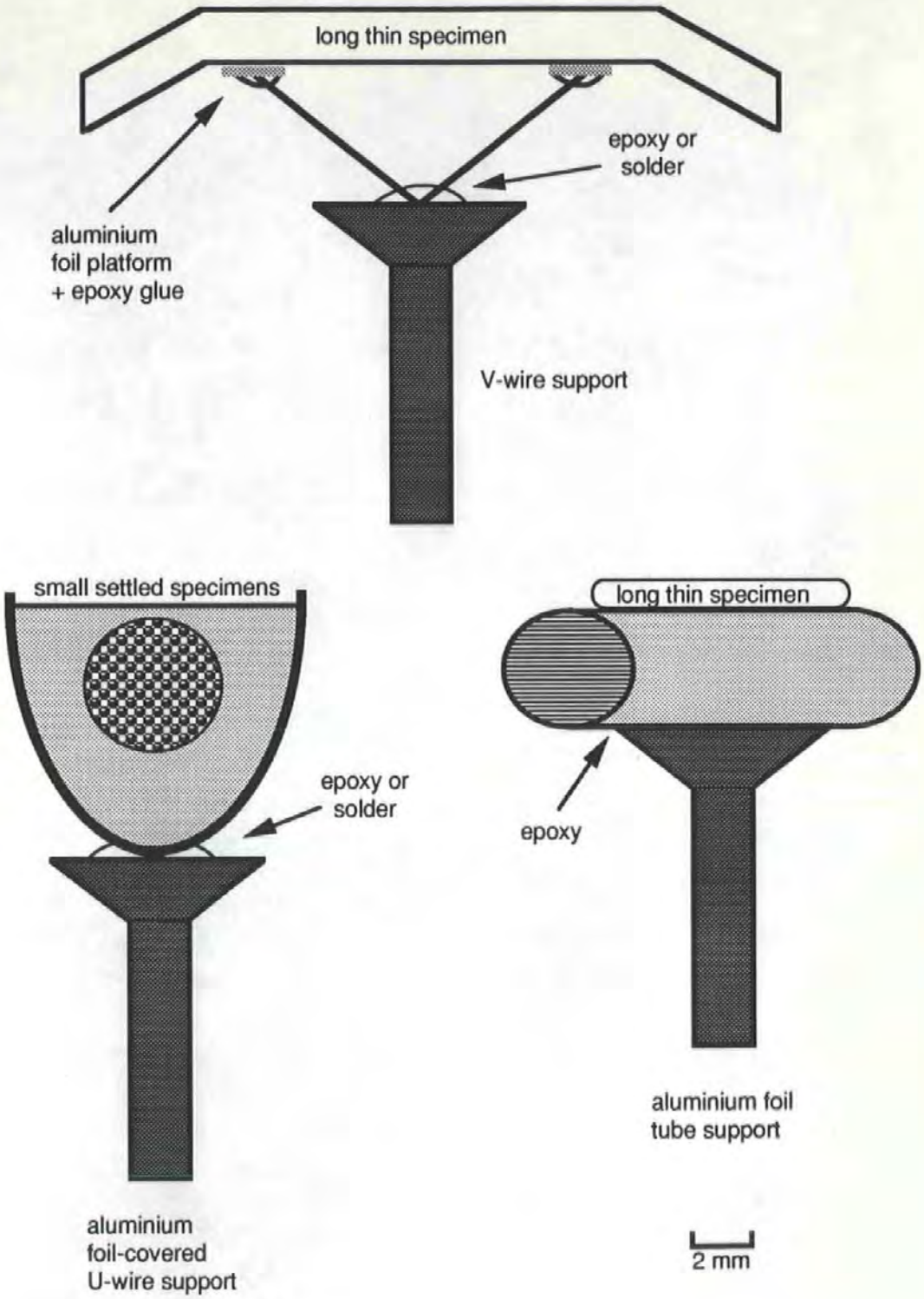

Figure 11. Low thermal mass specimen supports

These supports isolate specimens from bulky support pins which would delay specimen cooling. They enable faster cooling and also cooling from more than one direction (described in Section 3.18).

blocks of fresh spleen were also prepared which were frozen on the streamlined foil arch-type of support described above. These were dissected in a small plastic petri dish, the bottom of which was half covered with wet filter paper to maintain humidity and prevent drying of the tissue. These specimens were all freeze-substituted.

3.20 Cryoglues for cryomounting

Cryofixed arrowworm specimens were snapped off the Y-supports and then mounted into supports to fit the cryo-stage of a scanning electron microscope. This process is described in detail in Section 9. Essentially, low-melting point electroconductive adhesives were employed. These were standard Leit-C Conductive Carbon Cement (from Agar Scientific Ltd., Stansted, Essex) and Dotite Type D-550 silver cement (from J.E.O.L., Welwyn Garden City, Herts.). Both are normally used at ambient temperature for mounting specimens onto SEM specimen supports.

3.21 Carrot (Daucus) specimens

Pieces of cortical parenchyma 6 x 4 x 2 mm were cut from the storage tap root of specimens of *Daucus carotta* (Umbelliferae) and frozen by various methods for study by cold-stage scanning electron microscopy.

3.22 Scanning electron microscopy (SEM)

The microscope used in this work was a J.E.O.L. JSM 35C. Photographs were taken with the standard 120 roll film camera which was loaded with Ilford FP4. The films were developed in Paterson Acutol developer diluted 1 in 10 for 7.5 minutes at 20°C. Fixing, washing and further processing were as described under Transmission Electron Microscopy above. A Robinson back-scattered electron detector was used in

the final study to monitor the ingress of heavy metal during freeze-substitution.

3.23 Cryostage

The frozen arrowworm specimens were examined on a home-made cold stage. This was based on the original J.E.O.L. solid copper block which was cooled by copper braid from a LN_2 dewar. The system went to Hexland Instruments for conversion to direct cooling via PTFE tubing. The Hexland-modified stage was simply a cooled, solid copper block. Another version was designed by the author and built in-house by Mr. David Purse. This had a hole through the stage for the examination of frozen sections by cryo-scanning-transmission electron microscopy, a heater for regulating specimen temperature and a cold trap for anticontamination and freeze-etching/freeze-drying purposes. It proved very efficient for bulk specimens mounted on solid supports. Its construction was described in detail by Ryan *et al.* (1985a) and its performance during the observation of freeze-etching and freeze-drying processes by Ryan *et al.* (1985b).

3.24 X-ray microanalysis

The analysis of coelomic fluids in frozen arrowworm specimens was carried out with the scanning electron microscope using a Link Systems Model 860 system. The Link ZAF PB (= "atomic number-absorption-fluoresence peak-to-background") program was used to obtain quantitative data for the concentrations of elements in the specimens. Results were obtained in terms of %-weight and converted to mmol kg^{-1}. Sensitivity factors for the different elements were obtained from droplets of frozen seawater. Further details are given in Section 8.

3.25 Freeze-drying

During the investigation of the rate of freeze-substitution, specimens were removed from the solvent and transferred in LN_2 to a home-made freeze-drier system built on an Edwards 12E6 coating unit. The apparatus was a modified Polaron version of the Steere-Denton freeze-fracture module. It was modified in that the LN_2-cooled specimen stage was replaced by a brass block with 8 cavities to accept frozen specimens. The shroud was removed and cold trapping performed by the LN_2 trap of the modified vacuum system. The specimen temperature was controlled by thermocouple feedback from the stage which cut the power supply to the LN_2 pump so that the temperature of the specimen stage rose slowly to a preset value. Essentially, the small specimens were warmed to about 193 K (-80°C) by 11.00 h (mid-morning) and left overnight.

An Anavac mass spectrometer was used to monitor the partial pressure of water vapour in the vacuum. It was set to cut the LN_2 pump power supply automatically if the water vapour pressure rose too high. This was a safety measure because contaminating ice in the LN_2 occasionally causes blockage of the LN_2 pump. If this happened, the specimen would warm and water would come off rapidly and fire the cutout. The pump could concievably burn out if left working against a blockage overnight. With these specimens the process ran as intended, without cutting out.

The following morning the apparatus was turned off and the specimen allowed to come to ambient temperature under vacuum. The next morning the dried specimens were vented slowly with dried nitrogen gas, embedded in epoxy resin, planed in the ultramicrotome and mounted conventionally on SEM specimen supports with carbon paint. They were

then rotary coated with carbon ready for examination by back-scattered electron imaging.

3.26 Statistics and n = 2 to n = 6

Throughout this thesis, the presentation of data follows Costello & Corless (1978) by presenting mean cooling rates. The degree of replication is low, from n = 2 to n = 6; the reason for this was the extreme fragility of the specimens. It was deemed essential that data were accumulated from the *same* specimen within any one experiment, so that genuine comparison could be made between the coolants and/or plunge velocities which were used. When one specimen was replaced by another, it was always found that there was a small difference in thermal response, so that the results were not strictly comparable. The results reported in this work are those which were obtained from the first specimen to survive the required experiment.

The specimens had three main limitations: (1) fragility of the delicate thermocouple junctions (2) fragility of the thermocouple lead wires at the anchorage points and (3) the occasional tendency for exposed gelatin specimens to crumble with repeated freeze/thaw cycles and to shed small pieces, thereby changing the cooling response. The high velocity plunges were always more injurious to specimens. The acceleration of specimens to 6 ms^{-1} over a "throw" of a few centimeters, before entering the coolant, and the subsequent arrest was a dramatic event; there was invariably a degree of whiplash of the plunge-rod and sometimes the specimen struck the side of the tube which contained the coolant and thereby suffered damage.

In the thirty-four cooling experiment papers which were reviewed in Section 2.21, only five reported any statistical analyses of the results

(Costello & Corless, 1978; Robards & Severs, 1981; Knoll *et al.*, 1982; Robards & Crosby, 1983, and Costello *et al.*, 1984). Some of these reported on jet-cooling, where the specimen does not move, and some reported on cooling in soldered metal specimens, which are mechanically strong. Only Costello *et al.* (1984) reported any statistical analysis derived from plunging hydrated specimens (n = 3 and n = 4); they were encased in metal planchettes and plunged only 15 mm into coolants at low plunge velocities.

The general lack of statistics in the literature reflects the difficulty of performing plunge cooling experiments with hydrated specimens. The work reported in this thesis extends a measure of replication to the plunge cooling of exposed hydrated specimens. It also involves the plunging of both exposed and metal-sandwiched hydrated specimens at higher velocities than hitherto. The consistency of results from one specimen and comparison with another are shown in Table 6.

4 *Cooling in metal specimens (bare thermocouples)*

4.1 Summary

This Section describes an experiment which investigated the efficiency of coolants by plunging bare thermocouples into them. These are considered to be metal specimens, for rapid cooling purposes, and mimic the metal holders used in the cryofixation of freeze-fracture specimens. In order to perform the experiments it was first necessary to build a suitable plunge-freeze device in which coolants could be maintained at selected temperatures. The device was used to plunge a bare thermocouple into liquid ethane, liquid propane, isopentane-propane mixture, Freon 22 and liquid nitrogen. Ethane was found to cool the metal specimen more efficiently than the other coolants, even when 25 K above its melting point.

4.2 Introduction

The plunge cooling apparatus described here was developed from an early version which was described briefly by Ryan & Purse (1985a). The developments included an increase in the depth from 90 to 100 and finally to 130 mm, addition of a cartridge heater to control coolant temperature, modification of the plunge velocity sensor and provision of better elastic for accelerating the specimen.

The device is essentially a polystyrene box containing a piece of up-ended 20 mm copper water pipe, sealed basally, in which a stirred coolant is maintained. A gantry above it supports a thin rod, on the end of which the specimens are mounted. The rod is powered by elastic and injects the specimens down into the coolant.

Many liquid coolants have been tested in the past, as described in Section 2.16. It was decided for the purposes of this investigation to test the best of these, namely propane and Freon 22 as reported by Costello & Corless (1978) and Elder *et al.* (1982), against ethane.

4.3 Experimental Design

A cooling chamber was formed from a polystyrene Igloo box, from Jencons (Scientific) Ltd., Cherrycourt Way, Leighton Buzzard, Beds LU7 8UA, with internal measurements 125 mm square basally and 180 mm square at the top by 160 mm high with 12 mm thick walls. The 30 mm thick lid had a 100 mm diameter central hole (Figure 12). The box was mounted on a wooden bridge which located it over a IKA-Combimag magnetic stirrer, from FSA, Bishop Meadow Road, Leics LE11 0RG. The stirrer was set to maximum velocity, which prevented thermal gradients in the coolant and helped to maintain fluidity when supercooling the cryogens.

The chamber housed a brass plate which located the cryogen unit over the stirrer. The cryogen unit consisted of 2 concentric copper pipes, dimensions 130 x 20 mm diameter and 130 x 50 mm diameter, both fitted with end-plates. The narrower pipe was suspended within the wider one by 2 pins near the top and a spacing ring near the base. The original purpose of this arrangement was to form a thermal "break". This was to reduce cooling by liquid nitrogen contained in the polystyrene box, so that propane would not solidify. This proved to work over periods of 15 min or so but then it would solidify and require re-melting. Eventually a 5/16th x 1 inch 100 W cartridge heater, from Hedin Ltd, Raven Road, South Woodford, London E18 1HJ, was fitted in a copper block housed in the thermal break at the bottom of the inner pipe; this was applied to the inner tube but insulated from the outer tube. The coolants used are

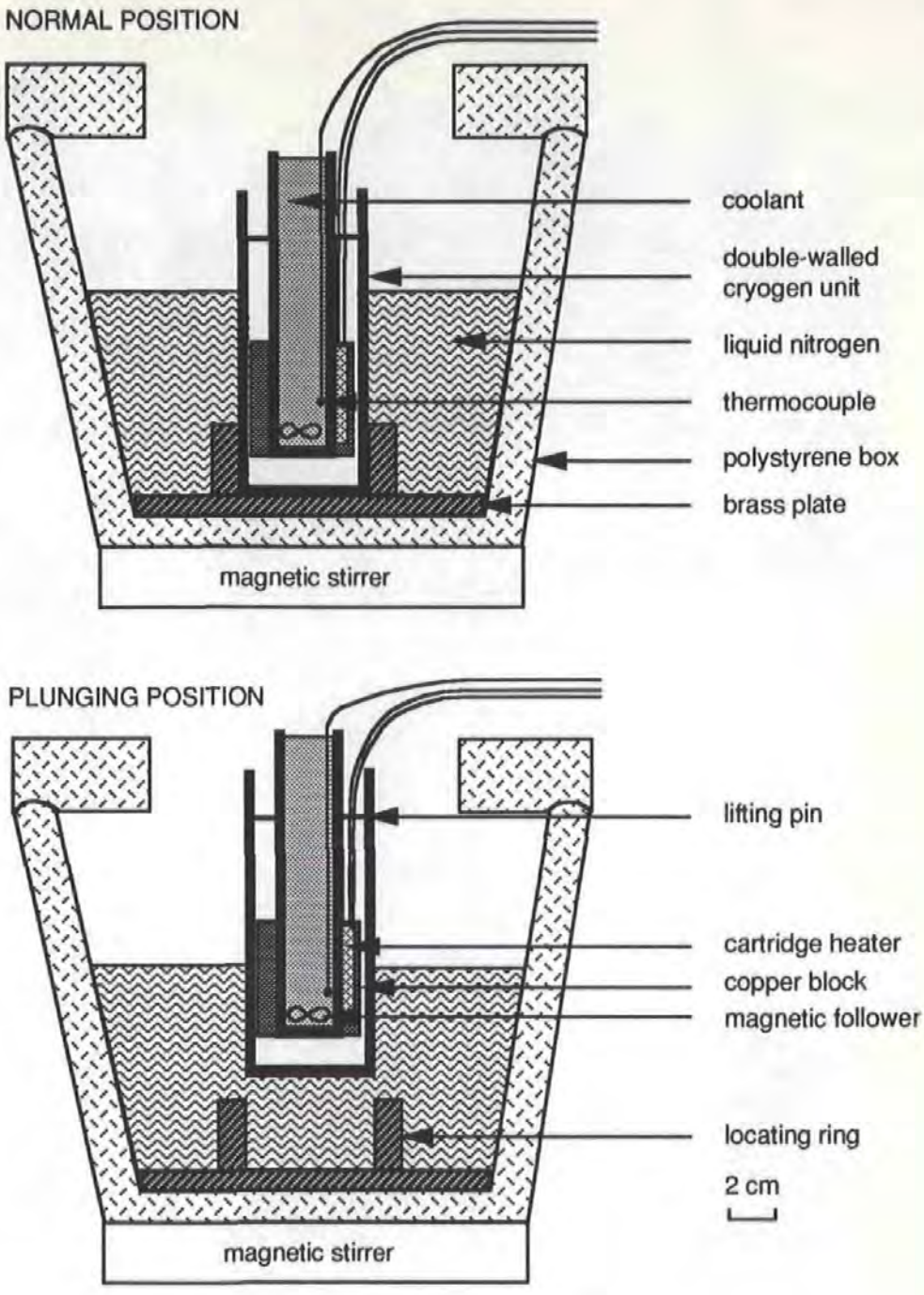

Figure 12. Benchtop plunge freezing device - I

In the normal position (upper diagram), the cryogen unit rests in the locating ring attached to the basal brass plate. Prior to freezing a specimen, the cryogen unit is raised (lower diagram). This minimises the prechilling of the specimen by exposure to a cold gas layer which can freeze the specimen relatively slowly before it reaches the cryogen.

described in Section 3.1 and their temperature was controlled as described in Section 3.4.

The thermal break area was not normally flooded with liquid nitrogen unless maximal cooling was required, as with a pentane-propane mixture or when propane gas was condensed, as in earlier experiments. A narrow-bore copper gas supply pipe was fitted for this purpose, which joined the inner coolant container at its base. It proved problematical in use and coolants were prepared as described in Section 3.3.

The gantry and plunge rod components are shown in Figure 13. The plunge rod had a side-arm with a vertical section which bore the scale of 10 mm high black and white bands for measuring plunge velocity (Sections 3.8 and 3.11). The bottom end of this side-arm rested on a metal block which was attached to the main gantry panel. Plunging was initiated by quickly removing a thin piece of card which was positioned under the end of vertical side-arm. The streamlined thermocouple (Figure 4) was taped to the bottom of the plunge-rod with Scotch tape. When coolants were ready for testing at a selected temperature, the cryogen unit was raised from its normal position by means of a wire handle. This brought the coolant almost out into room atmosphere and reduced the cold gas layer above the coolant which has been shown to prechill specimens and reduce cooling rates (Ryan & Purse, 1984).

Plunge velocity was set by tensioning the elastic which propelled the rod downwards into the coolant. Two velocities were used in this experiment, namely 1.12 and 2.25 ms^{-1}, and these were reproduced by clamping at predetermined marks on the elastic. These were chosen because 1.0 ms^{-1} was useful in modelling and is close to gravity values on

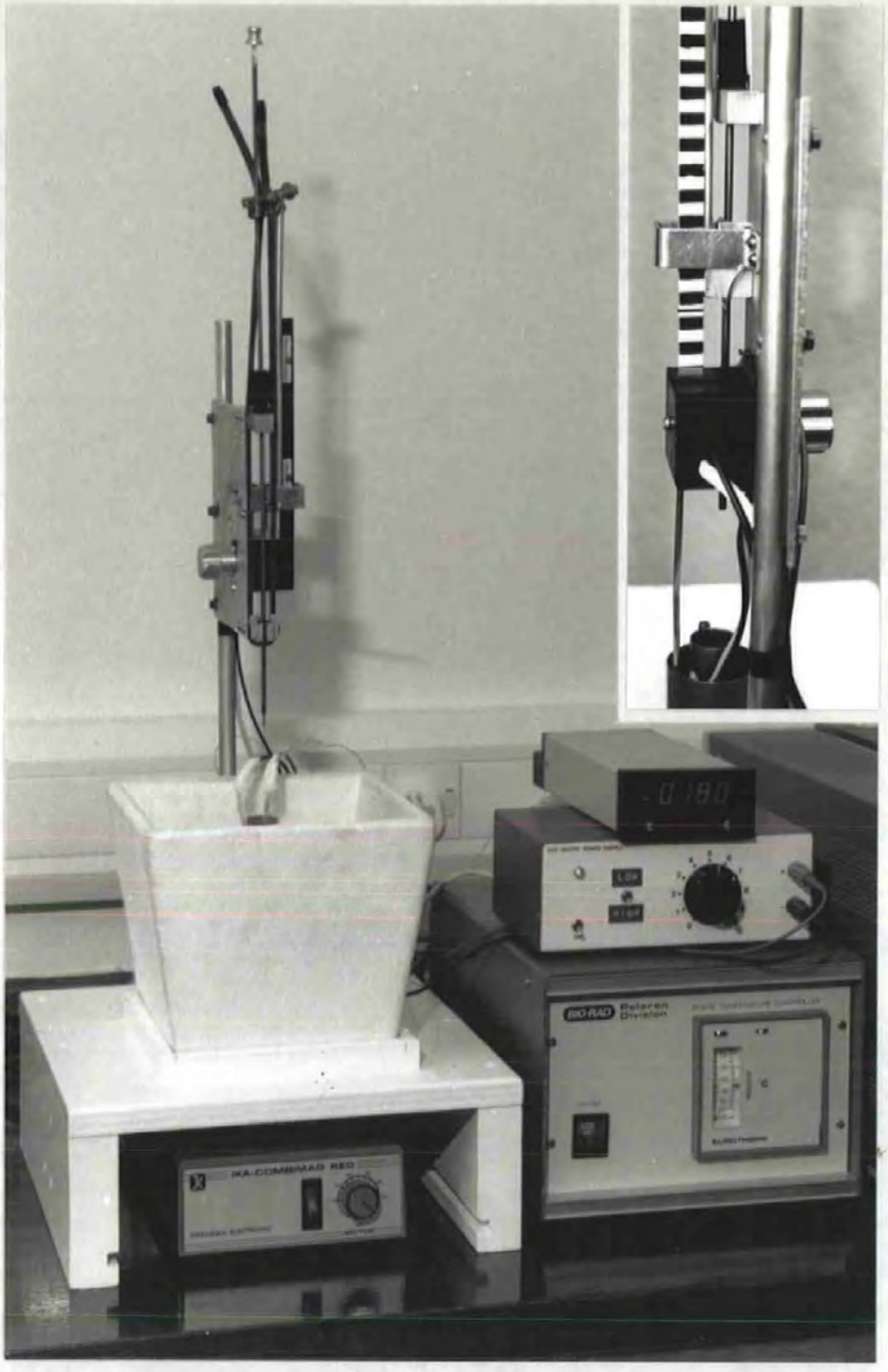

Figure 13. Benchtop plunge freezing device - II

The cooling chamber is shown with its lid removed. The thermocouple feedback control system is seen at the bottom right with the power supply above it. The digital thermometer gives a direct indication of coolant temperature. The inset shows the rear view of the motion sensor and plunge velocity scale, with the cryogen unit in the raised position.

this device and 2.25 ms^{-1} was near the upper velocity limit with regard to stretching the elastic.

The coolants were tested at 3 temperatures: (1) the lowest temperature maintainable, (2) 5 K above the melting point and (3) 25 K above the melting point.

4.4 Results

A typical experimental record from the stream-lined thermocouple is seen in Figure 14 and the cooling rates are seen in Table 2.

Ethane was cooled some 2 K below its melting point before it solidified and propane 4 K (the digital thermometer did not read fractions). The Freon 22 could not be cooled below its melting point without solidifying. The pentane-propane mixture cooled centrally to 1 K above liquid nitrogen temperature while peripherally 77 K could be measured. It became very viscous at these temperatures. The minimum temperatures could only be maintained for approximately 10 min before the coolants, other than the mixture, solidified.

4.5 Discussion

It is clear from the results that ethane produced the fastest cooling. It performed better than the other coolants even when it was warmed to 25 K above its melting point. The only exception to this was supercooled propane. The temperature of a coolant is important, as was illustrated by Costello (1980). He found that propane and Freon 22 cooled a thermocouple faster when they were near to the melting points than when they were up to 30 K above them.

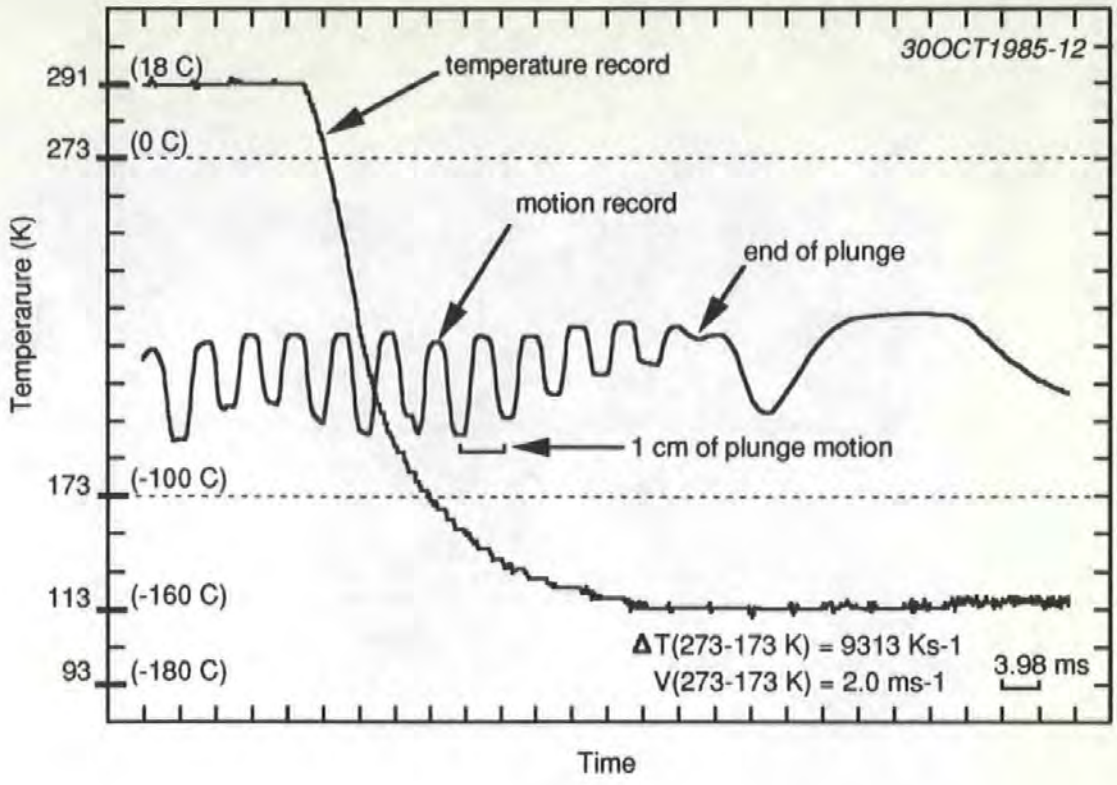

Figure 14. Typical record from the benchtop plunger

This record is from the experiments with a bare thermocouple which are described in this Section. The coolant was ethane which was maintained for this trial at 114 K (-159°C). The cooling rate (Δ T) and plunge velocity (V) over the temperature range 273-173 K are shown in the diagram. The figure was prepared by scanning the original XY plot on graph paper into a Macintosh computer, copying the records, graph framework and centimeter markers, and then erasing the graph lines for clarity. The electronic noise on the temperature record is useful because it shows that the signal was within the selected bandwidth of the recording system sensitivity and was not cut off at ambient or coolant temperature. The time scale is based on the 1 cm divisions of the original 28 x 19 cm graph paper, *note the 50% linear reduction.* The motion record shows that the thermocouple plunged approximately 80 mm into the coolant, before recoiling approximately 10 mm and then coming to rest.

Coolant	T_{mp} K (°C)	T K (°C)	Cooling rate (Ks^{-1}) 1.12 ms^{-1}	2.25 ms^{-1}
Ethane	89.7 (-183.3)	88 (-185)	12109 (517)	13038 (169)
		94 (-179)	10795 (116)	11634 (377)
		114 (-159)	8562 (299)	9978 (934)
Propane	83.3 (-189.7)	79 (-194)	8892 (350)	9787 (408)
		88 (-185)	7596 (586)	8695 (155)
		108 (-165)	6713 (242)	7652 (320)
3:1 Propane + isopentane	---------	78 (-195)	6886 (429)	8582 (192)
		98 (-175)	5973 (571)	7617 (425)
Freon 22	113.0 (-160.0)	113 (-160)	5959 (89)	6706 (162)
		118 (-155)	5540 (185)	6313 (55)
		138 (-135)	3895 (162)	4657 (406)
Nitrogen	63.1 (-209.9)	77 (-196)	569 (73)	731 (104)

Table 2. Cooling rates from a bare, streamlined thermocouple measured between 273 and 173 K (0/-100°C) while plunging in 130 mm depth of coolant: Mean (SD), n=3. Two velocities were tested. The melting point (T_{mp}) and temperature (T) of the coolants are indicated. The results for liquid nitrogen were extrapolated from the slope at 273 K as the thermocouple did not cool to 173 K under forced convection, during plunge motion. Modified, with permission, from Ryan *et al.* (1987), J. Microsc. 145, 89-96.

This ethane result is important, because previously it was assumed that propane was a better coolant for metal specimens (Bald, 1987). The reason for the assumption was that propane could be subcooled by 148 K (this being the difference between the boiling and melting points), whilst

ethane could only be subcooled by 95 K. Similarly, the colder mixture of pentane and propane (by 10-15 K) did not cool efficiently and actually cooled markedly less well than propane alone.

The importance of subcooling was previously ascribed to the fact that metal specimens cool so rapidly by conducting heat into coolants that they cause cryogens to form a thin insulating vapour layer at the specimen surface. This is because the coolant effectively boils during the initial stages of a plunge. Heat transfer is then impeded for a time interval which is significant to cryofixation. The assumption regarding the degree of subcooling may be correct in some circumstances and may explain the results of Rhebun (1972). He plunged a thermocouple soldered into a 1.4 mm diameter 2.75 mm long steel tube into various coolants, including propane and ethane. He reported a cooling rate of 5860 Ks^{-1} in propane and 4360 Ks^{-1} in ethane. It was improved in ethane when the tube was coated with a thin layer of dibutyl phthalate containing activated alumina.

The explanation for this seemingly unusual result is that the original specimen had high thermal conductivity. It would pass heat rapidly into the coolant and probably vapourise ethane more than propane, by film boiling. This process forms a complete layer of vapour around the specimen which insulates it somewhat from the coolant. The effect of coating with an insulator and a nucleating agent is that, initially, the specimen passes less heat into the coolant. Consequently, it does not form a vapour film but may still cause local vapourisation by nucleate boiling. Thus the coolant is in closer contact with the specimen and if the coating is not too thick then the resulting cooling efficiency can be improved.

The application of coatings was described by Cowley *et al.* (1961) and Luyet (1961), cited by Rhebun (1972, p.24 *et seq.*) for use with liquid nitrogen or other boiling coolants. The principle described by them is the same, except that liquid nitrogen is already a boiling liquid before the specimen is introduced into it; there is no subcooling.

The subject of subcooling was considered by Bald (1987) in his book, *Quantitative Cryofixation* (p.114), where he considers the results reported here and states:

> *"Ryan's experiments, however, show that the vapour film surrounding his 300 μm thermocouple was sufficiently thin to allow forced convection effects to override the advantages of a high degree of subcooling"*

Bald derived the following empirical expressions for the average surface heat transfer coefficients (in W cm^{-2} K^{-1}) over the range 273 to 173 K for:

ethane,	0.66 + 0.162V
propane,	0.46 + 0.154V
Freon 22,	0.46 + 0.185V, where V is plunge velocity in ms^{-1}.

These expressions were based on the following coefficients which he derived from the best cooling rates for each coolant (personal communication):

Coolant	T (K)	Measured ($Wcm^{-2}K^{-1}$) 1.12 ms^{-1}	2.25 ms^{-1}	Calculated ($Wcm^{-2}K^{-1}$) 1.12 ms^{-1}	2.25 ms^{-1}
Ethane	88	1.62	1.75	1.62	2.39
Propane	79	1.12	1.23	1.07	1.56
Freon 22	113	0.98	1.1	1.37	2.00

Table 3. Heat transfer coefficients derived from the best cooling rates for each coolant in Table 2 (these data were provided by W.B. Bald)

The agreements between measured and calculated heat transfer coefficients at 1.12 ms^{-1} are excellent for ethane and good for propane. At 2.25 ms^{-1} however, the agreement disappears. This concurs with observations by Robards & Crosby (1983), where entry velocity did not appreciably alter cooling rates in a thermocouple *during* the plunge motion. As Bald comments, these figures are a measure of the insulating effectiveness of the thin vapour film surrounding the thermocouple sample even in highly subcooled liquids.

Another possible source of discrepancy is the act of plunging through the coolant. A mean velocity of 2.25 ms^{-1} over the monitored cooling range (273 to 173 K) is achieved over a 40 mm "throw" to enter the coolant and this is a dramatic event. The entire plunge from rest to arrest, after approximately 150 mm of motion, is completed within a second. It is conceivable that cavitation occurs behind the rapidly plunging thermocouple, so that its entire surface is not flushed intimately by coolant.

The plunging device described here was little modified from that reported by Ryan & Purse (1985b) and the results in this Section were reported by Ryan *et al.* (1987). Copies of both papers are included as Appendices 4.1 and 4.2 to this thesis. The experiments were performed in late 1985 and 1986 and the data were communicated to W.B. Bald while he was compiling the book, *Quantitative Cryofixation.*

4.6 Conclusions

Of the coolants tested, ethane proved to be the most efficient for cooling the bare thermocouple. This constitutes a metal sample and is relevant to the cooling of metal-sandwiched specimens. These are used for freeze-fracture and freeze-etching purposes, where specimens are cooled either by plunging into coolant or by jetting coolant onto them. To date, ethane has not been reported as having been used for either method.

5 *Cooling in exposed, hydrated specimens*

5.1 Summary

This Section describes investigations into cooling in exposed, hydrated gelatin specimens which were constructed around thermocouples. There were essentially two experiments: (1) a specimen was plunged into a range of coolants and (2) a specimen was plunged more extensively into ethane and propane and comparisons were made with the cleaned, bare thermocouple and a similar specimen made from epoxy resin. Ethane was found to be more efficient for cooling the exposed, hydrated specimen than propane, isopentane-propane mixture, or Freon 22. High velocity plunging revealed ultimate cooling rates which were not limited by inadequate plunge depth and which reflected predicted cooling efficiencies.

5.2 Introduction

The plunge cooling apparatus used in this work was built as a much enlarged version of the earlier devices. There were several reasons for constructing such an apparatus. It was appreciated from earlier work that 0.5 mm^3 gelatin specimens did not cool under forced convection when plunged at 2 ms^{-1} into a 90 mm depth of coolant (Ryan & Purse, 1985a). Figure 5 in Ryan & Purse (1985a) is redrawn here as Figure 15, so as to form a link with the earlier work. In the earlier work the faster 0.5 mm^3 specimens were plunged, the sooner they reached plunge bottom (at increasingly warmer end-of-plunge temperatures) and the slower they cooled over the measured range, 273 to 173 K. The results underlined the concept for having an adequate minimum plunge depth.

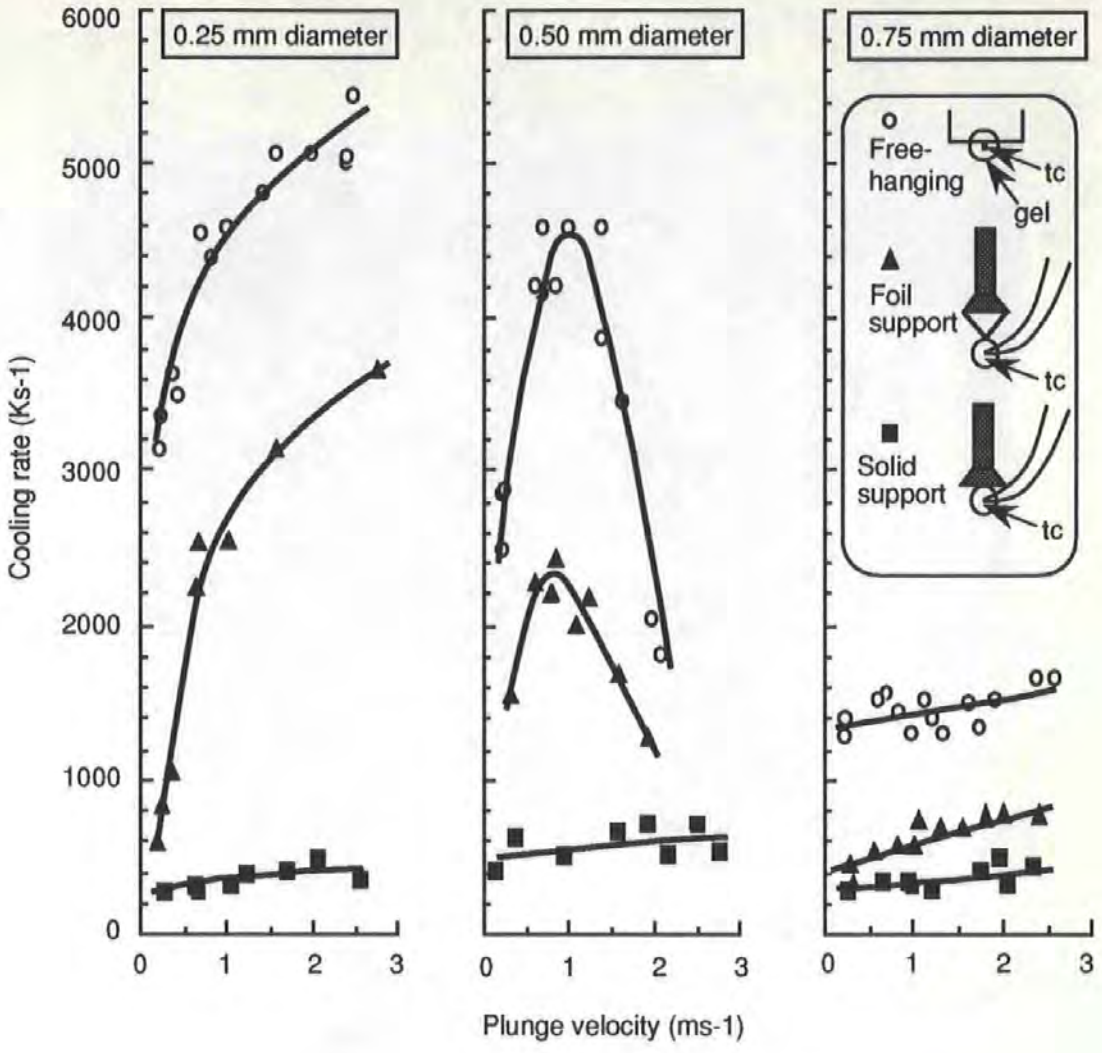

Figure 15. Determinants of cooling rates

This figure shows cooling rates from 3 sizes of hydrated gelatin specimen, each containing a thermocouple (tc). Each specimen was mounted in 3 ways: on a standard solid support, on a foil support and free-hanging with no support (as illustrated in the inset). The free-hanging and foil-mounted 0.25 mm diameter specimen showed increased cooling rates with increased plunge velocity, whereas the 0.50 mm diameter specimen showed slower cooling with increased plunge velocity. The coolant depth of 90 mm was a limiting factor. Increased plunge velocity appeared to have little effect on cooling in the 0.75 mm diameter specimen, motion records showed that it reached the bottom of the coolant before the thermocouple began to record cooling. Redrawn, with permission, from Ryan & Purse (1985a).

The objective in this work was to build as big a device as would fit in the room available, so as to maximise the potential for *maintaining* forced convective cooling. A corollary to this was that the device could incorporate a more powerful injection mechanism, thus maximising plunge velocity.

Preliminary experiments using fine thermocouples proved the difficulty of handling them, also that they were susceptible to the violent plunge experience, in that they were too delicate to withstand repeated high velocity plunges. It was decided, therefore, to take a seemingly self-defeating approach and use larger, butt-soldered 300 μm diameter wire thermocouples (as described in Sections 3.5 and 3.6). This proved successful, because the thermal events of interest were seen, through the motion record, to occur well before the specimens reached the end of the plunge.

5.3 Experimental Design

The cooling device was a 2.26 m high construction (Figure 16) and consisted of an upper section and a lower section which comprised the cooling chamber. The upper section could be swivelled away from the lower section and could be detached from it at a level just above the top of the cooling chamber.

The lower section was formed by a 730 x 220 diameter ABS plastic tube with a solvent-welded endplate. It was lined with strips of 23 mm thick polystyrene insulation and sealed internally by a tinplate liner tube. This retained the liquid nitrogen in a compartment which measured 690 deep x 140 diameter. Within the liner was an arrangement for locating the cryogen unit, which consisted of a round basal plate bearing a central locating ring, 3 upright rods and an upper locating ring to house the

Figure 16. Deep plunging device

The details of the construction of this device are given in Section 5.3 on page 124 *et seq.*

The upper gantry section can be swivelled with respect to the basal cooling chamber around the rear upright support. There is a joint which is located below the battery. The latter provides power for the velocity sensor.

For the purposes of the photograph, the supply lead to the heater and the output leads from the velocity sensor and from the thermocouple to the recording electronics are tied behind the device. The black and white scale for measuring plunge velocity has been rotated to face the camera. The 1.0 m long plunge rod (arrows) is screw clamped into the falling cross piece and extends to just below the battery.

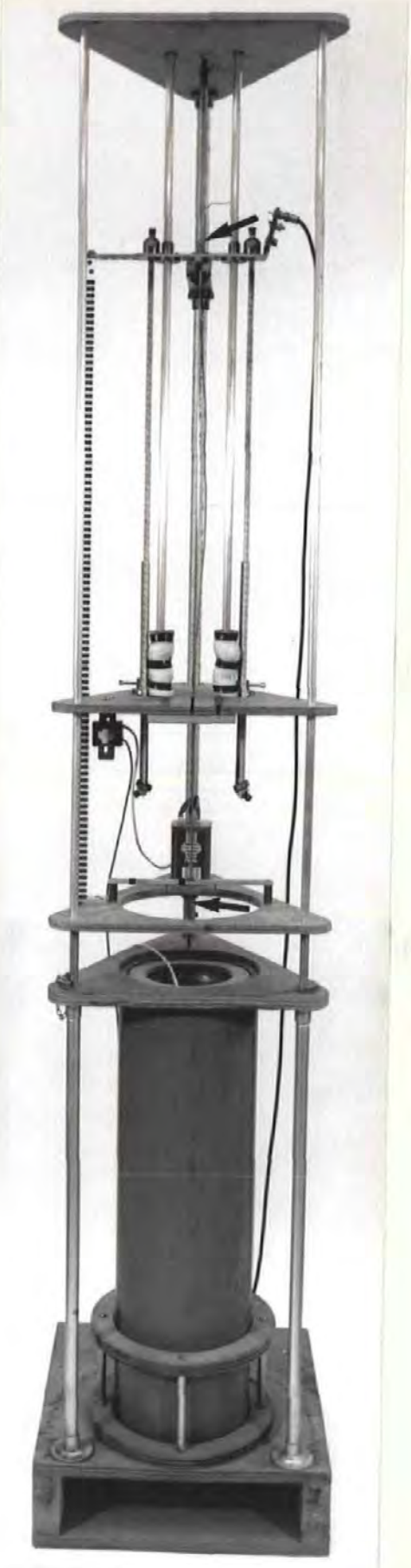

cryogen unit. The upper ring extended out to the inner liner and had spacious cutouts allowing access to the bottom of the outer container for topping up with liquid nitrogen. The whole section was encased and stabilised by a wooden framework which was tied together by upright metal rods.

The cryogen unit consisted of 2 concentric copper tubes with basal endcaps. These measured 610 deep by 50 mm diameter (outer tube) and 610 deep x 20 mm diameter (inner tube). The inner tube was removeable and suspended within the outer by a simple bayonet arrangement near the top. It had a narrow centering ring welded to it 45 mm above its base. A concentric copper block rested on this ring; it was slightly narrower than the outer tube so as not to make physical and thermal contact with it. The block housed a 100 W cartridge heater connected to the control system (Section 3.4).

The outer tube was fitted with an outer ring which was clamped near its upper end. Two pins protruded from the ring and these were used to raise the cryogen unit with the aid of a handle just prior to the moment of plunging. The handle hooked onto the cross-bar (see below) through which the plunge rod passed. The purpose of this was to obviate the cold gas layer above the coolant; the act of raising the cryogen unit brought the coolant meniscus up to the level of the top face of the cooling chamber.

The upper section was an extension in the framework described for the lower section. It housed twin upright aluminium rods which were the basis of the "guillotine" mechanism. A cross-piece slid vertically on the rods and was powered by 750 mm lengths of 8 mm elastic shock-cord (from C.R. Cload, Ships Chandlers, The Barbican, Plymouth). The cords were

attached to the bases of 2 vertical brass rods, with tension effected by sliding the rods downwards through ring fittings to positions at which the rods were fixed by pins through rods and housings. There were 6 settings for velocity, the highest of which corresponded to about 6 ms^{-1}. Higher velocities were possible with extra shock cord tied around the injector.

The falling cross-piece was arrested by foam rubber shock absorbers. The top end of the plunge rod was grub-screwed into the cross-piece. The rod was 1.0 m long and 2.95 mm outer diameter (wall thickness 0.325 mm). The bottom end slid through a centered bushing in a tied cross-bar. One end of the falling cross-piece bore 3 BNC terminals for thermocouple connection to the recording system. The opposite end of the cross-piece housed the upper end of a vertical scale which slid past the motion sensor. The sensor is shown in Figure 5.

The specimen consisted of a 125 μm thick layer of 20% gelatin around a thermocouple as described in Section 3.12 and illustrated in Figure 4. It was maintained in a water bath on the plunger until a few seconds before plunging, when the water was removed and the specimen drained with filter paper immediately before the plunge. As with all of the experiments, only a small number of plunges were performed in any one situation. This prolonged the life of the specimen and enabled results from only one specimen in each data set. Gel specimens or thermocouples which broke and were repaired did not subsequently produce comparable results.

5.4 Results

A typical plunge record from a gelatin specimen is shown in Figure 17 and the results from plunging a gelatin specimen at two velocities into a range of coolants are given in Table 4.

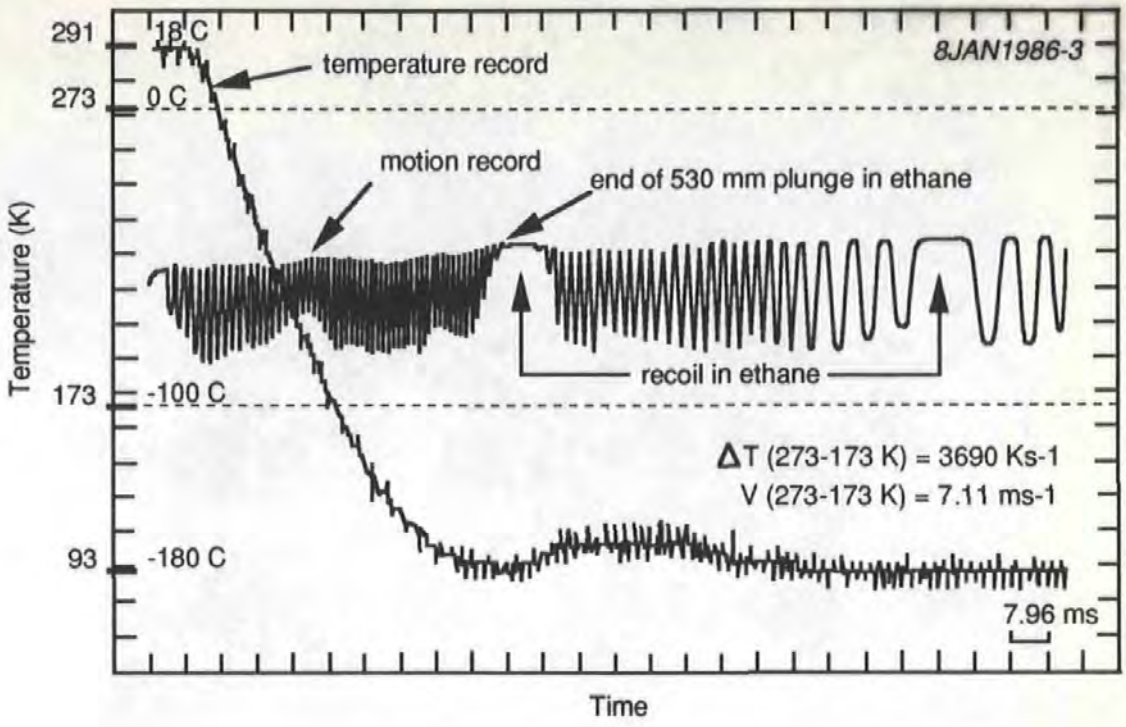

Figure 17. Typical record from the deep plunger

This record is from a high velocity plunge, at 7.11 ms^{-1}. The motion record shows that the 20% gelatin specimen recoiled approximately 270 mm in the coolant and that the specimen temperature rose to 110 K (-163 °C). This was because the specimen recoiled through coolant which had been slightly warmed by the plunge rod on which the specimen was mounted. The cooling rate (ΔT) and plunge velocity (V) over the temperature range 273-173 K are shown in the diagram. For details of the preparation of this figure see Figure 14.

Coolant	T	Cooling rate (Ks^{-1})	
	K (°C)	1.3 ms^{-1}	2.3 ms^{-1}
Ethane	94 (-179)	2103 (111)	2201 (54)
Propane	88 (-185)	1647 (138)	1858 (19)
Propane/Pentane	78 (-195)	1699 (89)	1806 (76)
Freon 22	118 (-155)	1138 (25)	1276 (82)

Table 4. Cooling rates from a 300 μm diameter thermocouple surrounded by a 125 μm thick layer of hydrated gelatin; mean (SD), n = 2. Cooling was performed under forced convection while plunging 0.55 m through the coolant. Modified, with permission, from Ryan *et al.* (1987), J. Microsc. 145, 89-96.

Results from a different but more or less identical specimen are given in Figure 18. This specimen was plunged into only 2 coolants, ethane and propane, but over a wide range of velocities. This figure also shows cooling rates from the thermocouple after the gelatin was removed and from a specimen of similar size and shape to the gelatin but made from epoxy resin.

The distances which are traveled while cooling from 273 to 173 K (0 to -100°C) were determined from the motion records and are shown in Figure 19.

Experiments were attempted with larger gelatin specimens but they tended to disintegrate. Possibly, because they cooled more slowly, they became honeycombed with crystal cavities after thawing which created

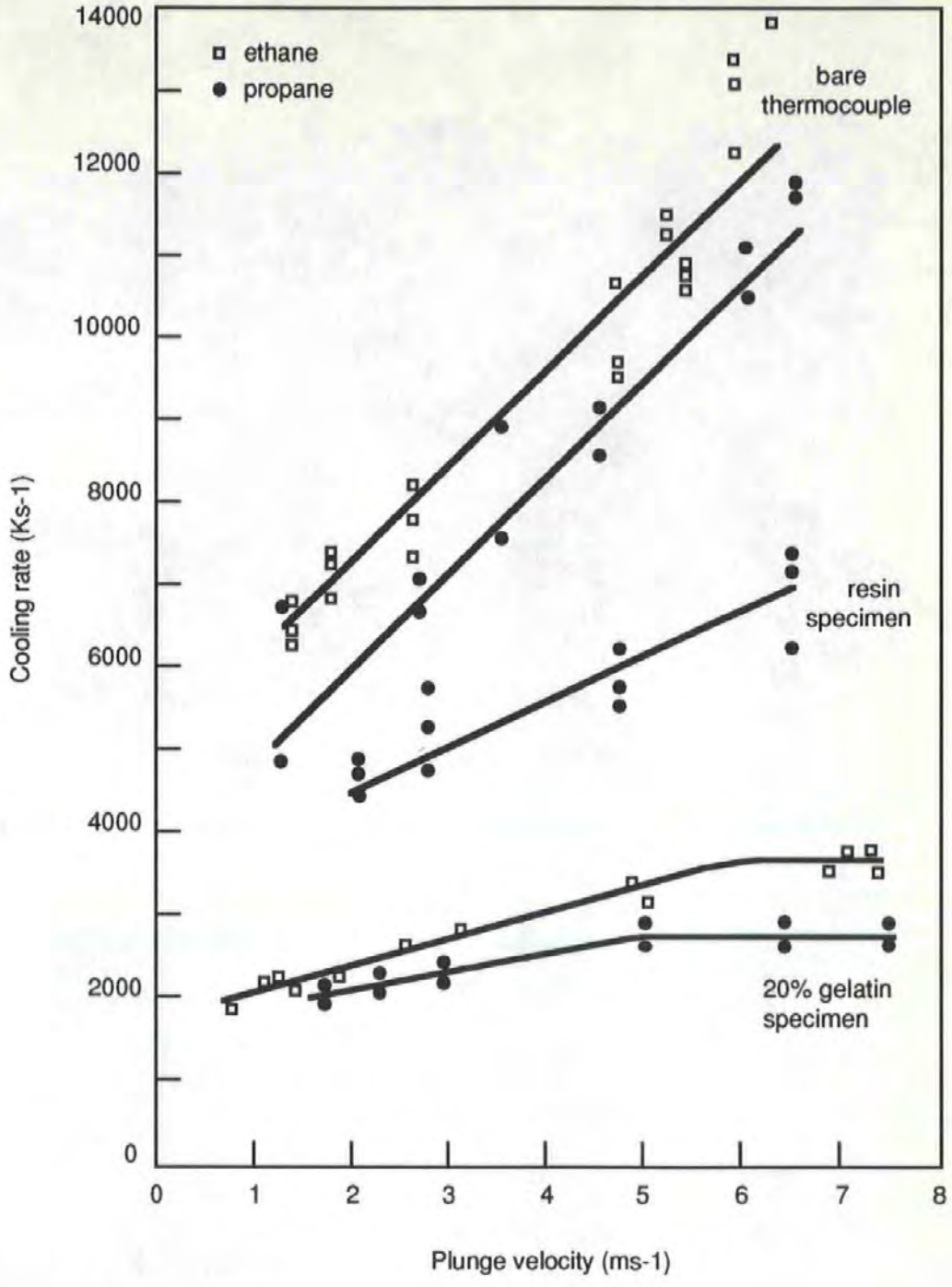

Figure 18. Cooling rates in exposed specimens

Cooling rates between 273-173 K in an exposed gelatin specimen of shell thickness 125 μm around the thermocouple, a resin specimen of similar size and the bare thermocouple plunged 550 mm into coolant. Note the uniform cooling rate in the gel specimen at plunge velocities above 5 ms^{-1} in propane and 6.5 ms^{-1} in ethane. Redrawn, with permission, from Ryan *et al.* (1987), J. Microsc. 145, 89-96.

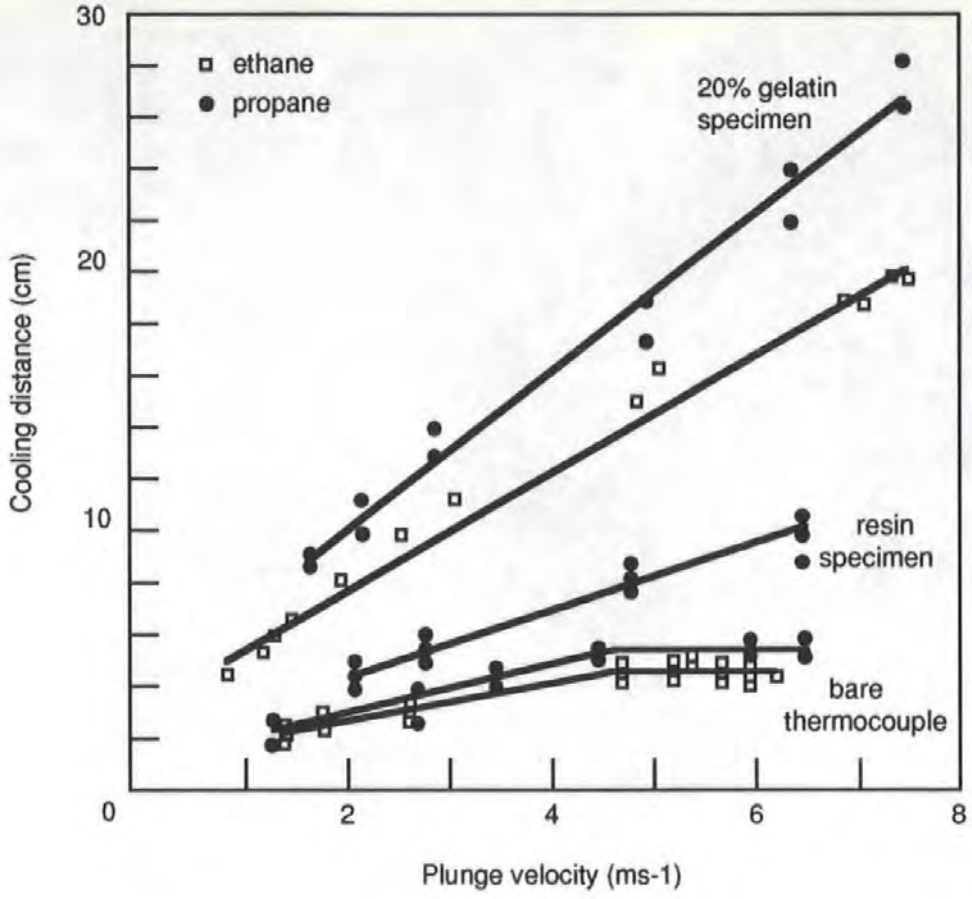

Figure 19. Cooling distances of exposed specimens

This figure shows the distances plunged by the gelatin and resin specimens and the bare thermocouple while cooling between 273 and 173 K. There is a general tendency to travel further with increased plunge velocity while cooling over the 273-173 K temperature range. Note the results for the bare thermocouple at high plunge velocities where this tendency is not followed. At plunge velocities greater than about 4.5 ms^{-1} the bare thermocouple cooled over a constant distance. This may indicate some suppression of the vapour film which forms by film boiling around the highly thermally conductive metal specimen. Redrawn, with permission, from Ryan *et al.* (1987), J. Microsc. 145, 89-96.

weaknesses, which may then have lead to crumbling during subsequent plunges. One specimen, 1.325 mm total diameter, plunged at 1.92 ms^{-1} in propane (88 K, -185°C) and 1.72 ms^{-1} in ethane (94 K, -179°C) cooled at 1112 and 1496 Ks^{-1} respectively.

5.5 Discussion

It can be seen in Table 4 that, of the range of coolants tested, the exposed hydrated specimen was cooled most efficiently by ethane. Propane and the propane-pentane mixture were markedly less efficient, although there was little to choose between the propane coolants. In fact, the fastest rates at 1.3 ms^{-1} were in the mixed coolant, but at the higher velocity propane alone had a faster mean cooling rate. From these initial results it was decided to test ethane and propane further.

The results presented in Figure 18 reveal several aspects of plunge cooling. The results at 1.3 ms^{-1} are very similar to those shown in Table 4. This indicates that the specimens and the technique are both consistent.

Both the hydrated specimen and the cleaned thermocouple cool faster in ethane than in propane. The specimens generally cool faster with increasing plunge velocity. However, certain critical velocities are reached beyond which the hydrated specimen does not cool any faster. This is clearly evident in the propane and indicated in the ethane. The fastest cooling rates of the gel specimen in ethane and in propane are 3650 and 2750 Ks^{-1} respectively, which ratio at 1.32:1.

Bald (1984) calculated that heat fluxes for an exposed 1.79 mm diameter water droplet during plunging in these coolants would be 97.4

Wcm^{-2} for ethane and 73.1 Wcm^{-2} for propane, which ratio at 1.33:1. This suggests that cooling is limited in this experiment by the predicted cooling efficiencies.

Ethane has been used previously in cryofixation. Dubochet & McDowall (1981) used it specifically to vitrify thin water films for cryo-TEM. Its advantage in this situation over propane is that, because of its higher vapour pressure, any cryogen remaining on the specimen when it is introduced into the microscope is more rapidly sublimed away in the vacuum (Dubochet *et al.*, 1988). Its higher vapour pressure is also useful in the cryoultramicrotomy situation, where residual cryogen can be removed from the specimen more easily (H. Sitte, personal communication). Silvester *et al.* (1982) tested ethane with thermocouples and found it the best of various coolants tested, although Bald (1984) calculated that their experiments were not performed under forced convection and thereby did not reveal the true potential for cryofixation.

The cleaned thermocouple showed increased cooling rates with increased plunge velocities. These rates cannot be compared with the results from bare thermocouple in Section 4, because the thermocouples are of different designs. As Figure 18 shows, there was considerable scatter in the results from each coolant. This was not the case for the results from the gel, which reflects perhaps the vagaries of vapour films around metal samples. The results show that ethane cools this bare thermocouple faster than propane, which supports the findings of Section 4.

A linear relationship between entry velocity and cooling rate was reported by Robards & Crosby (1983). They plunged a metal sandwich specimen 30 mm into propane at velocities of up to 6.35 ms^{-1}. The specimen

was 2 copper sheets, each 5 x 2 mm x 50 μm thick between which was soldered a 60 μm diameter thermocouple bead. It was probably thinner than the 300 μm diameter thermocouple used in the present investigation. The results of Robards & Crosby (1983) show that the cooling rate increased *after* the specimens came to rest at about 30 mm depth in the coolant, emphasising the Leidenfrost phenomenon and nucleate versus film boiling in subcooled fluids and differences between forced convection, transient conduction, and turbulent and laminar natural convection. The results obtained in the present work were definitely obtained during forced convective cooling. The thermocouple travelled a maximum of 50 mm while cooling from 273 to 173 K, while the overall plunge depth was from 410 to 420 mm.

An interesting phenomenon is seen in Figure 19, which shows the distances travelled by the specimen while cooling from 273 to 173 K. The gel specimen travelled increasingly further with increasing plunge velocity, which might be expected. At the highest velocities, of over 7 ms^{-1}, this specimen travelled 280 mm down through the coolant. The bare thermocouple shows unexpected results at high plunge velocities. The cooling rates between 4.5 to 6.5 ms^{-1} were obtained over a constant cooling distance. This did not represent the limit of thermocouple sensitivity because the cooling rates continued to increase with increasing plunge velocity. The phenomenon may signify the partial suppression of the insulating vapour film at the surface of the highly conductive metal sample and was discussed by Bald (1987) with respect to the results of Section 4.5.

Costello *et al.* (1984) report another linear relationship between plunge velocity and cooling rate in a thermocouple. They plunged a 40 μm

diameter bead 25 to 30 mm into propane, although the scatter in their Fig. 8(a) suggests little change with plunge velocity. A possible explanation for this is that the thermocouple may have been working close to the limits of its sensitivity (explained in Section 3.7). They also plunged a metal-sandwiched epoxy resin specimen and reported a fall-off in increased cooling at higher velocities of 1.5 to 2.5 ms^{-1}. This was probably because the specimen reached plunge-bottom at increasingly warmer low temperatures, as shown in gel specimens by Ryan & Purse (1985a).

In the present work, the resin specimen cooled approximately twice as fast as the gel specimen of similar size. Here, two factors are involved (1) thermal diffusivity and (2) latent heat release during the fusion of ice. Thermal diffusivity is the thermal conductivity divided by the product of density and heat capacity. For the resin used in this work, the thermal diffusivity was calculated as 0.151×10^{-6} m^2 s^{-1}. This was based on a thermal conductivity of 0.25 W m^{-1} K^{-1} allowing for air entrapment, a specific heat of 1375 J kg^{-1} K^{-1} and a specific gravity of 1200 kg m^{-3} (these properties were supplied by Mr. R. Searle, Ciba-Geigy Plastics Ltd., Duxford, Cambridge). The diffusivity of a fresh tissue (muscle) was calculated by Jones (1984) to be 0.107×10^{-6} m^2 s^{-1}. If the diffusivity of the gel is assumed to be similar to that of the tissue then it would cool more slowly than the resin.

The other factor is latent heat release. As the gel freezes then crystallisation probably occurs, releasing 334 Jg^{-1} at 273 K (equivalent to 80 cal at 0°C). This equates to a potential local temperature rise, antagonistic to the cooling in progress, of 80 degrees. Clearly, this must impede cooling in hydrated specimens! This aspect will be considered

further in Section 6. The results above were published by Ryan *et al.* (1987) and a copy of this report is included as Appendix 4.2 to this thesis.

5.6 Conclusions

1. Ethane was more efficient than propane for cooling exposed, hydrated specimens, which simulated exposed tissue specimens.

2. Increased plunge velocity produced increased cooling rates in all specimens.

3. During cooling under forced convection, or continuous plunge mode cooling, the rate of cooling in a hydrated specimen reached an absolute limit. The ultimate cooling rates in the two coolants reflected predicted heat fluxes.

4. Epoxy resin cooled much faster than hydrated specimens of similar size which indicated that a non-hydrated resin cannot model cooling in hydrated specimens where latent heat release can be an important factor.

5. Ethane was again seen to cool the cleaned thermocouple more efficiently than propane, supporting the findings in Section 4.

6 *Cooling in metal-sandwiched, hydrated specimens*

6.1 Summary

This Section describes the investigation of cooling rates, over several temperature ranges, in a hydrated specimen sandwiched between two thin copper sheets. The specimen is therefore a compound type which consists of both pure metal and hydrated gel and simulates a freeze-fracture specimen. Ethane was found to cool the specimen more efficiently than propane or Freon 22, which suggests that it should be tested in the jet-freezing technique. Arrested plunges induced slower cooling in a specimen than when it plunged to the full depth of the coolant, which demonstrated the need to maintain forced convective cooling. The effect of latent heat release during freezing, which is antagonistic to the cooling process, is discussed with regard to the shape of cooling curves from fine thermocouples which are surrounded by hydrated material. Plunge depths at which (1) the thermocouple registered 273 K (2) the specimen was calculated to have completed freezing and (3) the cooling curve entered a straight line phase, thereby reflecting conduction in a solid, are discussed. It is suggested that some other method of interpreting cooling curve phenomena may be more meaningful in the monitoring of specimen freezing rather than monitoring cooling over an arbitrary temperature range.

6.2 Introduction

The rapid freezing of specimens for freeze-fracture has generally used specimens mounted on, or encased in, some form of metal container. These have a variety of designs: from solid copper or gold discs of different geometries, sometimes involving central wells which may or may not be sandwiched together; hollow rivets of different designs for transverse or

longitudinal fracture, which may also be sandwiched together; to thin copper sheets designed for sandwiching specimens, which may also have central depressions. Robards & Sleytr (1985) surveyed holders in their Figure 6.2.

An important study of holders was carried out by Costello & Corless (1978) who plunged them 15 mm into a range of coolants at 0.49 ms^{-1}. Freons 12, 13 and 22, iso-pentane, propane, various mixtures of these, liquid nitrogen and slush nitrogen were tested. The conclusion was that propane was the most efficient coolant and that low specimen and specimen holder mass were of paramount importance in attaining high cooling rates.

The present study involves plunging the same hydrated gelatin specimen into different coolants over a range of plunge velocities. The specimen consisted of 20% gelatin-80% water which was contained in a cavity between two copper foils, in the centre of which was a miniature thermocouple.

6.3 Experimental Design

The freezing apparatus used was the deep plunger described in the previous Section. The specimen used in this experiment was a metal-sandwiched thermocouple surrounded by hydrated gelatin and was constructed as follows. The 1.0 m plunge-rod had to be removed from the big plunge cooling device. This entailed removing 2 screws which retained the cross-piece that the rod plunged through so that they merely rested in place, then the grub screw retaining the rod in the falling cross-piece was loosened enabling removal of the rod and bottom cross-piece.

The bottom end of the rod was then fitted with the 2-piece planchette assembly described in Section 3.13 and shown in Figure 10 and the removable planchette removed. Plastic catheters were slid along the rod so that about 10 mm protruded from the bottom end, near the planchette and about 150 mm protruded from the top. The long tails at the top were later taped to anchorages near the BNC connectors to the recording system so as to protect the delicate thermocouple wires from mechanical shock during plunging.

Narrow steel wires were passed along the plastic tubes to draw the 25 μm diameter thermocouple wires through. This, and the making of the thermocouple, are described in Section 3.6. The application of gelatin to make the final thermocouple-gel specimen is described in Section 3.13.

The specimen was plunged at velocities of up to 6 ms^{-1}, first into propane at 88 K (-185°C), then into Freon 22 at 118 K (-155°C), then into ethane at 93K (-180°C) and finally once more into propane as a control to confirm that similar cooling rates were obtained at the end of the experiment. This would indicate that the specimen was still intact and undamaged.

Cooling rates were measured at the centre of the specimen (Figure 20) over several temperature ranges: between ambient (291 K) and 273, 263, 253, 233 and 173 K (between 18 and 0, -10, -20, -40 and -100°C); also between the frequently used 273 and 173 K (0°C and -100°C) range. Distances plunged while cooling between 291 to 233 K (ambient to -40°C) were also measured.

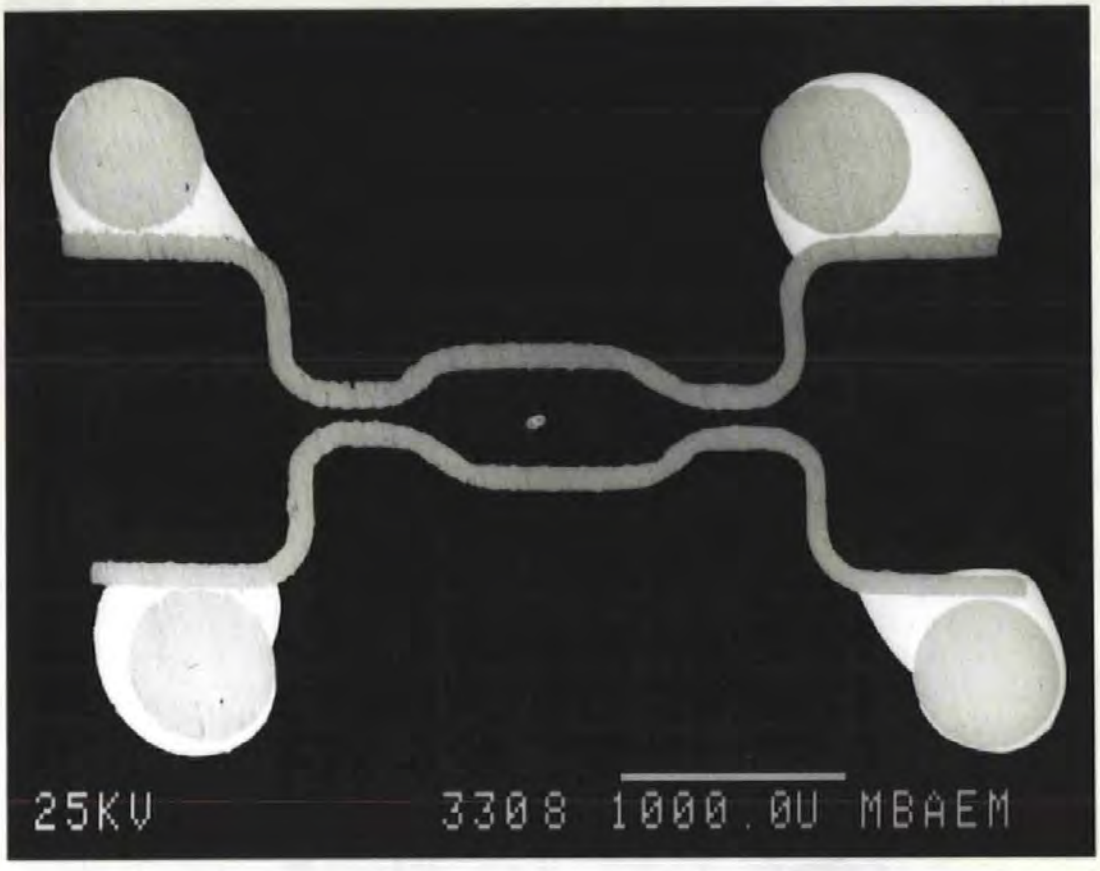

Figure 20. Back-scattered electron image of the sandwiched specimen

This image was obtained following the recording of the results shown in Figure 22. The specimen was embedded in resin and ground to show that the thermocouple junction was located at the centre of the specimen. The circular outlines at the corners are the support wires which are attached to the shaped planchettes by solder (which appears white). It was important that the thermocouple was centrally located and not displaced or touching a planchette. The cooling curves thus recorded the thermal history of the hydrated specimen with its latent heat phenomena. Scale bar: 1 mm.

The depths at which the recorded temperature reached 273 K (0°C) were measured and can be compared with theoretical minimum plunge depths to reach 273 K, which were calculated by Dr. W.B. Bald. A further plunge depth analysis was performed which measured the point at which the cooling curve entered a straight line phase.

Several duplicate specimens were plunged but most of these broke after only a few plunges, indicating the difficulty of handling such delicate, composite specimens in these experiments. One such specimen was plunged at 1.9 ms^{-1} into propane. It was allowed to plunge the normal depth of 420 mm as limited by the shock absorbers. It was then plunged again and arrested after plunging 40 mm in the coolant and then plunged again and arrested after 20 mm. The cooling rates were measured between 273 and 173 K.

Some results from early trials which were performed in a prototype bench-top plunger are included in this Section. They demonstrate the effect of latent heat release in hydrated specimens when they are frozen. During the trials a 0.5 mm^3 epoxy resin specimen and a 0.33 mm^3 gel specimen which both contained fine thermocouples were plunged at 1 ms^{-1} into a propane-pentane mixture, using a 90 mm deep prototype of the device described in Section 5. Other trials were performed by plunging a 0.25 mm^3 hydrated gelatin specimen on a fine thermocouple through a deep layer of cold nitrogen gas before it reached the cryogen.

6.4 Results

The specimen which was arrested after plunging only short distances into the propane gave the following cooling rates: arrested at 20

mm, 1051 Ks^{-1}; arrested at 40 mm, 1097 Ks^{-1}. When plunged over the whole depth of 420 mm the rate was 1538 Ks^{-1}.

A typical cooling curve from the main experiment is shown in Figure 21. The results from the main experiment, which measured cooling rates over different temperature ranges, are given in Figure 22.

The depths at which the recorded temperature reached 273 K (0°C) are given in Table 5.A and theoretical minimum plunge depths to reach 273 K are presented in Table 5.B. Depths at which cooling entered a straight line phase are shown in Table 5.C.

Cooling rates from 2 similar specimens to show (1) consistency of results with the same specimen over several trials and (2) comparison with another specimen are given in Table 6.

Results demonstrating latent heat release in hydrated gelatin specimens and its absence in a resin specimen are shown in Figures 23 and 24. Figure 25 shows depths plunged while cooling 273-173 K.

6.5 Discussion

The results from the specimen which was arrested after plunging only 20 and 40 mm into the coolant demonstrate very clearly the importance of plunge depth. If a specimen is plunged only a few mm into coolant and brought to a halt, it cools more slowly than if the plunge motion is continuous. In the specimen used here, the cooling rate increased by approximately 50% when the full coolant depth was used. This highlights the important concept of having sufficient coolant depth. This will be discussed further below, in relation to other results.

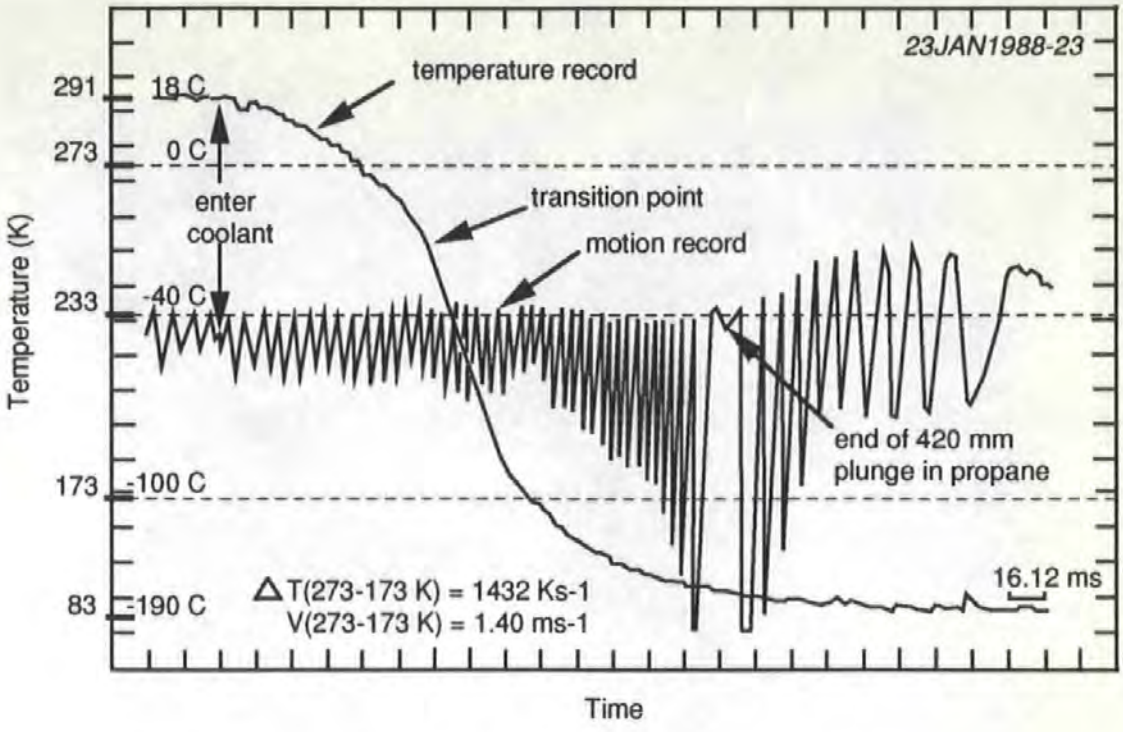

Figure 21. Typical record from the metal-sandwiched gel specimen

This figure shows the record of the final control plunge into propane and the cooling rate (ΔT) and plunge velocity (V) over the temperature range 273-173 K are shown in the diagram. A feature of the temperature record is that it commences with a rounded shoulder to the curve while the temperature falls to a transition point, after which there is a straight line relationship with plunge velocity over the central portion of the cooling curve. The rounded shoulder is probably due to the effect of latent heat release within the specimen which inhibits cooling. The transition point may indicate the end-point of the freezing of specimen water and may be a useful indicator. For details of the preparation of this figure see Figure 14. Redrawn, with permission, from Ryan *et al.* (1990), J. Microsc. 158, 365-378.

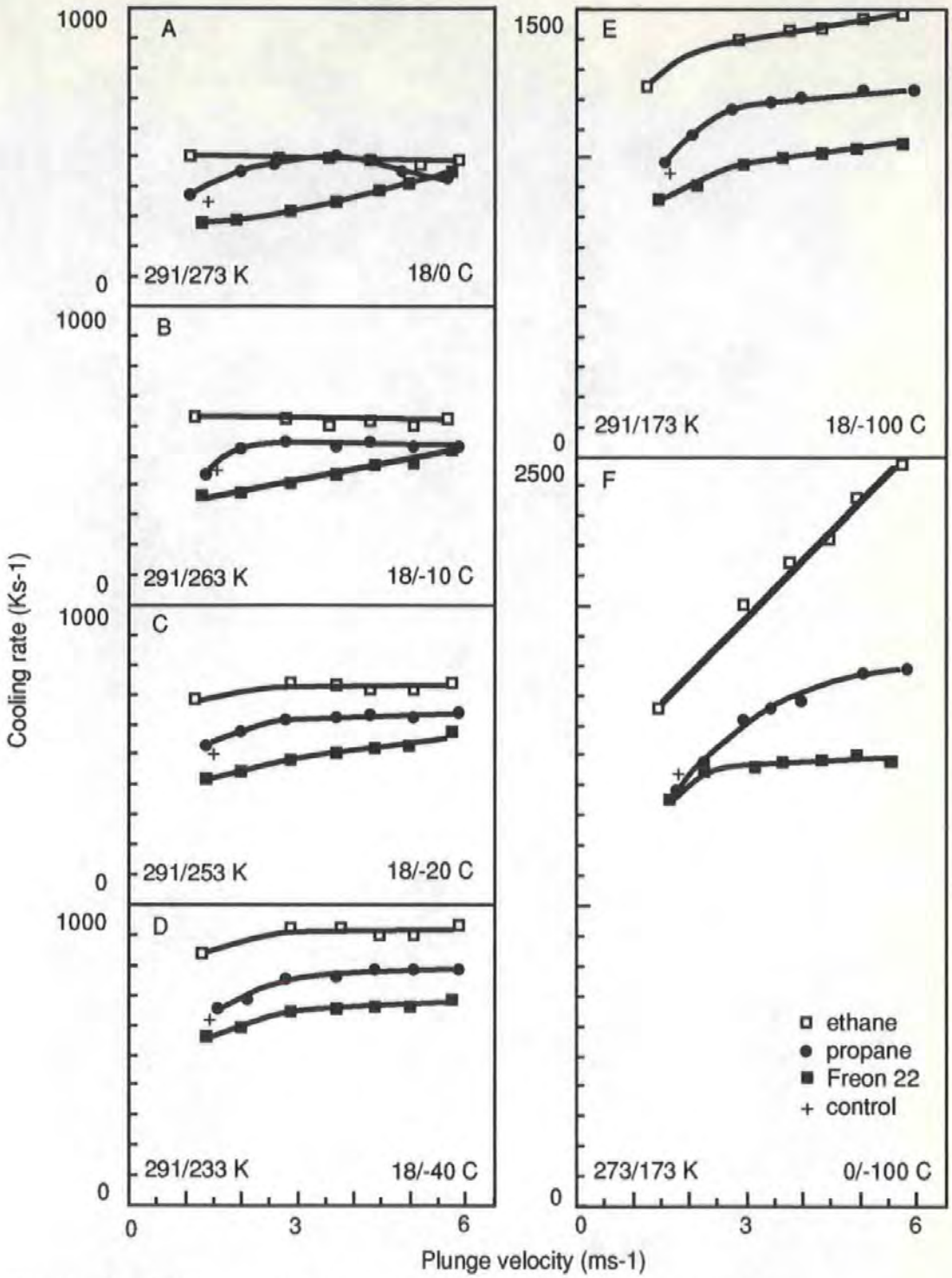

Figure 22. Cooling rates in the metal-sandwiched gel specimen

Cooling rates over different temperature ranges which are indicated in each sub-figure. Note that improvement in cooling rate with increased plunge velocity only occurs markedly when the monitoring range extends to 173 K, *i.e.*, well below the specimen freezing point. With permission from Ryan *et al.* (1990), J. Microsc. 158, 365-378.

Coolant	Plunge velocity (ms^{-1})					
(A)	1.2	2.0	3.5	4.3	5.1	5.7
Ethane	40	(70)	130	160	210	220
Propane	65	85	130	160	210	240
Freon 22	85	120	190	210	220	240
(B)	1.0	2.0	3.0	4.0	5.0	6.0
Ethane	68	124	171	212	250	282
Propane	79	140	189	232	270	300
Freon 22	86	148	198	240	280	312
(C)	1.3	2.1	3.7	4.4	5.1	5.8
Ethane	90	-----	230	285	320	340
Propane	140	175	280	310	370	390
Freon 22	140	190	290	370	----	----

Table 5. Measured and theoretical plunge depths (mm).

(A) Measured depths at which the specimen centre reached 273 K (0°C). The figure in parentheses is extrapolated from plotted data (n = 1).

(B) Theoretical minimum plunge depths at which the gelatin completely freezes. Calculated using equations (5.6) and (5.12) of Bald (1987) and ρ_1 = 0.86 gml^{-1}, K_1 = 0.015 $Wcm^{-1}K$ and L = 269 Jg^{-1} for 20% gelatin.

(C) Measured depths at which the cooling curve enters a straight line phase. The datum for ethane at 2.1 ms^{-1} is not feasible due to an imperfect record. At high velocities in Freon, the specimen hits the shock absorbers before the transition point is reached (n = 1). Modified, with permission, from Ryan *et al.* (1990), J. Microsc. 158, 365-378.

Specimen	Plunge velocity (ms^{-1})	Cooling rate (Ks^{-1})
1	2.40 ± 0.06 (n = 5)	929 ± 11 (n = 5)
	4.39 ± 0.10 (n = 5)	1139 ± 48 (n = 5)
2	2.15 ± 0.05 (n = 6)	890 ± 43 (n = 6)

Table 6. Plunge velocities and cooling rates from metal-sandwiched hydrated gelatin plunged into propane to show the consistency of results with one specimen and comparison with another. Reproduced with permission from Ryan *et al.* (1990), J. Microsc. 158, 365-378.

The cooling curve in Figure 21 shows the rounded shoulder at the beginning of cooling, which reflects the release of the latent heat of fusion of ice. This continues down to approximately 238 K (-35°C), after which the the curve enters a straight line phase which continues until the final cooldown. The significance of these phases will be discussed below.

The main results, in Figure 22, show a number of interesting features. Throughout, it can be seen that ethane produces the fastest cooling rates. In Figure 22.A there is a large deviation from linearity in the propane results. This may be caused by the release of latent heat at the centre of the specimen, which can reduce the measured cooling rate. It serves to highlight the errors which can arise when trying to monitor temperature changes near the specimen freezing point.

Over the various higher temperature ranges (those between ambient and 233 K/-40°C), increasing plunge velocity appears to make little difference to the cooling rate. It makes a difference when monitoring down

to 173 K (-100°C) and it is more pronounced when monitoring starts from 273 K (0°C), which is seen in Figure 22.F.

Clearly, this lower temperature range (273 to 173 K), which is frequently used for the measurement of cooling rates, covers the freezing of the specimen: it must be frozen when the temperature reaches 173 K. This means that the results reflect, in part, conduction through the solid phase which exists after freezing occurs. In other words, this temperature range straddles the freezing point and misses the potential to monitor the precise moment of freezing.

In most specimens, unless they are very small, true vitrification (as described in Section 2.6) is unlikely to occur. This means, therefore, that crystallisation will take place, with the release of the latent heat of fusion. As mentioned in the previous Section, this impedes the cooling process and manifests as a rounding of the shoulder early in the cooling curve (Silvester *et al.*, 1982). It is not seen in an epoxy resin specimen (0.5 mm^3, Rapid Araldite) constructed around fine thermocouples of the type used in this experiment. A dramatic illustration of this is seen in Figure 23. Unfortunately the specimens were of slightly different sizes, but the principle is seen in the shape of the cooling curve.

The resin specimen (Figure 23.A) shows prechilling over the first 20 mm in the cold gas layer that is still present after raising the cryogen unit in the prototype device. It then cools rapidly and soon enters a less steep, straight slope which is linear with velocity and levels off late in the process. The cooling rate (273-173 K) is 1724 Ks^{-1}. The smaller gel specimen (0.25 mm^3) shows no prechilling (Figure 23.B), then a rapid start

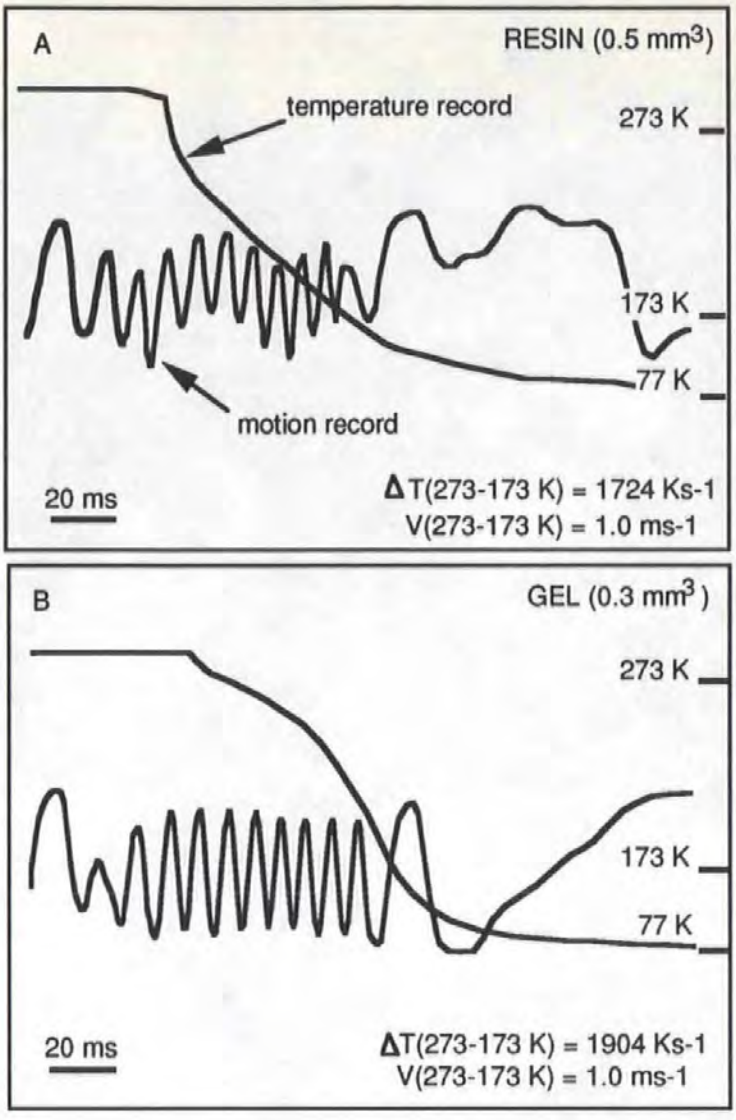

Figure 23. Cooling curves from a resin specimen and a gel specimen

A. The temperature record from the resin specimen showed a steep initial fall in temperature, followed by a straight line relationship with plunge velocity while plunge motion was maintained.

B. The hydrated gel specimen also showed a steep initial fall in temperature which rapidly entered a convex curved section in the cooling curve. This reflects rapid initial cooling to the freezing point, followed by the release of the latent heat of fusion of ice which impedes rapid cooling. Below 243 K (-30°C), the cooling rate increased again while plunge motion was maintained.

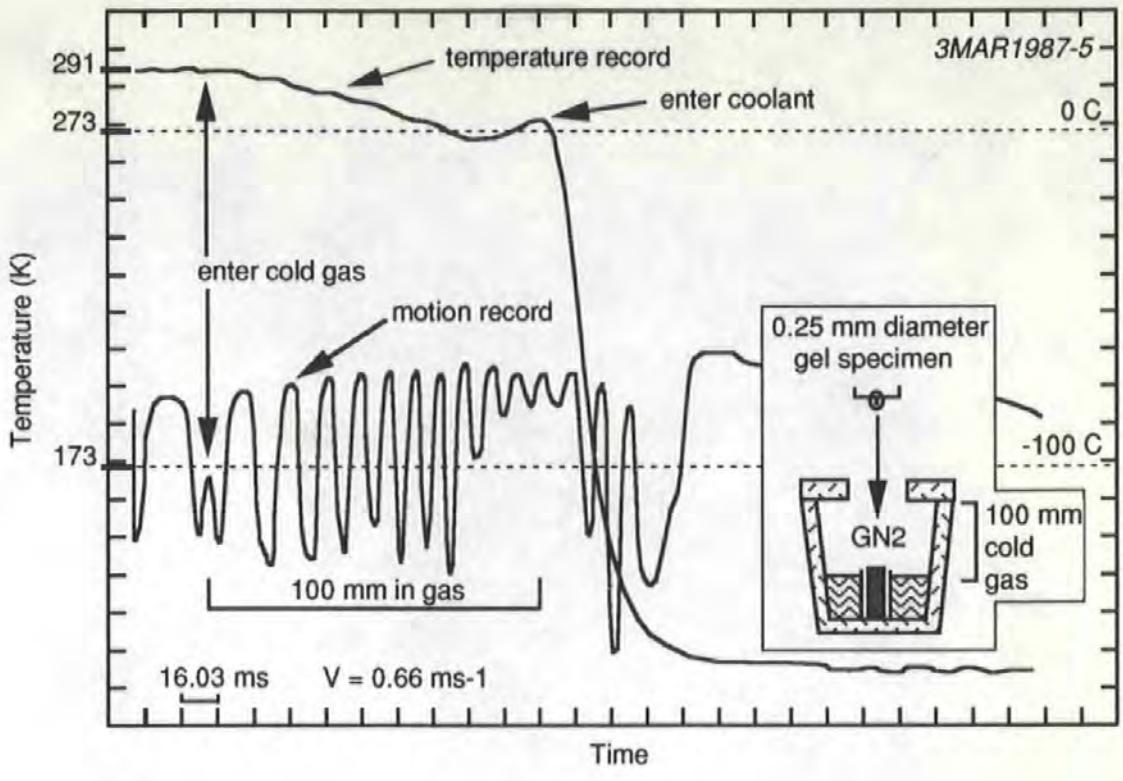

Figure 24. Rewarming of a specimen by latent heat during freezing

A free-hanging hydrated gel specimen was plunged by hand through a deep layer of cold gaseous nitrogen (GN_2), which originated from the boiling liquid nitrogen in the cooling chamber (inset). The specimen was cooled by the cold gas and its temperature fell slowly. While still plunging through the gas, the cooling curve underwent a reversal. This was probably due to latent heat being released faster during the freezing of the specimen than the cooling process could remove it. Thus, the specimen rewarmed and possibly thawed for a brief interval in this record. The specimen then reached the main coolant and cooled rapidly. The latent heat of fusion of ice is 334 Jg^{-1} at 273 K, or 80 calories. This is equivalent to a potential local rise in temperature of 80 degrees which explains the inhibitory effect of latent heat release on the cooling process. For details of the preparation of this figure see Figure 14.

to cooling (but less rapid than the resin) which enters a rounded shoulder phase that extends down to approximately 243 K (-30°C), where it then becomes almost linear with velocity. The cooling rate was 1904 Ks^{-1}.

The noted rounding of the slope is undoubtedly due to latent heat release. The process of heat release and specimen rewarming during freezing was predicted by Stephenson (1956) and illustrated in his Fig. 3 which was of computed cooling curves under different rates of heat removal (*i.e.* cooling). The phenomenal effect of specimen rewarming *while the specimen is undergoing cooling* is illustrated in a real specimen in Figure 24, which is from a slow plunge trial. The specimen passed through a deep layer of cold gas before reaching the coolant, so that cooling was very inefficient.

It is logical that prechilling the specimen to near freezing point before plunging would facilitate cryofixation; this is recommended by Bald (1987, p.130).

The distances plunged by the specimen while cooling are shown in Figure 25. They show that the cooling was carried out under forced convection (except in Freon 22 at the highest velocities). The figure shows that the sandwiched specimen (thicknesses - 0.1 mm copper; 0.415 mm gel; 0.1 mm copper) plunged up to 430 mm while cooling to 173 K (-100°C). This emphasises that coolant depth may need to be considerable to cool rapidly small bulk specimens such as tissue blocks.

The measured depths at which the centre of the specimen reached 273 K (Table 5.A) are less than the calculated depths (Table 5.B). This is attributed to supercooling, whereby the specimen reaches the melting

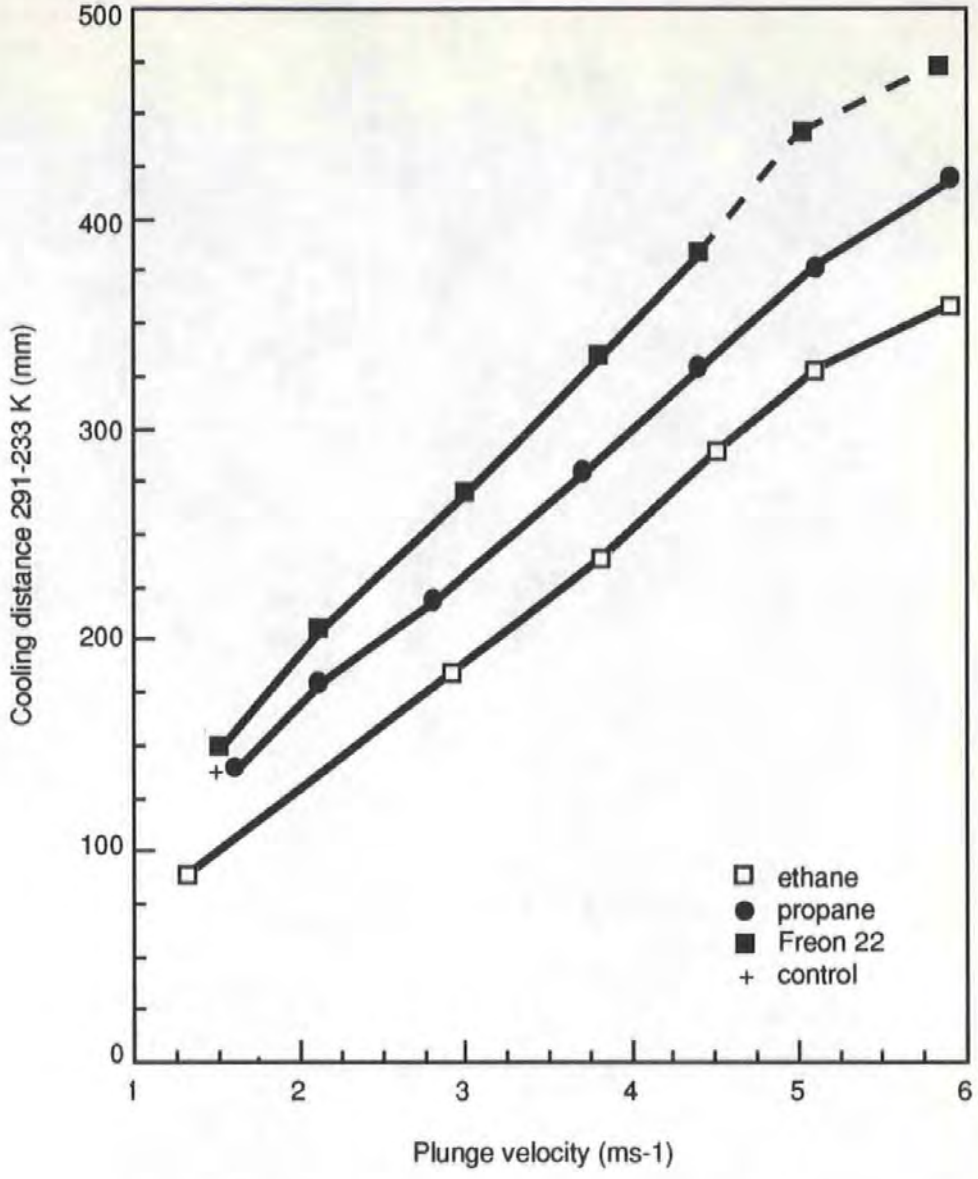

Figure 25. Cooling distances of the metal-sandwiched specimen

Cooling distances recorded simultaneously to the cooling rates shown in Figure 22.D. These are the depths plunged into the coolants while cooling from ambient (18°C) to 233 K (-40°C), at which temperature the specimens are assumed to be frozen. The specimens reached the plunge bottom at the highest plunge velocities in Freon 22 before cooling to 233 K and the data points were extrapolated from plotted data. The figure emphasises the minimum plunge depth concept if specimens are to be cooled by forced convection which is the most effective mode in plunge cooling. Redrawn, with permission, from Ryan *et al.* (1990), J. Microsc. 158, 365-378.

point of water but has not given up its latent heat of fusion. The calculated depths are *minimum* depths for complete freezing of the specimen. These are less than the depths presented in Table 5.C. This shows depths at which cooling entered a straight line phase and probably indicates conduction in the solid state. The transition point on the cooling curve thereby marks the end of latent heat release and the completion of freezing. These results may reflect *practical* depths for completely freezing the specimen. The results in Table 5.B assume perfect cooling technique, whereas it is easy after witnessing high velocity plunging to envisage that some cavitation must occur in the coolant. This implies non-ideal contact between the specimen and the coolant.

The temperatures at which the transition to a straight line occurred ranged irregularly in both ethane and propane between 234 and 239 K (-39 and -34°C) and between 242 and 250 K (-31 to -23°C) in Freon 22. This may indicate perhaps not that supercooling to these temperatures occurred, although that is not beyond reason, but that down to these temperatures latent heat was still being released.

There is little published work on cooling rates in plunged *hydrated* specimens with which these results can be compared. Stephenson (1956) published two cooling curves from pieces of liver which contained small thermocouples. He commented simply that the specimen which yielded the steeper curve contained smaller ice crystals. Costello & Corless (1978) tested the available freeze-fracture holders by filling them with 35% by weight of egg lecithin in water and plunging them under constant conditions into different coolants. They concluded that the fastest cooling was obtained in thin copper sandwiched specimens plunged into propane.

Costello *et al.* (1984) showed a cooling curve in their Fig. 7 from a 20-50 μm diameter miniature thermocouple embedded in 50% dilauryl lecithin which was clamped between 75 μm-thick copper sheets. The shape of the curve is almost identical to that from a similar sized epoxy resin specimen. They concluded that epoxy resin could be used to model cooling in hydrated specimens. They may have been correct regarding the thin specimen that they used, because it may have vitrified and thereby released no latent heat. With the larger specimens used here (Figures 23 and 24), this clearly is not the case.

The only other work which measured cooling rates in hydrated specimens was that of Van Venrooij *et al.* (1975). They measured cooling at different locations across a 2 mm diameter tubular specimen and correlated results to ice crystal size. They found that cooling was fastest in the centre of the specimen and slowest in the intermediate zone beneath the surface (discussed in Section 2.21, on cooling experiments). They related the results to measured crystal sizes in 1 mm diameter specimens after freeze-etch replication and found that the centre of the specimen contained the smallest crystals (referred to in Section 2.14, on modelling).

The results in this Section were reported by Ryan *et al.* (1990), except for the fine thermocouple trials which demonstrated the effects of latent heat release (Figures 23 and 24) and the results in Table 5.C.

6.6 Conclusions

1. Ethane produced faster cooling rates in the metal-sandwiched specimen than propane and Freon 22. This suggests that it should be tested in the jet-cooling method, which normally uses propane.

2. A specimen plunged only 20 or 40 mm into coolant, cools more slowly than when it is allowed to plunge 430 mm. This demonstrates the importance of maintaining forced convective cooling and having sufficient depth of coolant.

3. The temperature range over which cooling is monitored is important in thermocouple experiments. Different ranges yield different information. In this experiment it appears that the cooling rate in the metal-sandwiched specimen is not increased with increased plunge velocity at temperatures down to 233 K (-40°C).

4. Latent heat release in the freezing of hydrated specimens is demonstrably antagonistic to the cooling process.

5. The depths at which the specimen centre reached 273 K were measured at up to 240 mm. The *minimum* depths plunged while the specimen was completly frozen were calculated as up to 312 mm. A transition point to a straight line phase in the cooling curve, interpreted as marking the end of freezing and latent heat release, gave depths in excess of 390 mm.

6. Some other method of interpreting cooling curve phenomena may be more meaningful in the monitoring of specimen freezing, rather than simply monitoring an arbitrary temperature range.

7 *Crystal growth in metal-sandwiched, hydrated specimens*

7.1 Summary

This Section describes results from the analysis of ice crystal formation in cryofixed, freeze-substituted specimens. The specimens were either hydrated gelatin or fresh blood cells. They were sandwiched in copper, freeze-fracture planchettes which formed constant-sized samples, for meaningful analysis. Ethane was found to produce a smaller mean ice profile size than propane and Freon 22 produced the largest. Some of the results were in good agreement with predictions from modelling. Smaller ice profiles were more regularly seen in the centre of specimens than in subsurface zones.

7.2 Introduction

Coolant efficiency has long been tested by thermocouple thermometry (reviewed in Section 2.21), UV oscillography (Bald & Robards, 1978) and cooling rate metering (Robards, 1980), with the emphasis on thermocouple thermometry.

The experiments can be simple, where a bare thermocouple is cooled, or sophisticated, where a carefully constructed and maintained hydrated specimen is used. For cryofixation purposes, results from hydrated specimens are clearly more relevant. The previous Section shows that cooling rates give only a vague overview of specimen thermal history and that closer examination of the cooling curve may be more revealing.

These approaches are, however, only a view reflected by the thermocouple, which monitors one region within a specimen. It is a useful

indicator to coolant efficiency, which is linked by Stephenson (1956) to the real indicator of cooling efficiency, namely, resultant ice crystal size.

Since Stephenson's work, there have been surprisingly few systematic ice crystal studies from the viewpoint of cryofixation. Van Venrooij *et al.* (1975) analysed crystal size across a 1.0 mm diameter tubular specimen of 20% glycerol, using freeze-fracture replicas. They concluded that crystal size depended on position in the specimen and that good freezing could occur centrally.

Schwabe & Teraccio (1980) examined crystal formation in the surface layers of sliced kidney specimens after plunging into 5 coolants (stirred and unstirred), into flowing streams of liquid helium or liquid nitrogen and onto cold copper or mercury surfaces. It was concluded that copper was the most efficient coolant followed by propane.

Handley *et al.* (1981) illustrated results at the surface of blood samples in titanium foil envelopes after plunging at different velocities (1.25 and 10 ms^{-1}) into Freon 22. It was concluded that high immersion velocity reduced crystal development.

Elder *et al.* (1982) mounted muscle and liver samples on metal stubs and quenched them in a range of coolants. They concluded, among other aspects, that propane gave the best results and that there was a gradation to a zone of large ice crystals at some variable depth below the sample surface.

The paucity of studies on crystals reflects the technical difficulties that are involved in making the necessary measurements. Robards (1980)

noted that measuring cooling rates was an invaluable aid but appreciated that, ultimately, it was the size of the crystals that mattered, saying:

> *"The evaluation of cooling efficiency by measuring ice crystal dimensions, whatever method of electron microscopy is used, is necessarily an extremely time-consuming and tedious technique that is open to criticisms relating to the difficulties of ensuring comparable sampling procedures and accumulating statistically significant data".*

This study examined crystal size and distribution in specimens of constant-size which were plunge-frozen at different velocities and into different coolants. The results are compared with predictions modelled by Dr. W.B. Bald.

7.3 Experimental Design

The specimens were 20% gelatin and fresh blood from the flounder, *Platichthys flesus* (Section 3.14), mounted in copper planchettes (Section 3.13) and plunged into ethane, propane and Freon 22. Each coolant was maintained at 5 K above its melting point in the deep plunger (Section 5.3). Control samples of blood were plunged into liquid nitrogen. Some samples were plunged into ethane in the bench-top plunger (Section 4). After freezing, the specimens were freeze-substituted (Section 3.15), sectioned and examined by transmission electron microscopy (Section 3.16). Photographs were taken of erythrocyte cytoplasm along transects across the centre zone of specimens; at the surface, 10 μm below the surface and at 20 μm-intervals from the surface. Prints were made at a magnification of 122000, so that 1 mm represented 8.1 nm. Crystal dendrite diameter was measured with a ruler, as indicated in Figure 26.

7.4 Results

A typical field of view in a gelatin specimen is shown in Figure 26, where the branching, dendritic forms of the ice crystal cavities left after freeze-substitution are evident. Plotted data from this type of photograph are shown in Figure 27, as are the predicted dimensions.

Varied appearances of frozen blood cells are seen in Figures 28-31 and plotted measurements across specimens are presented in Figure 32. A summary of the experimental and modelling results for blood are given in Table 7.

7.5 Discussion

Critique of method

There are several sources of possible experimental error:

(1) *Freezing:* turbulence or cavitation effects at high plunge velocities due to specimen shape or plunge-rod whiplash, friction effects in the plunger and noise or instability in the electronics.

(2) *Physiology of the fish:* stress effects on the fish over a three-hour period of blood sampling on oxygen and carbon dioxide tensions and precise water content of the red blood cells.

(3) *Dimensions of the cells:* shrinkage during freeze-substitution and resin embedment, compression during sectioning and subsequent re-expansion by solvent vapour.

(4) *Photography:* accuracy of position in the specimen by using the TEM viewing screen calibrated to give field width measurement, selection of a cell at a given depth regarding ice crystal appearance, calibration of TEM and photographic magnifications.

(5) *Photographic interpretation:* contrast and grey levels, crystal orientation and graze effects, section thickness and overlay effects,

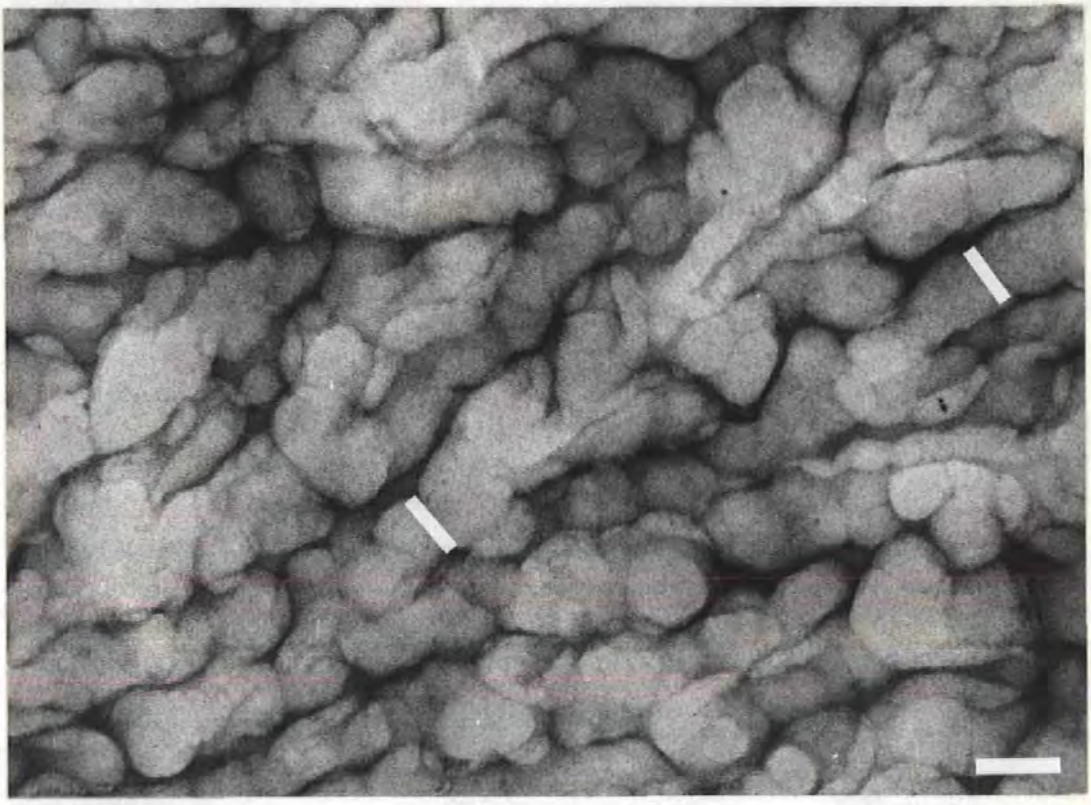

Figure 26. Typical appearance of a freeze-substituted gel specimen

This figure shows the branching nature of the cavity which remains after the frozen specimen water was removed by freeze-substitution (see Section 3.15 for details). The specimen was 20% gelatin in water and it was plunged into propane at 4.3 ms^{-1}. The field was 40 μm from the surface. The cooling front travelled from the bottom left to the top right of the field. Numerous overlap and graze effects can be observed and these make measurement of the profile diameters difficult. The criterion in this work was to measure just below where the profile branched. This is indicated by the bars which mark 75 nm diameter profiles, which was the figure derived from this field. Scale bar: 100 nm.

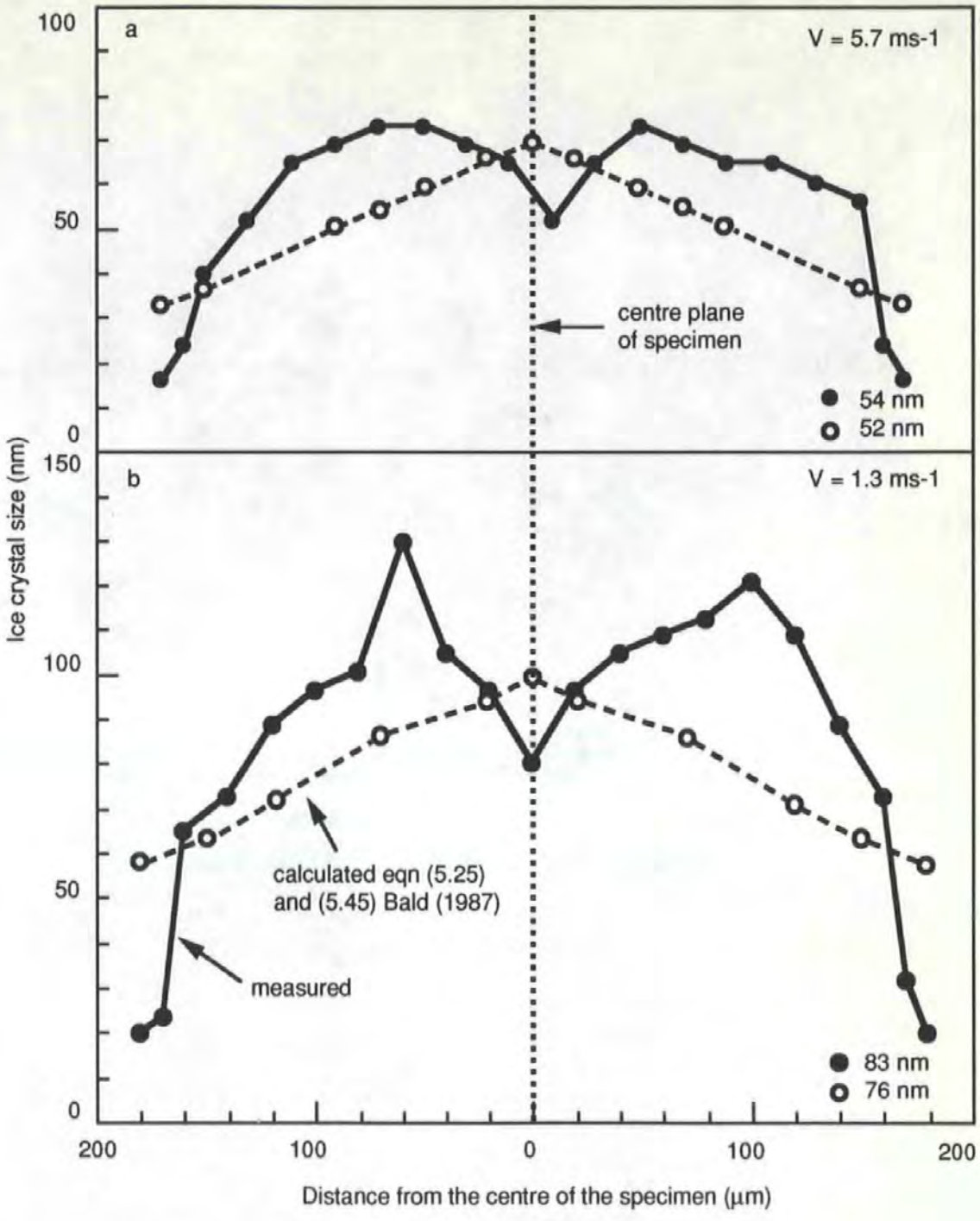

Figure 27. Transects of ice profile size across gel specimens

Measured and modelled ice profile sizes across metal-sandwiched 20% gel specimens freeze-substituted after plunging 420 mm into propane at 5.7 and 1.3 ms^{-1}. The mean ice profile size is shown at the right of each figure. Note the apparent agreement of the means between practice and theory, particularly in the upper figure. Reproduced, with permission, from Ryan *et al.* (1990), J. Microsc. 158, 365-378.

Coolant	Plunge Velocity (ms^{-1})	Ice crystal size (nm)	
		Measured	Theoretical
Ethane	6	38 ± 1	43
	3	42 ± 1	54
	1.3	46 ± 2	65
Propane	6	42 ± 2	46
	4.3	49 ± 2	53
	1.3	72 ± 1	73
Freon 22	6	48 ± 2	49
	3	55 ± 1	65
	1.3	76 ± 1	82

Table 7. Comparison between measured and theoretical mean ice crystal sizes in erythrocyte cytoplasm across Flounder blood samples frozen by plunging 410-430 mm into different coolants. Each measurement is derived from two analyses on the same photograph. Assumed properties for blood in theoretical calculations were U = 50 mm s^{-1} (ice crystal growth velocity), L = 250 J g^{-1} (latent heat of fusion), r* = 3 nm (radius of critical nucleus), ρ_1 = 0.98 g ml^{-1} (density of specimen frozen phase) and K_1 = 0.019 W cm^{-1} K (thermal conductivity of the frozen specimen). Modified, with permission, from Ryan *et al.* (1990), J. Microsc. 158, 365-378.

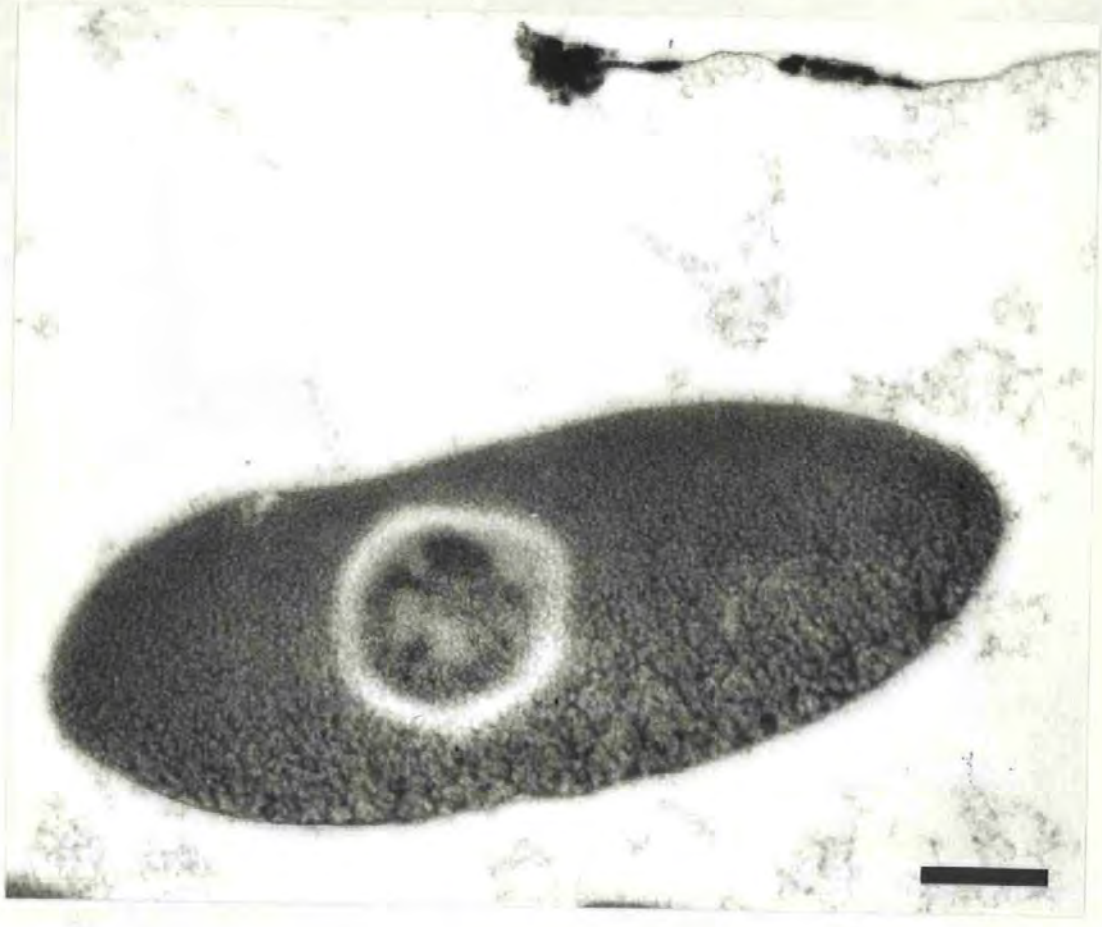

Figure 28. Appearance of freeze-substituted blood cells - I

Flounder *(Platichthys flesus)* red blood cell located at the surface of a 350 μm-thick sandwiched specimen which was plunged 430 mm deep in liquid ethane at 5.7 ms^{-1}. The surface of the specimen is marked at the top of the micrograph by osmium deposit from the freeze-substitution process. The gradation in ice profile size can be seen across the blood cell. The cooling front passed from the top of the micrograph to the bottom and the ice profiles in the cell increase in size towards the bottom of the photograph. Scale bar: 1 μm. Reproduced, with permission, from Ryan *et al.* (1990), J. Microsc. 158, 365-378.

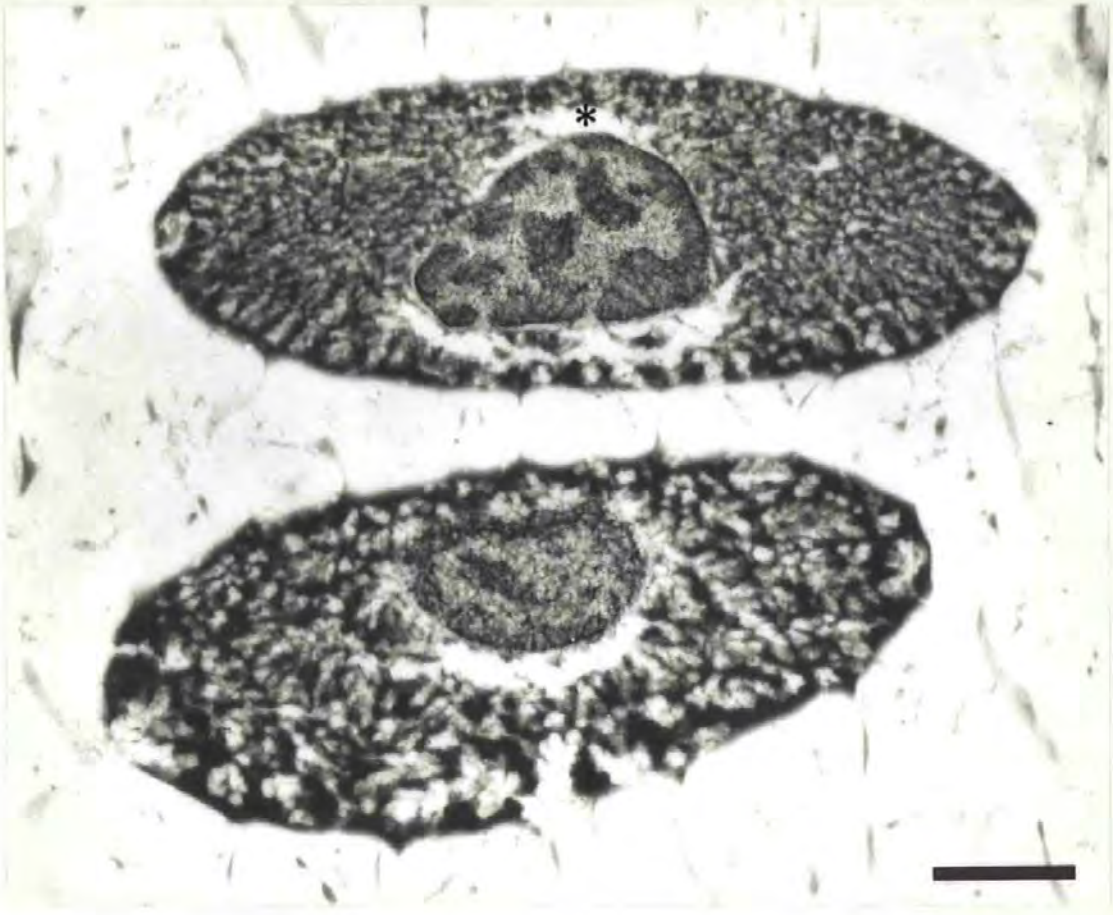

Figure 29. Appearance of freeze-substituted blood cells - II

Flounder red blood cells located halfway between the surface and the centre of a 350 μm thick sandwiched specimen plunged 430 mm deep in liquid propane at 5.9 ms^{-1}. The cooling front approached from the top of the figure and the ice profiles increase in size along this axis. The crystal dendrites of the extracellular medium also reflect this direction of cooling. Note that the possible nucleation point in the top cell is probably at the uppermost edge of the cell (asterisk) and that the dendrites radiate down into the cell from this point. This can also be seen less clearly in the lower cell. Note that the nucleus, which is normally taken to be a sensitive indicator of freezing damage, is less damaged than the erythrocyte cytoplasm. Scale bar: 1 μm. Reproduced, with permission, from Ryan *et al.* (1990), J. Microsc. 158, 365-378.

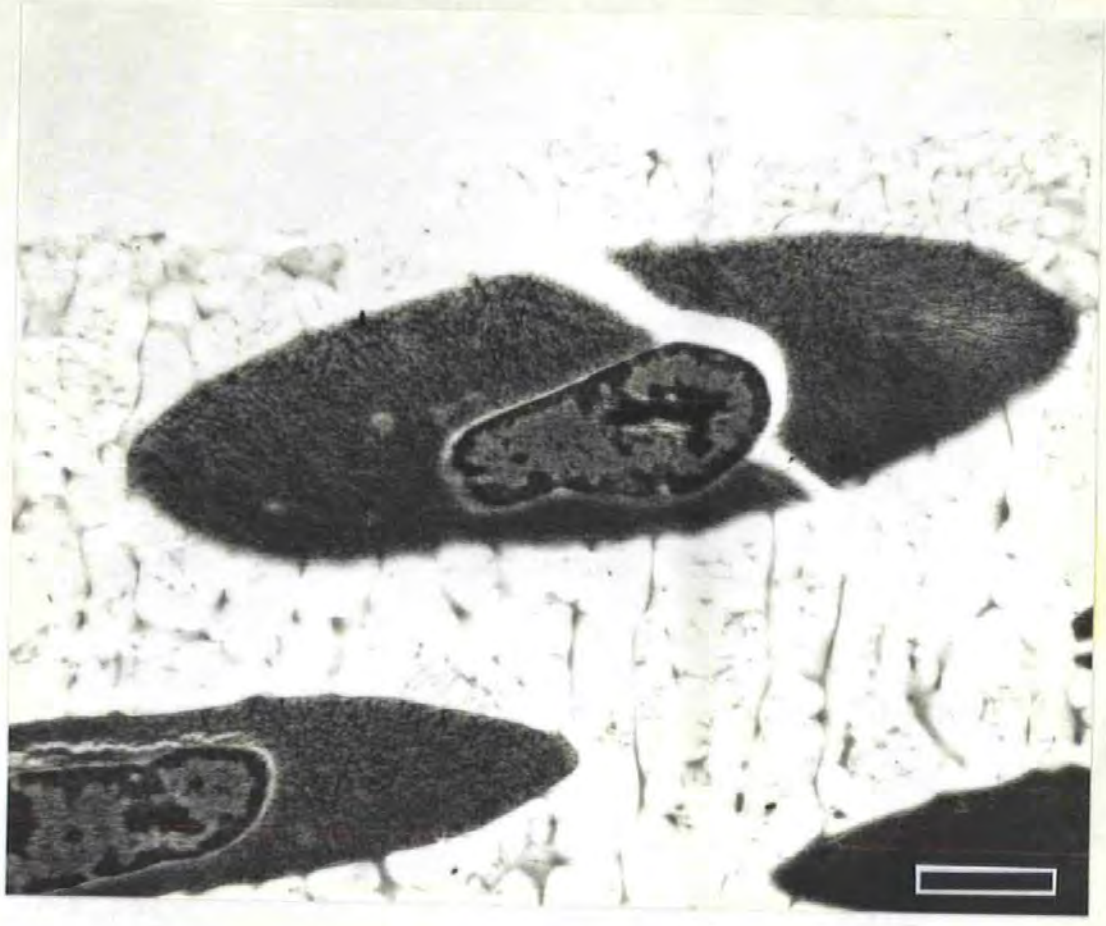

Figure 30. Appearance of freeze-substituted blood cells - III

Flounder red blood cells located near the centre of a 350 μm thick sandwiched specimen which was plunged 430 mm into liquid propane at 6 ms^{-1}. The cell at the centre shows freeze-fracture artifact. This was probably caused by the shearing apart of the copper (freeze-fracture) planchettes which may have occurred by striking the wall of the cryogen container during whiplash of the thin plunge rod after the high velocity plunging. The main fracture is across the top of the field with a small side fracture penetrating the blood cell. Scale bar: 1 μm. Reproduced, with permission, from Ryan *et al.* (1990), J. Microsc. 158, 365-378.

Figure 31. Appearance of freeze-substituted blood cells - IV

Flounder red blood cells located at the surface of a 350 μm thick sandwiched specimen which was plunged 410 mm deep at 2.0 ms^{-1} in liquid nitrogen. The surface of the specimen is marked at the top of the figure by dense osmium deposit from the freeze-substitution process. The cell nearest the surface shows large ice profiles, the adjacent cell shows fewer, larger profiles and is narrower. The cell at the bottom of the figure is more shrunken and is without obvious ice crystal damage. Scale bar: 1 μm. Reproduced, with permission, from Ryan et al. (1990), J. Microsc. 158, 365-378.

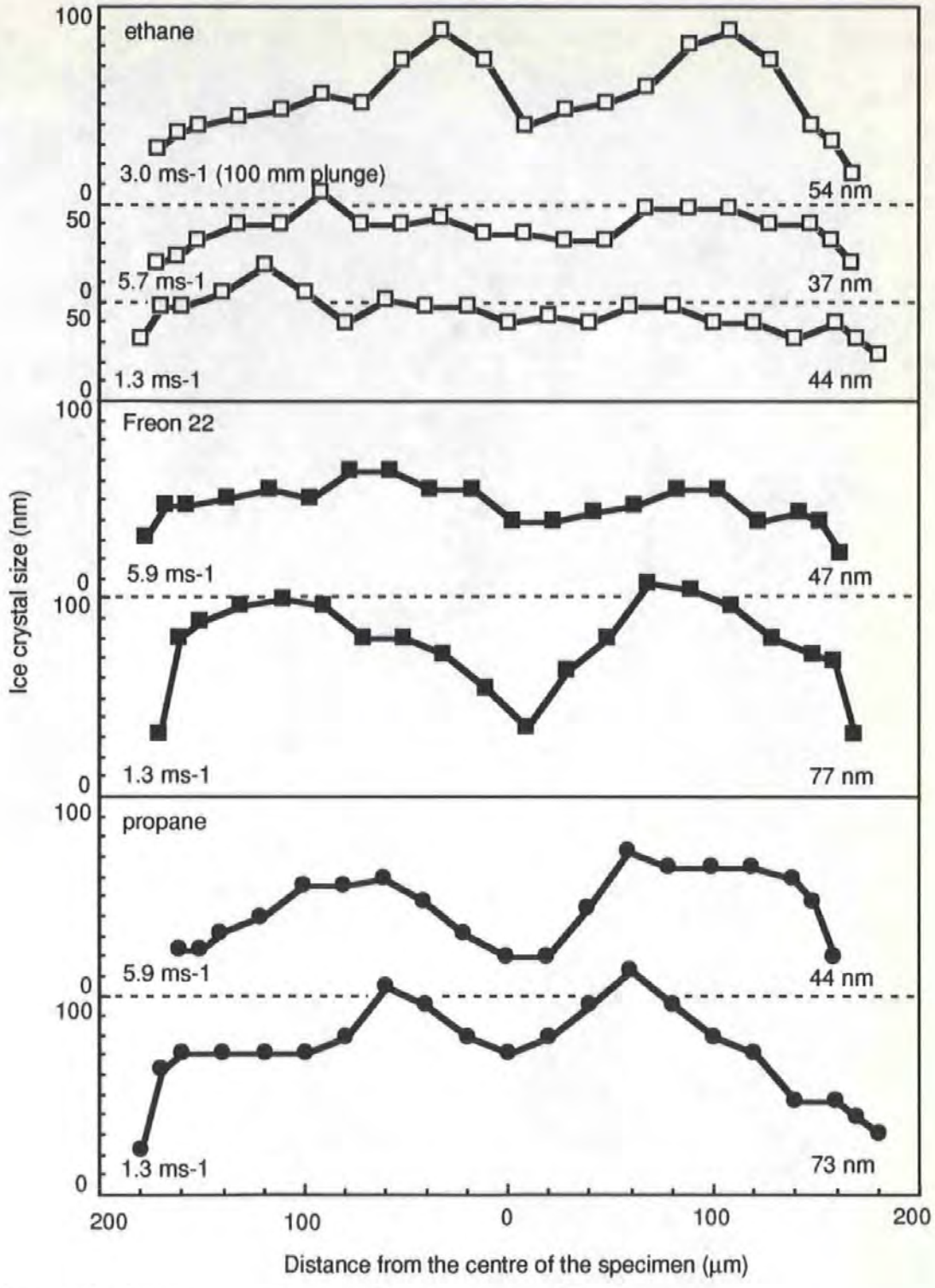

Figure 32. Transects of ice profile size across blood samples

The curves are labelled regarding the coolant and plunge velocity at left, with mean ice profile size shown at right. Note the small size of profile recorded at the centre of some specimens. Note also the mean result in the upper curve which was from an arrested plunge. With permission from Ryan *et al.* (1990), J. Microsc. 158, 365-378.

subdivision and branching of crystals, periodic crystal "waisting" or narrowing. Also granularity from resin, formvar support film, photographic film and occasional osmium deposits. Measurement on prints to the nearest 0.5 mm (= 4 nm). Gradation of crystal dendrite size across each cell.

(6) *Statistics:* only one fish was used for each coolant and normally only one sample examined for each plunge velocity (except for ethane, where plunging was repeated); only one photograph was taken at each depth in the specimen (total 665 photographs). A few micrometers were lost at one edge of each specimen when the planchettes were opened after freezing for freeze-substitution.

These limitations can be appreciated from Figure 26 and to this must be added the physiological state of the animal when considering the blood cell results.

The gelatin results in Figure 27 show the comparison between measured and predicted ice crystal size. The deviation between practice and theory at the centre of the sample arises from the "centre-line-effect", where cooling fronts converge and effective cooling increases. This was described originally by Van Venrooij *et al.* (1978) in their tubular specimen. The effect is not included in Balds theory for a flat specimen. It is interesting that despite the deviation from theory, when the data are considered for each specimen, the measured mean dendrite diameters are in reasonable agreement with the predicted mean diameters.

The micrographs of erythrocytes in Figures 28-31 show again the problems of measurement. The size of the ice cavity gradates across the cells and increase with distance from the cooled surface.

Results were not obtained from liquid nitrogen because it failed as a cryofixative. This is shown in Figure 31. The cell at the top, near the cooling face, froze with large crystals; the cell below it froze with larger crystals and the cell at the bottom froze without crystals. The explanation for the latter cell is that it shrunk during slow cooling which allowed the cell water to migrate to the growing crystal matrix in the extracellular medium. The cell membranes remain intact. This illustrates the principle of cryopreservation, where the objective is specimen revival after thawing.

The reason for gradation in dendrite diameter is that, as crystallisation proceeds into the specimen, latent heat is released. This reduces effective cooling and allows time for water molecules to migrate and join the growing crystal, which represents a lower energy state. It can be seen from Figure 29 that the dendrites originate from one area and this supports the statement of Dubochet & McDowall (1984) that a cell may have only one crystal which has many branches.

The results from transects across blood samples are seen in Figure 32. Generally, they show the "centre-line-effect", although it is less pronounced in the ethane results. However, it is clear in the top profile, which was from a specimen plunged only 100 mm in ethane at 3 ms^{-1}. The mean crystal dendrite diameter in this specimen was larger than in the other specimens plunged in ethane, including the one plunged more slowly. This again underlines the importance of minimum plunge depth, or having sufficient depth of coolant.

Comparisons between measured and theoretical crystal sizes are shown in Table 7. It is clear, again, that there are some remarkable agreements and some deviations. A problem in predicting crystal size is

the imprecise knowledge of the water content of the blood cells. For this study a figure of 70% was used. Published data for Carp (*Cyprinus carpio*) range between 64% for controls and 68.6% for 15 min *in vivo* air stress (Fuchs & Albers, 1988). The time lag in this study between removing blood and freezing it was 3-15 min. A number of samples were frozen from each bleeding, before taking more blood.

Other problems of ice crystal measurement include the distinction between small profiles, grey levels and granularity. A 15 nm profile magnified 122000 times measures only 1.8 mm on a micrograph. Computerised image analysis is not manageable because the continual manual intervention required. Crystal profiles of similar size have been measured previously, at 25 nm (Escaig, 1982) and 20 nm (von Zglinicki *et al.*, 1986). Silver section thickness is in the order of 60-80 nm, so clearly there could be overlay effects.

Another difficulty is that ice profiles may become smaller or even disappear during freeze-substitution. As ice is replaced by solvent then unfrozen eutectics between ice profiles may migrate and fill in the holes; also, the surrounding proteins may contribute to this process prior to their fixation.

The measured results in Table 7 range from 8 to 30% less than predicted. There is systematic, but unequal, "shrinkage" throughout which could be due to specimen processing artifacts, fish physiology disturbances or modelling assumptions. The means of the measured gelatin results in Figure 27 are 3.8 and 9.2% greater than predicted which suggests that there are errors associated with discrepancies in the assumed and/or experimental water content of the blood cells.

The freeze-fracture technique could provide a more faithful approach, in that freeze-substitution and resin embedding shrinkage and section compression artifacts would be avoided.

As in the previous Section, there is little published work with which to compare these results. Van Venrooij *et al.* (1975) measured ice crystal size across a tubular specimen perpendicular to the radial direction and found that it varied from about 1 μm at the surface and in the centre, to about 2.5 μm in the midway region. When they measured along the radial direction, the size in the intermediate zones was approximately 4 μm. It can be seen from the present work that the radial measurement, along the direction of cooling, merely samples the length of the dendrites and is of questionable value. The crystal sizes were two orders of magnitude larger than those reported here. This reflects the effects of cooling by immersion in Freon 22.

Elder *et al.* (1982) illustrated crystal sizes at different depths in rat liver plunged into propane on metal stubs which were coated with polyvinylpyrollidone. These specimens represent flat samples which were cooled from one direction (i.e. their free surface). The results showed a gradation in size up to a maximum of approximately 250 nm (measured on their Fig. 6c) at a depth of 45 μm from the specimen surface. Again, these crystal sizes are much larger than those reported here.

7.6 Conclusions

1. Measurement of ice crystal profiles in both hydrated gelatin and red blood cells shows encouraging confirmation of predicted ice profile size within a thin flat specimen after plunge-cooling. However, these specimens were chosen for their cytoplasmic homogeneity; greater difficulties arise

with the freezing of other cell systems, where the water content of different intracellular domains is not known.

2. Ethane proved the most efficient coolant with better results obtained at higher plunge velocities, provided that the coolant was deep enough to maintain the cooling process under forced convective conditions.

8 *Cryofixation and analysis of Chaetognath specimens*

8.1 Summary

This Section describes the investigation of two species of Chaetognath, *Sagitta setosa* and *S. elegans*, by cryofixation and low temperature scanning electron microscopy (cryoSEM). *S. elegans* was found to have a low concentration of sodium in the fluid which filled the body cavity and this was confirmed by other techniques. The sodium was found to be replaced by ammonia, which possibly acts as a buoyancy aid for this oceanic species. In ultrastructural studies, the use of low thermal mass specimen supports demonstrated the phenomenon of "centre-line-cryofixation", which gave good freezing in the centre of optimally supported specimens up to 80 μm from the surface.

8.2 Introduction

Low temperature scanning electron microscopy has been described by several workers as a method which enables specimens to be observed in a near-natural state. This is because cryofixation avoids the artifacts which are induced by wet chemical preparative methods (Echlin, 1973, 1978; Echlin & Moreton, 1974, 1976; Echlin & Saubermann, 1977; Robards & Crosby, 1979; Marshall, 1980a, 1980b; Echlin *et al.*, 1982).

This investigation forms part of a much wider investigation which is described fully in a report by Bone *et al.* (1987) and which is included as Appendix 4.4 to this thesis.

The work described here applied cryofixation and resulted in new knowledge. Living marine organisms with large fluid-filled body cavities were preserved in the fully hydrated state and analysed by X-ray

microanalysis. The water content of the cavities approximated to seawater, which is approximately 97% water.

In order to optimise cooling efficiency, specimens were frozen on low thermal mass supports, detached under liquid nitrogen and mounted in supports for cryoSEM by a new technique which is described in Section 9.

8.3 Experimental Design

The animals (Section 3.17) were normally mounted on low thermal mass supports (Section 3.18) and frozen in ethane using the benchtop device described in Section 4. After plunging, the specimens were collected in a small container of LN_2 in the cooling chamber, transferred to the cryomounting device and detached from the supports under LN_2 using cold forceps. They were then mounted in cryoSEM supports at 213 K (-60°C), as described in Section 9.

The specimens were examined in the SEM (Section 3.22) using a cryostage (Section 3.23). The SEM also had an airlock cold-stage on which the specimens could be freeze-fractured with a cold scalpel. They were then coated with a thin layer of evaporated carbon, to render them conductive, and examined by X-ray microanalysis (Section 3.24).

This analytical technique uses an energy dispersive system to characterise the X-rays which are emitted from a specimen when it is irradiated by the electron beam of the microscope. The X-rays have energies which are characteristic of the elements irradiated. The X-rays are collected by a solid state detector which produces a small voltage change proportional to the energy of each X-ray quantum. The voltage signals are amplified and processed in a multichannel analyser, or pulse

processor, to produce a spectrum which shows the number of X-rays collected for each energy level.

The ZAF PB (atomic number-absorption-fluorescence peak-to-background) program, from Link Systems Ltd., High Wycombe, Bucks., accommodates non-normal beam incidence and quantitates data from specimens of uncertain geometry by calculating peak to *local* background ratios (Statham, 1979). These are less geometry-dependent than the more usual polished specimen/net peak intensity approach.

The analysis was a demanding procedure. First, the general geometry, operating kV, eV/spectrum channel and calibration element were decided and stored in the system. Then the system resolution was determined by collecting calibration element spectra under different count rates. These were processed by the computer and a FWHM (full width half maximum) resolution value obtained for the artificial zero peak. An extra 5 eV was added to this value and it was stored in the system. Processed spectra were later degraded to this artifical value, so simulating a stable system without electronic noise and where resolution was unvarying.

Before analysing real specimens, it was necessary to build a computer library of peak profiles for the elements expected to occur in the specimen and also the elements detectable from the SEM, cryostage and specimen supports.

It was then necessary to derive two sensitivity factors for the elements in the specimen. One is a correction factor ("FST") generated by the program and the other ("RST") is a peak to background ratio for a peak

divided by the concentration of the element in the standard. These were then edited into the system's Standards File.

Many approaches were tried, such as doping gelatin with known salt concentrations and looking at these specimens frozen, or freeze-dried, or cryosectioned (hydrated and freeze-dried), similarly with PVP, starch, colloidal graphite preparations and minerals. Eventually, standard seawater was frozen as small drops on a specimen stub, fractured and data collected, from which the program yielded the sensitivity factors. It was essential that when these were applied to other frozen seawater droplets that the known concentrations of the elements in the standard were obtained.

A matrix file was also necessary. This contained information about light elements in the specimen which were undetectable by the system, but which generated background noise in the spectrum. The file was used by the system to compensate for this contribution of the non-specific biological matrix. The nominated matrix was water.

Calibration element spectra were collected regularly from copper with specimen spectra. The calibration spectra generated a Gain Factor and zero peak resolution which were used to compensate for minor drift in the zero peak and the gain of the spectrometer and pulse processor in processing subsequent analyses.

For analysis, a list of elements was required by the program and was compared to those found. This comparison was done after escape peaks were removed and the spectrum was digitally filtered to yield a set of peak profiles which were independent of the background. These were

then modified by the Gain Factor and resolution and filtered again. Peak areas were determined for the background-subtracted peaks by a filtered least squares (FLS) fit of the filtered peak profiles to the filtered spectrum. A Fit Index was then calculated over the filtered region, not the whole spectrum. This was a measure of the quality of the fit of the stored standard profiles to the unknown spectrum and should be close to 1.0. The complete profiles of peak plus their background were used in that process. The background-subtracted profiles were then scaled to match the unknown spectrum and stripped from it so that the background under the peaks could be determined. The continuum was then calculated from the first estimate of concentration and the true background fitted to it. Then, the G factor and interelement absorption and fluorescence corrections were calculated in an iterative process. The G factor is the mean of the (mass fraction x atomic number squared)/atomic weight for all the elements detected. It indicated the relative efficiency of background production.

There then followed a cycle of complicated iterative calculations of feasible specimen composition until concentrations were obtained within 0.005 (0.5%) of the previous values of the cycle. The results were then printed as % concentrations by weight.

This explanation of the microanalysis technique is a simplification of the Link Systems ZAF PB Program manual, it is only possible here to outline the principle of the method.

Besides the analysis, trunk segments of some specimens were frozen on the foil supports described by Ryan & Purse (1984), freeze-substituted (Section 3.15) and examined for ultrastructural appraisal using transmission electron microscopy (Section 3.16).

8.4 Results

A scanning electron micrograph of a frozen specimen is shown in Figure 33 and a typical X-ray spectrum is shown in Figure 34.A. This specimen is fully hydrated and the specimen can be compared with that in Figure 34.B which is derived from a freeze-dried specimen. A copy of the computer program printout for an analysis is shown in Figure 35. This figure is modified slightly by the inclusion of results also from *Sagitta setosa* and from seawater which was sampled with the animals. The overall results are summarised in Table 8.

Figure 36 shows surface cryofixation and Figure 37 shows the preservation in gut cells at the centre of a trunk segment which was frozen on a foil support.

8.5 Discussion

The X-ray microanalysis results represented more than six months of daily attempts at mastering the cryoSEM/quantitative X-ray technique. There were many erratic results initially which reflected the particular set of sensitivity factors applied to specimen spectra. It was only after using the seawater standard that believeable results were collected. There was considerable variation between animals and some of this was attributed to death prior to freezing. They were impossible to keep alive for more than than a few hours in the Laboratory. Additional variation occurred within each animal, depending on the size of the particular body compartment; in *S. elegans* large compartments were particularly low in sodium. Table 8 gives results from 17 animals and 6 samples of the seawater which was taken from the area where the animals were caught. The results from analysing standard seawater are also shown as a control.

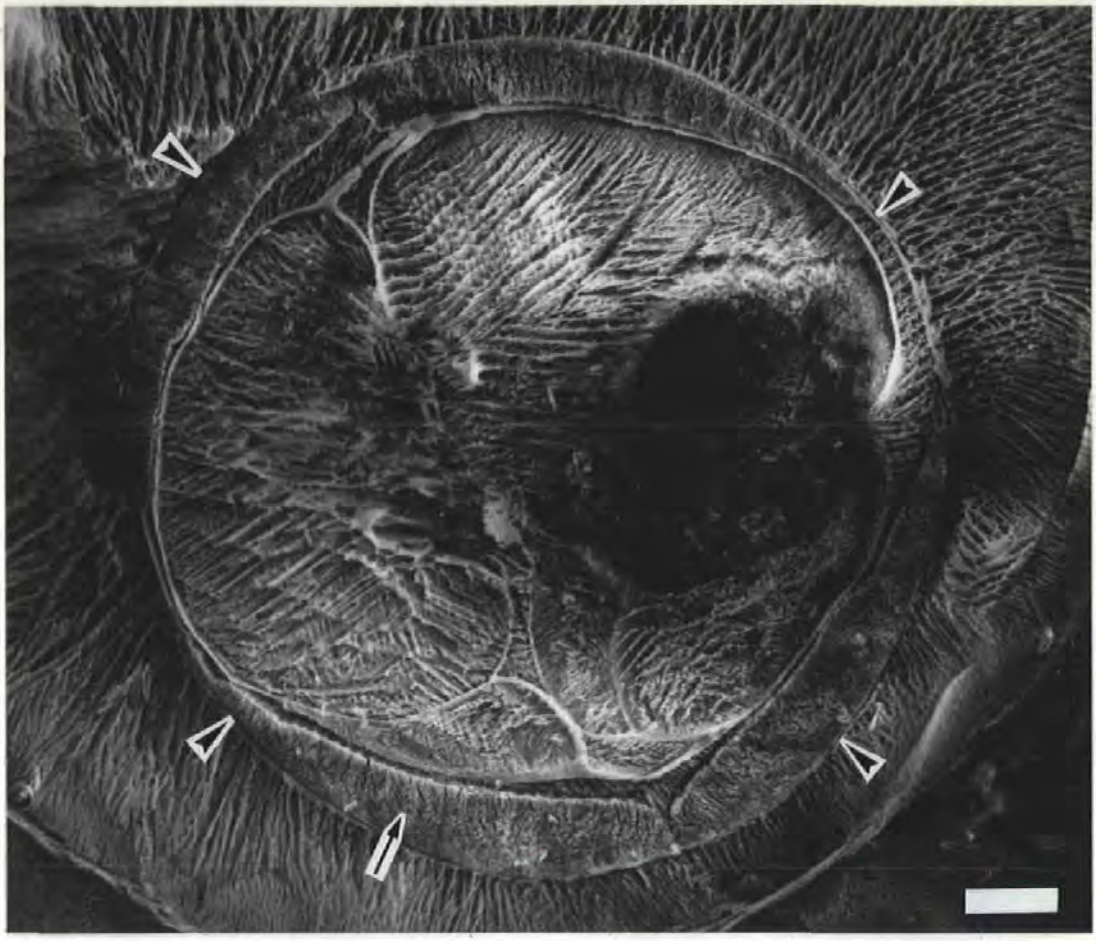

Figure 33. CryoSEM image of a Sagitta elegans

This figure shows a freeze-etched specimen which was frozen in a seawater-filled hole drilled through 2 specimen supports. These were held together, plunged in liquid nitrogen and then split apart. The outer surface of the specimen is indicated by arrowheads. The myofilament bundles of the body wall muscle (arrow) are separated due to ice crystal growth between them. The specimen is surrounded by crystallised seawater and the edge of the hole is seen at bottom left and right. The ice profiles in the body cavity are approximately 10 μm across and should be compared to the 2-μm crystals in Figure 41, which is of a cryomounted specimen. Cryomounting was normally used in this work and is described in detail in the following Section. It allowed optimised freezing which gave smaller ice crystals and less ionic redistribution. Scale bar: 100 μm.

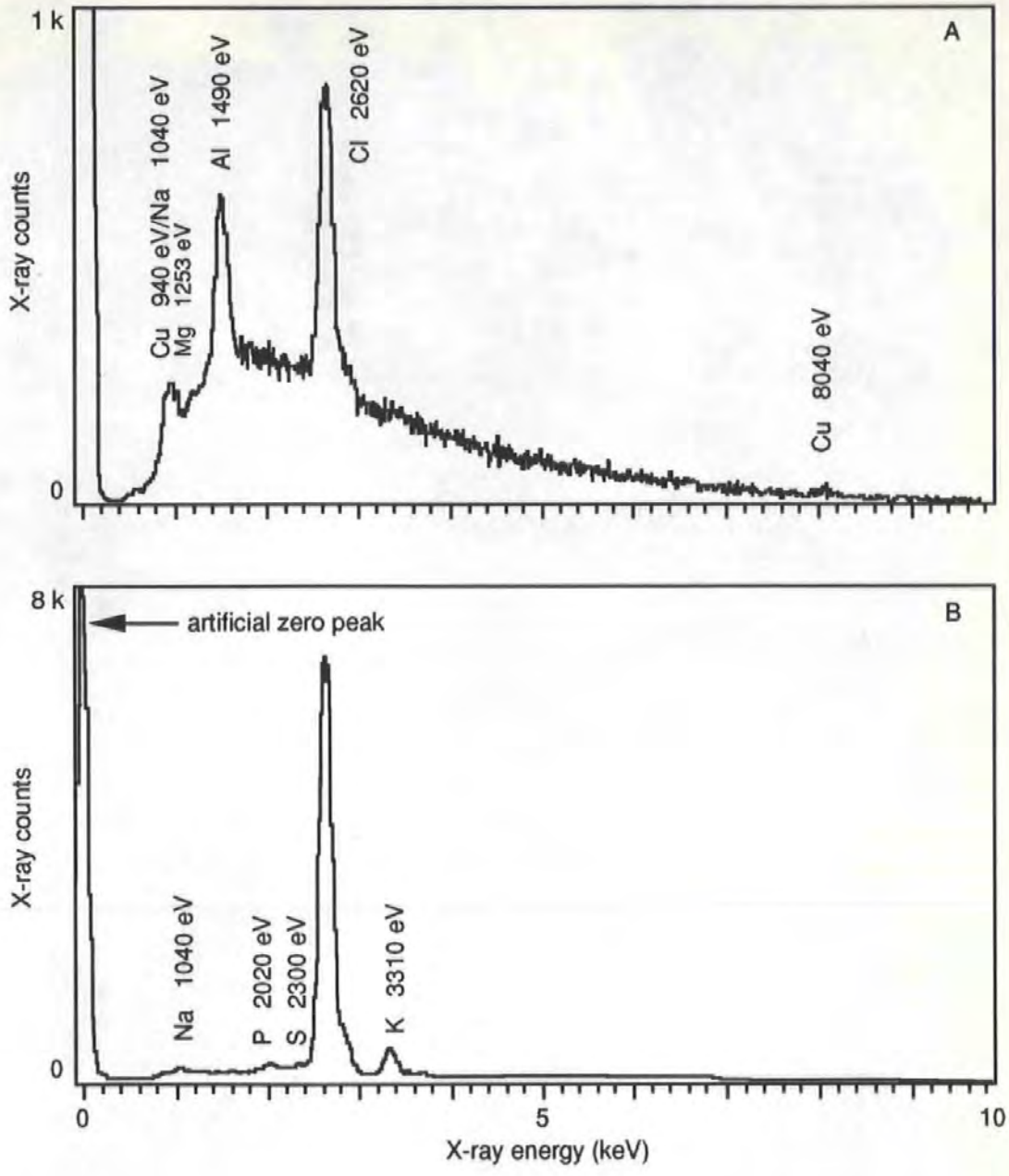

Figure 34. X-ray spectra from frozen Sagitta specimens

A. The spectrum from a frozen hydrated *Sagitta elegans* which gave the quantitative results which are shown in Figure 35.

B. A spectrum from a frozen *S. elegans* which was freeze-dried in the microscope. The counting time was 300 s for both spectra, under similar analytical conditions. Note the difference in the shape of the background after the water has been removed and the improved peak-to-background ratios.

TRACK-61 ELEGANS-1 FRACTURE LEVEL 1-1 LIVETIME (SPEC) 300 SECS

15KV TILT= .00 ELEV= 40 AZIM= .00 COSINE= .974

ENERGY RESOLN AREA

5.5 120.91 234700 TOTAL AREA= 117444

2 ITERATIONS G-FACTOR= 3.754 FIT INDEX= .92

SPECTRUM: TR61 ELEGANS-1 LEVEL 1-1 20:3:86 HYDRATED SAGITTA

ELEMENTS IN MATRIX: WATER - H2O - ICE

ELMT		AREA	AREA/BACKGROUND	ELEGANS %CONC	[SETOSA] [%CONC]	[S.W.] [%CONC]
AL	K	5210 +/- 218	.206 +/- .009			
CU	K	358 +/- 80	.275 +/- .062			
CU	L	2226 +/- 127	.329 +/- .019			
NA	K	339 +/- 157	.031 +/- .014	0.15	[1.00]	[1.12]
MG	K	185 +/- 179	.010 +/- .010	.04	[.11]	[.13]
S	K	-87 +/- 210	.003 +/- .008	-.01	[.16]	[.04]
CL	K	10529 +/- 287	.437 +/- .012	1.93	[2.00]	[1.87]
K	K	95 +/- 177	.005 +/- .010	.02	[.03]	[.02]
CA	K	47 +/- 167	.003 +/- .011	.01	[.03]	[.07]
MATRIX				97.86	[96.67]	[96.81]
TOTAL				100.00	[100.00]	[100.00]

Figure 35. ZAF PB computer printout of a typical X-ray analysis

The SETOSA and S.W. frozen hydrated results are added here from other printouts, for comparison. All three of these sets of results were chosen to illustrate results approximating to the mean final results for *Sagitta elegans, Sagitta setosa* and local seawater. Note the low sodium concentration in *S. elegans* and the similarity between the sodium concentrations in *S. setosa* and the seawater. The chlorine concentrations appear similar in the three specimens. The results were generated from the spectrum in Figure 34.A.

	Standard seawater	Channel seawater	*Sagitta elegans*	*Sagitta setosa*
Na	1.09 (.16)	0.97 (.27)	0.15 (.07)	1.10 (.21)
Cl	1.90 (.24)	1.86 (.43)	1.78 (.29)	2.01 (.41)
n	3	6	7	10
t	25	51	59	80

Table 8. Results of the X-ray microanalysis. Figures are given for the standard seawater of known composition (Na 1.055%, Cl 1.8979%, Mg 0.127%, S 0.0884%, K 0.038% and Ca 0.040%) which was used for calibration, as well as for the specimens analysed. The values given are the means (with standard deviations), n is the number of animals or seawater samples and t is the total number of analyses.

Table 8 shows that coelomic fluid in *Sagitta setosa* was very similar in composition to seawater; sodium and chlorine concentrations appeared to be marginally higher in the animal. The level of sodium in *S. elegans* was markedly low in all specimens. These results were confirmed by colleagues who used ion-sensitive electrode and flame emission and potentiometry methods, as described by Bone *et al.* (1987), in Appendix 4.4 to this thesis.

The results for sodium are notable. This was the lightest element which was normally detectable by the system and it occurred at low concentrations. The levels in *S. elegans*, of approximately 0.15% weight, were near the limit of detectability. Echlin & Taylor (1986) used a Link 860 Series II analysis system and the ZAF PB computer program to analyse physiological ions in tobacco leaves. They gave an overall value of

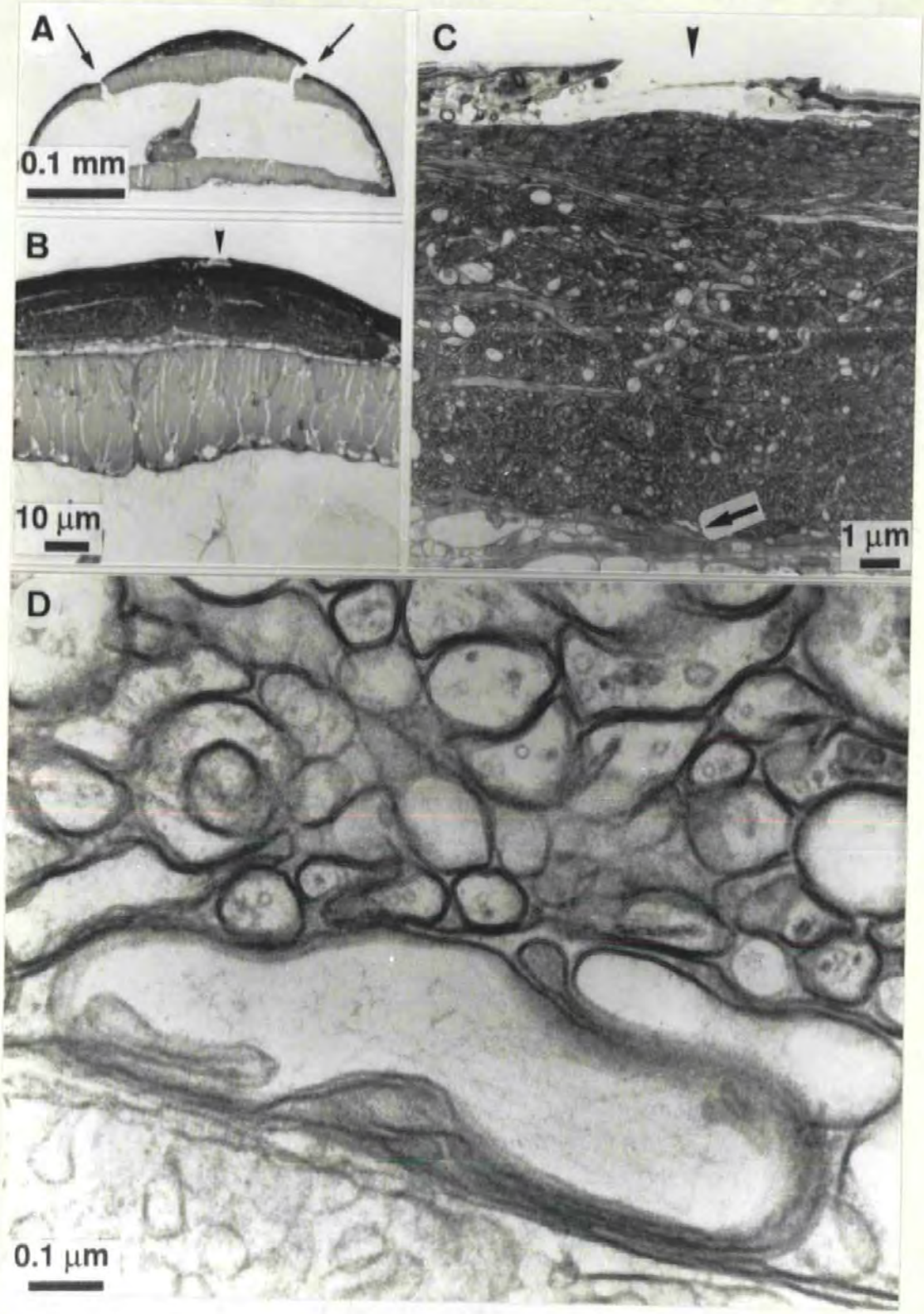

Figure 36. Electron micrographs showing surface cryofixation

A series of magnifications of a freeze-substituted *Sagitta* which was plunge frozen on an aluminium foil-arch support. Good cryofixation is shown to a depth of 13 µm. Arrows in A mark freeze-fracture artifact. The surface feature in B (arrowhead) is also seen in C.

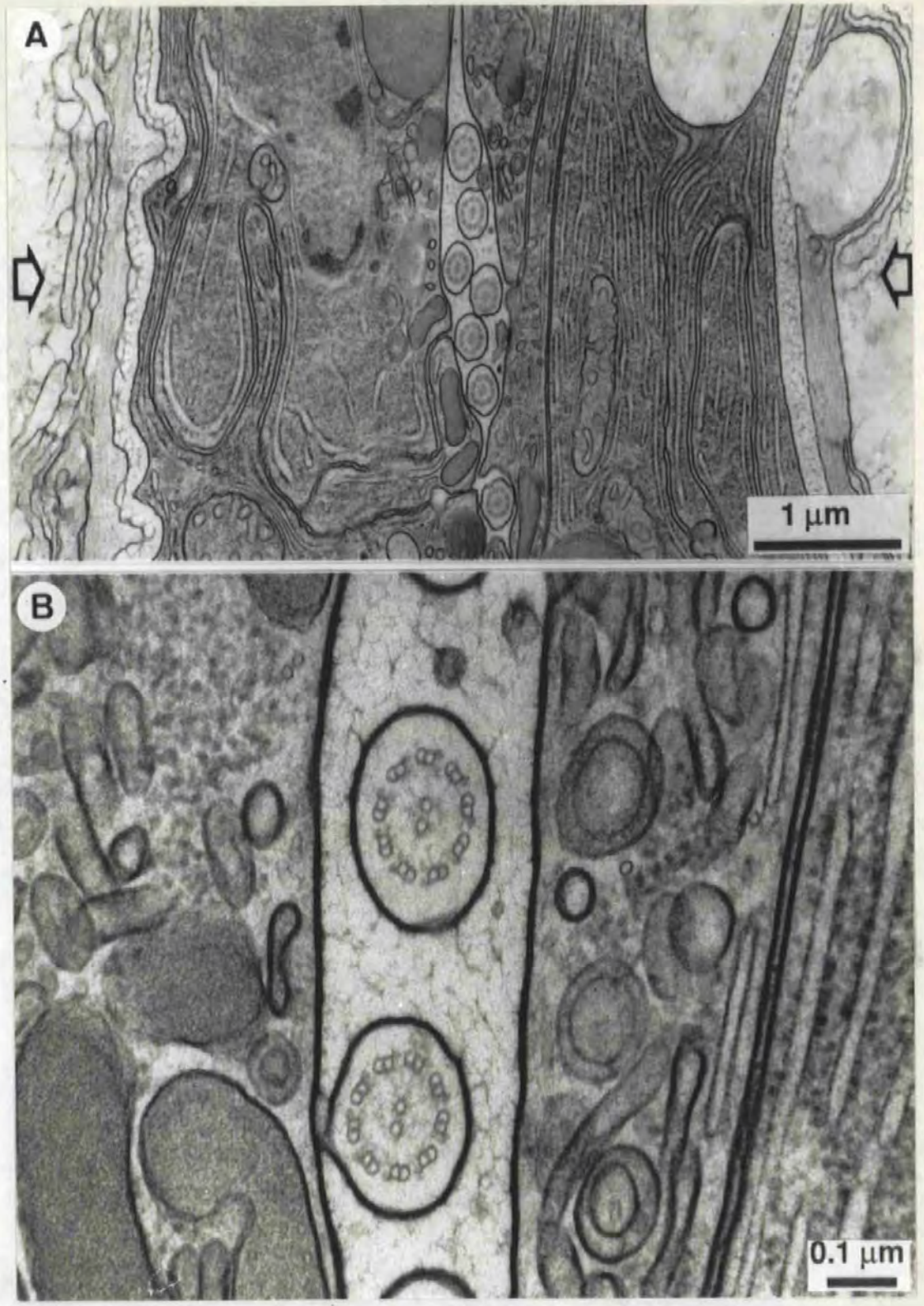

Figure 37. Electron micrographs showing centre-line-cryofixation

A. Detail of *Sagitta* gut from Figure 36.A, the directions of the cooling fronts are indicated by arrows. B. Gut lumen showing well preserved cilia which were 80 µm from the nearest surface of the specimen. Note the crystallisation of the fluid in the gut.

0.1% for sodium and the highest median elemental concentration was 0.89% for calcium in senescent leaves.

The work of Echlin & Taylor was more refined than that reported here. The specimens were coated with a thin layer of evaporated chromium, which gave better imaging and less charging. Thus, there was less distortion of the specimen-emitted signals, including X-ray photons.

An advantage of coating with chromium is that, unlike the carbon coating used in this work, it is detectable by the system. The computer program has a routine for recognising designated specimen holder and support grid elements which would contribute background to the spectrum.

In this work, the route chosen in the program was for the analysis of bulk specimens in a matrix of undetectable elements which formed the bulk of the material. It was anticipated that the absorption/fluorescence effects would be important and this route precluded the use of the grid-holder corrections. In retrospect, it is evident that the aluminium specimen support and the copper cryostage both contributed significant peaks to the spectra and, thus, significant background.

An interesting observation was that the uncoated fully hydrated specimens did not charge significantly. This could result from the natural conductivity of the body salts, which approximate to seawater - at least in *Sagitta setosa*.

The ultrastructure shows an unusual situation, namely, good preservation some 75 to 80 μm from the surface of the specimen (Fig. 37).

This is because the specimen support was of low thermal mass and cooling could occur from all sides. This is shown in Figure 38 and depicts the effect of the supports described originally by Ryan & Purse (1984). Normally good preservation is seen up to 20 μm from the surface; the intermediate zone, between the surface zone and the gut, suffered noticeable ice crystal damage. This result clearly demonstrates the principle of centre-line-cryofixation, where converging cooling fronts combine to increase the cooling rate at the centre of thin specimens. This supports the findings of the crystal analyses described in Section 7.

8.6 Conclusions

1. Cryofixation preserved the chemistry of specimens which was analysed by quantitative X-ray microanalysis using cryoSEM. The results were reasonably accurate and were corroborated by other techniques. This indicates that the method of physical preservation is valid.

2. The ultrastructure results show that the use of low thermal mass specimen supports can give good preservation in the centre of specimens. This corroborates the results of the crystal analyses.

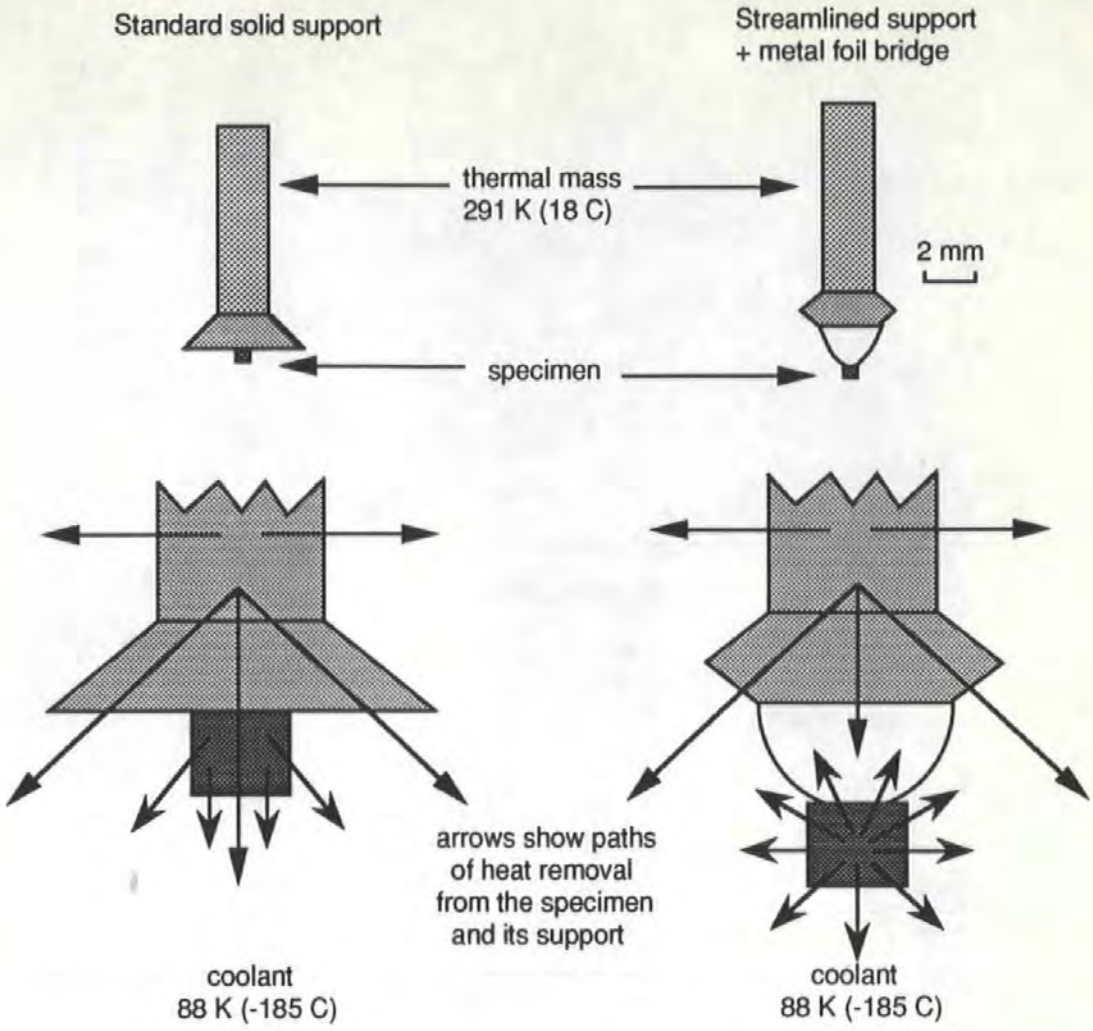

Figure 38. The centre-line-cryofixation principle

The standard solid support (at left) is a heat sink which retards cooling in the specimen. The foil-bridge support (at right) removes the specimen from this heat sink and enables coolant to reach it from all directions. Thus, cooling is omnidirectional and is greatly enhanced in the centre of the specimen where the cooling fronts converge. This gives better cryofixation in the centre of small specimens mounted on low thermal mass supports.

9 *Cryomounting of frozen specimens for cryoSEM*

9.1 Summary

This Section describes a method of mounting frozen specimens onto supports for cryo-scanning electron microscopy. The specimens were frozen between the ends of V-wire supports, detached under liquid nitrogen and glued into holes in SEM specimen stubs using electroconductive silver or graphite paints. The paints are solvent based and solidify at approximately 213 K (-60°C). Specimens mounted by this method showed less ice crystal damage than specimens mounted on standard supports before they were frozen.

9.2 Introduction

CryoSEM offers the possibility of examining biological specimens in a form that approaches their natural state, without the artifacts induced by other preparative methods (Echlin, 1973, 1978; Echlin & Moreton, 1974, 1976; Echlin & Saubermann, 1977; Robards & Crosby, 1979; Marshall, 1980a, 1980b; Echlin *et al.*, 1982).

Many cryoSEM specimens are frozen, inserted into the microscope and the external features observed (Sargent, 1986). This is a simple procedure which is very satisfactory, unless the specimen has to be fractured and the internal structure examined. As with other techniques which require the specimen to be frozen, ice crystal damage can disrupt its internal features. Normally, cryoSEM specimens are mounted on relatively large metal blocks and then frozen. The cryofixation process is affected by the thermal mass of the support, which greatly impedes cooling. The principle was demonstrated in work on determinants of cooling rates which was done before this thesis was undertaken (Ryan & Purse, 1985a).

In an attempt to improve on the standard technique, a method was required whereby specimens could be cryofixed as efficiently as possible and the specimen then mounted on a support for examination. Preliminary trials involving the mechanical clamping of frozen specimens proved ineffective because they invariably shattered, although Hagler & Buja (1984) used a clamping vise for holding frozen cryoultramicrotomy specimens. A suitable low temperature cement was then sought and the method described here was conceived through the work of Bachmann & Schmitt (1971), Karp *et al.* (1982), Steinbrecht & Zierold (1984) and Roos & Barnard (1985). Bachmann & Schmitt used butylbenzene, m.p. 185 K (-88°C), to glue frozen microdroplets together for freeze-fracturing; Karp *et al.* used toluene, m.p. 178 K (-95°C) for orienting and gluing frozen specimens for cryoultramicrotomy, Steinbrecht & Zierold used heptane, m.p. 182 K (-91°C) and Roos & Barnard used n-butylbenzene.

The novelty of this method was that, unlike cryoultramicrotomy specimens, electroconductivity was required against the charging of specimens in the microscope. Also, if freeze-etching or freeze-drying were required then a residual conductive matrix was necessary. For these purposes, the standard specimen cements, which are normally used and allowed to dry at ambient temperature, were found to be useful. Electroconductive paint has been used to fix fresh specimens to stubs *prior* to freezing (Echlin & Moreton, 1974).

9.3 Experimental Design

The equipment consisted of a temperature-controlled brass block which was housed in a polystyrene box. The box was also used as the cooling chamber of the benchtop plunging device (Section 4), fitted with a brass plate which formed a false bottom to the chamber (Figure 39). The

block measured 50 x 30 x 25 mm high and sat on a 5 mm thick layer of Tufnol insulation. A 100 W cartridge heater was inserted into one end and was connected to the power supply used with the plunger. The heater was controlled by a feedback thermocouple which was clamped into the block. A depression was milled in the top of the block (11 mm diameter x 4 mm deep) to house specimen supports. A screw-clamp held another thermocouple onto the specimen support for direct temperature measurement. In use, the base of the chamber was filled with liquid nitrogen, then the plate was added and flooded with liquid nitrogen to a depth of a few millimetres.

The specimens mounted after cryofixation were Chaetognaths (*Sagitta* species, Section 3.17) frozen on low thermal mass supports (Section 3.18) and carrot blocks (Section 3.21) which were mounted on aluminium foil strips which were attached to the plunge rod using Blutack. They were frozen by plunging either in ethane or in liquid nitrogen.

After cryofixation, the specimens were detached from their freezing supports and mounted on modified supports for cryoSEM. The standard cryo-support was a 5 mm high x 10 mm diameter aluminium stub. These were modified in two ways: for use with Chaetognaths, a 4 mm deep blind hole was drilled into the centre of the stubs and 2 mm wide x 2 mm deep slots were milled into the stubs for use with carrots.

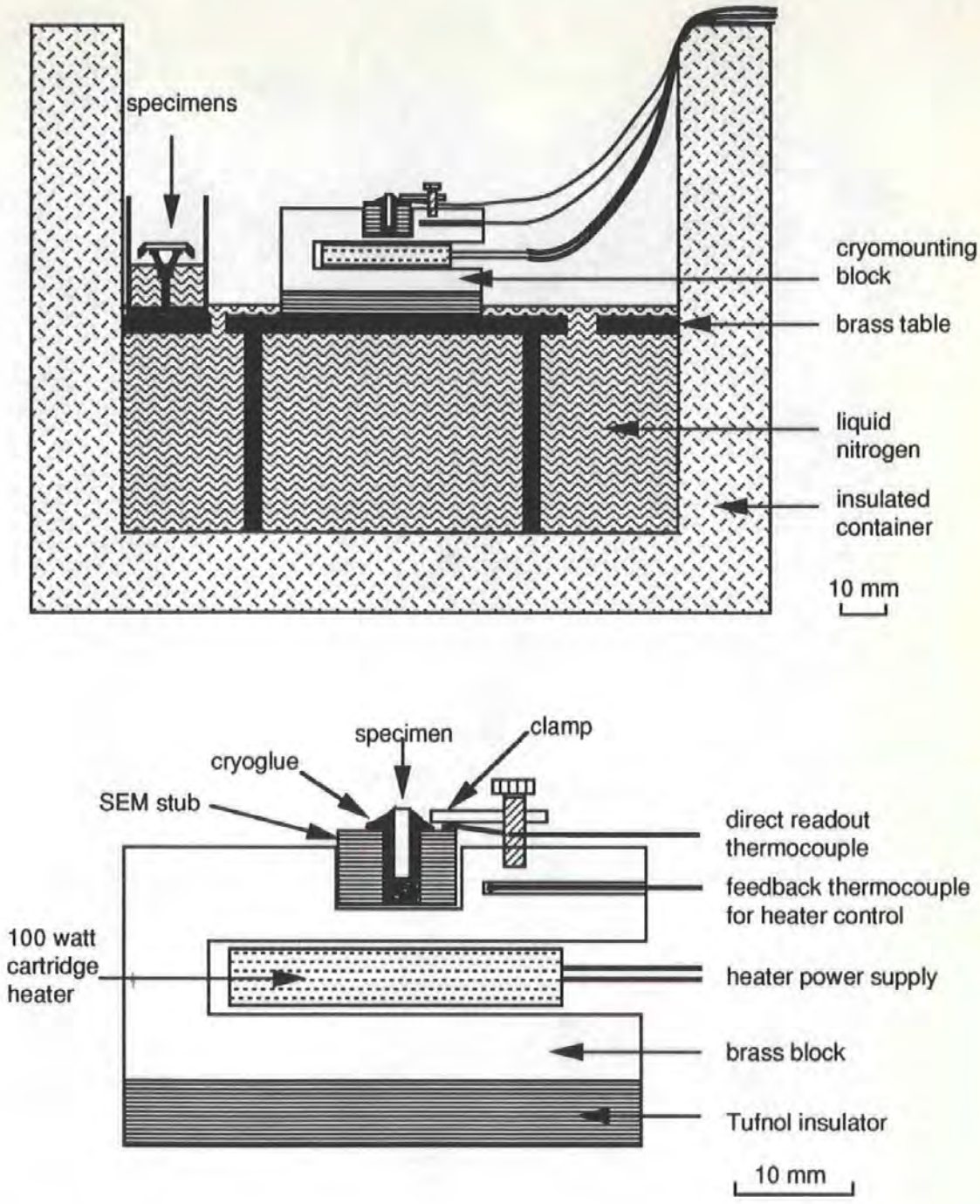

Figure 39. Cryomounting chamber

The complete assembly is shown at the top with the cryomounting block enlarged below. Optimally frozen specimens are mounted in cryoSEM specimen supports using silver or carbon paints at 213 K (-60°C). The specimens are then recooled to liquid nitrogen temperature for storage or for transfer to the cryoSEM. The effect of exposure to high subzero temperature is discussed in Section 10.

The method of mounting involved cooling the mounting block to an equilibrium state, which was normally 213 K (-60°C) and was controlled by the thermocouple-power supply system. A support was loaded as required with electroconductive cement, placed in the mounting block, clamped with the second thermocouple on the edge of the cement and allowed to cool to the desired temperature (Figure 40).

The cements were Dotite Type D0550 silver paint (supplied by J.E.O.L. (UK) Ltd., Welwyn Garden City, Herts.) and Leit C Carbon Conductive Cement (from Agar Scientific, Stansted, Essex). The latter is useful for X-ray microanalysis because it cannot be detected in the spectrum, although it does contribute to the background. The solvent for the silver cement is iso-butyl methyl ketone (m.p. 189 K/-84°C) and that for the carbon cement is a commercial product (m.p. 150 K/-123°C) containing xylene. At temperatures near the solvent melting points, the cements did not "wet" the specimens readily. This was the reason for using them at 213 K (-60°C), at which they were more liquid.

As a control, some Chaetognaths were mounted so that they protruded from holes in the stubs which were filled with seawater. These were frozen in liquid nitrogen.

When ready for observation, the specimens were examined by cryoSEM as described in Sections 3.22, 3.23 and 8.3.

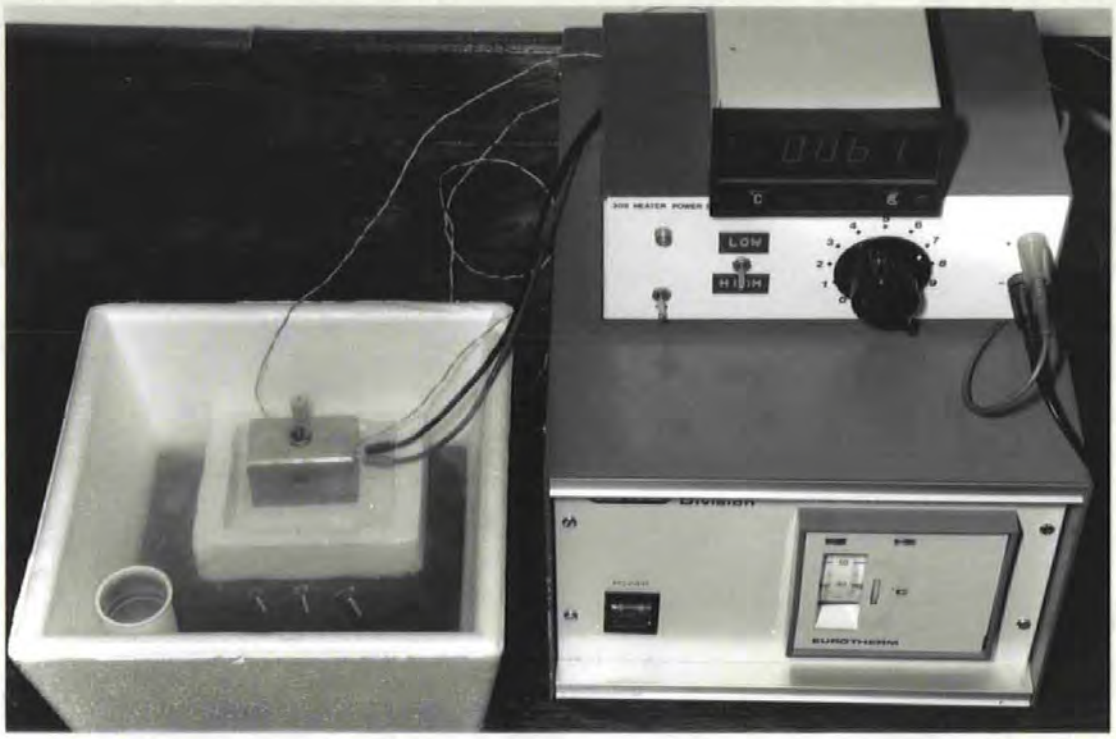

Figure 40. Cryomounting system

The brass cryomounting block is seen in the cooling chamber, at left. In this photograph it is on an extra layer of insulation. Frozen specimens on Y-frame supports are seen under liquid nitrogen on the base of the chamber, they were transported from storage in the aluminium container. A specimen is seen on the mounting block embedded in carbon paint in a cryoSEM specimen stub. At bottom right is seen the thermocouple feedback control unit which regulates the power unit above it, this controls the cartridge heater in the mounting block. The digital thermometer gives a direct readout of the cryomounting medium (see Figure 39, lower section).

9.4 Results

Figures 41 and 42 show results from two freeze-fractured and freeze-etched Chaetognath specimens. The specimen in Figure 41 was optimally cryofixed on a V-wire support, in liquid ethane as a coolant and subsequently cryomounted. The specimen in Figure 42 was mounted in the stub in seawater and frozen in liquid nitrogen.

The specimen frozen in ethane (Figure 41) showed internal crystal domains which were 0.4 to 0.9 μm in width, except for the outer zone at the surface of the specimen. This was 25 μm in depth and showed no damage, as observed by cryoSEM

The specimen frozen in the stub in liquid nitrogen (Figure 42) showed extensive internal segregation artifacts. Both the body wall and the body cavity showed large crystal cavities; those in the body wall measured 0.54 to 5.40 μm across and those in the body cavity were up to 8.8 μm across.

A stereoscopic cryo-scanning electron micrograph of a carrot root cortical parenchyma cell is shown in Figure 43. The specimen was frozen in ethane, cryomounted and freeze-dried in the microscope after freeze-fracturing. The cell was located approximately 1 mm from the nearest surface and shows an extensive honeycomb-like cavity which was formed by ice.

9.5 Discussion

The use of cryomounting techniques for cryoSEM purposes seems to be hitherto unreported, although they were used 20 years ago in a freeze-fracture method (Bachmann & Schmitt, 1971) and more recently in

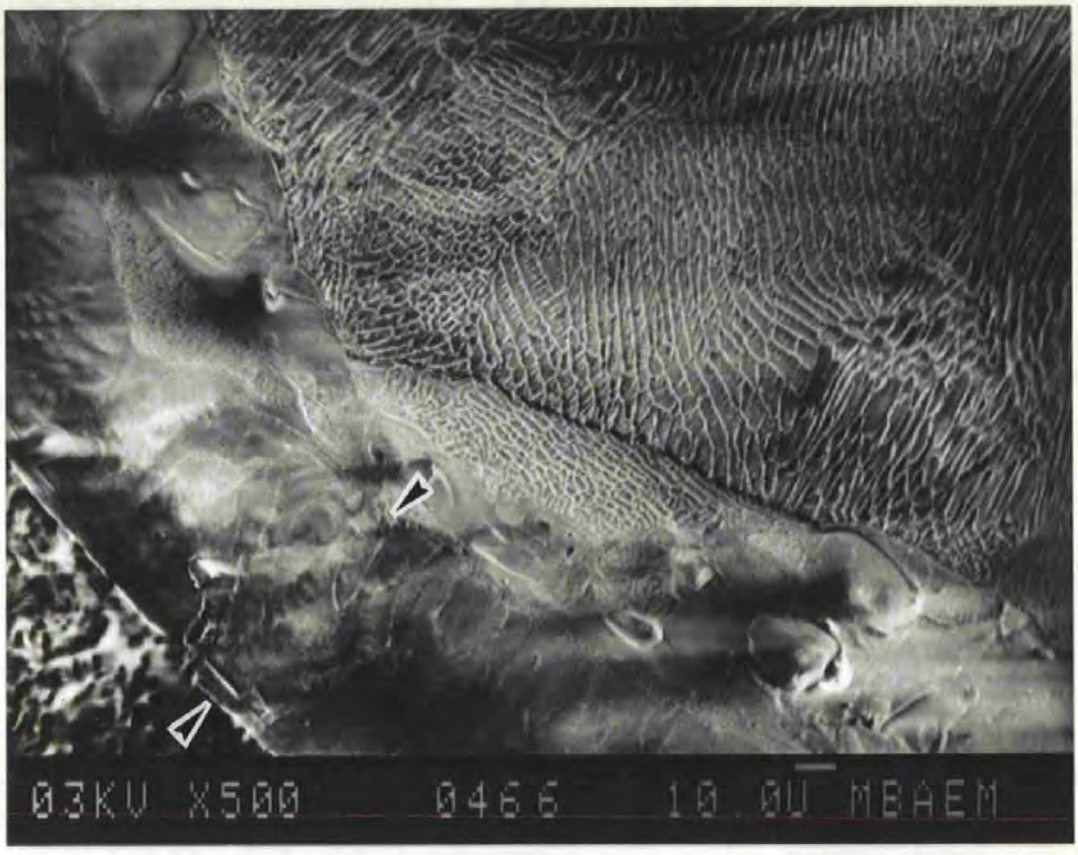

Figure 41. CryoSEM image of a cryomounted Sagitta elegans

This specimen was plunge-frozen on a V-wire support in ethane, cryomounted, fractured in the cryoSEM and then freeze-etched. The outer surface of the specimen is at bottom left, where carbon particles are seen in the graphite cryoglue. Note that the body wall (between arrowheads) shows little relief compared to the crystallised internal body cavity, where profiles up to 5 μm wide are seen. The body wall, 60 μm thick between the arrowheads, is well cryofixed with little sign of freezing damage at this magnification. This figure should be compared with Figure 42 which shows a more conventionally prepared specimen. Scale bar: 10 μm.

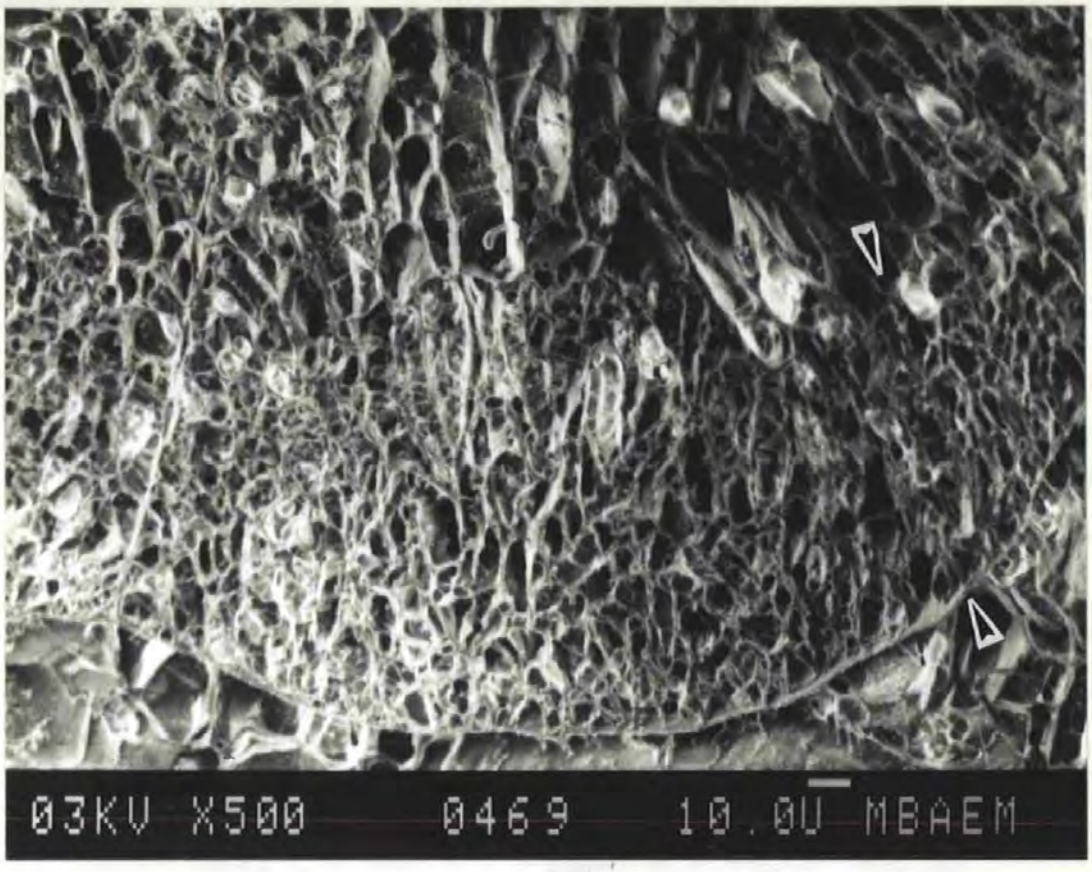

Figure 42. CryoSEM image of a non-cryomounted Sagitta elegans

Specimen frozen in liquid nitrogen while protruding from a seawater-filled hole in a 5 x 10 mm diameter aluminium specimen support. The specimen was fractured after insertion into the cryoSEM. The body wall is marked by arrowheads, the outer surface of the specimen is seen at the bottom of the figure. Compared to the image of an optimally frozen, cryomounted specimen in Figure 41, gross internal freezing damage has occurred. Scale bar: 10 μm. Reproduced, with permission, from Ryan *et al.* (1988) Cryo-Letters 9, 418-425.

cryoultramicrotomy (Karp et al., 1982; Steinbrecht & Zierold, 1984; Roos & Barnard, 1985). Recently, a new lower temperature glue which consisted of 30% ethanol, 30% methanol and 40% water was introduced by Martin Michel (*pers. comm.*). Its melting point was 133 K (-140°C) and it was designed to mount vitrified material from high pressure freezing onto cryoultramicrotomy pins without devitrifying the specimen.

The Chaetognath results (Figures 41 & 42) show a marked difference between the specimen frozen on the standard specimen support and the specimen frozen optimally and then cryomounted onto its support. While there is still obvious crystal artifact in the cryomounted specimen the result is important for X-ray microanalysis because it means that there is less redistribution of elements. Thus, scanned fields of view are less disturbed from the normal ionic concentration by the cryomounting method. This should be beneficial for X-ray microanalysis, because improved homogeneity of the body cavity fluids would give more reproducible results.

The apparent absence of artifact in the body wall layer of Figure 41 is significant because it suggests that frozen specimens can be subjected to the relatively high subzero temperature of 213 K (-60°C) without inducing observable additional crystal artifact, at least by the present imaging method of cryoSEM. The question of the growth of ice crystals will be addressed further in Section 10.

The image presented in Figure 43 is interesting in that it provides a "ghost" version of a situation described by Dubochet & MacDowall (1984). They reported that, because electron diffraction patterns from frozen sections were typical of single crystals, the frozen water in a cell formed a

Figure 43. Anaglyph of a carrot cell showing the ice cavity

Carrot root parenchyma cell located approximately 1 mm from the surface of the tissue block, frozen by plunging into liquid ethane, fractured, freeze-dried and gold-coated within the cryoSEM. The cell interior shows the honeycomb of salts and organic solutes which were deposited in the eutectic during freezing. This figure demonstrates the continuous nature of the ice cavity, showing that the water formed perhaps only one crystal which ramified through the cell. Crystal nucleation probably occurred on the right side of the cell and laminar dendrites radiated from this point. Perforations through the deposited laminar sheets serve to illustrate further the continuity of the crystal. Scale: field width = 140 μm.

This figure should be viewed using the red-green stereo viewers which are located inside the rear cover

single, ramifying, dendritically branched crystal. In Figure 43, the cell water has been sublimed away by freeze-drying. The resulting matrix in the cell shows that the space that was occupied by frozen water is continuous and supports the findings of Dubochet & MacDowall.

The ice cavity varies in width. Around the edge of the cell the ice space is narrow, reflecting the lower water content of the peripheral cell cytoplasm. The large central vacuolar area shows wider spacing, reflecting the higher water content. The observed matrix consists of salts and amino acids which separated out from the water as it crystallised and which were deposited in the eutectic mixture which formed between the crystal dendrites (described in Section 2.9). These specimens normally collapsed when removed from the microscope and then re-examined later.

The results shown in Figure 43 would probably not be obtained if previously used solvent-only low temperature cements were used. These would sublime away while the specimen freeze-dried in the microscope and result in detachment of the specimen from its support.

The cryomounting method described here was reported by Ryan *et al.* (1988).

9.6 Conclusions

1. Standard solvent-based electroconductive cements were used to attach frozen specimens to supports at temperatures in the region of 213 K (-60°C).

2. Specimens were cryofixed while supported by a low thermal mass support, so that cooling was more efficient and ice crystal damage was reduced. They were then oriented as required for observation by cryoSEM.

3. The specimens were freeze-etched and freeze-dried as required and remained attached to the supports by an electro-conductive matrix.

4. The method did not induce additional observable ice crystal artifact which was observable by cryoSEM.

10 The effect of exposure to subzero temperatures

10.1 Summary

The growth of ice crystals was studied in red blood cells in 100 μm-thick slices of flounder spleen which were optimally plunge-frozen on low thermal mass supports. The specimens were stored at subzero temperatures for periods of up to 8 days. There appeared to be no observable change after 8 days at 193 K (-80°C) and 2 days at 213 K (-60°C). Specimens stored at 233 K (-40°C) showed fine-order mottling after 8 days, this appeared after only 45 minutes in specimens stored at 253 K (-20°C). These specimens developed crystals which were up to 40 nm in width which did not increase in size with further exposure of up to 8 days. The cells appeared to shrink during this period and the extracellular space enlarged. Cells stored at 263 K (-10°C) showed no signs of crystal damage, but after 45 min they had shrunk and lay in enlarged extracellular spaces.

10.2 Introduction

The objectives of this Section were to investigate two areas. The first question was to ascertain if crystals might grow during storage at 193 K (-80°C), as this was the temperature at which freeze-substitution was carried out. It was envisaged that the results of the crystal analysis in Section 7 (Crystal growth in metal-sandwiched specimens) might not result from the original cryopreparation but from some metamorphosis induced by processing at that particular temperature. The second related question was whether exposure to 213 K (-60°C) during cryomounting would induce crystal growth in specimens which were otherwise optimally frozen.

Some of this concern may have arisen from the work of Meryman (1957) who found that when replicas of amorphous ice films were exposed to 193 K (-80°C) for 5.5 minutes they developed 0.5 μm crystals. Nei (1973) showed that when glycerinated erythrocytes were exposed for 30 minutes to 203 K (-70°C) they also developed small crystals and that similar crystals developed during 14 days storage at 193 K (-80°C).

In view of the above, it would seem that some investigation in this area would be worthwhile, particularly as Meryman (1957) and Nei (1973) used freeze-fracture replicas to measure crystals. Replication provides a rapid and direct method of measurement compared to the 48 hour freeze-substitution method used in the present work, during which time a great deal of change in ice crystal size might be envisaged.

10.3 Experimental Design

Both fresh and prefixed flounder spleen (Section 3.19) were used in this study. Prior experience with prefixed material showed that, when the 5% glutaraldehyde was washed out with saline, it behaved as fresh material as regards the formation of ice crystals that occurs during rapid freezing.

The prefixed material was sliced at 100 μm thickness with a vibrating microtome as described in Section 3.19. The slices were mounted on low thermal mass supports built on a U-frame covered with aluminium foil (see Figure 11) and rapidly frozen in the deep plunging device (Section 5). The specimens were recovered from the coolant and stored in plastic cryotubes in liquid nitrogen to await the various post-treatments at different temperatures.

Exposure at 193 K (-80°C), 213 K (-60°C) and 233 K (-40°C) was achieved on a thermal gradient in a long-necked 25 l LN_2 dewar which was about one-third full. This was the same method as described in Section 3.15 for freeze-substitution. Essentially, a brass gauze basket was suspended at the required temperature, as measured by a thermocouple attached to its base. Exposure at 253 K (-20°C) was done in a chest freezer, the temperature of which cycled between 253 and 255 K (-20 and -18°C). Exposure at 263 K (-10°C) was done in the freezer compartment of a domestic refridgerator where the temperature cycled between 262 and 264 K (-11 and -8°C).

When the temperature had stabilised at the required setting, the frozen specimens were retrieved from storage in liquid nitrogen and transferred to a polystyrene box which contained liquid nitrogen. Here the tubes were emptied of LN_2, recapped loosely and inserted in the dewar neck. This procedure was adopted so that the specimens reached the set temperature quickly. The specimens exposed to 193 K (-80°C) reached the temperature in approximately 15 minutes, those exposed to 213 K (-60°C) reached the temperature in 35 minutes and those exposed to 233 K (-40°C) reached the temperature in 50 minutes. The specimens exposed to 263 K (-10°C) were placed in the freezer box in a precooled aluminium block which had holes drilled to accept the tubes, they reached temperature in 10 minutes. This method was also used at 253 K (-20°C), with a similar time response. The timed exposures started from when the nominated temperatures were reached.

The prefixed material was treated at 193, 233, 253 and 263 K (-80, -40, -20 and -10°C) for periods from 45 minutes up to 8 days. After exposure, a liquid nitrogen-containing polystyrene box was brought to just

above the specimen. A cryotube full of liquid nitrogen was placed alongside the tube containing the exposed specimens and the sample was inserted into the liquid nitrogen. It was stored for subsequent freeze-substitution (Section 3.15) and transmission electron microscopy (Section 3.16). Fresh flounder spleen was cryofixed on the foil-arch type of low thermal mass support as described by Ryan & Purse (1984). These specimens were stored at 213 K (-60°C) for 48 hours before freeze-substitution. Freeze-substitution was always performed at 193 K (-80°C) for 48 hours.

10.4 Results

The prefixed tissue stored at 193 K (-80°C) showed no signs of ice crystal development, as seen in Figures 44.A and 45.A. The only possible sign is the clarity of the perinuclear space in Figure 45.A, although this appearance occurred somewhat irregularly and was not seen in the specimens stored at 213 K (-60°C). Figures 44.B and 45.B show results from exposure to 233 K (-40°C) for 8 days, there are crystals in the high magnification image and signs of an enlarged perinuclear space in the low magnification field. Figure 45.B does show clear spaces between the cells, but similar spaces are seen in chemically processed specimens also, so they may not be directly attributed to ice artfact.

The specimens exposed to 253 K (-20°C) showed a mottled appearance at high magnification as seen in Figure 44.C, where the profiles are measured at approximately 40 nm in width. They showed this from the 45 minute exposure through to the 8 days exposure, without any apparent increase in crystal size. The low magnification field in Figure 45.C shows a marked development in that the cells have shrunk and lie in large, clear spaces. These can be observed after 1 day at this temperature.

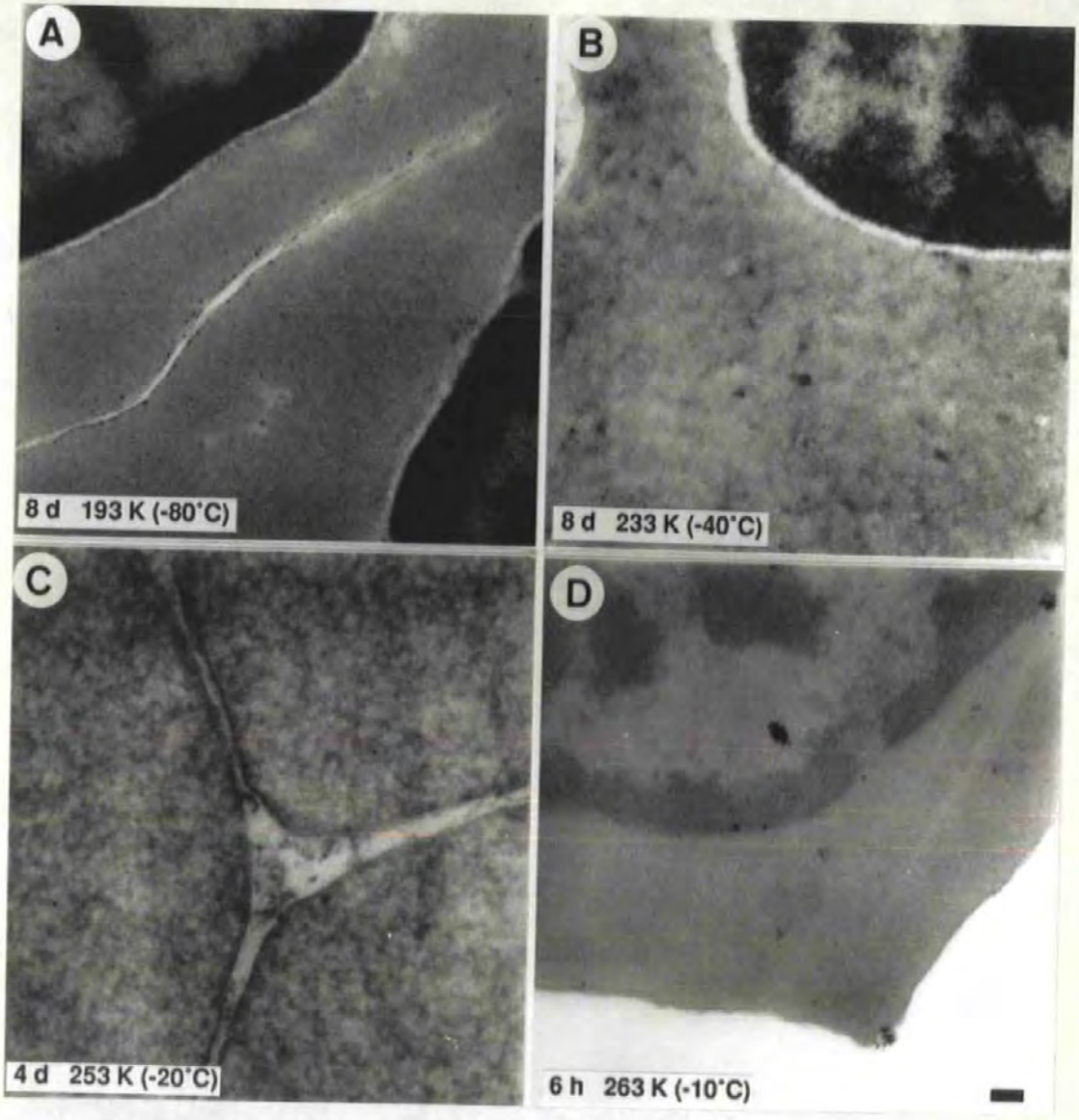

Figure 44. Frozen cells stored at high subzero temperatures - I

High magnification images of rapidly frozen red blood cells stored at different subzero temperatures for periods of up to 8 days, followed by freeze-substitution at 193 K (-80°C) over 48 h. No discernible intracellular crystal development can be observed in (A). (B) and (C) show crystal formation and (D) does not appear to show intracellular ice crystals. The blood was obtained from flounder, *Platichthys flesus*. Scale bar: 100 nm.

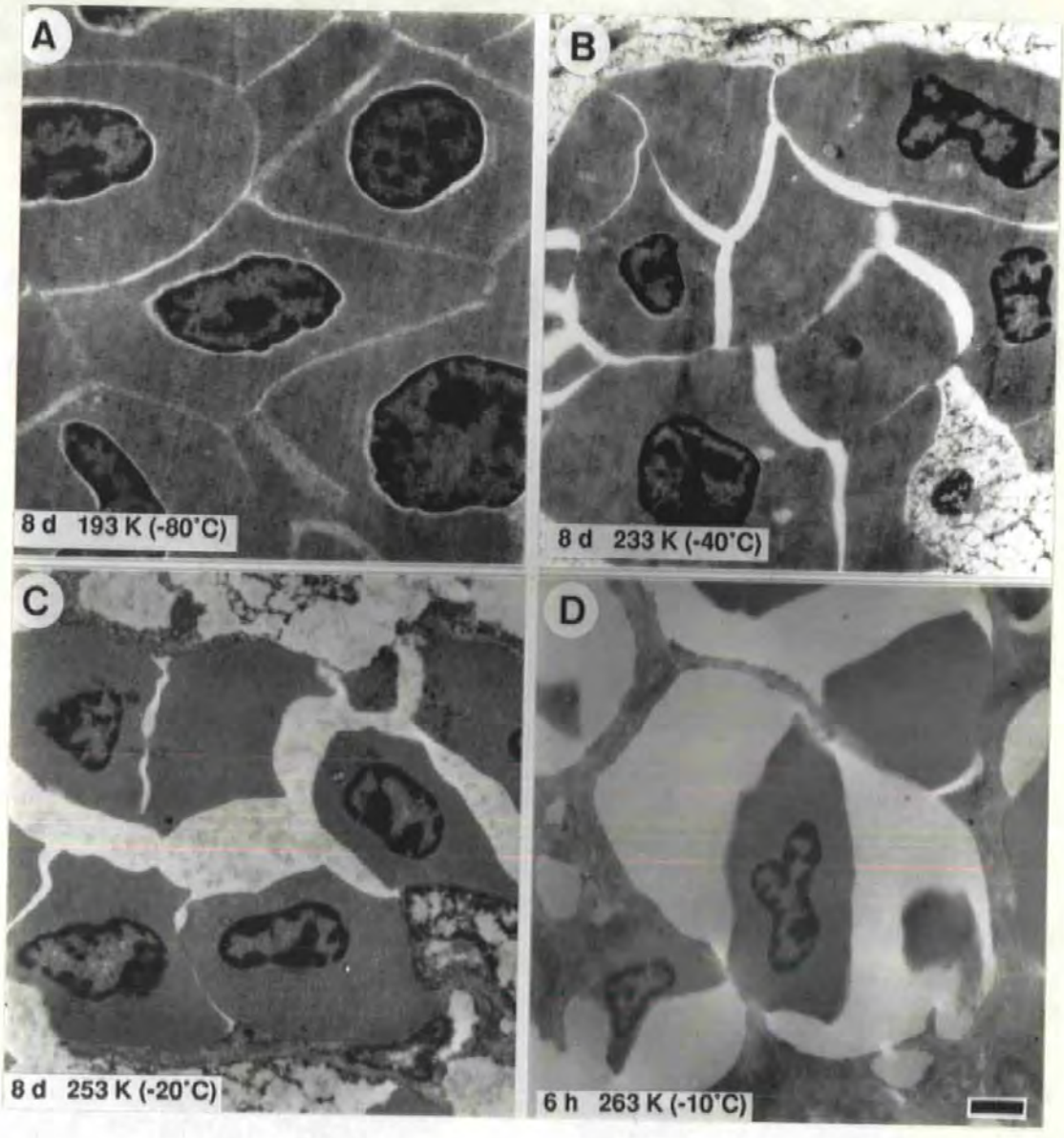

Figure 45. Frozen cells stored at high subzero temperatures - II

Low magnification images of rapidly frozen red blood cells stored at different subzero temperatures, followed by freeze-substitution at 193 K (-80°C) over 48 h. (A) The erythrocytes show no signs of crystal development. (B) and (C) The extracellular space is enlarged and the cells show fine-order mottling due to crystal formation. (D) The cells are shrunken and the extracellular space is enlarged. The blood was obtained from flounder, *Platichthys flesus*. Scale bar: 1 μm.

Exposure to 263 K (-10°C) produces smooth red blood cell cytoplasm which is devoid of apparent crystal artifact, after 45 minutes (Figure 44.D). The cells are obviously shrinking after 45 minutes and after 6 hours they are noticeably shrunken and surrounded by large cavities (Figure 45.D).

The cells in the fresh material which was stored at 213 K (-60°C) for 48 hours showed no signs of crystal damage and the intercellular spacing similarly shows no sign of disturbance by ice crystal artifact (Figure 46).

10.5 Discussion

The results in this study were quite unexpected. It had been assumed that some progressive development in crystal growth with higher temperatures would be encountered at some stage and that some reasonable correlation of time versus temperature would be forthcoming. Instead, there was an indefineable result at the remarkably high subzero temperature of 253 K (-20°C). This took the form of crystals which appeared in the blood cells after 45 min but which did not appear to grow in the cells. The extracellular crystals appeared to grow at the expense of the intracellular medium, by migration of water molecules from the small intracellular crystals to the larger extracellular crystals. The larger crystals represent a lower energy state (Section 2.12) and the process results in shrinkage of the red blood cells.

Two conclusions can be drawn from these results. Firstly, the 8 days storage at 193 K (-80°C) did not induce crystal artifact and therefore the results of the crystal analysis in Section 7, where specimens were exposed to 193 K for only 48 hours during freeze-substitution, are valid. Secondly, 2 days at 213 K (-60°C) did not induce crystal growth, therefore the

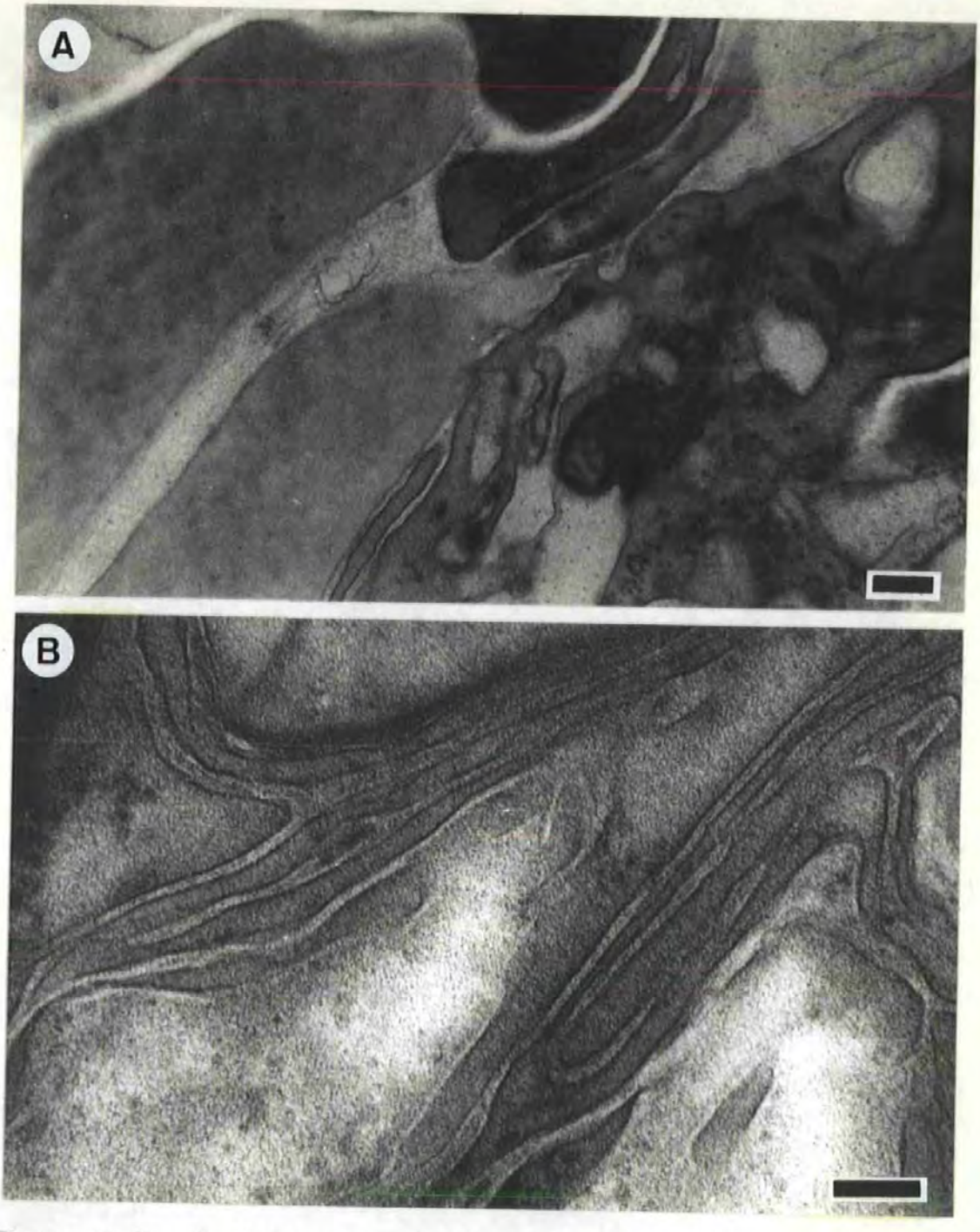

Figure 46. Cryofixed spleen stored at 213 K (-60°C) for 48 hours

A. The red blood cells, at left, and reticular cells, at right, show no sign of ice crystal formation. Scale bar: 100 nm.

B. The extracellular space between the tissue elements in this field shows no sign of ice crystal formation. Scale bar: 100 nm

cryomounting process, which involved approximately 10 minutes at this temperature, did not induce further crystal artifact.

These results are not without precedent as there are several pieces of evidence in the literature. Some were supplied by the pioneering cryobiologist, Luyet (1960). He coined the term *"irruptive recrystallisation"* to describe the development of crystals in crystal-free films which were warmed to certain specific temperatures. These events were governed by the molecular weight of solute that they contained. For glycerol, it was 208 K (-65°C); for sucrose, it was 242 K (-31°C); for gelatin, 261 K (-12°C) and for soluble starch solution, it was 267 K (-6°C).

Luyet also used the term *"migratory recrystallisation"* to describe the growth of larger crystals in solution at the expense of smaller ones. A frozen solution of 10% glycerol showed this after 15 min at 253 K (-20°C). The same solution of gelatin showed no growth after 36 hours at 253 K, which supported the findings relevant to irruptive recrystallisation.

The results of Meryman (1958), which are mentioned in the Introduction to this Section, may be explained by the technique that he used to show crystal growth. The temperature of the specimen during etching and shadowing may not have been controlled. Inadvertently, there can be an input of considerable heat from evaporative metal shadowing. This problem has been addressed by Robards *et al.* (1981) and Echlin *et al.* (1985).

Nei (1973) reported crystal growth at 193 K (-80°C) in *glycerinated* blood cells, but this report also repeats earlier work (Nei, 1971), where blood cells without cryoprotectant were frozen and exposed to 243 K

(-30°C) for 30 minutes without inducing crystal growth. In this case it was the presence of glycerol which lowered the recrystallisation temperature.

Further evidence for the high thermal stability of cryofixed specimens at fairly high temperatures is seen in the results of Woolley (1974) and Barlow & Sleigh (1979) who freeze-substituted specimens at 223 K (-50°C) while retaining good preservation. Steinbrecht (1985) exposed cryofixed moth sensory hairs to 230 K (-43°C) without damage after 45 minutes, although just 2 minutes at 250 K (-23°C) produced obvious secondary damage.

These reported results all support the findings of MacKenzie (1980), who used differential thermal analysis to investigate crystal growth in a wide range of frozen gels. He found that they were remarkably stable up to between 238 and 263 K (-35 and -10°C) when they exhibited *"antemelting"*, this describes their aquisition of new translational mobility. At between 243 and 267 K (-30 and -6°C) they manifested exotherms from migratory recrystallisation, or growth of already-frozen ice crystals.

From these results, it may be surmised that freeze-substitution and freeze-drying might be performed at somewhat higher temperatures than the traditional 193 K (-80°C), as indeed has already been shown by Woolley and Barlow & Sleigh. The only *proviso* is that when the specimens contain very watery areas then these may undergo some metamorphosis at temperatures down to 193 K. Similarly, cryosectioning may be carried out at up to 243 K (-30°C) without seriously altering ice crystal damage in native-frozen specimens, although cryoprotected material would be adversely affected.

10.6 Conclusions

1. The erythrocytes did not show secondary ice crystal growth after prolonged exposure to 193 K (-80°C). Therefore the results of the ice crystal analysis in Section 7 are valid.

2. The specimens exposed to 213 K (-60°C) for 48 hours did not show secondary crystal growth, therefore the cryomounting process did not alter crystal damage brought about during cryofixation.

11 The rate of cryosubstitution

11.1 Summary

The rate of freeze-substitution was investigated in blocks of frozen gelatin which were substituted at 193 K (-80°C) in methanol containing 4% uranyl acetate. Samples were taken out at intervals between 1.5 and 48 hours, drained at 193 K and then stored in liquid nitrogen. The specimens were subsequently freeze-dried, embedded in resin, planed and examined by back-scattered electron imaging. The maximum penetration of uranium measured on micrographs was found to be 320 μm, although after allowing for the linear shrinkage of up to 50% which occurred during freeze-drying this distance could be almost doubled.

11.2 Introduction

The objective of this final investigation was to ascertain how quickly frozen specimens might be freeze-substituted by the method which was chosen earlier in the work to measure ice crystal damage in hydrated specimens, namely using methanol at 193 K (-80°C).

Without such an investigation, an important question would remain as to whether the freeze-substitution process was completed during the experiments or whether it was terminated prematurely, *i.e.* after 48 hours? If the latter were the case, then the results of the crystal analyses in Section 7 may not be valid. They might be properly substituted at the surface layers but within the specimen there may be some alteration brought about as the unsubstituted areas warmed up or thawed, thus altering the effective crystal size which occurred on cryofixation.

The original intention was to perform a multifaceted study which involved cryomounting time-resolved stages of freeze-substitution for freeze-fracture and examination by cryoSEM. The fractured specimens were to be gently etched in the vacuum, in anticipation that the solvent would sublime away before the frozen water in the specimen. The intention of this was to reveal the solvent-water interface in the specimen, so that progression of solvent penetration could be measured. This was to be followed by back-scattered imaging and X-ray line-scan profiling to identify the penetration of the heavy metal fixing agent, namely uranium.

The correlation between solvent penetration and heavy metal penetration would be of great interest in the cryosubstitution process, unfortunately several initial trials proved not to be successful in these aims. The solvent demonstrated a propensity for liquefying on the cryostage of the SEM at a few degrees below its nominal melting point. This occurred almost immediately during slow rewarming when the first trace of any methanol in the vacuum was recorded by mass spectroscopy. It then welled up to obscure the fracture face which became covered with deposited uranyl acetate, thus precluding meaningful measurements.

As with the previous Section, there is a lack of reported results regarding the rate of freeze-substitution. Zalokar (1966) observed the extraction of methylene blue from soaked filter papers which were frozen and concluded that acetone was not very efficient although this has subsequently been shown to be otherwise. Ornberg & Reese (1981) measured the extraction of tritiated water by acetone from 10 μl droplets. Humbel & Müller (1986) also used the extraction of tritiated water from filter papers as a measure of freeze-substitution in different solvents. The

observation method used in the present work seems to be previously unused.

11.3 Experimental Design

Pieces of prefixed gelatin were washed out in distilled water and cut into strips, approximately 1 mm square by 5 mm long. The cross-sectional dimensions of 6 specimens taken from the same strips were 1.26 mm (SD 0.063) by 1.15 mm (SD 0.16). The specimens were suspended from the tips of fine forceps and plunge-frozen in ethane in the benchtop plunger (Section 4). The specimens were collected in liquid nitrogen and placed in Nunc cryotubes containing 1.0 ml of methanol with 4% weight of uranyl acetate added. These tubes were put to freeze-substitute at 193 K (-80°C) in the neck of a dewar as described in Section 3.15.

The specimens were freeze-substituted for periods of 1.5, 3, 6, 12, 24 and 48 hours. After the selected time interval, the top was removed from the cryotube, the specimen retrieved with precooled forceps, drained on precooled filter paper stored beside the cryotube, transferred to a precooled empty cryotube and stored in liquid nitrogen until required for freeze-drying (described in Section 3.25). During freeze-drying, the Anavac system was used to record mass spectra of the residual gases in the vacuum.

After freeze-drying, the specimens were embedded in epoxy resin (Spurr, 1969), planed on an ultramicrotome, carbon-coated and examined by SEM (Section 3.22) using back-scattered electron imaging by means of a Robinson detector.

11.4 Results

Partial pressures which were recorded during freeze-drying are shown in Figure 47. The top spectrum shows nitrogen and oxygen in the same proportions as they occur in air. This indicates that they were the residual air gases remaining shortly after the specimens were introduced into the freeze-drying system. This was done at 1015 h. The second spectrum from the top of the figure is recorded at 10 times the sensitivity of the first and shows the appearance of methanol peaks in the vacuum at 143 K (-130°C). Water appeared at about 183 K (-90°C) and is evident in the fourth spectrum, which was recorded at 203 K (-70°C). Water was recorded in the vacuum until the specimen reached approximately 273 K (0°C). These spectra were recorded during a later, accelerated process so as to record the events which would normally occur overnight.

The freeze-dried specimens are shown in Figure 48, where the white outer zone represents the presence of uranium penetrating the gelatin. There are obvious cracks and fissures in the specimens, some of which are produced by the rapid freezing process and others by the freeze-drying process. The cross-sectional dimensions of the specimens as measured on the micrographs are 0.76 mm (SD 0.08) by 0.58 mm (SD 0.096).

The penetration of uranium was measured against the SEM scale bar and plotted in Figure 49. This shows both minimum and maximum penetrations of the uranium. The minimum and maximum penetrations after 48 hours were 160 and 320 μm respectively. These results are effectively minimal penetrations, because the tubes were not disturbed during the freeze-substitution process. In other words, there was no stirring or replenishment of the freeze-substitution medium.

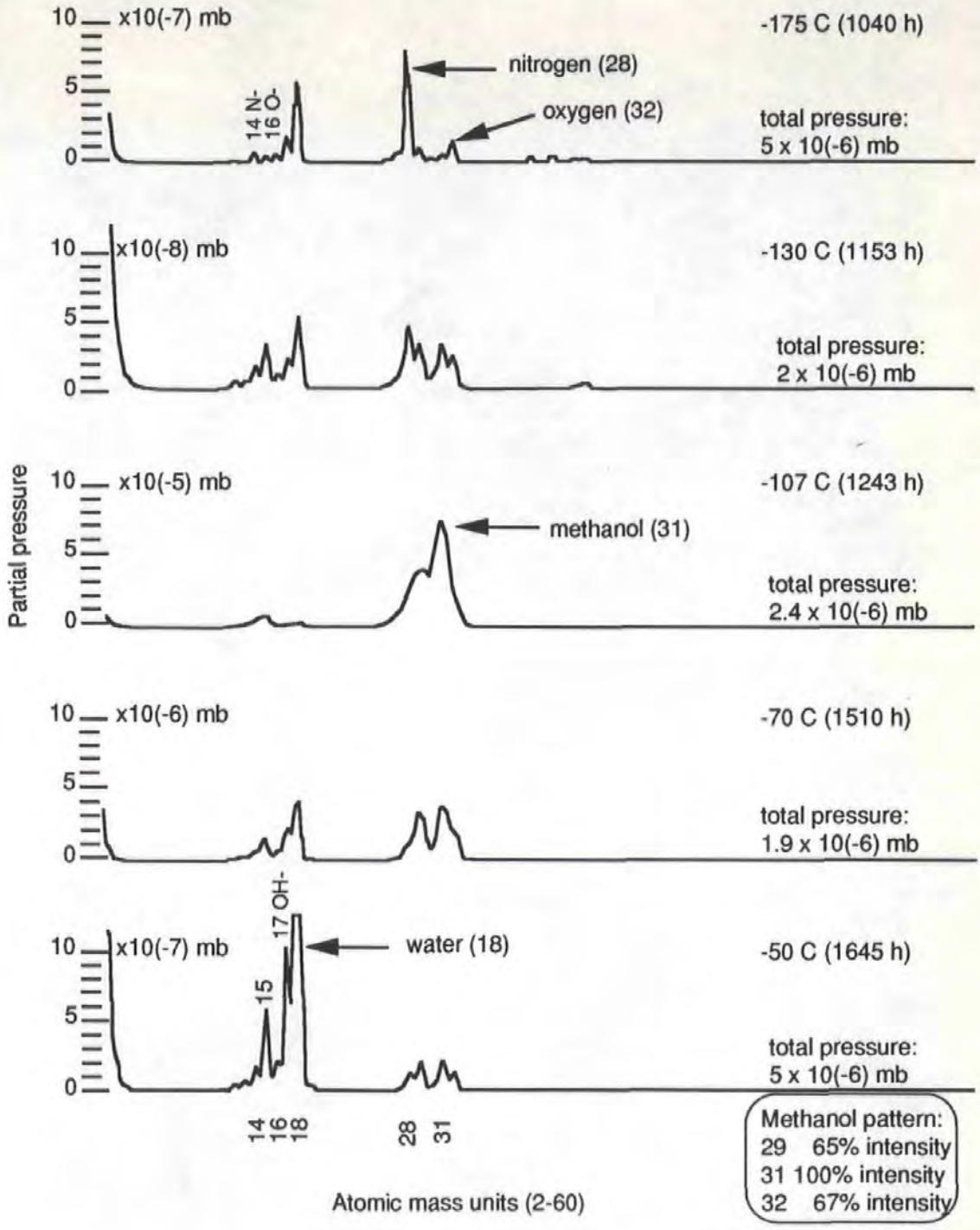

Figure 47. Partial pressures recorded during freeze-drying

Mass spectra recorded during the freeze-drying of specimens which had been partially freeze-substituted in 4% uranyl acetate in methanol. Note the residual air gases in the top spectrum, the methanol in the three central spectra and the relative amounts of water and methanol in the bottom spectrum.

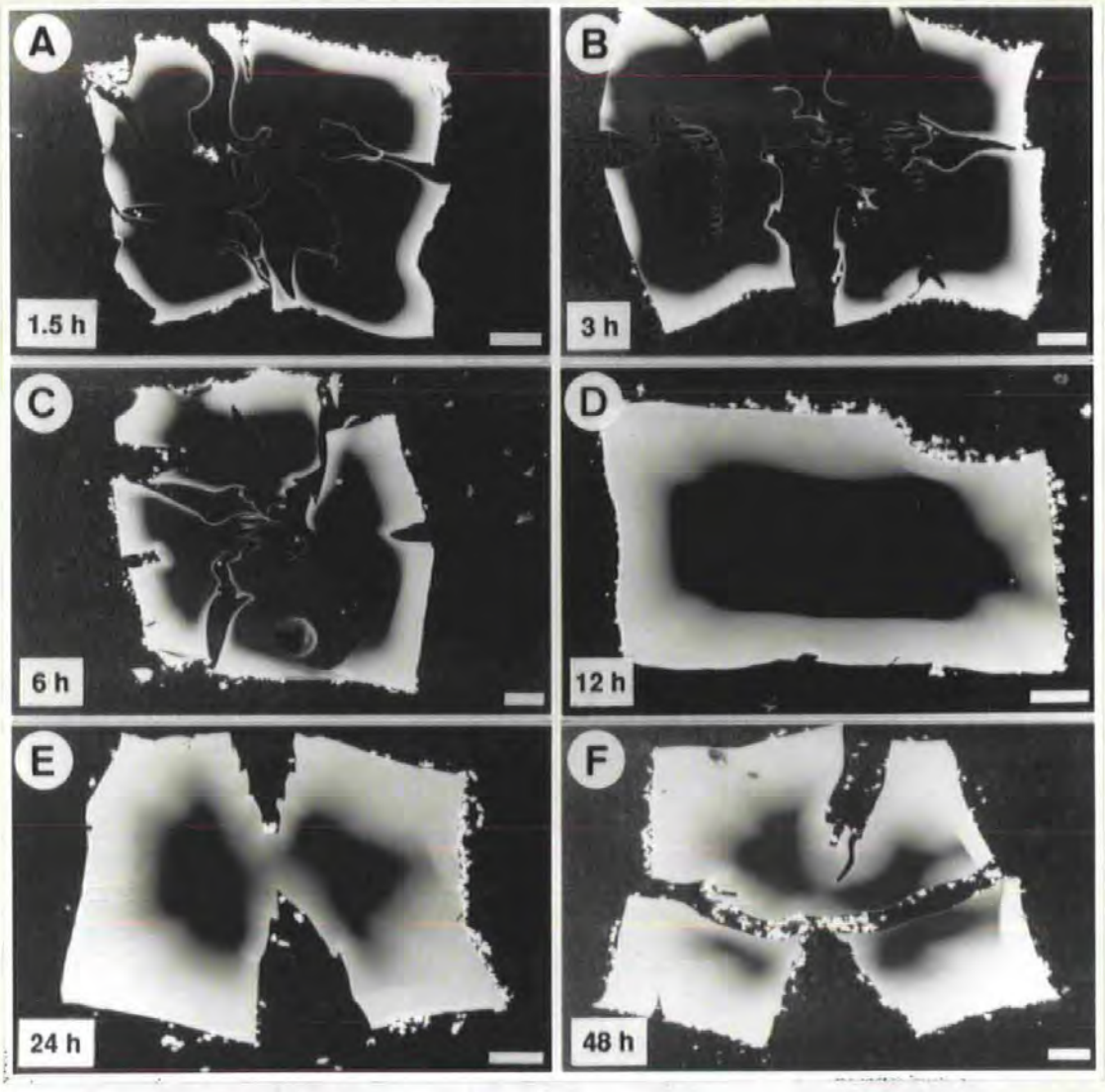

Figure 48. Images of uranium penetration during cryosubstitution

Back-scattered electron images of cross-sectional views of gelatin blocks which were freeze-substituted over timed intervals at 193 K (-80°C) in methanol containing 4% uranyl acetate. The blocks were then freeze-dried, embedded in resin, planed and coated with carbon before viewing. The various freezing cracks have distorted during the shrinkage which is associated with freeze-drying. It is possible that the results, plotted in Figure 49, underestimate the penetration of osmium because uranium is a heavier ion and will diffuse more slowly into the specimens. The 40-50% linear shrinkage of the specimen (see Section 11.5) will also underestimate the penetration. Scale bar: 100 μm.

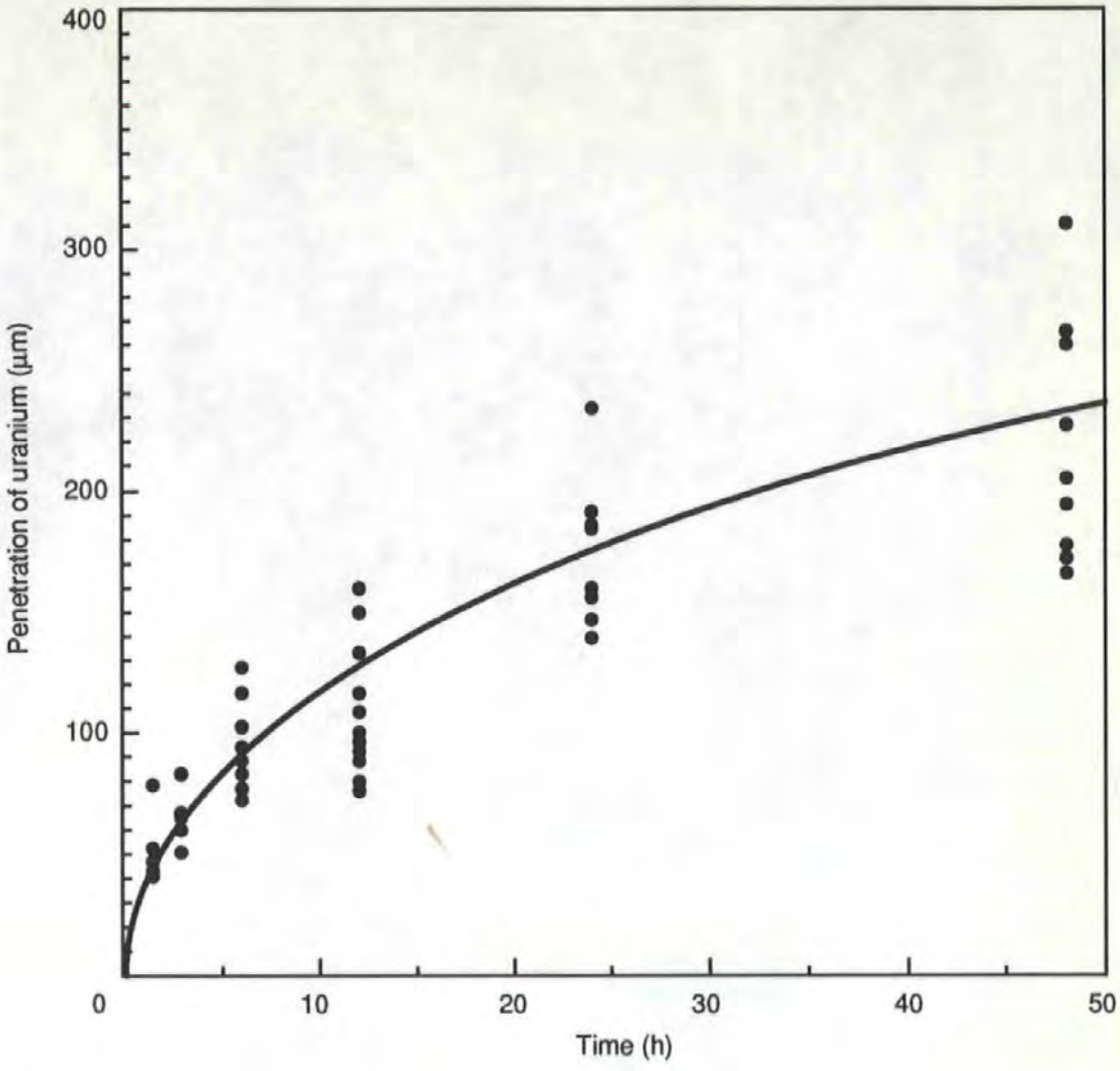

Figure 49. The penetration of uranium during freeze-substitution

Depths to which uranium penetrated into frozen gelatin blocks during 1.5, 3, 6, 12, 24 and 48 h exposure periods to 4% uranyl acetate in methanol at 193 K (-80°C), thus monitoring the process of freeze-substitution. After the exposure, the specimen was cooled in liquid nitrogen, freeze-dried and examined by back-scattered scanning electron microscopy, the results are shown in Figure 48. This figure shows the scatter of results and these should be interpretted with regard to freeze-drying shrinkage which is as high as 50% in these specimens, as discussed in Section 11.5, thus giving maximum uranium penetrations of 500-600 μm. These results may underestimate the solvent penetration depths due to different diffusion rates.

11.5 Discussion

The results of this simple investigation indicate that the freeze-substitution process proceded to the extent that the uranium could penetrate 320 μm during the 48 hour time interval routinely allowed for the process. This was in some ways the worst case situation because there was probably a diffusion lag between the heavy metal penetration and the ingress of the methanol. Also there was no stirring in this process, it was purely diffusion driven.

Mean specimen size, based on 6 measured specimens, was 1.26 x 1.15 x 5.2 mm, giving a volume of 7.25 μl where 5.8 μl of this was water. During freeze-substitution it would be immersed in a 1.0 ml volume of medium so that there was a solvent/specimen volume ratio of about 170:1. This was important because it meant that the maximum water content of the methanol would become 0.58% which would not affect the efficiency of freeze-substitution. The work of Humbel & Müller (1986) showed that methanol would continue to substitute tritiated water from frozen filter papers at 183 K (-90°C) with up to 10% water present.

Ornberg & Reese (1981) substituted 10 μl samples in 10 ml acetone at 190 K (-83°C). They found that the samples which were frozen on a helium-cooled copper block and contained small ice crystals, were substituted in about 25 hours. The specimens quenched in Freon 22, and which contained larger crystals, appeared to be only 70% substituted in the same time.

The mean cross-section size of the six freeze-dried specimens, 0.76 x 0.58 mm, indicates that considerable shrinkage occurred during the drying process. Unfortunately, the specimens were not measured before freezing

and freeze-drying, but when they are compared with the mean size of six specimens from the same batch, namely 1.26 x 1.15 mm, it can be suggested that 40-50% linear shrinkage occurred. This means that the maximum depth to which the uranium penetrated, which was measured in Figure 48.F as 320 μm, can be nearly doubled to 640 μm.

An additional point concerning freeze-substitution relates to the difference in mass between the methanol molecule with a molecular weight of 32 and uranyl acetate ($UO_2(C_2H_3O_2)_2.2H_2O$) with a molecular weight of 424.15. This implies that uranium ions (A.W. 238.03) will penetrate the gelatin much more slowly than the methanol, because, as Sjöstrand (1990) states:

> *"the laws of mechanics apply to translational motions. At a given temperature, the mean translational kinetic energy, E_M, of a population of molecules with mass m and velocity v is $E_M = ½mv^2$*

He continued, and derived (1) that in a population of molecules with different molecular weights the heavy molecules will move more slowly than the lighter molecules, (2) that the mean translational kinetic energy is a function of temperature and (3) that there is an inverse relationship between the rate of diffusion and viscosity.

11.6 Conclusions

1. The penetration of uranyl acetate during 48 hours of freeze-substitution at 193 K (-80°C) reached a measured maximum of 320 μm, as measured on the micrographs. Allowing for the 40-50% linear shrinkage which occurred during the freeze-drying process, the maximum penetration can be estimated to be in excess of 600 μm.

2. The penetration of the substituting medium, namely, methanol, ingressed in front of the heavy metal ions. Therefore, the real progress of freeze-substitution was better than was measured by the back-scattered electron imaging technique.

3. From the results in this Section, it can be concluded that the metal-sandwiched gelatin and blood specimens, which were 360 μm thick, were properly freeze-substituted and their ice-crystal analyses in Section 7 were valid.

12 General Conclusions

The overiding conclusion of the investigations in this work is that ethane is a superior coolant for cryofixation than propane or Freon 22. This was established in Section 4, by measuring cooling rates with a bare thermocouple which represented a metal specimen. It was repeated at other stages of the work such as in Section 5, where cooling was measured in hydrated specimens; in Section 6, where cooling was measured in composite, metal-sandwiched hydrated specimens; and in Section 7, where crystal growth was analysed in hydrated specimens after they were frozen in the different coolants.

The cooling efficiencies of ethane and propane were found in Section 5 to have ultimate limits, where the final cooling rates in a hydrated specimen could be ratioed and found to reflect predicted cooling efficiencies. Ethane cooled the exposed, hydrated specimen 33% more efficiently than propane.

A conclusion of Section 6 was that the depth of the coolant was important and that arrested plunges produced slower cooling rates and larger mean ice profile size, as is seen in measured crystal sizes in Section 7. A corollary to this was that the release of the latent heat of the fusion of ice was antagonistic to the cooling of the specimen, to the point of remelting it during slow cooling.

The depths at which the specimen centre reached 273 K (0°C) and the calculated depths at which the specimen completely froze showed disparity. The calculated depths, which were minimum plunge depths, were appreciably greater than the measured depths at which 273 K was

reached. This was attributed to the specimen not having frozen and given up its latent heat at 273 K.

A third depth was measured at which cooling curves entered a straight line phase. This was interpreted as the point at which the specimen completed freezing. This was deeper than the calculated depths and was interpreted as indicating that cooling in the experiments was not ideal, probably because of cavitation effects.

An important aspect of monitoring cooling was raised in Section 6. This concerned temperature ranges over which cooling rates are measured. Cooling rates have been said to improve with increased plunge velocity, but this depends on the temperature range over which cooling is monitored. When temperatures down to 233 K were monitored, the cooling rate was quite uniform and independent of the plunge velocity. It was concluded that a more meaningful approach to the monitoring of cooling would be useful.

There was good agreement between experimentally measured and theoretically predicted ice crystal sizes shown in Section 7. This shows that modelling can successfully predict cryofixation results, although it must be emphasised that the specimens were chosen for their cytoplasmic homogeneity. Most specimens manifest variation in water content across the cellular domains.

The cryoSEM investigation in Section 8 proved the potential of cryofixation. Cryofixed specimens were found to manifest ecophysiological differences between two species which were related to their occurrence in different water masses in the sea off Plymouth. The use of low thermal

mass supports with these specimens revealed another potential in cryofixation, the phenomenon of centre-line-cryofixation. This occurs when cooling fronts can converge from different directions and it results in sudden improvement in the cooling rate in the centre of thin specimens.

The cryomounting technique described in Section 9 was shown to be useful for mounting specimens for cryoSEM after they had been optimally frozen on low thermal mass supports. Taken with the results of Section 10, it was shown that exposure of the specimens to the cryomounting temperature of 213 K (-60°C) for 10 minutes did not induce secondary ice crystal growth, nor did exposure to this temperature for 48 hours.

The results on the effects of exposure to subzero processing temperatures in Section 10 are remarkable. They show that despite the metastability of frozen specimens in the vitreous and cubic ice phases, they are remarkably stable in the hexagonal ice phase up to quite high subzero temperatures. There is evidence in the literature for this although it seems to have been overlooked during recent years. It has significance for the temperatures at which cryosectioning, freeze-drying and cryosubstitution are performed.

The assessment of the penetration of heavy metal ions during cryosubstitution, as reported in Section 11, appears to be the first time that direct observation of the process has been attempted using electron microscopy, albeit here after freeze-drying. This is quite surprising in view of the fact that cryosubstitution was introduced into electron microscopy over thirty years ago (Fernández-Morán, 1960). The purpose of the present investigation was to check if the process was completed in the 48 hours

allowed. The reason was to ascertain if the ice crystal analyses were valid, which they were found to be.

The final conclusion of the experiments is that the ice crystal damage observed in this work after freeze-substitution is primary freezing damage. That is, it is caused during the cryofixation process and not during subsequent cryoprocessing.

The overall conclusions of this work are that cryofixation has much to offer in biological electron microscopy. It has already achieved the true vitrification of thin specimens, as shown by Dubochet and his collaborators. However, as Sjöstrand (1990) noted:

> *"Cryofixation is an example of a word that has perpetuated a misconception. The word "fixation" has been used by microscopists to characterise a treatment that aims at stabilising the structure of cells enough to prevent structural damage during embedding in a suitable medium. The word "cryofixation" therefore conveys the impression that freezing fixes the tissue and consequently prevents structural modifications from occurring during the embedding of the frozen tissues..... The two methods used for embedding frozen tissues are freeze-drying and freeze-substitution. These procedures have been referred to as involving physical fixation in contrast to conventional chemical fixation."*

Sjöstrand continued, stating that care is necessary in the further cryoprocessing of specimens if structural and molecular conformational changes are to be avoided. The native conformation of protein molecules is imposed by thermodynamic forces which are weakened when temperature

is lowered, rendering the proteins more susceptible to denaturing by the diffusion of the sidechain components and to the denaturing action of solvents and embedding media. Therefore, the time of exposure to the action of these chemicals should be minimised. The use of small specimens is an aid to this end.

It is clear that, while cryofixation and other cryotechniques are powerful tools in biological electron microscopy, there is still much that needs further investigation. For instance, is there a critical size of metal-sandwiched, freeze-fracture specimen above which subcooling factors become important, whereby propane becomes the more efficient coolant? This could be important where relatively large hinged holders are used, although the general rule of reducing specimen and holder mass to a minimum should be ever borne in mind.

Questions of a similar nature relate to the rapid freezing of exposed tissue specimens. These are, again, fundamental points: (1) what is the largest size of tissue block that can be frozen without ice crystal damage and (2) what is the thickest tissue slice that can be frozen without ice crystal damage? These could be tested by plunge cooling with the present equipment; an important aspect would be to use low thermal mass specimen supports.

The question of optimal specimen size could not be answered completely without using all of the available freezing methods. Equipment for jet-cooling and slam-cooling would be needed and the methods would also need to be optimised. The jet method would need to ensure perfect coolant delivery (as discussed in Section 2.19) and the metal mirror method

would need to ensure that there was no mirror frosting and an absence of specimen bounce (as discussed in Section 2.20).

Both the jet-cooling and cryoblock-cooling methods prompt further questions. The results of this thesis show that thin metal-sandwiched specimens were cooled more efficiently in ethane than in propane. Therefore, since the jet device uses the same type of specimen, would ethane be a better choice of coolant rather than the normally used propane? In the cryoblock method, should copper or silver blocks should be used? Also, at what working temperatures? Should liquid nitrogen or liquid helium be used to cool them? For the ultimate cryoblock efficiency, it would be necessary to test the blocks at temperatures that bracket the theoretical optimal working temperatures regarding heat transfer properties (Bald, 1983).

These questions could be answered with minimal funding and reasonable workshop facilities. Obviously, attention should be paid to the high pressure freezing method, although this does not lend itself to easy do-it-yourself experiments; the investment of time and funding behind the commercial device is considerable. In an ideal situation, however, the size of the specimen chamber and, thus, the specimen, could be varied and tested.

A problem that attends all of the above questions is that of specimen perturbation prior to cryofixation (Sitte *et al.*, 1977). Often, too much time is devoted to sampling and rendering tissue samples down to dimensions that are suitably small for rapid freezing. This is done at the expense of specimen integrity, both structural and physiological. It may be that, with the exception of some naturally ideally-sized cell suspensions which can be

used in spray freezing, there will always be a compromise between specimen size and integrity. More attention should perhaps be given to methods of *in situ* cryofixation (Monroe *et al.*, 1968; Chang *et al.*, 1980; Zyglinicki *et al.*, 1986; Hagler *et al.*, 1989). This is certainly true where ionic analysis is the objective.

Finally, the last two questions addressed in this thesis, namely, the effects of exposure of cryofixed specimens to subzero temperatures and the rate of freeze-substitution, bear further attention. These are fundamental aspects of cryotechnique and yet they are little understood. After cryofixation, specimens must be further processed at low temperatures, unless they are examined at below the devitrification temperature. This means that specimens pass some time interval at an elevated subzero temperature at which water molecules may migrate to join small ice crystals. It is important to know at what temperature this begins and also what are the dynamics? How long a time can be passed at a certain temperature before crystals grow to an observable size?

The attempt in this thesis at answering these questions is restricted to work on blood cells in plasma (Section 10). It is probable that effects occurred in the plasma at temperatures lower than those at which they were seen to occur in the blood cells, namely 233 K (-40°C). Any alterations which did occur in the extracellular matrix may have been lost by redistribution during the freeze-substitution process. However, it was quite clear that the exposure to 213 K (-60°C) for 48 h did not induce crystal growth. Further investigation should be carried out between these temperatures using a more homogeneous tissue, such as liver, rather than blood cells. It would seem from these results that fresh frozen tissue is more resistant to relatively high subzero temperatures than might be

imagined; this was suggested by MacKenzie (1981) and found to be the case by Nei (1971, 1973) who also found that cryoprotected material showed crystal growth after only 30 minutes at 203 K (-70°C). This distinction between fresh and cryoprotected material seems not to be widely appreciated.

The final question asked in this thesis regarding the rate of freeze-substitution should be further investigated. The original proposal was to use differential etching in the cryo-SEM of cryo-fractured specimens after timed intervals of freeze-substitution and this still offers the most accurate and useful approach. The true progress of substitution would be revealed because it would show the solvent-ice interface. This is the most important aspect of freeze-substitution and not heavy metal penetration, particularly as freeze-substitution sometimes does not involve the use of heavy metal fixing agents (Monaghan & Robertson, 1990). Another important factor regarding accurate measurement of the process is that the shrinkage that derived from the freeze-drying which was used in this work would be avoided. This question could probably be answered quite easily using the equipment already to hand when sufficient time is devoted to the etching process. It is anticipated that answers from this area of investigation will be forthcoming.

Bibliography

Allison, D.P., Daw, C.S. & Rorvik, M.C. (1987) The construction and operation of a simple inexpensive slam freezing device for electron microscopy. J. Microsc. 147, 103-108.

Altmann, R. (1890) Die Elementarorganismen und ihre Beziehungen zu den Zellen. Veit u. Co., Leipzig. 145 pp., 20 plates.

Akahori, H., Yamada, E., Usukura, J. & Takahashi, H. (1980) Development of a rapid freezing device. J. Clin. Electron Microscopy 13, 576-577.

Angell, C.A. (1970) The data gap in solution chemistry: the ideal glass transition puzzle. J. Chem. Educ. 47, 583-587.

Angell, C.A. (1983) Supercooled water. Ann. Rev. Phys. Chem. 34, 593-630.

Angell, C.A. & Choi, Y. (1986) Crystallization and vitrification in aqueous solutions. J. Microsc. 141, 251-261.

Bachmann, L. & Schmitt, W.W. (1971) Improved cryofixation applicable to freeze-etching. Proc. Natl. Acad. Sci. USA, 68, 2149-2152.

Bachmann, L. & Schmitt-Fumian, W.W. (1973) Spray-freezing and freeze-etching. In: *Freeze-etching: Techniques and Applications* (eds. E.L. Benedetti and P. Favard) pp. 73-79. Société Française de Microsopie Électronique, Paris.

Bachmann, L. & Schmitt-Fumian, W.W. (1973) Spray-freeze-etching of dissolved macromolecules, emulsions and subcellular components. In: *Freeze-etching: Techniques and Applications* (eds. E.L. Benedetti and P. Favard) pp. 63-71. Société Française de Microsopie Electronique, Paris.

Bachmann, L. & Mayer, E. (1987) Physics of water and ice: implications for cryofixation. In: *Cryotechniques in Biological Electron Microscopy* (eds. R.A. Steinbrecht and K. Zierold) pp. 3-34. Springer-Verlag, Berlin, Heidelberg.

Baker, J. (1966) *Cytological Technique: the principles underlying routine methods,* 5th edition. Chapman & Hall, London.

Baker, H.D., Ryder, E.A. & Baker, N.H. (1961) *Temperature Measurement in Engineering*, Vol 2, Chap. 6, Rapidly changing temperatures. John Wiley & Sons, New York & London.

Bald, W.B. (1983) Optimizing the cooling block for the quick freeze method. J. Microsc. 131, 11-23.

Bald, W.B. (1984) The relative efficiency of cryogenic fluids used in the rapid quench cooling of biological samples. J. Microsc. 134, 261-270.

Bald, W.B. (1985) The relative merits of the various cooling methods. J. Microsc. 140, 17-40.

Bald, W.B. (1986) On crystal size and cooling rate. J. Microsc. 143, 89-102.

Bald, W.B. (1987) *Quantitative Cryofixation*. Adam Hilger, Bristol.

Bald, W.B. (1988) Theory of rapid freezing. Inst. Phys. Conf. Ser. No. 93: Vol. 3, Chap. 1, pp.9-14.

Bald, W.B. & Robards, A.W. (1978) A device for the rapid freezing of biological specimens under precisely controlled and reproducible conditions. J. Microsc. 112, 3-15.

Barlow, D.I. & Sleigh, M.A. (1979) Freeze substitution for preservation of ciliated surfaces for scanning electron microscopy. J. Microsc. 115, 81-95.

Barnard, T. (1980) Ultrastructural effects of high molecular weight cryoprotectants dextran and polyvinyl pyrolidone on liver and brown adipose tissue. J. Microsc. 120, 93-104

Bell, L.G.E. (1952a) The application of freezing and drying techniques in cytology. Int. Rev. Cytol. 1, 35-63.

Bell, L.G.E (1952b) Cooling bath for cytological investigations. Nature 170, p.719.

Bernhard, W. & Leduc, E.H. (1967) Ultrathin frozen sections. I Methods and ultrastructural preservation. J. Cell Biol. 34, 757-771.

Bone, Q. & Ryan, K.P. (1972) Osmolarity of osmium tetroxide and glutaraldehyde fixatives. Histochem. J. 4, 331-347.

Bone, Q., Brownlee, C., Bryan, G.W., Burt, G.R., Dando, P.R., Liddicoat, M.I., Pulsford, A.L. & Ryan, K.P. (1987) On the differences between the two "indicator" species of Chaetognath, *Sagitta setosa* and *S. elegans*. J. mar. biol. Ass. U.K. 67, 545-560.

Bouin, P. (1897) Études sur l'évolution normale et l'involution du tube séminifère. Arch. d'Anat. micr. 1, 225-263.

Boutron, P. (1984) More accurate determination of the quantity of ice crystallized at low cooling rates in the glycerol and 1,2-propanediol aqueous solutions: comparison with equilibrium. Cryobiology 21, 183-191.

Boyde, A. & Wood, C. (1969) Preparation of animal tissues for surface-scanning electron microscopy. J. Microsc. 90, 221-249.

Boyde, A., Bailey, E., Jones, S.J. & Tamarin, A. (1977) Dimensional changes during specimen preparation for scanning electron microscopy. Scanning Electron Microscopy/1977 Vol. 1 IITRI Chicago, Illinois, pp. 507-518.

Boyne, A.F. (1979) A gentle, bounce-free assembly for quick-freezing tissues for electron microscopy: application to isolated torpedine ray electrocyte stacks. J. Neurosci. Meth. 1, 353-364.

Buchheim, W. (1972) Zur Gefrierfixierung wassringer Lossungen. Naturwissenschaften 59, p.121.

Buchheim, W. (1977) Cryofixation of tissue without cryoprotectants. Naturwiss. 64, 270.

Buchheim, W. & Welsch, U. (1977) Freeze-etching of unglycerinated tissue dispersions by application of the oil emulsion technique. J. Microsc. 111, 339-349.

Bullivant, S. (1965) Freeze substitution and supporting techniques. Lab. Investig. 14, 440/1178-457/1195.

Burstein, N. & Maurice, D.M. (1978) Cryofixation of tissue surfaces by a propane jet for electron microscopy. Micron 9, 191-198.

Burton, E.F. & Oliver, W.F. (1935) X-ray patterns of ice. Nature 135, 505-506.

Chang, S.H., Mergner, W.J., Pendergrass, R.E., Bulger, R.E., Beresky, I.K. & Trump, B.F. (1980) A rapid method of cryofixation of tissues *in situ* for ultracryomicrotomy. J. Histochem. Cytochem. 28, 47-51.

Chang, Z-H. & Baust, J.G. (1991) Ultra-rapid freezing by spraying/ plunging: pre-cooling in the cold gaseous layer. J. Microsc. 161, 435-444.

Clark, J., Echlin, P., Moreton, R., Saubermann, A. & Taylor, P. (1976) Thin film thermocouples for use in low temperature scanning electron microscopy. Scanning Electron Microscopy/1976 1, 84-90.

Coetzee, J. & Merwe, F. van der (1984) Extraction of substances during glutaraldehyde fixation of plant cells. J. Microsc. 135, 147-158.

Cole, R., Matuszek, C.S. & Rieder, C.L. (1990) A simple pneumatic device for plunge-freezing cells grown on EM grids. J. Electron Microsc. Technique 16, 167-173.

Costello, M.J. (1980) Ultra-rapid freezing of biological samples. Scanning Electron Microscopy II, 361-370.

Costello, J.M. & Corless, M.J. (1978) Direct measurement of temperature changes within freeze-fracture specimens during quenching in liquid coolants. J. Microsc. 112, 17-37.

Costello, M.J., Fetter, R. & Corless, J.M. (1984) Optimum conditions for the plunge freezing of sandwiched samples. In: *The Science of Biological Specimen Preparation* (eds. J.-P. Revel, T. Barnard and G.H. Haggis) pp.105-115. SEM Inc., AMF O'Hare, IL 60666.

Costello, M.J., Fetter, R. & Hoechli, M. (1982) Simple procedures for evaluating the cryofixation of biological samples. J. Microsc. 125, 125-136.

Coulter, H.D. & Terracio, L. (1977) Preparation of biological tissues for electron microscopy by freeze-drying. Anat. Rec. 187, 477-494.

Dowell, L.G. & Rinfret, A.P. (1960) Low temperature forms of ice as studied by X-ray diffraction. Nature 188, 1144-1148.

Dubochet, J. & McDowall, A.W. (1981) Vitrification of pure water for electron microscopy. J. Microsc. 124, RP3-4.

Dubochet, J. & McDowall, A.W. (1984) Cryoultramicrotomy: study of ice crystals and freezing damage. In: *Proc. 8th Eur. Congr. Elec. Microsc., Budapest* (eds. A. Csanády, P. Röhlich, and D. Szabó), vol. 2, pp. 1407-1410. Programme Committee of the Eighth European Congress on Electron Microscopy, Budapest.

Dubochet, J., Adrian, J., Chang, J.-J., Homo, J.-Cl., Lepault, J., McDowall, A.W. & Schultz, P. (1988) Cryo-electron microscopy of vitrified specimens. Quart. Rev. Biophys. 21, 129-228.

Dubochet, J., Adrian, M. & Vogel, R.H. (1983) Amorphous solid water obtained by vapour condensation or by liquid cooling: a comparison. Cryo-Letters 4, 233-240.

Dubochet, J., Lepault, J., Freeman, R., Berriman, J.A. & Homo, J.-Cl. (1982) Electron microscopy of frozen water and aqueous solutions. J. Microsc. 128, 219-237.

Echlin, P. (1973) Scanning microscopy at low temperature. In: *Freeze-etching: Techniques and Applications* (eds. E.L. Benedetti and P. Favard) pp. 211-222. Société Française de Microsopie Électronique, Paris.

Echlin, P. (1978) Low temperature scanning electron microscopy: a review. J. Microsc. 112, 47-62.

Echlin, P. & Moreton, R. (1974) The preparation of biological materials for X-ray microanalysis. In: *Microprobe Analysis as Applied to Cells and Tissue* (eds. T. Hall, P. Echlin and R. Kaufmann) pp. 159-174. Academic Press, London.

Echlin, P. & Moreton, R. (1976) Low temperature techniques for scanning electron microscopy. Scanning Electron Microscopy/1976 1, 753-761.

Echlin, P. & Saubermann, A.J. (1977) Preparation of biological specimens for X-ray microanalysis. Scanning Electron Microscopy, 1, 621-637.

Echlin, P. & Taylor, S.E. (1986) The preparation and X-ray microanalysis of bulk frozen hydrated vacuolate plant tissue. J. Microsc. 141, 329-348.

Echlin, P., Gee, W. & Chapman, B. (1985) Very low voltage sputter coating. J. Microsc. 137, 155-169.

Echlin, P., Lai, C. & Hayes, T.L. (1982) Low temperature X-ray microanalysis of the differentiating vascular tissue in root tips of *Lemna minor L.* J. Microsc. 126, 285-306.

Edelmann, L. (1989) The contracting muscle: a challenge for freeze-substitution and low temperature embedding. Scanning Microscopy Supplement 3, 241-252.

Eisenberg, D. & Kauzmann, W. (1969) *The structure and properties of water.* Oxford University Press, Oxford.

Elder, H.Y. & Robards A.W. (1988) Cryopreparation techniques in electron microscopy. Microscopy and Analysis, Issue 7 (Sept.1988), 7-10.

Elder, H.Y., Gray, C.C., Jardine, A.G., Chapman, J.N. & Biddlecombe, W.H. (1982) Optimum conditions for cryoquenching of small tissue blocks in liquid coolants. J. Microsc. 126, 45-61.

Elgsaeter, A., Espevik, K., Kopstad, G., Mikkelsen, A. & Stokke, B.T. (1984) Freeze-etching of macromolecules. In: *The Science of Biological Specimen Preparation* (eds. J.-P. Revel, T. Barnard and G.H. Haggis) pp. 195-201. SEM Inc., AMF O'Hare, IL 60666.

Eränkö, O. (1954) Quenching of tissues for freeze-drying. Acta anat. 22, 331-336.

Escaig, J., Géraud, G. & Nicolas, G. (1977) Congélation rapide de tissus biologiques. Mesures des témperatures et des vitesses de congélation par thermocouple en couche mince. C.R. Acad. Sci. Paris D, 284, 2289-2292.

Escaig, J. (1982) New instruments which facilitate rapid freezing at 83 K and 6 K. J. Microsc. 126, 221-229.

Escaig, J. (1984) Control of different parameters for optimal freezing conditions. In: *The Science of Biological Specimen Preparation* (eds. J.-P. Revel, T. Barnard and G.H. Haggis) pp. 117-122. SEM Inc., AMF O'Hare, IL 60666.

Espevik, T. & Elgsaeter, A. (1981) *In situ* liquid propane jet-freezing and freeze-etching of monolayer cell cultures. J. Microsc. 123, 105-110.

Fahmy, A. (1967) An extemporaneous lead citrate stain for electron microscopy. Proc. 25th Ann. Conf. E.M.S.A. (ed. C.J. Arcenaux), p. 148, Ethyl Corporation, Baton Rouge.

Feder, N. & Sidman, R.L. (1958) Methods and principles of fixation by freeze-substitution. J. Biophys. Biochem. Cytol. 4, 593-600.

Fernández-Morán, H. (1957) Electron microscopy of nervous tissue. In: *Metabolism of the Nervous System* (ed. D. Richter) pp. 1-34. Pergamon Press, Oxford.

Fernández-Morán, H. (1960) Low-temperature preparation techniques for electron microscopy of biological specimens based on rapid freezing with liquid helium II. Ann. N.Y. Acad. Sci. 85, 689-713.

Flemming, W. (1884) Mittheilungen zur Farbetechnik. Zeit. wiss. Mikr. 1, 349-361.

Franks, F. (1977) Biological freezing and cryofixation. J. Microsc. 111, 3-16.

Franks, F. (1982) The properties of aqueous solutions at subzero temperatures. In: *Water: A Comprehensive Treatise*, Vol. 7 (ed. F. Franks) pp. 215-338. Plenum Press, New York.

Fuchs, D.A. & Albers, C. (1988) Effect of adrenaline and blood gas conditions on red cell volume and intra-erythrocytic electrolytes in the Carp, *Cyprinus carpio*. J. Exp. Biol. 137, 457-477.

Gersch, I. (1932) The Altmann technique for fixation by drying while freezing. Anat. Rec. 53, 309-337.

Gersh, I. (1956) The preparation of frozen-dried tissue for electron microscopy. J. Biophys. Biochem. 2, (Suppl.), 37-43.

Gersch, I., Isenberg, I., Stephenson, J.L. & Bondareff, W. (1957a) Submicroscopic structure of frozen-dried liver specifically stained for electron microscopy. Part I, Technical. Anat. Rec. 128, 91-111.

Gersch, I., Isenberg, I., Bondareff, W. & Stephenson, J.L. (1957b) Submicroscopic structure of frozen-dried liver specifically stained for electron microscopy. Part II, Biological. Anat. Rec. 128, 149-168.

Gilkey, J.C. & Staehelin, L.A. (1986) Advances in ultrarapid freezing for the preservation of cellular ultrastructure. J. Electron Microsc. Techn. 3, 177-210.

Glaeser, R.M. (1975) Radiation damage and biological electron microscopy. In: *Physical Aspects of Electron Microscopy and Microbeam Analysis* (eds. B.M. Siegel and D.R.Beaman) pp. 205-231. Wiley, New York.

Glauert, A.M. (1975) Fixatives. In: *Fixation, Dehydration and Embedding of Biological Specimens* Vol. 3 Part 1 of Practical Methods in Electron Microscopy (ed. A.M. Glauert) pp. 5-65. North-Holland, Amsterdam.

Glover, A.J. & Garvitch, Z.S. (1974) The freezing rate of freeze-etch specimens for electron microscopy. Cryobiology 11, 248-254.

Golgi, C. (1878) Un nuovo processo di tecnica microscopia. Rendic. Ist. Lombardo Sc., 12, 206-210.

Gulik-Krzywicki, T. & Costello, M.J. (1978) The use of low temperature X-ray diffraction to evaluate methods used in freeze-fracture electron microscopy. J. Microsc. 112, 103-113.

Gupta, B.L. & Hall, T.A. (1984) Role of high concentrations of Ca, Cu, and Zn in the maturation and discharge *in situ* of sea anemone nematocysts as shown by X-ray microanalysis of cryosections. In: *Toxins, Drugs, and Pollutants in Marine Animals* (eds. L. Bolis, J. Zadunaisky and R. Gilles) pp. 77-95. Springer-Verlag, Berlin, Heidelberg.

Gupta, B.L., Hall, T.A. & Moreton, R.B. (1977) Electron probe X-ray microanalysis. In: *Transport of Ions and Water in Animals* (eds. B.L. Gupta, R.B. Moreton, J.L. Oschman and B.J. Wall) pp. 83-143. Academic Press, London.

Haggis, G.H. (1986) Study of the conditions necessary for propane-jet freezing of fresh biological tissues without detectable ice formation. J. Microsc. 143, 275-282.

Hagler, H.K. & Buja, L.M. (1984) New techniques for the preparation of thin freeze-dried cryosections for X-ray microanalysis. In: *The Science of Biological Specimen Preparation* (eds. J.-P. Revel, T. Barnard and G.H. Haggis) pp. 161-166. SEM Inc., AMF O'Hare, IL 60666.

Hagler, H.K. & Buja, L.M. (1986) Effect of specimen preparation and section transfer techniques on the preservation of ultrastructure, lipids and elements in cryosections. J. Microsc. 141, 311-317.

Hagler, H.K., Morris, A.C. & Buja, L.M. (1989) X-ray microanalysis and free calcium measurements in cultured neonatal rat ventricular myocytes. In: *Electron Probe Microanalysis, Applications in Biology and Medicine* eds. K. Zierold & H. Hagler, Springer Series in Biophysics, Vol. 4 pp. 181-197. Springer Verlag, Berlin Heidelberg.

Hallbrucker, A. & Mayer, E. (1987) Calorimetric study of the vitrified liquid water to cubic ice phase transition. J. Phys. Chem. 91, 503-505.

Handley, D.A., Alexander, J.T. & Chien, S. (1981) The design and use of a simple device for rapid quench freezing of biological samples. J. Microsc. 121, 273-282.

Harvey, D.M.R., Hall, J.L. & Flowers, T.J. (1976) The use of freeze-substitution in the preparation of plant tissue for ion localisation studies. J. Microsc. 107, 189-198.

Hayat, M.A. (1981) *Fixation for Electron Microscopy*. Academic Press, New York, London.

Heath, B. (1984) A simple and inexpensive liquid helium cooled 'slam freezing' device. J. Microsc. 134, 75-82.

Heide, H.-G. & Zeitler, E. (1984) Water in cryomicroscopy. In: *Electron microscopy, 1984* vol. 2 (eds. A. Csanády, P. Röhlich and D. Szabó) pp. 1388-1392. Programme Committee of the Eighth European Congress on Electron Microscopy, Budapest, 1984.

Heide, H.-G. & Zeitler, E. (1985) The physical behaviour of solid water at low temperatures and the embedding of electron microscopical specimens. Ultramicroscopy 16, 151-160.

Heuser, J.E., Reese, T.S., Dennis, M.J., Jan, Y, Jan, L. & Evans, L. (1979) Synaptic vesicle exocytosis captured by quick freezing and correlated with quantal transmitter release. J. Cell Biol. 81, 275-300.

Hippe, S. (1984) Rapid cryofixation by a simple propane-double-jet device adapted to a modified specimen table of the Bioetch 2005. Mikroskopie (Wien) 41, 289-301.

Hoch, H.C. (1986) Freeze-substitution of fungi. In: *Ultrastructure Techniques for Microorganisms* (eds. H.C. Aldrich and W.J. Todd) pp. 183-212. Plenum Publishing Corporation, New York.

Hoerr, N.L. (1936) Cytological studies by the Altmann-Gersch freeze-drying method. Anat. Rec. 65, 293-313.

Humbel, B.M. & Müller, M. (1986) Freeze-substitution and low temperature embedding. In: *The Science of Biological Specimen Preparation, 1985* (eds. M. Müller, R.P. Becker, A. Boyde amd J.J. Wolosewick) pp. 175-183. SEM, A.M.F. O'Hare, IL 60666.

Jehl, B., Bauer, R., Dorge, A. & Rick, R. (1981) The use of propane/isopentane mixtures for rapid feeezing of biological specimens. J. Microsc. 123, 307-309.

Jones, G.J. (1984) On estimating freezing times during tissue rapid freezing. J. Microsc. 136, 349-360.

Kay, D.H. (1965) ed. *Techniques for Electron Microscopy,* 2nd edn. Blackwell Scientific Publications, Oxford.

Kaeser, W., Koyro, H.-W. & Moor, H. (1989) Cryofixation of plant tissues without pretreatment. J. Microsc. 154, 279-288.

Kanno, H., Speedy, R.J. & Angell, C.A. (1975) Supercooling of water to -92°C under pressure. Science 189, 880-881.

Kellenberger, E. (1987) The response of biological macromolecules and supramacromolecular structures to the physics of specimen cryopreparation. In: *Cryotechniques in Biological Electron Microscopy* (eds. R.A. Steinbrecht and K. Zierold) pp. 35-63. Springer-Verlag, Berlin, Heidelberg.

Kistler, S.S. (1936) The measurement of "Bound" water by the freezing method. J. Am. Chem. Soc. 58, 901-907.

Knoll, G., Oebel, G. & Plattner, H. (1982) A simple sandwich- cryogen-jet procedure with high cooling rates for cryofixation of biological materials in the native state. Protoplasma 111, 161-176.

Knoll, G. & Plattner, H. (1990) Time resolved electron microscopy and parallel biochemistry: combination of rapid mixing and rapid freezing for analysis of subcellular dynamics. Abstracts of 4th Int. Meet. on Low Temperature Biological Microscopy and Analysis, in Proc. R. Micr. Soc. 25, (2) Suppl. p.S17.

Kopstad, G. & Elgsaeter A. (1982) Theoretical analysis of specimen cooling rate during impact freezing and liquid jet freezing of freeze-etch specimens. Biophys. J. 40, 163-170.

Lepault, J., Erke, I., Nicolas G. & Ranck, J.-L. (1991) Time-resolved cryo-electron microscopy of vitrified muscular components. J. Microsc. 161, 47-57.

Lepault, J., Freeman, R. & Dubochet, J. (1983) Electron beam induced "vitrified ice". J. Microsc. 132, RP3-RP4.

Livesey, S.A., Buescher, E.S., Krannig, G.L., Harrison, D.S., Linner, J.G. & Chiovetti, R. (1989) Human neutrophil granule heterogeneity: immunolocalisation studies using cryofixed, dried and embedded specimens. Scanning Microscopy Suppl. 3, 231-240.

Lovelock, J.E. (1953) The mechanism of the protective action of glycerol against haemolysis during freezing and thawing. Biochim. Biophys. Acta 11, 28-36.

Luyet, B. (1960) On various phase transitions occurring in aqueous solutions at low temperatures. Ann. N.Y. Acad. Sci. 85, 549-569.

Luyet, B. & Gonzales, F. (1951) Recording ultrarapid changes in temperature. Refrig. Engng. 59, 1191-1193 (plus p.1236).

MacKenzie, A.P. (1969) Apparatus for the partial freezing of liquid nitrogen for the rapid cooling of cells and tissues. Biodynamica 10, 341-351.

MacKenzie, A.P. (1981) Modelling the ultra-rapid freezing of cells and tissues. In: *Microprobe Analysis of Biological Specimens* (eds. T.E. Hutchinson and A.P. Somlyo) pp. 397-421. Academic Press, New York & London.

MacKenzie, A.P. & Luyet, B.J. (1967) Electron microscope study of recrystallization in rapidly frozen gelatin gels. Biodynamica 10, 95-122.

Marchese-Ragona, S.P. (1984) Ethanol, an efficient coolant for rapid freezing of biological material. J. Microsc. 134, 169-171.

Marshall, A.T. (1980a) Frozen-hydrated bulk specimens. In: *X-ray Microanalysis in Biology* (ed. M.A. Hayat) pp. 167-196. University Park Press, Baltimore and MacMillan, London.

Marshall, A.T. (1980b) Frozen-hydrated sections. In: *X-ray Microanalysis in Biology* ed. M.A. Hayat) pp. 197-206. University Park Press, Baltimore and MacMillan, London.

Mathes, G. & Hackenseller, H.A. (1981) Correlations between purity of dimethyl sulphoxide and survival after freezing and thawing. Cryo-Letters 2, 389-392.

Mayer, E. (1988) Hyperquenching of water and dilute aqueous solutions into their glassy states: an approach to cryofixation. Cryo-Letters 9, 66-77.

Mayer, E. & Hallbrucker, A. (1987) Cubic ice from liquid water. Nature 325, 601-602.

Meisner, J. & Hagins, W.A. (1978) Fast freezing of thin tissue by thermal conduction into sapphire crystals at 77 K. Biophys. J. 21, p.149a.

Mengold, R.B., Lüttge, B. & Kaiser, W. (1974) Zum Einfrieren von Suspensionen für elektronenmikroskopische Untersuchungen. Colloid Polymer Sci. 252, 530-537.

Mengold, R.B. & Lüttge, B. (1979) Freeze-etching of dispersions without contamination of the fracture faces. Microscopica Acta 81, 317-327.

Menco, B.Ph.M. (1986) A survey of ultra-rapid cryofixation methods with particular emphasis on applications to freeze-fracturing, freeze-etching, and freeze-substitution. J. Elec. Microsc. Techn. 4, 177-240.

Meryman, H.T. (1957) Physical limitations of the rapid freezing methods. Proc. R. Soc. Lond. B, 147, 452-459.

Monaghan, P. & Robertson, D. (1990) Freeze-substitution without aldehyde or osmium fixative: ultrastructure and implications for immunocytochemistry. J. Microsc. 158, 355-363.

Monson, K.L. & Hutchinson, T.E. (1981) X-ray microanalysis of freeze-dried muscle: techniques and problems. In: *Microprobe Analysis of Biological Specimens* (eds. T.E. Hutchinson and A.P. Somlyo) pp. 157-176. Academic Press, New York & London.

Monroe, R.G., Gamble, W.J., La Farge, C.G., Gamboa, R., Morgan, C.L., Rosenthal, A. & Bullivant, S. (1968) Myocardial ultrastructure in systole and diastole using ballistic cryofixation. J. Ultrastruct. Res. 22, 22-36.

Moor, H. (1987) Theory and practice of high pressure freezing. In: *Cryotechniques in Biological Electron Microscopy* (eds. R.A. Steinbrecht and K. Zierold) pp. 175-191. Springer-Verlag, Heidelberg, Berlin.

Moor, H. & Riehle, U. (1968) Snap-freezing under high pressure: a new fixation technique for freeze-etching. In: *Electron Microscopy 1968*, (ed. S. Bocciarelli) Vol 2 Proc. 4th Eur. Reg. Conf. Electron Microsc., pp. 33-34, Rome.

Moor, H., Mueller, M. & Kistler, J. (1976) Freezing in a propane jet. Experientia 32, p.805.

Morgan, A.J. (1980) Preparation of specimens: changes in chemical integrity. In: *X-ray Microanalysis in Biology* (ed. M.A. Hayat) pp. 65-166. MacMillan, London and Basingstoke.

Moreton, R.B., Echlin, P., Gupta, B.L., Hall, T.A. & Weis-Fogh, T. (1974) Preparation of frozen hydrated tissue sections for X-ray microanalysis in the scanning electron microscope. Nature 247, 113-115.

Mueller, M. (1990) High pressure freezing and follow up procedures. In: Abstracts of 4th Int. Meeting on Low Temperature Biological Microscopy and Analysis, Proc. Roy. Micr. Soc. 25 (2, Suppl) p.S7.

Mueller, M. & Moor, H. (1984) Cryofixation of thick specimens by high pressure freezing. In: *The Science of Biological Specimen Preparation* (eds. J.-P. Revel, T. Barnard and G.H. Haggis) pp. 131-138. SEM Inc, AMF O'Hare, IL 60666.

Mueller, M., Meister, N. & Moor, H. (1980) Freezing in a propane jet and its application in freeze-fracturing. Mikroskopie (Wien) 36, 129-140.

Murray, P.W. Le R., Robards, A.W. & Waites, P.R. (1989) Countercurrent plunge cooling: a new approach to increase reproducibility in the quick freezing of biological tissue. J. Microsc. 156, 173-182.

Nei, T. (1971) Hemolysis during the rewarming process of frozen erythrocytes. Proc. XIIIth Int. Congr. Refrig. 10, 907-911.

Nei, T. (1973) Growth of ice crystals in frozen specimens. J. Microsc. 99, 227-223.

Ornberg, R.L. & Reese, T.S. (1981) Quick freezing and freeze-substitution for X-ray microanalysis of calcium. In: *Microprobe Analysis of Biological Systems* (eds. T.E. Hutchnison and A.P. Somlyo) pp. 213-230. Academic Press Inc., New York.

Padron, R., Alamo, L., Craig, R. & Caputo, C. (1988) A method for quick-freezing live muscles at known instants during contraction with simultaneous recording of mechanical tension. J. Microsc. 151, 81-102.

Pease, D.C. (1964) *Histological Techniques for Electron Microscopy*, 2nd edn. Academic Press, New York.

Pease, D.C. (1967a) Eutectic ethylene glycol and pure propylene glycol as substituting media for the dehydration of frozen tissue. J. Ultrastruct. Res. 21, 75-97.

Pease, D.C. (1967b) The preservation of tissue fine structure during rapid freezing. J. Ultrastruct. Res. 21, 98-124.

Pease, D.C. (1973) Substitution techniques. In: *Advanced Techniques in Biological Electron Microscopy* (ed. J.K. Koehler) pp. 35-66. Springer-Verlag, New York.

Pearse, A.G.E. (1980) The chemistry and practice of fixation. In: *Histochemistry: Theoretical and Applied* by A.G.E. Pearse 4th ed. Vol.1 Preparative and Optical Technology pp. 97-158. Churchill Livingstone, Edinburgh, London and New York.

Plattner, H. & Bachmann, L. (1982) Cryofixation: a tool in biological ultrastructural research. Intl. Rev. Cytol. 79, 237-304.

Plattner, H. & Knoll, G. (1984) Cryofixation of biological materials for electron microscopy by the methods of spray-, sandwich-, cryogen-jet- and sandwich-cryogen-jet-freezing: a comparison of techniques. In: *Science of Biological Specimen Preparation* (eds. J.-P. Revel, T. Barnard and G.H. Haggis) pp. 139-146. SEM Inc., AMF O'Hare, IL 60666.

Plattner, H., Schmitt-Fumian, W.W. & Bachmann, L. (1973) Cryofixation of single cells by spray-freezing. In: Freeze-etching: Techniques and Applications (eds. E.L. Benedetti and P. Favard) pp. 63-71. Société Française de Microsopie Électronique, Paris.

Polian, A. & Grimsditch, M. (1984) New high pressure phase of H_2O: Ice X. Phys. Rev. Lett. 52, 1312-1314.

Pollard, T.D., Maupin, P., Sinard, J. & Huxley, H.E. (1990) A stopped-flow/rapid-freezing machine with millisecond time resolution to prepare intermediates in biochemical reactions for electron microscopy. J. Electron Microsc. Technique 16, 160-166.

Pryde, J.A. & Jones, G.O. (1952) Properties of vitreous water. Nature 170, 685-688.

Pscheid, P., Schudt, C. & Plattner, H. (1981) Cryofixation of monolayer cell cultures for freeze-fracturing without chemical pre-treatments. J. Microsc. 121, 149-167.

Rapatz, G. & Luyet, B.J. (1959) Recrystallisation at high subzero temperatures in gelatin gels subjected to various cooling treatments. Biodynamica 8, 85-105.

Rasmussen, D.H. (1982) Ice formation in aqueous systems. J. Microsc. 128, 176-174.

Rebhun, L.I. (1965) Freeze-substitution: fine structure as a function of water concentration in cells. Fed. Proc. 24, S217-S232.

Rebhun, L.I. (1972) Freeze-substitution and freeze-drying. In: *Principles and techniques of Electron Microscopy, Biological Applications Vol.2.* (ed. M.A. Hayat) pp.3-52. Van Nostrand Reinhold Co., New York.

Reimer, L. (1975) Review of the radiation damage problem of organic specimens in electron microscopy. In: *Physical Aspects of Electron Microscopy and Microbeam Analysis* (eds. B.M. Seagel and D.R. Beaman) pp. 231-245. Wiley, New York.

Rey, L.R. (1960) Thermal analysis of eutectics in freezing solutions. Annls. N.Y. Acad. Sci. 510-534.

Riehle, U. (1968) Schnellgefrieren organischer Preparate für die Elektronen Mikroskopie: die Vitrifizierung verdunnter wassriger Losungen. Chemie Ingenier Technik 40, 213-218.

Riehle, U. & Hoechli, M. (1973) The theory and technique of high pressure freezing. In: *Freeze-etching Technique and Applications* (eds. E.L. Benedetti and P. Favard), pp.31-61. Société Française de Microscopie Électronique, Paris.

Richards, A.G., Steinbach, H.B. & Anderson, T.F. (1943) Electron microscope studies of squid giant nerve axoplasm. J. Cell. & Comp. Physiol. 21, 129-143.

Robards, A.W (1980) A microprocessor controlled rapid cooling rate meter. Cryo-Letters 1, 384-391.

Robards, A.W. (1984) Fact or artifact - a cool look at biological electron microscopy. Proc. R. Microsc. Soc. 19, 195-208.

Robards, A.W. & Crosby, P. (1979) A comprehensive freezing, fracturing and coating system for low temperature scanning electron microscopy. Scanning Electron Microscopy/1979 2, 324-344.

Robards, A.W. & Crosby, P. (1983) Optimisation of plunge-freezing: linear relationship between cooling rate and entry velocity into liquid propane. Cryo-Letters 4, 23-32.

Robards, A.W. & Severs, N.J. (1981) A comparison between cooling rates achieved using a propane jet device and plunging into liquid propane. Cryo-Letters 2, 135-144.

Robards, A.W. & Sleytr, U. (1985) *Practical Methods in Electron Microscopy*, (ed. A. Glauert); Vol. 10, Low Temperature Methods in Biological Electron Microscopy. Elsevier, Amsterdam.

Robards, A.W., Wilson, A.J. & Crosby, P. (1981) Specimen heating during sputter coating. J. Microsc. 124, 143-153.

Roos, N & Barnard, T. (1985) A comparison of subcellular element concentrations in frozen-dried, plastic-embedded, dry-cut sections and frozen-dried cryosections. Ultramicroscopy 17, 335-344.

Roos, N. & Morgan, A.J. (1990) *Cryopreparation of Thin Biological Specimens for Electron Microscopy: Methods and Applications*. Oxford University Press, Oxford.

Rosenkranz, J. (1975) Course of temperature variation in an object during freeze-etching procedure. Arzneim Forsch. (Drug Res.) 25, 454-455.

Ryan, K.P. & Bald, W.B. (1990) Ice crystal growth during cryofixation. In: Abstracts of 4th Int. Meeting on Low Temperature Biological Microscopy and Analysis, Proc. R. Microsc. Soc. 25 (2, Suppl) p.S14.

Ryan, K.P. & Purse, D.H. (1984) Rapid freezing: specimen supports and cold gas layers. J. Microsc. 136, RP5-RP6.

Ryan, K.P. & Purse, D.H. (1985a) Plunge-cooling of tissue blocks: determinants of cooling rates. J. Microsc. 140, 47-54.

Ryan, K.P. & Purse, D.H. (1985b) A simple plunge-cooling device for preparing biological specimens for electron microscopy. Mikroskopie (Wien) 42, 247-251.

Ryan, K.P. & Liddicoat, M.I. (1987) Safety considerations regarding the use of propane and other liquefied gases as coolants for rapid freezing purposes. J. Microsc. 147, 337-340.

Ryan, K.P., Bald, W.B. Neumann, K., Simonsberger, P., Purse, D.H. & Nicholson, D.N. (1990) Cooling rate and ice crystal measurement in biological specimens plunged into liquid ethane, propane, and Freon 22. J. Microsc. 158, 365-378.

Ryan, K.P., Bateson, J.M., Grout, B.W.W., Purse, D.H. & Nicholson, D.N. (1988) Cryo-scanning electron microscopy of ice crystal damage in rapidly frozen, cryomounted specimens. Cryo-Letters 9, 418-425.

Ryan, K.P., Purse, D.H., Robinson, S.G. & Wood, J.W. (1987) The relative efficiency of cryogens for plunge-cooling biological specimens. J. Microsc. 145, 89-96.

Ryan, K.P., Purse, D.H. & Wood, J.W. (1985a) A transmission cryo-stage with a heater and integral anti-contaminator for a scanning electron microscope. Mikroskopie (Wien) 42, 225-229.

Ryan, K.P., Purse, D.H. & Wood, J.W. (1985b) Cryo-stage performance and observation of freeze-etching and freeze-drying in a scanning electron microscope. Mikroskopie (Wien) 42, 196-205.

Sabatini, D.D., Bensch, K. & Barnett, R.J. (1963) Cytochemistry and electron microscopy. The preservation of cellular ultrastructure and enzymatic activity by aldehyde fixation. J. Cell Biol. 17, 19-58.

Sargent, J.A. (1986) Cryo-preservation for scanning electron microscopy avoids artefacts induced by conventional methods of specimen preparation. Tissue & Cell 18, 305-311.

Saubermann, A.J. & Echlin, P. (1975) The preparation, examination and analysis of frozen hydrated tissue sections by scanning transmission electron microscopy and X-ray microanalysis. J. Microsc. 105, 155-191.

Schwabe, K.G. & Teraccio, L. (1980) Ultrastructural and thermocouple evaluation of rapid freezing techniques. Cryobiology 17, 571-584.

Scott, G.H. (1933) A critical study and review of the method of microincineration. Protoplasma 20, 133-151.

Silvester, N.R., Marchese-Ragona, S. & Johnston, D.N. (1982) The relative efficiency of various fluids in the rapid freezing of protozoa. J. Microsc. 128, 175-186.

Simpson W.L. (1941) An experimental analysis of the Altmann technique of freezing-drying. Anat. Rec. 80, 173-189.

Sitte, H. (1979) Cryofixation of biological material without pretreatment - A review. Mikroskopie (Wien) 35, 14-20.

Sitte, H., Edelmann, L. & Neumann, K. (1987) Cryofixation without pretreatment at ambient pressure. In: *Cryotechniques in Biological Electron Microscopy* (eds. R.A. Steinbrecht and K. Zierold) pp. 87-113. Springer-Verlag, Heidelberg, Berlin.

Sitte, H., Fell, H., Hobl, W., Kleber, H. & Neumann, K. (1977) Fast freezing device. J. Microsc. 111, 35-38.

Sitte, H., Neumann, K. & Edelmann, L. (1986) Cryofixation and cryosubstitution for routine work in transmission electron microscopy. In: *The Science of Biological Specimen Preparation* (eds. M. Mueller, R.P. Becker, A. Boyde and J.J. Wolosewick) pp. 103-118. SEM Inc., AMF O'Hare, IL 60666.

Sitte, H., Neumann, K. & Edelmann, L. (1987) Safety rules for cryopreparation. In: *Cryotechniques in Biological Electron Microscopy* (eds. R.A. Steinbrecht and K. Zierold) pp. 285-290. Springer-Verlag, Heidelberg, Berlin.

Sjöstrand, F.S. (1990) Common sense in electron microscopy: about cryofixation, freeze-substitution, low temperature embedding and low denaturation embedding. J. Struct. Biol. 103, 135-139.

Sjöström, M. (1980) The skeletal muscle. In: *X-ray Microanalysis in Biology* (ed. M.A. Hayat) pp. 263-306. University Park Press, Baltimore and MacMillan, London.

Skaer, H. (1982) Chemical cryoprotection for structural studies. J. Microsc. 125, 137-147.

Somlyo, A.V., Schuman, H. & Somlyo, A.P. (1977) Elemental distribution in striated muscle and the effects of hypertonicity. Electron probe analysis of cryosections. J. Cell Biol. 74, 828-857.

Somlyo, A.V., Bond, M., Silcox, J.C. & Somlyo, A.P. (1985) Direct measurements of intracellular elemental composition utilising a new

approach to freezing *in vivo*. Proc. 43 Ann. Meet. EMSA, p.10. San Francisco Press, San Francisco.

Spurr, A.R. (1969) A low-viscosity epoxy resin embedding medium for electron microscopy. J. Ultrastruct. Res. 26, 31-43.

Statham. P.J. (1979) A ZAF procedure for microprobe analysis based on measurement of peak-to-background ratios. In: *Microbeam Analysis* ed. D.E. Newbury, pp. 247-253. San Francisco Press Inc., San Francisco.

Steere, R.L. (1957) Electron microscopy of structural detail in frozen biological specimens. J. biophys. biochem. Cytol. 3, 45-60.

Steinbrecht, R.A. (1985) Recrystallisation and ice crystal growth in a biological specimen, as shown by a simple freeze substitution method. J. Microsc. 140, 41-46.

Steinbrecht, R.A. & Zierold, K. (1987) eds. *Cryotechniques in Biological Electron Microscopy*. Springer-Verlag, Heidelberg, Berlin.

Stephenson, J.L. (1954) Caution in the use of liquid propane for freezing biological specimens. Nature 174, p.235.

Stephenson, J.L. (1956) Ice crystal growth during the rapid freezing of tissues. J. biophys. biochem. Cytol. 2 (Suppl.), 45-52.

Stephenson, J.L. (1960) Ice crystal formation in biological materials during rapid freezing. Annls. N.Y. Acad. Sci. 85, 535-540.

Stolinski, C. (1977) Freeze-fracture replication in biological research: development, current practice and future prospects. Micron 8, 87-111.

Studer, D. Michel, M. & Mueller, M. (1989) High pressure freezing comes of age. Scanning Microscopy Supplement 3, 253-269.

Taylor, K.A. & Glaeser, R.M. (1976) Electron microscopy of frozen hydrated biological specimens. J. Ultrastruct. Res. 55, 448-456.

Tokuyasu, K.T. (1973) A technique for ultracryotomy of cell suspensions and tissues. J. Cell Biol. 57, 551-565.

Tokuyasu, K.T. (1980) Immunocytochemistry of ultrathin frozen sections. Histochem. J. 12, 381-403.

Toscano, W.M., Cravalho, E.G., Silvares, O.M. & Huggins, C.E. (1975) The thermodynamics of intracellular ice nucleation in the freezing of erythrocytes. Trans. ASME J. Heat Transfer, 97, 326-332.

Trinick, J. & Cooper, J. (1990) Concentration of solutes during preparation of aqueous suspensions for cryo-electron microscopy. J. Microsc. 159, 215-222.

Tvedt, K.E., Halgunset, J., Kopstad, G. & Haugen, O.A. (1988) Quick sampling and perpendicular cryosectioning of cell monolayers for the X-ray microanalysis of diffusible substances. J. Microsc. 151, 49-59.

Umrath, W. (1974) Cooling bath for rapid freezing in electron microscopy. J. Microsc. 101, 103-105.

Umrath, W. (1975) Rapid freezing in open cooling baths. Arzneim.- Forsch. (Drug Res.) 25, p.450.

Van Harreveld, A. & Crowell, J. (1964) Electron microscopy after rapid freezing on a metal surface and substitution fixation. Anat. Rec. 149, 381-386.

Van Harreveld, A. & Trubatch, J. (1979) Progression of fusion during rapid freezing for electron microscopy. J. Microsc. 115, 243-256.

Van Harreveld, A., Crowell, J. & Malhotra, S.K. (1965) A study of extracellular space in central nervous tissue by freeze-substitution. J. Cell Biol. 25, 117-137.

Van Harreveld, A., Trubatch, J. & Steiner, J. (1974) Rapid freezing and electron microscopy for the arrest of physiological processes. J. Microsc. 100, 189-198.

Van Venetie, R., Hage, W.J., Bluemink, J.G. & Verkleij, A.J. (1981) Propane jet-freezing: a valid ultra-rapid freezing method for the

preservation of temperature dependent lipid phases. J. Microsc. 123, 287-292.

Venrooij, G.E.P.M. (1975) Studies on freezing velocity and crystal size. Arzneim.-Forsch. (Drug Res.) 25, p.451.

Van Venrooij, G.E.P.M., Aertsen, A.M.H.J., Hax, W.M.A., Ververgaert, P.H.J.T., Verhoeven, J.J. & Van der Horst, H.A. (1975) Freeze-etching: freezing velocity and crystal size at different locations in samples. Cryobiology 12, 46-61.

Verna, A. (1983) A simple quick-freezing device for ultrastructure preservation: evaluation by freeze-substitution. Biol. Cell 49, 95-98.

Wendt-Gallitelli, M.F. & Isenberg, G. (1989) Single isolated cardiac myocytes frozen during voltage-clamp pulses: a technique for correlating X-ray microanalysis data on calcium distribution with calcium inward current in the same cell. In: *Electron Probe Microanalysis, Applications in Biology and Medicine* eds. K. Zierold & H. Hagler, Springer Series in Biophysics, Vol. 4 pp. 265-279. Springer Verlag, Berlin Heidelberg.

Westwater, J.W. (1959) Boiling heat transfer. Amer. Sci. 47, 427-446.

Williams, R.C. (1954) The application of freeze-drying to electron microscopy. In: *Biological Applications of Freezing and Drying* (ed. R.J.C. Harris) pp.303-328. Academic Press, New York.

Wilson, A.J. & Robards, A.W. (1982) Some experiences in the use of a polymeric cryoprotectant in the freezing of plant tissue. J. Microsc. 125, 287-298.

Woolley, D.M. (1974) Freeze-substitution: a method for the rapid arrest and chemical fixation of spermatozoa. J. Microsc. 101, 245-260.

Young, J.Z. (1935) Osmotic pressure of fixing solutions. Nature, 135, 823-824.

Zalokar, M. (1966) A simple freeze-substitution method for electron microscopy. J. Ultrastruct. Res. 15, 469-479.

Zasadzinski, J.A.N. (1988) A new heat transfer model to predict cooling rates for rapid freezing fixation. J. Microsc. 150, 137-149.

Zierold, K. (1991) Cryofixation methods for ion localization in cells by electron probe microanalysis: a review. J. Microsc. 161, 357.

Zierold, K., Gerke, I. & Schmitz, M. (1989) X-ray microanalysis of fast exocytotic processes. In: *Electron Probe Microanalysis, Applications in Biology and Medicine* eds. K. Zierold & H. Hagler, Springer Series in Biophysics, Vol. 4 pp. 281-292. Springer Verlag, Berlin Heidelberg.

Zglinicki, T. von, Rimmler, M. & Purz, H.-J. (1986) Fast cryofixation technique for X-ray microanalysis. J. Microsc. 141, 79-90.

Collaborators

Four papers have been published based on work in this thesis (see Appendix 3) and these are appended at the end of this thesis, as Appendices 4.1-4.4. The papers were contributed to by the following colleagues, who were coauthors. Their contributions to the work are described below.

Mr. David Purse was Engineering Workshop manager at the Marine Biological Association when the work began. He interpreted my drawings of apparatus into engineering possibilities and constructed them.

Mr. 'Robbie' Robinson was Electronics Workshop manager at the Marine Biological Association and designed and built the sensor device used for monitoring plunge motion, following my original enquiry about using a linear resistor.

Mr. John Wood assembled the double oscilloscope and transient recorder electronics system. He also modified the thermocouple-feedback power supply system for regulating coolant supply and specimen temperature during freeze-drying.

Mr. David Nicholson, the Laboratory Senior Photographer, provided photographic assistance, together with help and encouragement throughout the work.

Dr Klaus Neumann (University of Homburg) and Dr. Peter Simonsberger (University of Salzburg) took an interest in the work from 1985 onwards, when I first returned to Austria to give talks at Seefeld and Salzburg. They are electron microscopists who are involved in the use and

development of cryotechniques and they have given advice on the use of metal planchettes, freeze-substitution and the liquefaction of large volumes of flammable gases.

Dr Bill Bald (University of York) calculated theoretical ice crystal sizes which were given in a published paper. They are presented here in Section 8, to compare with measured, experimental ice crystal sizes.

Regarding the paper by Bone *et al.* (1987), Dr. Quentin Bone coordinated the work and performed microelectrode analyses of ionic content with Dr. Colin Brownlee; Mr. Malcolm Liddicoat performed ammonia analyses, Dr. Geof Bryan and Mr. Gary Burt performed analyses by atomic absorption, Dr. Paul Dando analysed free amino acids by high pressure liquid chromatography, and Dr. Ann Pulsford carried out investigations on sectioned specimens using conventional transmission electron microscopy.

Activities undertaken in connection with this research

16 Jan. 1985: Gave a seminar at the Marine Biological Association, Plymouth, entitled "Plunge-cooling in practice".

16. Feb. 1985: Talked to Cardiff E.M. Club during a Reichert Open Day, on "Rapid freezing of tissue blocks for cryoultramicrotomy".

1-4 April 1985: Attended the 3rd International Low Temperature Biological Microscopy and X-ray Microanalysis Meeting, Cambridge. Gave a paper entitled "Plunge-cooling of tissue blocks".

25 Sept.-4 Oct. 1986: Gave a seminar at Workshop no. 34 on "Cryomethods in Biological Ultramicrotomy and Electron Microscopy" at Seefeld, Austria, organised by Prof. Hellmuth Sitte.

14 Oct. 1986: Gave a lecture entitled "Cryotechniques in electron microscopy with special reference to plunge-cooling experiments" at the Institute of Zoology, University of Salzburg, Austria.

15 Oct. 1986: Gave a tutorial to Dr Hannes Pohla's group at the University of Innsbruck, Austria.

19 Oct. 1987: Organised a lecture at the Marine Biological Association, Plymouth, by Dr Wolfgang Probst, of Carl Zeiss, Oberkochen, Germany, entitled "Electron spectrosocopic imaging and image analysis in the transmission electron microscope". This included the processing of images from frozen, hydrated specimens.

9-10 Dec. 1987: Organised a Carl Zeiss seminar and demonstration at the Marine Biological Association, Plymouth, of the Zeiss EM 902 microscope, with a tutorial about cryo-T.E.M.

19 Feb. 1988: Gave a paper entitled "Plunge-freezing experiments and quantified X-ray microanalysis using cryo-S.E.M." at the Southern Cryo Users Meeting, at the International Mycological Institute, Kew, London.

17 May 1988: Attended the Bristol Fine Structure Group meeting at the University of Bristol on "Principles and applications of freeze-fracture and freeze-etching", given by Prof A.W. Robards.

28 June 1988: Awarded the first Geoffrey Meek Memorial Prize by the Royal Microscopical Society for technical advances in Microscopy, at the Royal Society, Carlton House, London.

21 Oct. 1988: Attended the Southern Cryo Users Meeting II at the Royal Veterinary College, London, on "Cryo-SEM and freeze-fracture".

12-16 Dec. 1988: Attended the Royal Microscopical Society "Cryo-techniques Course in Electron Microscopy" at the University of Glasgow, organised by Prof Hugh Elder and Prof Tony Robards.

3 Mar. 1989: Attended the Cryo-Microscopy Group meeting entitled "Cryomicroscopy and analysis of hydrated specimens" at the Eastman Dental Hospital, London.

Also, elected Honorary Treasurer of the Cryo-Microscopy Group.

6-15 Mar. 1989: Gave seminars at Workshop no. 40 on "Cryomethods in Biological Electron Microscopy" at Seefeld, Austria.

22 Mar. 1989: Gave a paper to the Biological X-ray Microanalysis Group meeting at the Medical Society, London, entitled "Freezing of biological specimens".

11-12 Oct. 1989: Visited Carl Zeiss, Oberkochen, Germany, with Dr Jim Nott for demonstrations of the Zeiss Cryo EM 902 and the Zeiss plunge freezing device.

13 Oct. 1989: Gave a talk to the Faculty of Natural Sciences, University of Salzburg, with Dr Jim Nott, on "Cryotechniques and the localisation of elements in cells and tissues".

15-19 Oct. 1989: Gave seminars at Workshop no. 45 on "Cryomethods in Biological Electron Microscopy" at Seefeld, Austria.

29 Nov. 1989: Gave paper entitled "Rapid cooling techniques for use with freeze-substitution and low temperature embedding" at the Cryo-Microscopy Group meeting, Royal Veterinary College, London.

13 Feb. 1990: Gave a talk to the Bristol Fine Structure Group entitled "Chilling tales: cryofixation and low temperature electron microscopy" at the University of Bristol.

2-6 April 1990: Attended the 4th International Meeting on Low Temperature Microscopy and Analysis at Cambridge and gave a paper

entitled "Ice crystal growth during cryofixation", with Dr W.B. Bald as coauthor.

13 July 1990: Attended a workshop given by RMC and Prof. Herb Hagler, Dallas, Texas, at the University of Wales, Cardiff, on "Cryoultramicrotomy and Cryotechniques".

23 Oct.-3 Nov. 1990: Gave seminars at Workshop no 49A on "Cryomethods in Biological Electron Microscopy" and Workshop no. 49B on "Cryofixation, Cryosubstitution and Low Temperature Embedding" at Seefeld, Austria, organised by Prof. H. Sitte.

28 Nov. 1990: Attended the Cryo-Microscopy Group meeting entitled "The ever expanding world of cryo-SEM", at the Royal Veterinary College, London.

21-23 April 1991: Attended the "X-ray Microanalysis in Biology: Experimental Techniques and Applications" meeting at the University of Manchester.

22 May 1991: Gave a talk entitled "Freeze-drying tissue samples for X-ray microanalysis" at the Cryo-Microscopy Group meeting at the Royal Veterinary College, London.

Publications associated with this research

1 Ryan, K.P. & Purse, D.H. (1985) A simple plunge-cooling device for preparing biological specimens for cryo-techniques. Mikroskopie (Wien) 42, 247-251.

2 Ryan, K.P., Purse, D.H., Robinson, S.G. & Wood, J.W. (1987) The relative efficiency of cryogens used for plunge-cooling biological specimens. J. Microsc. 145, 89-96.

3 Ryan, K.P., Bald, W.B., Neumann, K., Simonsberger, P., Purse, D.H. & Nicholson, D.N. (1990) Cooling rate and ice crystal measurement in hydrated metal-sandwiched specimens plunged into liquefied ethane, propane, and Freon 22. J. Microsc. 158, 365-378.

4 Bone, Q., Brownlee, C., Bryan, G.W., Burt, G.R., Dando, PR., Liddicoat, M.I., Pulsford, A.L. & Ryan, K.P. (1987) On the differences between the two 'indicator' species of Chaetognath, *Sagitta setosa and S. elegans*. J. mar. biol. Ass. U.K. 67, 545-560

Mikroskopie (Wien) 42, 247–251 (1985)
Verlag Georg Fromme & Co., Wien (Oesterreich)

Mikroskopie

Short Technical Communication

Marine Biological Association of the U. K., The Laboratory, Plymouth, England

A Simple Plunge-cooling Device for Preparing Biological Specimens for Cryo-techniques

(Eine einfache Eintauch-Kühlvorrichtung zum Herstellen biologischer Präparate für die Kryo-Technik)

By Keith P. RYAN[1]) and David H. PURSE

With 3 figures

(Received 6th May 1985, revised version 30th August 1985)

Summary

An inexpensive device is described for rapidly cooling specimens by plunging them into a cryogen which is 130 mm deep. Propane, ethane, Freon 22 and a mixture of propane and iso-pentane have been used as cryogenic fluids. The cryogens are cooled by liquid nitrogen and but are maintained above their freezing points. Plunge velocity is varied with elastic catapult tension and monitored with a sensor connected to an oscilloscope. Specimens can be prepared for cryo-sectioning, cryo-substitution, freeze-fracture and freeze-drying.

Zusammenfassung

Es wird eine billige Einrichtung beschrieben, die es erlaubt, das rasche Einfrieren durch Einschießen in Stickstoff mit einer Tiefe von 130 mm zu erreichen. Als kryogene Flüssigkeiten wurden Propan, Äthan, Freon 22 und eine Mischung aus Propan und Iso-Pentan verwendet. Die kryogenen Flüssigkeiten werden in flüssigem Stickstoff gekühlt und oberhalb ihres Gefrierpunktes gehalten. Die Einschußtechnik wird durch ein elastisches Katapultsystem gewährleistet, dessen Spannung über ein Oszilloskop kontrolliert wird. Es können Objekte für die Gefriersubstitution, das Gefrierbrechen, Gefriertrocknen und zum Gefrierschneiden eingefroren werden.

Introduction

Rapid cooling is becoming an increasingly important method of preparing biological specimens for electron microscopy. This report is a preliminary description of an apparatus under development which, with modified specimen supports, has produced improvement in the freezing of small tissue blocks (RYAN and PURSE, 1984) and has been used in freeze-substitution studies of muscle tissue (BONE et al., 1985) and lysosomal membranes (NOTT et al., 1985). It is also used in experiments where thermocouples are embedded in hydrated gelatin specimens; results from these experiments demonstrate the importance of block size,

[1]) Address for Correspondence: Mr. Keith RYAN, B. Sc., CIBiol., Marine Biological Association of the U. K., The Laboratory, Citadel Hill, Plymouth PL 1 2 PB, England.

method of specimen support and plunge velocity in a practical situation (RYAN and PURSE, 1985).

The apparatus incorporates a number of practical features: the cryogen is deep and its temperature can be controlled; thermal gradients within the cryogen are eliminated by a magnetic stirrer; the cold gas layer above the cryogen is eliminated at the time of plunging; and high speed injection can be performed. A simple transfer technique minimises rewarming of specimens after plunging. Forceps have been fixed on the plunger rod for bare grid technique. Designs for specimen supports are described.

Construction and use of the aparatus

The freezing chamber is a polystyrene box which contains liquid nitrogen; it is supported on a wooden baseboard over a magnetic stirrer. A brass plate fits the bottom of the box in the centre of which is fixed a brass ring, this houses the main cryogen unit and locates it with respect to the stirrer. The cryogen unit consists of two concentric copper pipes (dimensions in this model are 15 × 130 and 40 × 130 mm), these are fitted with end-plates. The smaller pipe is suspended inside the larger pipe by two pins near the top and by a spacing ring near the bottom. Liquid nitrogen is maintained in the polystyrene box near the top of the outer pipe, the space between the pipes is not normally flooded unless the propane: pentane mixture is used (JEHL et al., 1981) when maximum cooling is required.

The space between the copper pipes provides a site for liquifying propane or ethane gas, a narrow copper tube runs down in the space to join the inner pipe near its base. Gas is fed into the top of the tube from a supply cylinder by plastic tubing, this is pushed onto the copper tube by about 2 mm only as it is removed after the cryogen is prepared.

The sizes of the pipes and the gap between them can be altered and this, combined with the level of liquid nitrogen maintained in the polystyrene box, can control the temperature of the cryogen. Temperature is controlled more easily by a cartridge heater fitted in a copper block between the two pipes, this is connected to a safe, variable power supply. For some

---

Fig. 1 a: Side view of the cooling device with the plunger and cryogen unit in the raised position. Plunge velocity is controlled by the tension of the elastic. Scale bar 50 mm.

Fig. 1 b: Detail of the scale attached to the plunger side-arm which rests on a metal block prior to release. Also seen are the retaining bracket which guides the scale past the sensor (black box) which monitors plunge motion, this is adjustable in the vertical axis with a locking knob. A neoprene rubber shock absorber is at the top of the figure.

Fig. 2: Experimental result from 0.25 mm diameter hydrated gelatin specimen containing a central thermocouple. Specimen plunged 50 mm into propane: pentane mixture at 0.85 ms^{-1} entry velocity under gravity acceleration. The temperature record (t) shows a cooling rate of 4,720 Ks^{-1} between 273 and 173 K. Cooling is by forced convection during plunge motion as shown by the simultaneously recorded plunge motion record (m) where each cycle represents 1 cm of plunge. Entry point marked by arrow. A 0.25 mm cube tissue block plunged under these conditions without cryo-protection would show restricted ice-crystal damage after cryo-substitution. Temperature scale markers are 273 K, 173 K and 77 K. Time scale bar: 10 ms.

Fig. 3: Experimental result from 1.0 mm diameter gelatin specimen plunged 80 mm at 0.6 ms^{-1}. The cooling rate is 1,080 Ks^{-1} and cooling is seen to occur mainly after plunge motion has ceased, by the slower processes of natural convection and conduction. A 1.0 mm cube tissue block plunged under similar conditions would show extensive ice-crystal damage. Time scale bar: 50 ms.

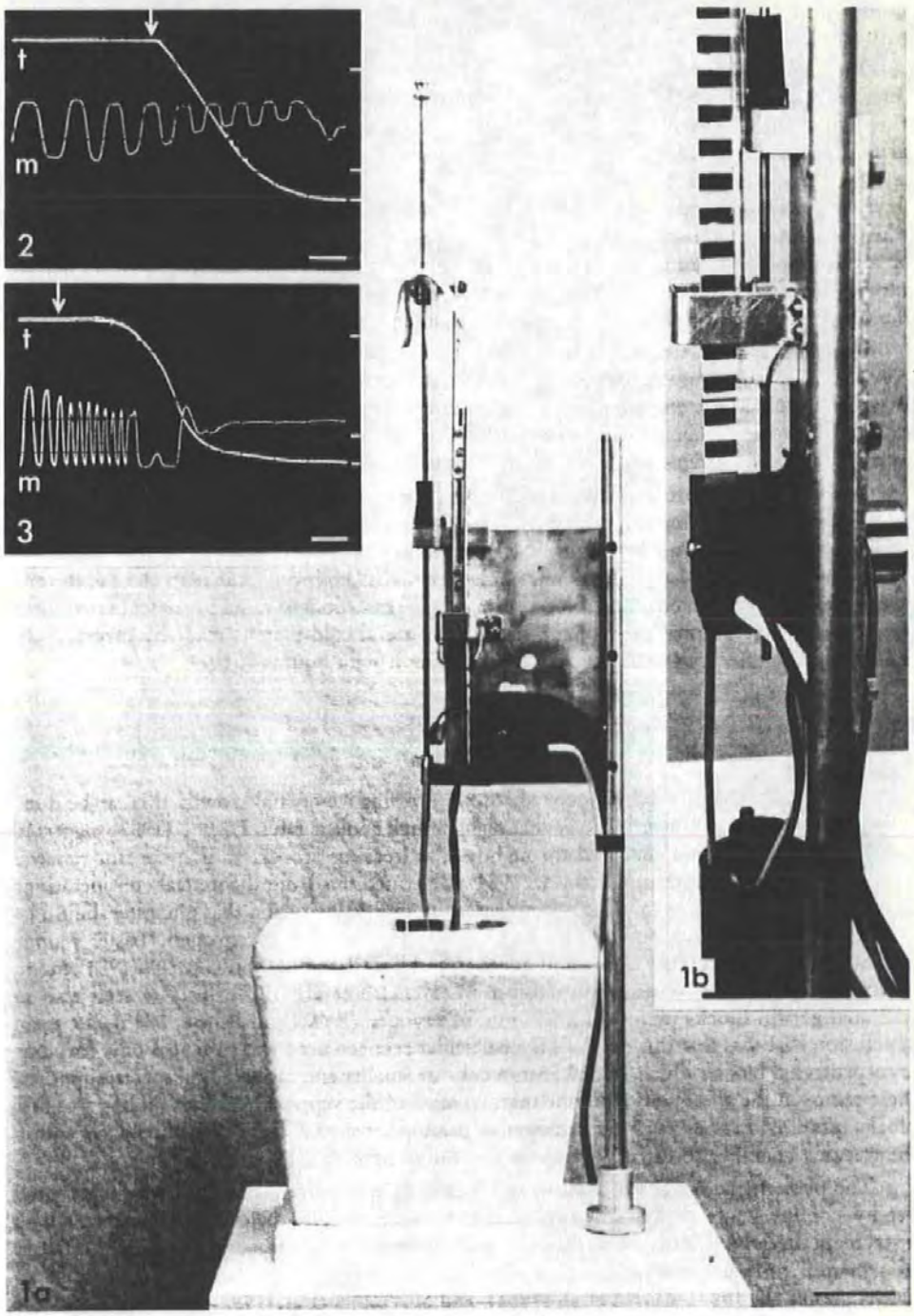
t
m
2
t
m
3
1b
1a

applications the device has been used as described up this point for plunging by hand; also specimens have been allowed to fall through the cryogen into a mesh basket which has a long wire handle for retrieval.

For high speed immersion a plunger is mounted on a gantry above the freezing chamber (Fig. 1a). The gantry swivels on a vertical pole set into the baseboard. Two brackets support a wire handle which is used to raise the cryogen unit just before a plunge. The unit is raised so that the cryogen surface is level with the lid of the polystyrene box, this eliminates the cold gas layer which can pre-chill specimens. The plunger has a side-arm with a long vertical section, this rests on a block until released for the plunge. The side-arm bears a scale of 5 mm black and white bands which are scanned by an infra-red sensing device (Fig. 1b), this produces a signal on an oscilloscope enabling monitoring of plunge motion (Figs. 2, 3). Velocity is controlled by varying the length of a piece of elastic looped around the gantry and plunger rod. The end of the rod is drilled out to hold the necessary specimen supports.

After plunging the cryogen unit is lowered but the specimen remains immersed in the cryogen. A liquid nitrogen container is hooked onto the side of the cryogen unit, the specimen is raised to just above the copper pipe, the gantry is quickly swivelled and the specimen is lowered into the container. The specimen is then detached from the plunger under liquid nitrogen and can be removed from the freezing chamber in the container as required.

A specimen support used recently is a Reichert pin with a wire V-frame attached to it with epoxy, long specimens are mounted between the ends of the V. The V can be covered with aluminium foil for use with thin sheet-like specimens. A support for tissue blocks is made by removing the head of a standard pin, a hole is then drilled through the shaft close to the end of the pin which is then chamfered for streamlining. These designs reduce contact between the specimen and the thermal mass of the support. A useful cold-plate is made by inverting the baseplate in the freezing chamber and just flooding it with liquid nitrogen.

Discussion

The success of rapid-cooling depends on suppressing ice-crystal growth, this can be done by using cryo-protectants or by achieving high enough cooling rates. ESCAIG (1982) suggested that plunge motion be maintained throughout the freezing process so that coolant renewal over the specimen is continuous. BALD (1984) confirmed this from theoretical considerations but established also that cooling is dependent on plunge velocity and that plunging should be performed as rapidly as possible **through a sufficient depth of cryogen.** Faster plunge velocity has produced faster cooling in metal assemblies (ROBARDS and CROSBY, 1983) and in epoxy and thin layer aqueous suspensions (COSTELLO et al., 1984). This is seen also in hydrated gelatin blocks plunged into 90 mm of cryogen (RYAN and PURSE, 1985); the main conclusion here was that this depth of the particular cryogen used was sufficient only for non-cryo-protected blocks which were 0.25 mm cube or smaller and mounted on special supports, these removed the specimens from the thermal mass of the support. Another finding was that blocks mounted in this way were sensitive to passing through a deep layer of cold gas within the freezing chamber so the cryogen unit was raised (after ELDER et al., 1982).

The performance of the model described here (130 mm deep) has not been investigated yet by cooling curve experiment. The device was constructed before the Reichert KF 80 instrument became available and does not incorporate safety features seen on the latter. Information on plunge-technique and safety matters can be found in the publications of COSTELLO et al. (1984), ELDER et al. (1982), and SILVESTER et al. (1982).

Acknowledgements:

We wish to thank Mr. S. G. ROBINSON for constructing the infra-red sensor.

References

BALD W.: The relative efficiency of cryogenic fluids used in the rapid quench cooling of biological samples. J. Microsc. **134**, 261–270 (1984).

BONE Q., C. J. P. GRIMELIJKHUIZEN, A. L. PULSFORD and K. P. RYAN: Possible transmitter functions of acetycholine and an RFamide-like substance in *Sagitta* (Chatognatha). Proc. R. Soc. Lond. B. (Submitted, 1985).

COSTELLO M. J., R. FETTER and J. M. CORLESS: Optimum conditions for the plunge freezing of sandwiched samples. In: The Science of Biological Specimen Preparation (Eds. J.-P. Revel, T. Barnard and G. H. Haggis) pp. 105–115, SEM Inc., AMF O'Hare (Chicago), IL 60666–0507, U.S.A. (1984).

ELDER H. Y., C. C. GRAY, A. G. JARDINE and W. H. BIDDLECOMBE: Optimum conditions for cryoquenching of small tissue blocks in liquid coolants. J. Microsc. **126**, 45–61 (1982).

ESCAIG J.: New instruments which facilitate rapid freezing at 83 K and 6 K. J. Microsc. **126**, 221–229 (1982).

JEHL B., R. BAUER, A. DORGE and R. RICK: The use of propane/isopentane mixtures for rapid freezing of biological specimens. J. Microsc. **123**, 307–309 (1981).

NOTT J. A., M. N. MOORE, L. MAVIN and K. P. RYAN: The fine structure of lysosomal membranes in the digestive gland of *Mytilus edulis* exposed to anthracene and phenanthracene. Marine Environmental Research (in press, 1985).

ROBARDS A. W., and P. CROSBY: Optimisation of plunge-freezing: Linear relationship between cooling rate and entry velocity into liquid propane. Cryoletters **4**, 23–32 (1983).

RYAN K. P. and D. H. PURSE: Rapid freezing: specimen supports and cold gas layers. J. Microsc. **136**, pp. RP 5–RP 6 (1984).

RYAN K. P. and D. H. PURSE: Plunge-cooling of tissue blocks: determinants of cooling rates. J. Microsc. (in press, 1985).

SILVESTER N. R., S. MARCHESE-RAGONA and D. N. JOHNSTON: The relative efficiency of various fluids in the rapid freezing of protozoa. J. Microsc. **128**, 175–186 (1982).

Journal of Microscopy, Vol. 145, *Pt* 1, *January* 1987, *pp.* 89–96.
Received 19 *May* 1986; *accepted* 8 *October* 1986

The relative efficiency of cryogens used for plunge-cooling biological specimens

by K. P. RYAN, D. H. PURSE, S. G. ROBINSON *and* J. W. WOOD, *Marine Biological Association of the U.K., The Laboratory, Citadel Hill, Plymouth PL1 2PB*

KEY WORDS. Cryogens, plunge-cooling, coolants, ethane, propane, thermocouples, cooling rates, hydrated gelatin specimens, epoxy resin specimens, latent heat, vapour formation.

SUMMARY

Coolants used for freezing biological specimens were tested for cooling performance in the continuous plunge mode. Results from bare thermocouples showed that ethane cooled faster than propane or a propane:pentane mixture, even when warmed to 25 K above its freezing point. Propane coolants were more efficient than Freon 22 and the slowest cooling occurred in boiling liquid nitrogen. Hydrated gelatin specimens showed similar results with ethane cooling about 33% faster than propane. Epoxy resin specimens cooled faster than hydrated gelatin specimens of similar size. Hydrated and resin specimens cooled over increasing distances as plunge velocity increased. A bare thermocouple, however, cooled over a constant distance when plunged above a critical velocity. This phenomenon may reflect vapour formation and its suppression at high plunge velocities. The rate of cooling in hydrated specimens is shown to have an absolute limit and cannot be modelled by bare thermocouples or resin specimens.

INTRODUCTION

Liquid air was used by Gersch (1932) in a combined cryo-block and plunging technique; since then several coolants have been proposed for freezing biological specimens. Improved freezing results have been attributed to the use of ethanol (Scott, 1934), iso-pentane (Hoerr, 1936), liquid propane (Bell, 1952a), Freon 12 (Bell, 1952b), Freon 22 (Rhebun, 1965) and Freon 21 (Monson & Hutchinson, 1981). Liquid helium II at 2 K has also been used (Fernández-Morán, 1960) although liquid propane proved more efficient (Bullivant, 1965; Bald, 1984).

Liquid ethane was found more recently to cool faster than liquid propane (Silvester *et al.*, 1982); in accord with these experimental results heat transfer analysis revealed that ethane should be the more efficient coolant (Bald, 1984). The analysis also indicated, however, that the result of Silvester *et al.* was not obtained under forced convection and did not detect the real potential for cryo-fixation. Consideration of thermophysical properties indicates that liquid nitrogen should be the most efficient coolant if vapour formation can be suppressed (Bald, 1984); subcooled nitrogen was used by Umrath (1974, 1975). Both ethane and propane have vitrified pure water (Dubochet & McDowall, 1981).

Experimental results are available regarding cooling rates recorded by bare thermocouples and by thermocouples embedded inside metal and epoxy specimens (see review by Costello & Corless, 1978; Costello, 1980; Elder *et al.*, 1982; Robards & Crosby, 1983; Costello *et al.*, 1984). There are, however, few data regarding hydrated specimens which are exposed directly to the coolant. This paper addresses the biologically more relevant question of whether liquid ethane improves cooling rates in exposed, hydrated specimens under conditions of forced convection.

MATERIALS AND METHODS

The coolants used in these experiments were: ethane CP grade and propane CP grade (re-named Grade N1.5(Tech)), both from British Oxygen Company, Special Gases division), Freon 22 (BOC Industrial Gases division), liquid nitrogen (CryoServices Ltd, Worcester) and iso-Pentane (BDH Chemicals Ltd, Poole).

Two plunge-cooling devices were used: one device had a coolant depth of 13 cm and has been described previously (Ryan & Purse, 1985a). The other is essentially similar but with a coolant depth of 60 cm.

Two types of thermocouple were made using 0·3 mm diameter copper and constantan wires. For plunging with a bare thermocouple the wires were trimmed to an angle of 45° and these facets were soldered together. This resulted in a streamlined structure strong enough to withstand repeated plunging; this thermocouple was plunged in the 13 cm deep device.

The second type was made primarily for recording cooling rates from inside a layer of hydrated gelatin, although it was also used without gelatin. The wires were carefully trimmed square at the ends and then soldered end-to-end. 20% gelatin in distilled water was maintained in a water bath and applied to the thermocouple using warmed needles. Gelatin specimens were constructed under a binocular microscope with a calibrated eye-piece graticule. The specimen was maintained hydrated and fixed in 5% glutaraldehyde in distilled water. The results reported here are mostly from specimens with a gelatin thickness of 125 μm around the thermocouple. A larger specimen 1·375 mm in diameter was also used.

The streamlined, bare thermocouple was taped to the end of the plunger rod on the small plunging device. On the deep device the wires from the gelatin:thermocouple specimen were fed through the 1·0 m tube which forms the plunger rod. The gelatin specimen was maintained in a water bath on the plunging apparatus and prior to plunging this was removed and excess water was drained. In some experiments the gelatin was replaced by rapid curing epoxy resin.

Thermocouple output was amplified by a Tektronix 5110 oscilloscope and fed to a Datalab 902 transient recorder, and thence to an XY plotter via the oscilloscope. Plunge motion was monitored with an infra-red sensor (Ryan & Purse, 1985a, b) whose output was treated similarly. The temperature and motion records stored in the transient recorder were displayed on a second oscilloscope. Plunge velocity was set by changing the length of elastic driving the plunger, and mean plunge velocity obtained by timing the plunge over a period during which the specimen cooled from 273 K to 173 K. Cooling distance was measured as being the distance plunged while cooling from 273 K to 173 K.

RESULTS

Table 1 shows cooling rates from the streamlined, bare thermocouple plunged into coolants maintained at various temperatures. Ethane and propane remained supercooled for approximately 10 min with the magnetic stirrer operating before they solidified. Freon 22 never cooled below its freezing point; it stayed at its freezing point for about 10 min before solidifying. The 3:1 mixture of propane and pentane cooled to 78 K and was very viscous.

Table 2 presents results from the thermocouple surrounded by a layer of hydrated

Table 1. Cooling rates obtained from the bare, streamlined thermocouple cooling between 273 K and 173 K while plunging into a 13 cm depth of coolant: Mean (SD), $n=3$. Two plunge velocities were used. The melting point (T_{mp}) and temperature (T) of the coolants are indicated. The results for liquid nitrogen are extrapolated from the slope at 273 K as the thermocouple did not cool to 173 K during the plunge.

Coolant	T_{mp} (K)	T (K)	Cooling rate (K s^{-1}) 1·12 m s^{-1}	2·25 m s^{-1}
Ethane	89·7	88	12109 (517)	13038 (169)
		94	10795 (116)	11634 (377)
		114	8562 (299)	9978 (934)
Propane	83·3	79	8892 (350)	9787 (408)
		88	7596 (586)	8695 (155)
		108	6713 (242)	7652 (320)
Propane/pentane	—	78	6886 (429)	8582 (192)
		98	5973 (571)	7617 (425)
Freon 22	113·0	113	5950 (89)	6706 (162)
		118	5540 (185)	6313 (55)
		138	3895 (162)	4657 (406)
Nitrogen	63·1	77	569 (73)	731 (104)

gelatin, these results were all obtained from the same specimen. The coolant temperatures shown in Table 2 were those used as working temperatures in the 60 cm deep plunger; they were about 5 K above the coolant freezing points and were chosen so as to avoid solidification of the coolant.

Figure 1 compares cooling rates from hydrated specimens and the cleaned, bare thermocouple plunged into ethane and propane, results from an epoxy resin specimen plunged into propane are also given. The results were obtained using the same thermocouple as used in Table 2. The gel specimens were intact after the experiments; this occurred only twice in eleven specimens plunged into propane and once in twelve specimens plunged into ethane.

The cooling rate in the hydrated specimens shows a steady increase as plunge velocity increases up to a critical velocity, above which the cooling rate remains constant. When the gelatin is replaced on the same thermocouple by a layer of epoxy resin of similar thickness the cooling rates are noticeably faster. The cooling rate in the bare thermocouple also shows a linear relationship with plunge velocity, although at the highest velocities it may not be linear.

The distance travelled by the specimens while cooling from 273 K to 173 K are shown in Fig. 2. All specimens cooled over increasing distances as plunge velocity increased. Above a critical velocity the bare thermocouple cooled over a constant distance.

Experiments with larger gelatin specimens were difficult to perform because they were

Table 2. Cooling rates obtained from the non-streamlined thermocouple surrounded by a 125 μm thick layer of hydrated gelatin (the total thickness of the gelatin and thermocouple assembly was 0·55 mm): Mean (SD), $n=2$. Cooling in different cryogens was performed under forced convection while plunging 55 cm through coolant; two plunge velocities were used. Each coolant was maintained about 5 K above its melting point except for the propane : pentane mixture which does not solidify when cooled by liquid nitrogen.

Coolant	T (K)	Cooling rate (K s^{-1}) 1·3 m s^{-1}	2·3 m s^{-1}
Ethane	94	2103 (111)	2201 (54)
Propane	88	1647 (138)	1858 (19)
Propane/pentane	78	1699 (89)	1806 (76)
Freon 22	118	1138 (25)	1276 (82)

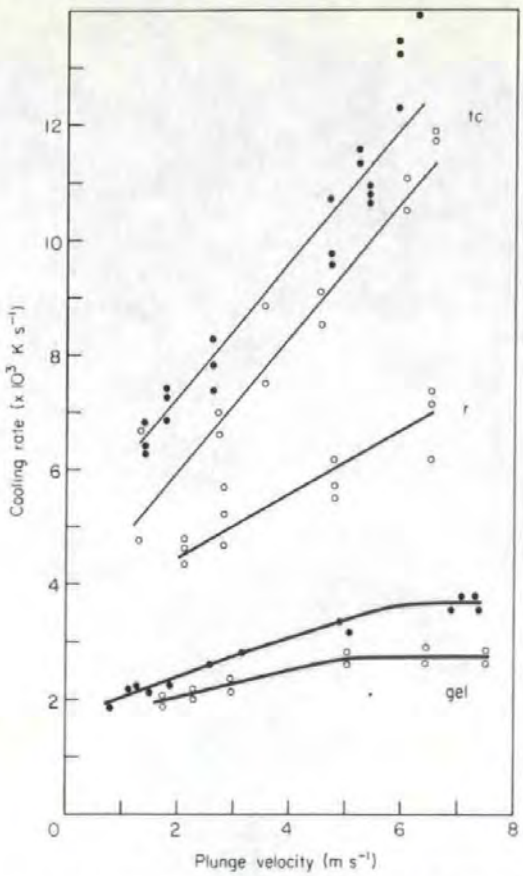

Fig. 1. Cooling rates from a bare thermocouple (tc), hydrated gelatin specimens (gel) and an epoxy resin specimen (r) cooling from 273 K to 173 K. The specimens were plunged 55 cm into ethane maintained at 94 K (closed circles) and propane at 88 K (open circles). The thickness of the gelatin or resin layer around the thermocouple was 125 μm. Note the linear relationship between cooling rate and plunge velocity in the gelatin specimens up to about 5 m s^{-1} in propane and 6·5 m s^{-1} in ethane followed by a uniform cooling rate above those velocities.

easily damaged; as a result, no experiment was completed using both coolants. A 1·325 mm diameter specimen plunged into propane (88 K) at 1·92 m s^{-1} and ethane (94 K) at 1·72 m s^{-1} gave cooling rates of 1112 and 1496 K s^{-1} respectively. The cooling distances over the measured 100 K were 17 cm (propane) and 11 cm (ethane).

DISCUSSION

Cooling of the streamlined thermocouple in a range of coolants

Ethane cooled the bare thermocouple faster than any of the other coolants tested (Table 1). It remained more efficient even when warmed to 25 K above its freezing point, then only supercooled propane cooled faster. Freon 22 was a less efficient coolant compared to ethane and propane, whilst boiling liquid nitrogen was least efficient. The performance of propane, Freon 22 and liquid nitrogen followed the order reported by Costello (1980) and Elder *et al.* (1982).

The thermocouple used in this work was thicker than many freeze-fracture metal sandwich specimens. This suggested that ethane may cool those specimens faster than

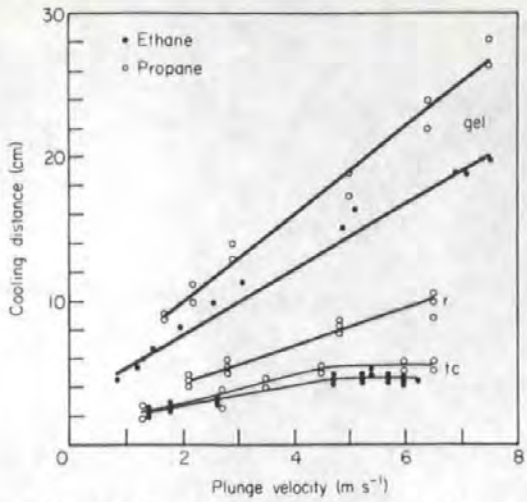

Fig. 2. Cooling distances of the bare thermocouple (tc), hydrated gelatin specimens (gel) and epoxy resin specimen (r) measured simultaneously to the cooling rates presented in Fig. 1. The cooling distance is the distance travelled while cooling from 273 K to 173 K. Coolants: ethane (closed circles) and propane (open circles). Note the linear relationship between cooling distance and plunge velocity in the bare thermocouple up to about 4·5 m s^{-1} followed by a constant cooling distance above that velocity.

propane which is normally used. Trials were performed with a layer of silver cement 1 mm thick sandwiched in Balzers planchettes; it cooled almost 50% faster in ethane than in propane (unpublished results).

Cooling of exposed, hydrated gelatin in a range of coolants

When the thermocouple is surrounded by a layer of hydrated gelatin, ethane cools the specimen faster that the propane coolants (Table 2); Freon 22 cools the specimen less efficiently than propane. These results are at variance with the predictions of Bald (1984) where ethane is the best coolant followed by Freon 22 and propane in that order. This discrepancy is due to the necessity of extrapolating viscosity values for the Freon near its melting point (Bald, personal communication).

High velocity plunging of hydrated specimens in ethane and propane

The results at 1·3 m s^{-1} in Fig. 1 for the hydrated gelatin specimen cooling in ethane are similar to those shown in Table 2, indicating that the specimens and technique are consistent (some variation may be attributed to the size and water content of the specimens at the moment of plunging). The bare thermocouple results in Table 1 cannot be compared as they are from the streamlined thermocouple.

Cooling in the gelatin specimens is dependent on plunge velocity, although plunging above a certain velocity produces no increase in cooling. This situation is not due to limited coolant depth as the specimens are less than half way down the coolant column when this occurs (see Fig. 2). Clearly another limitation to the cooling process arises at this point.

One explanation for the constant cooling rate seen above certain plunge velocities could be that the cooling process is limited by the thermal diffusivity of the specimen. This is probably not the limiting factor in these results because different ultimate cooling rates are obtained using different coolants.

The fastest cooling rates of hydrated gelatin in Fig. 1 are 3650 K s^{-1} (ethane) and 2750 K s^{-1} (propane), i.e. 1·32:1. This ratio is in good accord with the ratio of heat fluxes from specimen to coolant calculated by Bald (1984), these are 97·4 and 73·1 W/cm^2 for

ethane and propane respectively; a ratio of 1·33:1. The cooling rates thus appear to be limited by the predicted coolant efficiencies.

Cooling in large hydrated gelatin specimens

Larger hydrated gelatin specimens cool more rapidly in ethane than in propane. The 1·375 mm diameter gelatin specimen shows cooling rates of 1496 K s^{-1} in ethane and 1112 K s^{-1} in propane, a ratio of 1·34:1 reflecting again, the respective heat fluxes expected under forced convection (Bald, 1984).

Cooling in epoxy specimens

Cooling in a resin specimen is faster than in a hydrated gelatin specimen of the same size, despite the lower thermal conductivity of the resin. This is due largely to two factors: differences in thermal diffusivity and in the release of latent heat which occurs in hydrated specimens during fusion of ice.

The thermal diffusivity of the resin used in this work is estimated to be $0{\cdot}151\times10^{-6}$ m^2 s^{-1} (based on a thermal conductivity of 0·25 W m^{-1} K^{-1} allowing for air entrapment, a specific heat of 1375 J kg^{-1} K^{-1}, and a specific gravity of 1200 kg m^{-3}; Searle, personal communication). The diffusivity of fresh muscle has been calculated to be $0{\cdot}107\times10^{-6}$ m^2 s^{-1} (Jones, 1984). Thus the resin may be expected to cool faster than the hydrated gel. The situation is complicated, however, by the phase transition which occurs during freezing in the hydrated specimen. As the water crystallizes it releases its latent heat, thus retarding the cooling process.

The release of latent heat cannot retard cooling in a non-hydrated resin specimen. It may be negligible or absent in small hydrated specimens that cool fast enough to vitrify rather than crystallize (predicted in Fig. 3 of Stephenson, 1956, and demonstrated in Fig. 7 of Costello *et al.*, 1984). Evidently, therefore, resin cannot be used to model cooling in tissue blocks.

High velocity plunging of a bare thermocouple in ethane and propane

The bare thermocouple used with gelatin and resin specimens showed a linear relationship between cooling rate and plunge velocity (Fig. 1). At the highest velocities cooling may be enhanced by virtue of vapour suppression (see following section on cooling distance).

A linear relationship was reported in metal sandwich specimens plunged 3 cm into propane by Robards & Crosby (1983). However, as they pointed out, increased heat flux occurred after their specimen came to rest. At higher velocities it did not cool to 173 K under forced convection. These velocities gave shorter plunge times resulting in specimen temperature being higher at the moment of arrest, so magnifying the Leidenfrost effect (Bald, 1985).

Linear correlation of cooling rate with plunge velocity in a bare thermocouple was reported also by Costello *et al.* (1984). The thermocouple was 40 μm in diameter and plunged 2·5–3·0 cm into propane. A heat transfer analysis revealed it would have reached coolant temperature in less than 0·5 cm (Bald, 1985).

Cooling in Costello's 30 μm thick epoxy sample sandwiched between copper sheets, however, could be limited by the plunge depth (Costello's Fig. 8b). The copper sheets were up to 100 μm thick; analysis reveals that to cool a 100 μm thick sample holder plunging at 2·5 m s^{-1} to 173 K would require a plunge depth of about 5 cm (Bald, 1985).

Coolant depth was not a limiting factor in the present work. The specimens plunged 55 cm through coolant and the bare thermocouples cooled to 173 K within 6 cm.

Costello's bare thermocouple results were summarized in their Fig. 8(a), the scatter suggests little change in cooling rate with plunge velocity. A possible explanation is that the thermocouple is so small that it is operating close to the limit of its sensitivity. Another

explanation may be flexing of the thermocouple at higher plunge velocities. If the thermocouple can flex during plunging then it will dwell longer in coolant that is warmed, thus it will not cool optimally.

Costello's Fig. 6 reveals that a smaller thermocouple (30 μm diameter) plunging at 0·7 m s^{-1} cools to 173 K in 0·4 ms, i.e. 0·3 mm of plunge. Experiments in this laboratory indicate that both rigidity in the mounting of fine thermocouples and coolant surface temperature are very important.

Distance plunged while cooling from 273 K to 173 K

Cooling occurred over longer distances in all specimens as plunge velocity increased. In the bare thermocouple, however, this process appears to alter at high velocities; this may reflect specimen thermal diffusivity and coolant vaporization at its surface.

As the bare thermocouple cools a layer of vaporized coolant is presumed to form on its surface due to the high thermal diffusivities of the metals (Bald, 1984). High plunge velocity may suppress the formation of this layer to some extent by enhancing coolant renewal, although heat flux would increase as would the potential for further vaporization. Possibly an equilibrium is reached above a critical velocity where vapour formation is suppressed so permitting faster cooling over a shorter distance.

Cooling over a constant distance is not seen in the gel and resin specimens. This probably reflects their poorer thermal diffusivities which preclude the formation of excessive vapour at their surfaces.

The phenomenon of cooling over a constant distance does not signify that the limit of thermocouple sensitivity is reached, because cooling rates continue to increase with the bare thermocouple. Indeed, at the highest plunge velocities there is a hint that cooling improves further and that the curve may inflect upwards (Fig. 1). This phenomenon could be investigated in a high pressure plunger as described by Bald & Robards (1978). In such a device the coolant is maintained at supercritical pressure thus preventing vapour formation and enhancing the rate of cooling.

CONCLUSIONS

1. Ethane produced the fastest cooling in bare thermocouples followed by propane, an iso-pentane:propane mixture, Freon 22 and liquid nitrogen in that order. Ethane at 25 K above its melting point cooled more efficiently than the other coolants near their melting points (with the exception of supercooled propane).

2. Ethane produced faster cooling than the other coolants in a test specimen of exposed, hydrated gelatin which simulated a tissue block.

3. Epoxy resin specimens cooled faster than hydrated gelatin specimens of the same size. The resin has a higher thermal diffusivity than the gel, also it does not release the latent heat of fusion of ice. It cannot be used to model cooling in relatively large, hydrated specimens.

4. Increased plunge velocity produced improved cooling rates in bare thermocouples, resin specimens and exposed, hydrated gelatin specimens. During continuous plunging the rate of cooling in hydrated specimens reached an absolute limit.

5. The rate of cooling in small hydrated specimens has been shown previously to depend on block size, method of support, plunge velocity and coolant depth. This study shows that under continuous forced convection the particular coolant is a limiting factor.

6. Ethane may be a more efficient coolant than propane for freeze fracture specimens sandwiched in metal planchettes.

7. The distance plunged while cooling from 273 K to 173 K increased with plunge velocity. However, when a bare thermocouple was plunged above a critical velocity cooling occurred over a constant distance. This demonstration may highlight the problem of vapour formation which occurs when plunging at atmospheric pressure.

ACKNOWLEDGMENTS

We wish to thank Dr Quentin Bone F.R.S. and Dr Jim Nott for continued encouragement, Mrs Linda Mavin for maintaining liquid nitrogen supplies and Mr David Nicholson for various photographic services. Mr R. Searle of Ciba-Geigy Plastics, Duxford, Cambridge, provided information about epoxy resins. We are grateful to Dr W. B. Bald for criticism of an early draft of the manuscript.

REFERENCES

Bald, W.B. (1984) The relative efficiency of cryogenic fluids used in the rapid quench cooling of biological samples. *J. Microsc.* **134**, 261–270.

Bald, W.B. (1985) The relative merits of various cooling methods. *J. Microsc.* **140**, 17–40.

Bald, W.B. & Robards, A.W. (1978) A device for the rapid freezing of biological specimens under precisely controlled and reproducible conditions. *J. Microsc.* **112**, 3–15.

Bell, L.G.E. (1952a) The application of freezing and drying techniques in cytology. *Int. Rev. Cytol.* **1**, 35–63.

Bell, L.G.E. (1952b) Cooling bath for cytological investigations. *Nature*, **170**, 719.

Bullivant, S. (1965) Freeze-substitution and supporting techniques. *Lab. Invest.* **14**, 1178–1195.

Costello, M.J. (1980) Ultra-rapid freezing of thin biological samples. *Scanning Electron Microscopy II*, 361–370.

Costello, M.J. & Corless, J.M. (1978) The direct measurement of temperature changes within freeze-fracture specimens during rapid quenching in liquid coolants. *J. Microsc.* **112**, 17–37.

Costello, M.J., Fetter, R. & Corless, J.M. (1984) Optimum conditions for the plunge freezing of sandwiched samples. *The Science of Biological Specimen Preparation* (ed. by J.-P. Revel, T. Barnard and G. H. Haggis), pp. 105–115. SEM Inc., AMF O'Hare (Chicago), Illinois.

Dubochet, J. & McDowall, A.W. (1981) Vitrification of pure water for electron microscopy. *J. Microsc.* **124**, RP3–RP4.

Elder, H.Y., Gray, C.C., Jardine, A.G., Chapman, J.N. & Biddlecombe, W.H. (1982) Optimum conditions for cryoquenching of small tissue blocks in liquid coolants. *J. Microsc.* **126**, 45–61.

Fernández-Morán, H. (1960) Low temperature preparation techniques for electron microscopy of biological specimens based on rapid freezing with liquid helium II. *Ann. N.Y. Acad. Sci.* **85**, 689–713.

Gersch, I. (1932) The Altmann technique for fixation by drying while freezing. *Anat. Rec.* **53**, 309–337.

Hoerr, N.L. (1936) Cytological studies by the Altmann–Gersch freezing-drying method. *Anat. Rec.* **65**, 293–313.

Jones, G.J. (1984) On estimating freezing times during tissue rapid freezing. *J. Microsc.* **136**, 349–360.

Monson, K.L. & Hutchinson, T.E. (1981) X-ray microanalysis of freeze-dried muscle: techniques and problems. *Microprobe Analysis of Biological Systems* (ed. by T. E. Hutchinson and A. P. Somlyo), pp. 157–176. Academic Press, New York.

Rhebun, L.I. (1965) Freeze-substitution: fine structure as a function of water concentration in cells. *Fed. Proc.* **24**, S217–S232.

Robards, A.W. & Crosby, P. (1983) Optimisation of plunge-freezing: Linear relationship between cooling rate and entry velocity into liquid propane. *Cryoletters*, **4**, 23–32.

Ryan, K.P. & Purse, D.H. (1985a) A simple plunge-cooling device for preparing biological specimens for cryo-techniques. *Mikroskopie*, **42**, 247–251.

Ryan, K.P. & Purse, D.H. (1985b) Plunge-cooling of tissue blocks: determinants of cooling rates. *J. Microsc.* **140**, 47–54.

Scott, G.H. (1934) A critical study and review of the method of microincineration. *Protoplasma*, **20**, 133–151.

Silvester, N.R., Marchese-Ragona, S. & Johnston, D.N. (1982) The relative efficiency of various fluids in the rapid freezing of protozoa. *J. Microsc.* **128**, 175–186.

Stephenson, J.L. (1956) Ice crystal growth during the rapid freezing of tissues. *J. biophys. biochem. Cytol.* **2** (Suppl.), 45–52.

Umrath, W. (1974) Cooling bath for rapid freezing in electron microscopy. *J. Microsc.* **101**, 103–105.

Umrath, W. (1975) Rapid freezing in open cooling baths. *Arzneim.-Forsch. (Drug Res.)*, **25**, 450–451.

Journal of Microscopy, Vol. 158, *Pt* 3, *June* 1990, *pp.* 365–378.
Received 20 *September* 1989; *revised and accepted* 30 *November* 1989

Cooling rate and ice-crystal measurement in biological specimens plunged into liquid ethane, propane, and Freon 22

by K. P. RYAN, W. B. BALD*, K. NEUMANN†, P. SIMONSBERGER‡, D. H. PURSE *and* D. N. NICHOLSON, *Plymouth Marine Laboratory, Citadel Hill, Plymouth PL1 2PB, England, *Wolfson Unit for Applied Cryobiology, Institute for Applied Biology, University of York, York YO1 5DD, England, †Fachrichtung 3.5 Medizinische Biologie, Universität des Saarlandes, D-6650 Homburg-Saar, F.R.G. and ‡Institut für Zoologie, Naturwissenschaftliche Fakultät, Universität Salzburg, Hellbrunner Strasse 34, A-5020 Salzburg, Austria*

KEY WORDS. Cryofixation, coolants, hydrated specimens, plunge-cooling, cooling rates, ethane, propane, Freon 22, freeze-fracture, cryotechniques.

SUMMARY

Specimens sandwiched between copper planchettes were plunged up to a depth of 430 mm into coolants used for cryofixation. Hydrated gelatin containing a miniature thermocouple was used to mimic the behaviour of tissue during freezing. Gelatin and red blood cells were used for ice-crystal analysis. Ethane produced the fastest cooling rates and the smallest ice-crystal profiles, and Freon 22 produced the slowest cooling rates and the largest crystal profiles. Smaller crystal profiles were often seen in the centre of the specimens than in subsurface zones. The results show that ethane, rather than propane, should be used for freezing metal-sandwiched freeze-fracture specimens by the plunging method, and probably also in the jet-cooling method. They further suggest that good cryofixation could occur at the centre of thin specimens rather than only at their surfaces. Comparison between theoretical and experimental ice-crystal sizes was satisfactory, indicating that where the experimental parameters can be defined then realistic predictions can be made regarding cryofixation results.

INTRODUCTION

Specimens for electron microscopical cryotechnique need to be frozen rapidly, so as to minimize ice-crystal damage (Stephenson, 1956). Liquid samples and cell suspensions, for example, are placed in metal holders and frozen by plunging into a liquid coolant (Costello & Corless, 1978) or by jet cooling (Müller *et al.*, 1980). Practical aspects of the various freezing methods are considered by Sitte *et al.* (1987).

Metal-sandwiched specimens present a complex heat transfer situation, where the coolant first cools the metal holder which in turn cools the hydrated sample. Several workers have measured cooling rates in sandwiched specimens, but they were either all-metal assemblies (Robards & Severs, 1981; Robards & Crosby, 1983), or epoxy-resin sandwiches (Costello 1980; Costello *et al.*, 1984), which, while useful, do not

model cooling in hydrated specimens where the latent heat of fusion of ice is an important factor (Stephenson, 1956; Bald, 1984; Ryan *et al.*, 1987).

Thermocouple results from plunged hydrated specimens (Costello & Corless, 1978; Costello *et al.*, 1984) must be affected by limited plunge depth (Bald, 1985), while those from jet-cooled hydrated specimens (Pscheid *et al.*, 1981; Plattner & Knoll, 1984) were obtained only with propane. The main advantage of thermocouple plunge tests is to measure the heat-transfer coefficient for different cryogens (Bald, 1987).

Cooling efficiency is evaluated more usefully by analysing resultant ice-crystal formation: Stephenson (1956) showed that faster cooling produced smaller crystals. Van Venrooij *et al.* (1975) correlated crystal size and cooling rate with position in a cylindrical specimen, and Schwabe & Terracio (1980) and Elder *et al.* (1982) correlated crystal size in tissue slices with a range of coolants. Theoretical aspects of crystal size and cooling rate were considered by Bald (1986).

This paper describes quench cooling in hydrated, metal-sandwiched specimens under the continuous plunge mode in different coolants, using a thermocouple and an analysis of ice crystals. The thermocouple measurements give some indication of the relative efficiency of the different cryogens but, more importantly, define the minimum plunge depth for each experiment.

MATERIALS AND METHODS

Plunge-cooling was performed using a 2·26-m-high guillotine device, powered by elastic shock-cords (Fig. 1). The basal section houses a tube (20 mm diameter and 600 mm deep) which contains the coolant; this was developed from a smaller device described previously (Ryan & Purse, 1985a).

The upper section supports the plunge-rod. This is a 1·0-m steel tube (3 mm diameter) attached to a cross-bar, which slides vertically on two poles. The cross-bar is held by a latch, against which it is tensioned by the shock-cords; their length is adjustable and controls the plunge velocity.

The test coolants were ethane (93 K), propane (88 K), and Freon 22 (118 K), and were condensed in a cooled glass bottle device having a gas connector, a handle and a pouring spout. The temperatures refer to the bulk of the coolant column; after equilibrating, a small thermal gradient formed in the top layer (20–30 mm deep) with the surface being 4 or 5 K warmer. This was mixed with a rod cooled in liquid nitrogen prior to plunging, resulting in an apparent uniform temperature. Some specimens were frozen in liquid nitrogen. Normal safety precautions were exercised

---

Fig. 1. The plunge-cooling device, 2·2 m high, housing a 610 mm deep cryogen container, and powered by elastic shock-cords (arrowheads). The motion sensor (broad arrow) scans a scale of 5 mm high black and white bands, producing a record of plunge motion (as shown in Fig. 5).

Fig. 2. Side view of the test specimen, showing the two-piece planchette-clamping assembly which is attached to the end of the 1·0-m plunge rod by small screws. The 25 μm diameter thermocouple wires can be seen passing into catheter tubes inside the plunge-rod.

Fig. 3. Face view of one of the planchettes sandwiching the test specimen, showing the centrally positioned thermocouple. The planchette is 4·5 mm wide.

Fig. 4. Section through the test specimen, embedded in resin and ground to show the small thermocouple mid-way between the 110 μm thick planchettes (back-scattered electron image).

Fig. 5. x–y plot showing simultaneously recorded traces of plunge motion and temperature from the control plunge in propane. Arrows indicate contact with the coolant (which is also marked by adjustment of the sensor and a 1-mm black strip on a white scale band) and the end of the 410-mm plunge. The specimen recoils several tens of mm from the foam-rubber buffers. The temperature record shows cooling from room temperature (291 K) to the propane temperature (88 K). Note the rounded shoulder of the cooling curve during freezing, it then enters a straight-line phase before final cooldown. Each cycle on the motion record represents 10 mm of plunge; this specimen plunged 85 mm (at 1·40 m/s) before cooling to 273 K, and 210 mm before reaching 173 K. Markers at right indicate 273, 233 and 173 K. Scale bar = 50 ms.

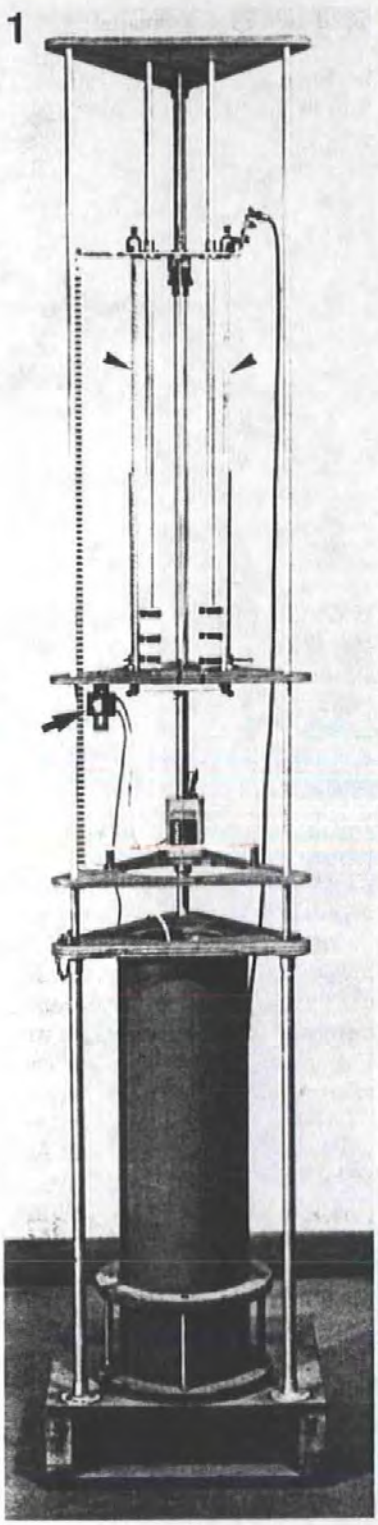
1

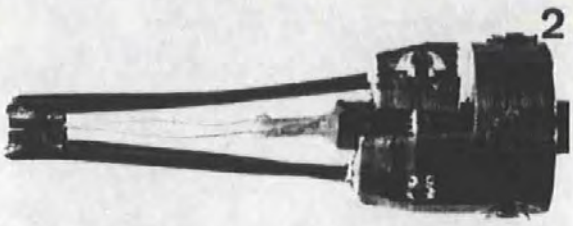
2


3

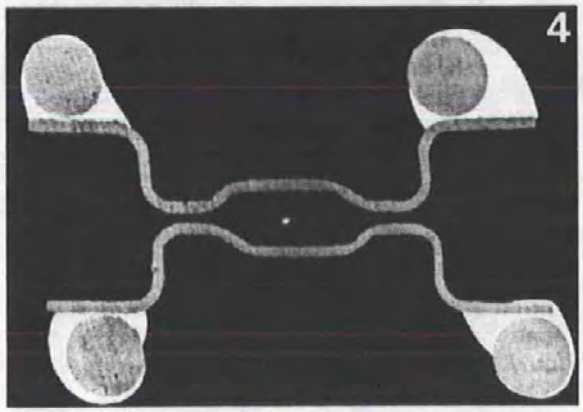
4

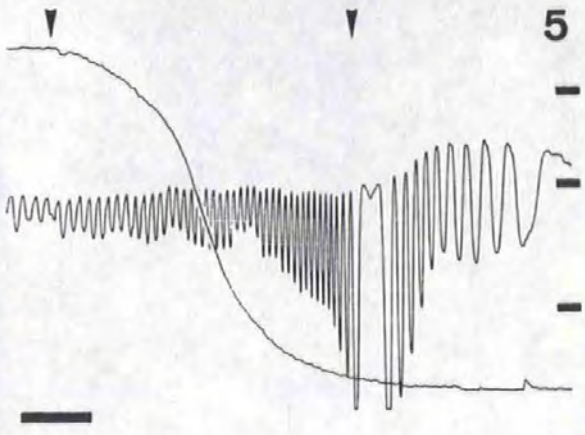
5

(Ryan & Liddicoat, 1987), although the plunger would not fit any available fume cupboard.

Gelatin (20%) in distilled water was used to measure specimen cooling rates and plunge depths. The gelatin was sandwiched between copper planchettes (Balzers BUO 12 057T, 110 μm thick) which were soldered on to supporting wires. These formed part of a two-piece clamp assembly, which was attached to the plunger rod (Fig. 2). The gelatin was warmed and applied quickly to the planchettes with a warm needle; the planchettes were also warmed. The final specimen was maintained in water between plunges.

The specimen which yielded the most complete set of results was embedded in resin after the experiment and ground down to show the position of the thermocouple (see Fig. 4).

Thermocouples were made by soldering together 25 μm chromel and constantan wires, which were fixed to the edge of one planchette with epoxy (Fig. 3). These were of the type that could record maximum cooling slopes of 500,000 K/s (Ryan & Purse, 1985b). Chromel/constantan was used for reasons of economy and greater signal output (9·793 mV over the range 291–77 K compared to 6·248 mV with copper/constantan). The planchettes were spaced 55 μm apart by small pieces of Scotch tape applied along two edges; the gelatin thickness was 415 μm. The wires passed up polythene tubes in the plunger rod to connect with the recording system.

Thermocouple output was amplified by a Tektronix 5103N oscilloscope and fed to a Datalab 902 transient recorder, and then to a plotter via the oscilloscope. Plunge motion was monitored by an i.r. sensor which scanned a scale of black and white bands attached to the cross-bar; its output was treated similarly. A second oscilloscope displayed the records.

Cooling rates at the centre of the gelatin specimen were measured between ambient (291 K) and 273, 263, 253, 243 and 173 K; they were also measured between 273 and 173 K. The distance plunged while cooling over the various temperature ranges was timed and used to calculate the mean plunge velocity. Specimens plunged a total distance of between 420 and 430 mm into the coolants depending on the plunge velocity and the compression of the foam rubber shock absorbers which were used to arrest the specimens.

Initial ice-crystal analysis was performed on 20% gelatin samples plunged into propane. The remainder of the ice-crystal analysis used fresh blood from Flounder (*Platichthys flesus*). Samples were 350 μm thick, excluding the planchettes which were not separated by Scotch tape. They were frozen at various plunge velocities in the three coolants. After plunging, the planchettes were opened under liquid nitrogen, freeze-substituted at 193 K for 48 h in methanol containing 1% OsO_4 and brought to ambient temperature over a 4-h period. The specimen was brought to acetone, carefully detached from the planchette that it adhered to, and embedded in resin (Spurr, 1969).

Ultrathin silver sections, 60–80 nm thick, were cut with a Reichert Ultracut ultramicrotome, collected on coated 2 × 1-mm slot grids and stained in lead citrate solution (Fahmy, 1967). The section plane passed through the centre of the specimen and was perpendicular to the faces which had contacted the planchettes (Fig. 4).

Water content of erythrocytes was estimated by X-ray microanalysis using a Link 860 system, after the method of Ingram & Ingram (1986). The chlorine peak of the resin was used as a label to represent 100% hydration in the medium surrounding the sample. The peak was reduced in the sample by the presence of cell constituents, thus reflecting the original local free-water content. Sections on naked grids were washed on water for 1 h on each side to remove any diffusible chlorine and other ions.

The sections were photographed in a Philips EM300 at the specimen surface, at 10 μm into the specimen and at 20-μm intervals thereafter through the specimen.

Prints were made at × 122,000 and crystal diameter was measured using a ruler (see Fig. 8).

RESULTS

Records of temperature and motion recorded simultaneously are shown in Fig. 5. Cooling rates over the various temperature ranges from a gelatin specimen are plotted in Fig. 6 and cooling distances between 291 and 233 K are shown in Fig. 7. Results were obtained first from propane, followed by ethane, and then from Freon 22. Finally, a control plunge was performed in propane, to check that the specimen gave a similar result to that obtained at the beginning of the experiment. This was the most complete set of results obtained from a single, undamaged specimen. The depths at which the centre of the gelatin specimen reached 273 K are given in Table 1(a). The calculated minimum depths at which the specimen freezes are given in Table 1(b), using the theoretical equations of Bald (1987).

Several other near-identical gelatin specimens were plunged. One specimen plunged at 1·9 m/s in propane gave a cooling rate between 273 and 173 K of 1538 K/s; when arrested after plunging 40 mm, the cooling rate was reduced to 1097 K/s, and when arrested after 20 mm, it was 1051 K/s. These results highlight the importance of the minimum plunge depth concept.

Table 2 presents data illustrating the consistency of results if a specimen is plunged several times under identical conditions. Results from a second specimen are also shown which demonstrate the consistency between specimens. Differences in cooling

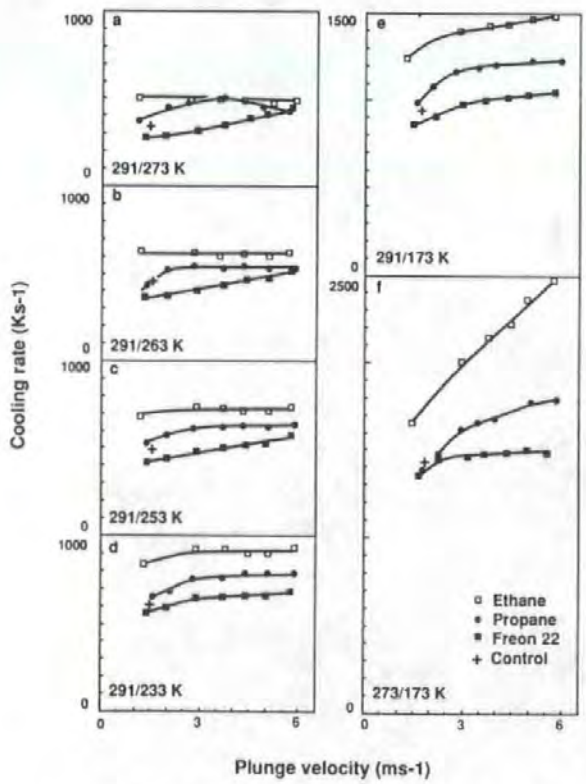

Fig. 6. Cooling rates, between 291 K and 273, 263, 253, 233 and 173 K and between 273 and 173 K, obtained by plunging the same gelatin test specimen first into propane, then ethane, and Freon 22. A final control plunge was performed in propane. Each coolant was 5 K above its melting point.

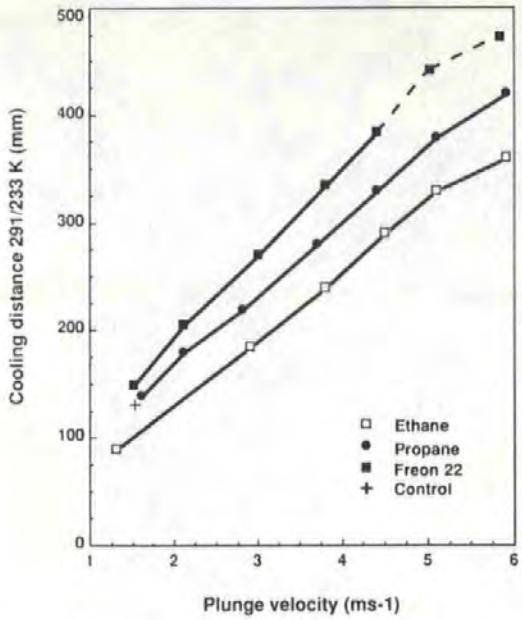

Fig. 7. Cooling distances recorded simultaneously to the cooling rates in Fig. 6(d). These are the distances plunged while cooling from 291 to 233 K. At the highest plunge velocities the specimen reached the plunge bottom in Freon 22 before cooling to 233 K, and the curve is extrapolated from plotted data.

Table 1. Measured (a) and theoretical minimum (b) plunge depths (mm).

	Plunge velocity (m/s)					
Coolant	1·2	2·0	3·5	4·3	5·1	5·7
(a)*						
Ethane	40	(70)	130	160	210	220
Propane	65	85	130	160	210	240
Freon 22	85	120	190	210	220	240
(b)†	1.0	2·0	3.0	4.0	5.0	6.0
Ethane	68	124	171	212	250	282
Propane	79	140	189	232	270	300
Freon 22	86	148	198	240	280	312

*Measured plunge depths at which the temperature in the centre of the gelatin specimen reached 273 K. The figure in parentheses is extrapolated from plotted data.

†Theoretical minimum plunge depths at which the gelatin specimen completely freezes. Calculated using equations (5.6) and (5.12) of Bald (1987) and $\rho_l = 0{\cdot}86$ g/ml, $K_l = 0{\cdot}015$ W/cmK, and $L = 269$ J/g for 20% gelatin.

response between similar specimens are attributed to differences in epoxy thickness separating the planchettes, through which the thermocouple wires pass.

Figure 8 shows the branching, dendritic nature of ice in a 20% gelatin sample. The appearance of erythrocytes at the surface of a specimen is seen in Fig. 9 and cells seen typically half way between the surface and the centre of the specimen are shown in Fig. 10. Figure 11 shows a cell at the centre of a specimen which manifests a freeze-fracture artefact and Fig. 12 shows a specimen frozen in liquid nitrogen.

The X-ray microanalysis results for estimating the water content of erythrocytes gave $71{\cdot}7 \pm 9{\cdot}7\%$ ($n = 10$) background-corrected Cl peak counts compared to those for empty resin, which constituted a peripheral standard.

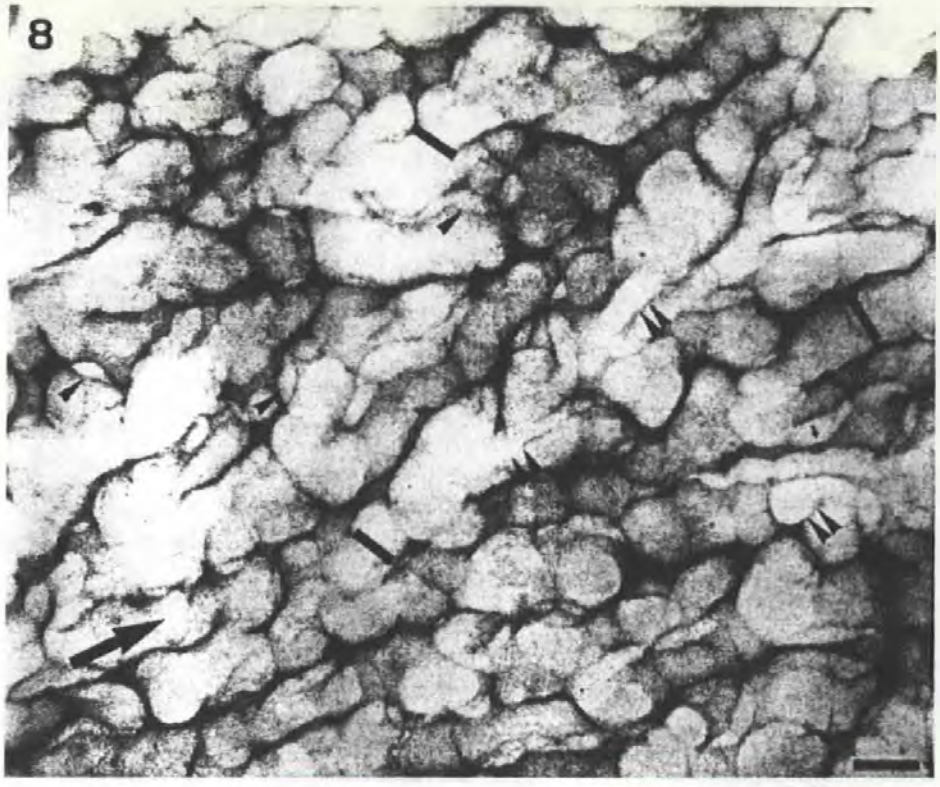

Fig. 8. Dendritic ice crystal formation, after freeze-substitution, in a 20% gelatin specimen plunged into propane at 4·3 m/s. The field was 40 μm from the specimen surface. The arrow indicates the direction of travel of the cooling front. Single pointers indicate crystal overlap. Double pointers indicate graze effects. The bars mark 75 nm diameter profiles, indicating the figure derived from this field. Scale bar = 100 nm.

Table 2. Plunge velocities (m/s) and cooling rates (K/s) from gelatin specimens plunged into propane, to show the consistency of results with one specimen and comparison with another.

Specimen	Plunge velocity	Cooling rate
1	2·40 ± 0·06 (n = 5)	929 ± 11·06 (n = 5)
	4·39 ± 0·10 (n = 5)	1139 ± 48·40 (n = 5)
2	2·15 ± 0·05 (n = 6)	890 ± 43·00 (n = 6)

Figure 13 shows the results of the ice crystal size distribution analysis across gelatin specimens plunged into propane. Figure 14 summarizes the results of the ice-crystal analysis on erythrocytes.

DISCUSSION

Thermocouple experiments

Bald (1984, 1987) has shown that forced convection is the most efficient mode for plunge cooling both exposed specimens and those in metal holders (this is demonstrated here by the slower cooling in the arrested plunges compared to the continuous plunging mode). He has also emphasized that plunging bare thermocouples into

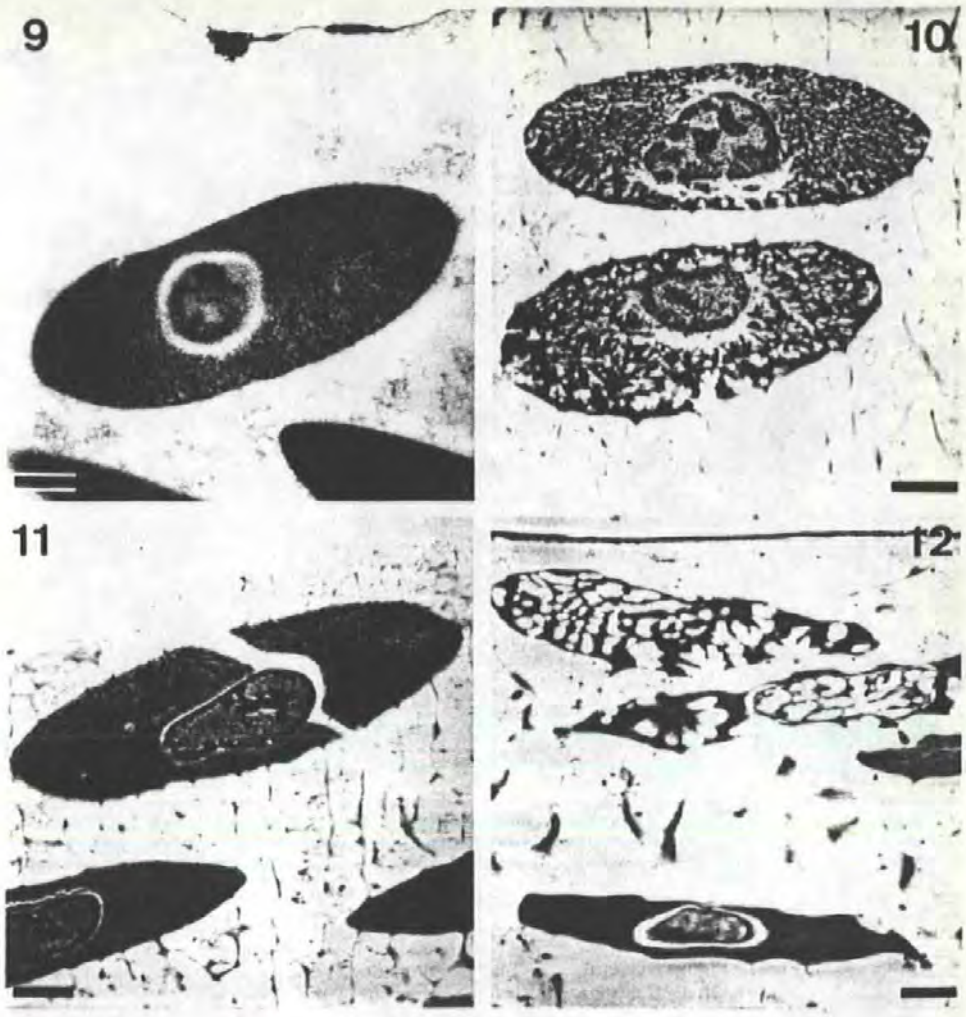

Fig. 9. Red blood cell at the surface of a specimen plunged 430 mm into liquid ethane at 5·7 m/s. The specimen surface is marked by scattered osmium precipitate at the top. Scale bar = 1 μm.
Fig. 10. Blood cells located halfway between the surface and the centre of a specimen frozen in propane at 5·9 m/s. The cooling front approached from the top of the figure. Note the gradation in crystal size along this axis, the dendritic form, and invasion of the cell membrane by the crystallized matrix of plasma. Scale bar = 1 μm.
Fig. 11. Blood cell located near the centre of a specimen plunged into propane at 6 m/s. The cell shows freeze-fracture artefact due to planchette separation during whiplash of the plunge-rod. Scale bar = 1 μm.
Fig. 12. Blood cells plunged 410 mm into liquid nitrogen at 2 m/s. The surface of the specimen is marked by osmium precipitate. The cell nearest the surface shows large ice-crystal profiles, the adjacent cell shows larger crystal profiles and is narrower. The cell at the bottom is shrunken and without obvious ice-crystal damage. Scale bar = 1 μm.

coolants does not give a direct indication of cooling efficiency but merely defines the heat-transfer coefficient for a particular coolant.

It is important that a hydrated specimen is used, because Ryan *et al.* (1987) have shown that epoxy resin does not model cooling in a specimen approximating to a 0·25 mm^3 tissue block.

The results of Fig. 6 show clearly that ethane is the most efficient coolant for the gelatin/thermocouple specimens followed by propane and Freon 22. Considering

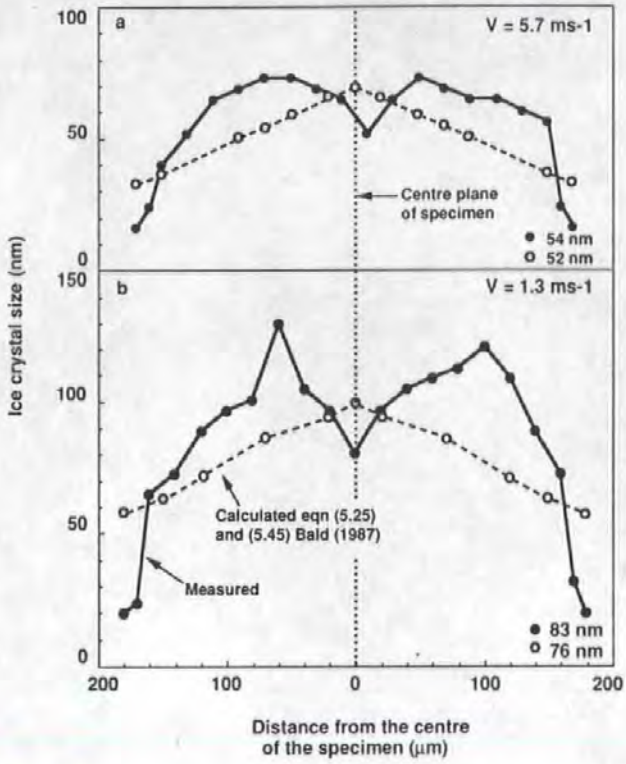

Fig. 13. Ice-crystal size in 20% gelatin samples plunged into propane at 1·3 and 5·7 m/s. Experimental and predicted mean ice-crystal size across each specimen is shown at the right.

temperature ranges from ambient (291 K) down to 233 K, cooling is dependent on the particular coolant but appears almost independent of plunge velocity (Fig. 6a–d). However, Fig. 6(f) shows that after the specimen is frozen, cooling rates increase with faster plunge velocities as would be expected.

The reason for the cooling rate being independent of plunge velocity in Fig. 6(a–d) is caused by the initial non-linear portion of the cooling curve of Fig. 5. This non-linearity is due to the combined effect of measuring the temperature at the centre of the specimen and the poor thermal conductivity of the unfrozen gelatin. These effects could be eliminated to some extent by pre-cooling the specimens to near their freezing point prior to plunging (see Bald, 1987, p. 130).

Figure 6(a) shows the measured cooling rates at the centre of the gelatin sample from ambient to 273 K. The large deviation from linearity in the propane results is probably caused by the release of latent heat at the centre which can suddenly reduce the measured cooling rate. This highlights the errors which can arise in trying to monitor temperature changes near the specimen freezing point.

Cooling rates in propane are slower, and apparently level off at high plunge velocities over the range 291–173 K (Fig. 6e). This was reported in an exposed hydrated specimen by Ryan *et al.* (1987) and was interpreted as a limitation due to coolant efficiency, because the specimen was only half way down the coolant column at that time. In the present results, it is because the specimen reaches plunge bottom a little before it has cooled to 173 K, and then cools by less-efficient processes. This highlights the usefulness of simultaneous plunge motion records (Fig. 5). The effect was more pronounced with Freon 22 in Fig. 6(f).

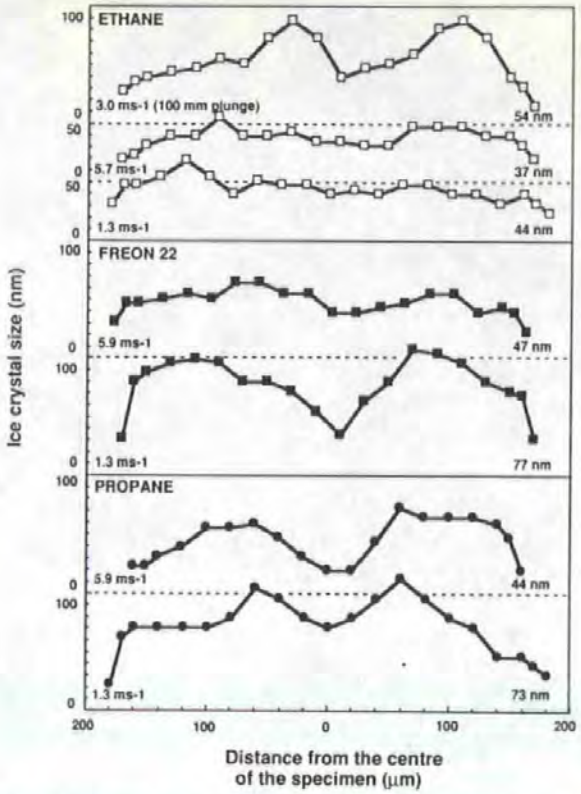

Fig. 14. Ice profile size in sandwiched blood cells. The curves are labelled regarding coolant and plunge velocity (at the left), with mean ice-crystal size at the right. The specimens were plunged 410–430 mm into coolant, depending on plunge velocity, except for the top curve where the specimen was plunged 100 mm into ethane.

Similar results were reported by Costello *et al.* (1984) from a sandwiched epoxy specimen plunged 25 mm into propane. Their thermocouple bead was 30 μm in diameter and sandwiched in planchettes 50–100 μm thick. At entry velocities greater than 1 m/s the cooling rate increased progressively less. This suggests, in the light of our results, that theirs were also affected by insufficient propane depth, as indicated by Bald (1985). However, this does not mean that excellent results cannot be obtained from 10–15 μm thick specimens (Costello *et al.*, 1985).

Figure 7 shows that the more efficient cooling capabilities of ethane requires less plunge distance to cool the centre of the gelatin sample from ambient to 233 K than either propane or Freon 22. There is some indication at the highest plunge velocities of downward deflection in the curves. This was seen previously in bare thermocouple results and was attributed to vapour film suppression (Ryan *et al.*, 1987).

Table 1(b) shows the theoretically calculated *minimum* plunge depths to freeze completely the gelatin specimen at different plunge velocities in the three coolants. These values were obtained using equations (5.6) and (5.12) of Bald (1987). Nominal plunge velocities were used in these calculations because of the variations in the actual plunge velocity referred to earlier.

Comparing the calculated values of Table 1(b) and the measured values of Table 1(a) it can be seen that the theoretical values are consistently greater than the measured. This is attributed to supercooling effects whereby at a measured centre temperature

of 273 K the specimen has not completely yielded up its latent heat of fusion. Pre-cooling the specimen would also improve accuracy (see Bald, 1987, p. 130).

Ice-crystal analysis

Figures 8–14 summarize the results of ice-crystal analysis in the gelatin and blood samples.

Figure 13 shows the comparison between the measured ice-crystal size distributions across the 20% gelatin sample plunged into propane and theoretical predictions. The deviation between theory and experiment at the centre of the specimen is caused by the 'centre-line effect' where cooling rates rise rapidly as the cooling fronts converge. This effect is not included in Bald's theory for a flat specimen.

For the blood samples, surface cells, close to the planchettes, normally froze well, but those slightly deeper showed crystal damage (Fig. 9). Cells well away from the surface always showed extensive damage, as seen in Fig. 10. These are interesting in that each cell shows a gradation in ice profile size, which increases *away* from the cooling specimen surface.

This phenomenon is due to the cooling process within the cell; in the present situation cooling is insufficient to produce vitrification so crystallization occurs. The water nearest the approaching cooling front normally nucleates first and, as crystallization proceeds, the latent heat of fusion of ice is released. This impedes the freezing front so that adjacent water freezes progressively more slowly, resulting in larger crystal profiles across the cell. The holes in the cytoplasm are not individual crystals but dendritic branches of a ramifying crystal (Fig. 8); there is electron diffraction evidence of there being only one crystal in a cell (Dubochet *et al.*, 1988). Other evidence of the 3-D branching nature of the cell crystal was demonstrated recently by Ryan *et al.* (1988, Fig. 10).

Cells at the centre of specimens normally showed reduced ice profile sizes, as reported by Van Venrooij *et al.* (1975). The cell in Fig. 11 shows this and also another artefact: it was plunged at high velocity which can cause whiplashing of the 1·0 m long plunge-rod, the frozen specimen may then strike the side of the coolant tube causing the planchettes to shear apart, thus effecting a freeze-fracture.

A specimen plunged 430 mm into liquid nitrogen showed another phenomenon (Fig. 12). Cells near the specimen surface showed large ice profiles, which increased in size in deeper cells. Those deeper again froze so slowly that the cells had time to dehydrate by losing their water to the freezing matrix around them. They then froze in a shrunken state without apparent crystal formation. This is the basis of cryopreservation, after which cells can be revived, providing membranes are intact.

The results of the ice-crystal analysis on blood are summarized in Fig. 14. The mean ice-crystal sizes of Fig. 14 are compared with theoretically predicted values in Table 3. Theoretical values were calculated using the weighted mean cooling rate equation (5.53) of Bald (1987) together with equation (5.45).

The comparison between theory and measurement is reasonably good but there are difficulties in measuring and predicting ice-crystal sizes in real cell and tissue systems. The comparison between measured and predicted results for the homogeneous gelatin specimen in Fig. 13 is satisfactory but with the erythrocyte there is more variation, although the erythrocyte cytoplasm was chosen for its apparent homogeneity.

A problem in predicting crystal size is imprecise knowledge of the water content of the blood cells. For this study a figure of 70% was used. Published data for Carp (*Cyprinus carpio*) range between 64% for controls and 68·6% for 15 min *in vivo* air stress (Fuchs & Albers, 1988). The time lag in this study between removing the fish from water and plunge-freezing the blood sample was 3–15 min, because several samples were frozen from each bleeding. Measurement of water content on one sample

Table 3. Comparison between measured and theoretical mean ice-crystal sizes in erythrocyte cytoplasm across Flounder blood samples frozen by plunging 410–430 mm into different coolants.

Coolant	Plunge Velocity ($m s^{-1}$)	Ice crystal size (nm)	
		Measured	Theoretical
Ethane	6	38 ± 1	43
	3	42 ± 1	54
	1·3	46 ± 2	65
Propane	6	42 ± 2	46
	4·3	49 ± 2	53
	1·3	72 ± 1	73
Freon 22	6	48 ± 2	49
	3	55 ± 1	65
	1·3	76 ± 1	82

The measured figures are derived from two analyses on the same specimen. Assumed properties for blood in theoretical calculations were U = 5 cm/s, L = 250 J/g, r^* = 3 nm, ϱ_l = 0·98 g/ml, and K_l = 0·019 W/cm K.

indirectly by X-ray microanalysis gave 71·7%. This can be corrected by the normal ionic and free amino-acid content (1·66% of the mass of the intracellular water; Fugelli & Rohrs, 1980) to give a final estimate of 70·5%, assuming that leaching of diffusibles was complete.

There are other problems relating to this type of investigation. Prominent among them is the measurement of small profiles; a 15-nm profile magnified 122,000 times becomes 1·8 mm on a photographic print. Crystal profiles of this order of magnitude have been measured previously, for example 25 nm by Escaig (1982) and 20 nm by Zglinicki *et al.* (1986). Silver section thickness is in the region of 60–80 nm, so that overlay may occur with the smaller crystals.

Another difficulty regarding measurement is the possibility of ice profiles becoming smaller or even disappearing during freeze-substitution. As ice is replaced by solvent then unfrozen eutectics between the ice profiles may fill in the holes, also surrounding proteins may contribute to this process prior to their fixation. Responsibility for measurements in this present study lay with the first author.

CONCLUSIONS

(1) The plunge tests using thermocouples clearly demonstrate that ethane is more efficient for rapidly cooling biological tissue than either propane or Freon 22. Bald (1984) has predicted that, for exposed biological specimens, supercritical nitrogen is potentially the best coolant. However, he concluded that it is less efficient for specimens in metal holders (Bald, 1987), and that these cool faster in highly subcooled, subcritical liquids. This, and the results reported here, suggest that ethane is the most efficient coolant for plunge-cooling, and presumably for jet-cooling, metal-sandwiched specimens.

(2) Thermocouple measurements during rapid plunging highlight the importance of the minimum plunge depth concept for efficient cryofixation. This requirement further indicates the use of ethane as the preferred coolant, although cost and safety considerations may influence this choice (Ryan & Liddicoat, 1987).

(3) Ice-crystal measurements in a 20% gelatin model show encouraging confirmation of the theoretically predicted ice-crystal sizes within a thin flat specimen during plunge-cooling.

(4) Measurements of ice-crystal size within the red cells of fresh Flounder blood show similarly encouraging correlation with predicted crystal sizes. However, these

cells were chosen for their cytoplasmic homogeneity; difficulties arise in dealing with the rapid freezing of other real cell systems, where the water content of different domains within cells is not known.

ACKNOWLEDGMENTS

We are grateful to Dr Quentin Bone, F.R.S., and Dr James Nott, Plymouth Marine Laboratory, and Professor Hans Adam, University of Salzburg, Austria, for their continuing support; to Dr Ann Pulsford for providing blood from the Flounder; to George Best for loaning the Leitz hand microtome used to prepare Fig. 4; and to Albert Nutty for workshop services. This paper is dedicated to Professor Hellmuth Sitte on the occasion of his 60th birthday, in appreciation of his contributions to ultramicrotomy and cryotechniques.

REFERENCES

Bald, W.B. (1984) The relative efficiency of cryogenic fluids used in the rapid quench cooling of biological samples. *J. Microsc.* **134**, 261–270.

Bald, W.B. (1985) The relative merits of different cooling methods. *J. Microsc.* **140**, 17–40.

Bald, W.B. (1986) On crystal size and cooling rate. *J. Microsc.* **143**, 89–102.

Bald, W.B. (1987) *Quantitative Cryofixation*. Adam Hilger, Bristol.

Costello, M.J. (1980) Ultra-rapid freezing of thin biological samples. *Scanning Electron Microsc.* **2**, 361–370.

Costello, M.J. & Corless, J.M. (1978) The direct measurement of temperature changes within freeze-fracture specimens during rapid quenching in liquid coolants. *J. Microsc.* **112**, 17–37.

Costello, M.J., Fetter, R. & Corless, J.M. (1984) Optimum conditions for the plunge freezing of sandwiched samples. *The Science of Biological Specimen Preparation for Microscopy and Microanalysis* (ed. by J.-P. Revel, T. Barnard and G.H. Haggis), pp. 105–116. SEM Inc., Chicago.

Costello, M.J., Fetter, R.D. & Frey, T.G. (1985) Complementary replicas of ultra-rapidly frozen specimens. *The Science of Biological Specimen Preparation for Microscopy and Microanalysis 1985* (ed. by M. Mueller, R.P. Becker, A. Boyde and J.J. Wolosewick), pp. 95–101. SEM Inc., Chicago.

Dubochet, J., Adrian, M., Chang, J.-J., Homo, J.-C., Lepault, J., McDowall, A.W. & Schultz, P. (1988) Cryoelectron microscopy of vitrified specimens. *Quart. Rev. Biophys.* **21**, 129–228.

Elder, H.Y., Gray, C.C., Jardine, A.G., Chapman, J.N. & Biddlecombe, W.H. (1982) Optimum conditions for cryoquenching of small tissue blocks in liquid coolants. *J. Microsc.* **126**, 45–61.

Escaig, J. (1982) New instruments which facilitate rapid freezing at 83 K and 6 K. *J. Microsc.* **126**, 221–229.

Fahmy, A. (1967) An extemporaneous lead citrate stain for electron microscopy. *Proc. 25th Ann. Conf. E.M.S.A.* (ed. by C. J. Arceneaux), p. 148. Ethyl Corporation, Baton Rouge.

Fuchs, D.A. & Albers, C. (1988) Effect of adrenaline and blood gas conditions on red cell volume and intra-erythrocytic electrolytes in the Carp, *Cyprinus carpio*. *J. Exp. Biol.* **137**, 457–477.

Fugelli, K. & Rohrs, H. (1980) The effect of Na^+ and osmolarity on the influx and steady state distribution of taurine and gamma-aminobutyric acid in Flounder (*Platichthys flesus*) erythrocytes. *Comp. Biochem. Physiol.* **67A**, 545–551.

Ingram, F.D. & Ingram, M.J. (1986) Cell volume regulation studies with the electron microprobe. *The Science of Biological Specimen Preparation for Microscopy and Microanalysis 1985* (ed. by M. Mueller, R. P. Becker, A. Boyde and J. J. Wolosewick), pp. 95–101. SEM Inc., Chicago.

Müller, M., Meistner, N. & Moor, H. (1980) Freezing in a propane jet and its application to freeze-fracturing. *Mikroskopie*, **36**, 129–140.

Plattner, H. & Knoll, G. (1984) Cryofixation of biological materials for electron microscopy by the methods of spray-, sandwich-, cryogen-jet- and sandwich-cryogen-jet-freezing: a comparison of techniques. *The Science of Biological Specimen Preparation for Microscopy and Microanalysis* (ed. by J.-P. Revel, T. Barnard and G.H. Haggis), pp. 139–146. SEM Inc., Chicago.

Pscheid, P., Schudt, C. & Plattner, H. (1981) Cryofixation of monolayer cell cultures for freeze-fracturing without chemical pre-treatments. *J. Microsc.* **121**, 149–167.

Robards, A.W. & Crosby, P. (1983) Optimisation of plunge freezing: linear relationship between cooling rate and entry velocity into liquid propane. *Cryo-Letters*, **4**, 23–32.

Robards, A.W. & Severs, N.J. (1981) A comparison between cooling rates achieved using a propane jet device and plunging into liquid propane. *Cryo-Letters*, **2**, 135–144.

Ryan, K.P., Bateson, J.M., Grout, B.W.W., Purse, D.H. & Wood, J.W. (1988) Cryo-scanning electron microscopy of ice crystal damage in rapidly frozen, cryomounted specimens. *Cryo-Letters*, **9**, 418–425.

Ryan, K.P. & Liddicoat, M.I. (1987) Safety considerations regarding the use of propane and other liquefied gases as coolants for rapid freezing purposes. *J. Microsc.* **147**, 337–340.

Ryan, K.P. & Purse, D.H. (1985a) A simple plunge-cooling device for preparing biological specimens for cryo-techniques. *Mikroskopie*, **42**, 247–251.

Ryan, K.P. & Purse, D.H. (1985b) Plunge-cooling of tissue blocks: determinants of cooling rates. *J. Microsc.* **140**, 47–54.

Ryan, K.P., Purse, D.H., Robinson, S.G. & Wood, J.W. (1987) The relative efficiency of cryogens used for plunge-cooling biological specimens. *J. Microsc.* **145**, 89–96.

Schwabe, K.G. & Terracio, L. (1980) Ultrastructural and thermocouple evaluation of rapid freezing techniques. *Cryobiology*, **17**, 571–584.

Sitte, H., Edelmann, L. & Neumann, K. (1987) Cryofixation without pretreatment at ambient pressure. *Cryotechniques in Biological Electron Microscopy* (ed. by R. A. Steinbrecht and K. Zierold), pp. 85–113. Springer-Verlag, Heidelberg.

Spurr, A.R. (1969) A low-viscosity epoxy resin embedding medium for electron microscopy. *J. Ultrastruct. Res.* **26**, 31–43.

Stephenson, J.L. (1956) Ice crystal growth during the rapid freezing of tissues. *J. Biophys. Biochem. Cytol.* **2**, 45–52.

Van Venrooij, G.E.P.M., Aertsen, A.M.H.J., Hax, W.M.A., Ververgaert, P.H.J.T., Verhoeven, J.J. & Van Der Vorst, H.A. (1975) Freeze-etching: freezing velocity and crystal size at different locations in samples. *Cryobiology*, **12**, 46–51.

von Zglinicki, T., Rimmler, M. & Purz, H.-J. (1986) Fast cryofixation technique for X-ray microanalysis. *J. Microsc.* **141**, 79–90.

J. mar. biol. Ass. U.K. (1987), **67**, 545–560
Printed in Great Britain

ON THE DIFFERENCES BETWEEN THE TWO 'INDICATOR' SPECIES OF CHAETOGNATH, *SAGITTA SETOSA* AND *S. ELEGANS*

Q. BONE, C. BROWNLEE, G. W. BRYAN, G. R. BURT, P. R. DANDO, M. I. LIDDICOAT, A. L. PULSFORD AND K. P. RYAN
The Laboratory, Marine Biological Association, Citadel Hill, Plymouth PL1 2PB

(Figs. 1–4)

Two species of chaetognath that have been regarded as 'indicators' of different water masses, *Sagitta setosa* and *S. elegans*, differ in structure, for the latter, (but not the former) has gut cells that are vacuolated to such an extent that the vacuoles almost obliterate the coelomic cavity. In the vacuoles of the gut cells NH_4^+ largely replaces Na^+; up to 500 mM-NH_4^+ is found in the larger vacuoles. In contrast to this, the coelomic cavity in *S. setosa* contains a fluid very similar in composition to sea water. As a result of the lift provided by the replacement of Na^+ by NH_4^+, *S. elegans* is significantly less dense than *S. setosa*. It is also less active when captured in plankton tows, and it is suggested that in the sea, it is close to neutral buoyancy and may operate as an ambush predator, instead of actively seeking up and down in the water column as *S. setosa* apparently does. Further studies of the behaviour of the two species in the sea or in culture will be required before it is possible to decide whether this postulated difference in behaviour could account for the difference in distribution of the two species.

INTRODUCTION

The suggestion that the two chaetognath species *Sagitta setosa* and *S. elegans* were 'indicators' of different water masses was first made by Meek (1928), working off Northumberland, and subsequently developed by Russell (1933, 1935, 1939) in his classical work on their distribution as indicators of 'Channel' and 'Western' water off Plymouth. The alternation in dominance of the two species during the well-known changes in the Western Channel off Plymouth during the past 60 years (which have been termed the 'Russell' cycle; Cushing & Dickson, 1976) have most recently been reviewed and discussed by Southward (1984).

Although *S. elegans* attains a slightly larger maximum size than *S. setosa*, the two species are in most respects very similar. In preserved plankton samples they may be distinguished by such features as the shape of the seminal vesicles; the size of the collarette; the position of the second pair of lateral fins; and by a different opacity of the anterior region (Fraser, 1957).

In living specimens, where the body is almost perfectly transparent, these differences are much less obvious than a striking difference between the two species in the appearance of the body cavity. *S. elegans* has a series of thin but conspicuous 'partitions' or 'septa' dividing up the space between the gut and the inner border of the muscle layer: these are absent in *S. setosa*. Unfortunately, the

'septa' are not readily visible in intact preserved samples, but in samples of living material their presence is the simplest way of distinguishing *S. elegans* from *S. setosa*. These 'septa' in *S. elegans* are actually the walls of enormously vacuolated gut cells, as Meek (1928) was the first to suggest. He observed that the gut behind the oesophageal region 'undergoes a most remarkable vacuolation', to such a degree that the gut vacuoles fill almost the whole of the body cavity.

Similar 'septa' were first seen in another species, *S. minima* by Grassi (1883), who supposed them to be coelomic septa; Doncaster (1902) indicated their true nature as the boundaries of gut cells. Most recently, Dallot (1970) has surveyed the occurrence of this curious gut vacuolation in the group for its value as a taxonomic character, but Meek is the only worker who speculated on its function. He was evidently struck by the resemblance of the 'septated' body cavity in *S. elegans* to the notochord of vertebrate embryos and suggested that the gut vacuoles acted as an hydrostatic skeleton, their turgor stiffening the body. The difficulty in accepting this view of the role of the gut vacuoles in *S. elegans* will be evident, for there is no obvious difference in the movements of the two species.

In fact, despite much work on the abundance and distribution of the two species in the Western Channel and elsewhere (see Fraser, 1952; Southward & Barrett, 1983; Southward, 1984), behavioural and physiological differences between the two, (which must underlie their differences in distribution and hence their value as indicator species) have not been examined. We show in this note that *S. elegans* is of a lower density than *S. setosa* by virtue of storage of ammonium ions in the vacuolated gut cells, and suggest that this difference between the two species may be significant in determining their distribution.

MATERIALS AND METHODS

Sagitta elegans Verrill and *S. setosa* Müller were collected from the plankton off Plymouth during the period 1984–7 and examined in a variety of ways. For transmission electron microscopy they were either fixed in seawater glutaraldehyde (5% buffered with sodium cacodylate), or in mixtures of seawater glutaraldehyde and paraformaldehyde; or alternatively they were plunge-frozen in ethane in a simple plunge-freezing device (Ryan & Purse, 1985), and subsequently freeze-substituted in osmic acid in acetone. After embedment in epoxy resin, thin sections were examined in a Philips EM300. For X-ray analysis, whole animals plunge-frozen and subsequently mounted on aluminium stubs, were fractured transversely and examined on a cryo stage fitted to a JEOL 35C scanning microscope (Ryan, Purse & Wood, 1985), using a Link detector and 860 analysis system. X-ray counts processed by the Link systems ZAF/PB programme yielded values in % wt. which could be converted to mM/kg. Sensitivity factors for the programme were obtained from sea water frozen in depressions on aluminium stubs. The ionic content of the fluids within the coelom of *S. setosa* and within the vacuoles of *S. elegans* were also estimated by two other approaches.

First, the fluids were collected by decapitating living animals (previously blotted dry on filter paper), and gently expressing the contained fluid by squeezing the body. From a single animal, around 1–2 μl of fluid could be collected in this way. Fluids from 5–10 animals were collected and transferred to preweighed tubes for storage in a deep-freeze prior to analysis.

Some other analyses were carried out using whole animals, weighed after blotting dry. Na^+ and Cl^- were estimated by flame emission and potentiometrically; NH_4^+ by the method of Liddicoat, Butler & Knox (1975); and free amino acids by HPLC after derivitisation by the methods given in Dando *et al.* (1986). Secondly, in *S. elegans*, direct estimates of the ionic content and pH of the

vacuolar fluid were obtained using liquid ion-exchange microelectrodes for H^+, Na^+, Cl^-, and NH_4^+ (Thomas, 1978). All liquid ion sensors were obtained from Fluka AG (Switzerland). The NH_4^+ sensor was based on nonactin (10% nonactin; 89% nitrophenyl octyl ether; 1% sodium tetraphenyl borate). The animals were pinned out on Sylgard using *Opuntia* spines, and opened to expose the vacuolated cells which were impaled with an ion sensitive electrode and a conventional KCl-filled potential measuring electrode. For each impalement, the potential of the reference electrode was subtracted electronically from the total ion selective electrode potential and fed to a chart recorder. Electrode potentials were compared with appropriate calibration curves to give concentrations of the free ions.

The density of living animals was determined by varying the density of the sea water in which they were collected by the addition of isosmotic CsCl until mixtures of sea water and the denser CsCl were obtained in which the animals just sank or just floated. The density of these solutions, and of the original sea water were measured with a density bottle. pH measurements of the gut lumen were difficult to make since the gut was usually empty in the animals examined, and had only a virtual lumen, with both sides closely apposed; a rough estimate was made by injecting various indicator solutions into the gut via the oesophagus. The pH of the vacuolar fluid was measured directly with a pH microelectrode.

The rhythmic activity of freshly caught animals in a small container was monitored visually, or by recording from intact animals using a suction electrode attached to the tail. Alternatively, electrical activity from locomotor muscle fibres was recorded intracellularly from pinned out animals.

OBSERVATIONS

Morphology

With darkfield lighting or semi-darkfield transmitted light, living specimens of the two species can immediately be distinguished by the appearance of the body cavity. In *S. setosa*, this shows a thin line of gut, and is otherwise empty. In *S. elegans*, it is subdivided by a series of thin-walled sacs on either side of the gut (Fig. 1A). The sac walls are readily visible in transverse section (Fig. 1B, C).

These structures in the body cavity are part of the gut, rather than septa passing between the gut and the inner border of the muscle layers, for if the gut is pulled out of the trunk, the sacs remain attached to it: it is hardly surprising that the structure of the gut in the two species is very different. That of *S. setosa* has been described at the ultrastructural level by several authors (including Welsch & Storch, 1983, who supposed that they were examining *S. elegans*, but evidently actually examined *S. setosa*) but that of *S. elegans* has not previously been examined in any detail.

In *S. setosa* the gut consists of a single layer of relatively large cuboidal cells, some 4–10 μm thick, which are interdigitated with each other, and coupled by a variety of junctional types, including gap junctions (Duvert, Gros & Salat, 1980). Many cells contain large agranular membrane-bound inclusions adjacent to their luminal surfaces (Fig. 2A) whilst others have elaborately folded endoplasmic reticular (ER) profiles within them. The gut lumen is normally only virtual, since unless there is prey within it (which is rare) the opposing luminal surfaces are close together, often separated only by a single row of closely packed cilia. Duvert *et al.* (1980) follow Parry (1944) in dividing the gut cells into two types, absorptive and secretory, but it is not yet entirely clear if the two types may not perhaps be but stages in the cycling of a single cell type. The outer

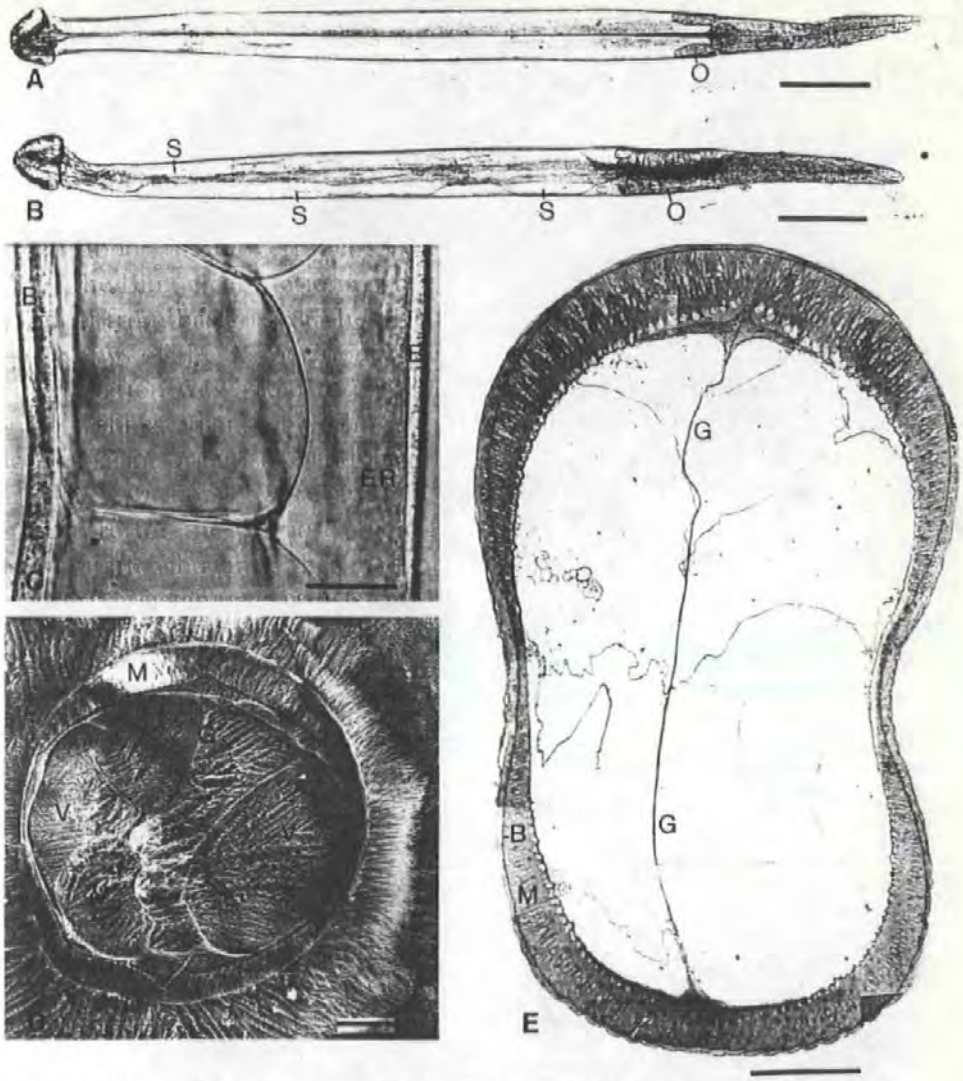

Fig. 1. (**A**) Living *S. setosa*, transmitted light. O, Ovaries. Scale bar, 2 mm. (**B**) Living *S. elegans*, transmitted light. O, Ovaries; S, gut cell sacs. Scale bar, 2 mm. Animals in **A** and **B** immobilized with d-tubocurarine. (**C**) *S. elegans*. Mid-trunk region of living specimen showing rounded walls of vacuolated gut sacs. ER, Granular band of cells rich in endoplasmic reticulum; B, optical section of body wall. Scale bar, 100 μm. (**D**) *S. elegans*. Mid-trunk region cryo-fractured and photographed after etching (to show the structure more clearly). G, Gut; M, muscle layer; V, vacuolated gut sacs. Scale bar, 100 μm. (**E**) *S. elegans*. Transverse semi-thin resin section stained with toluidine blue showing basement membrane, B, separating the outer epithelium from the muscle layer, M. The gut, G, divides the body cavity, in which parts of the walls of several gut sacs are seen in section. Scale bar, 100 μm.

(coelomic) surface of the gut is covered with a thin layer of smooth muscle cells whose fibres run circumferentially (Fig. 4). Presumably these are responsible for the peristaltic movements of the gut described by Burfield (1927). The arrangement is seen schematically in his fig. 8a.

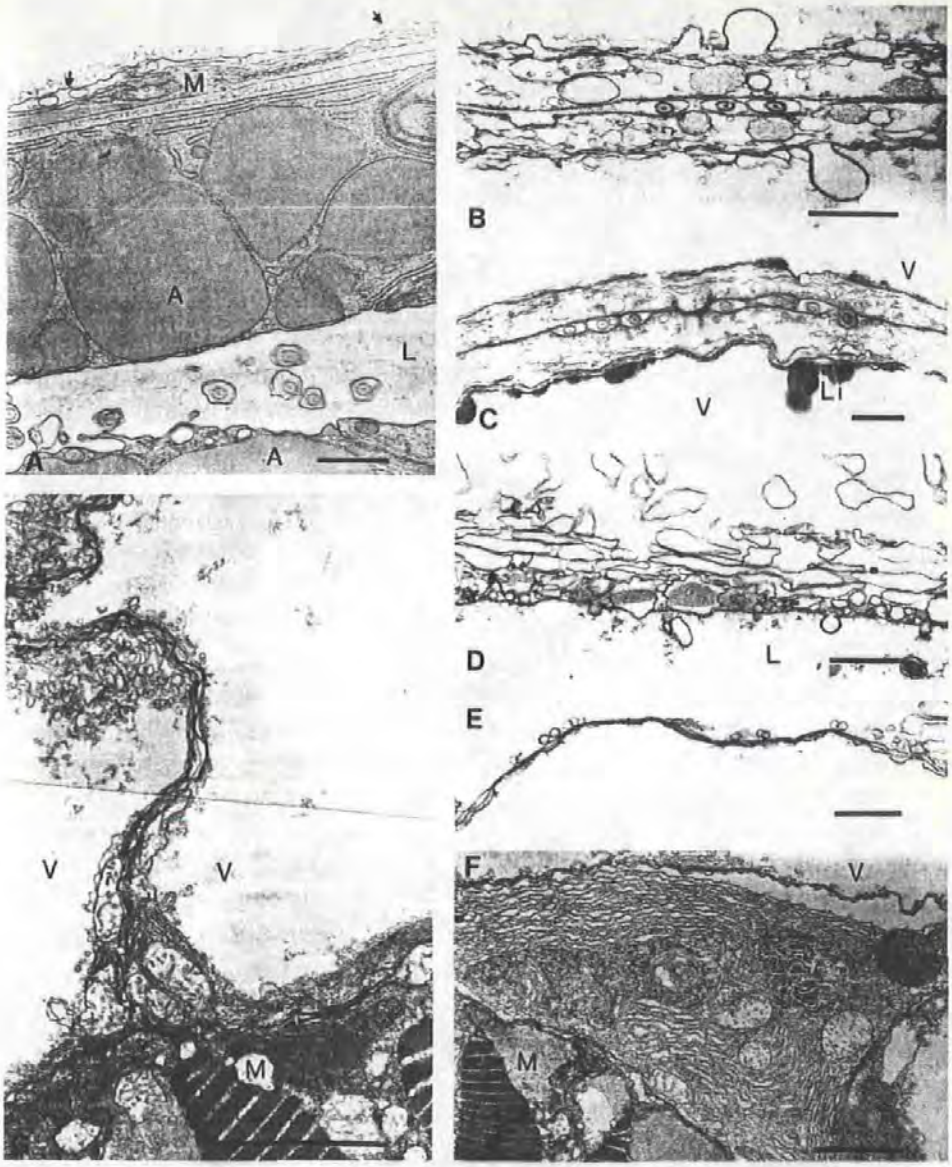

Fig. 2. (**A**) *S. sertosa*. Transverse section of portion of gut plunge-frozen and freeze-substituted showing agranular secretory (?) vesicles, A, within the gut cells and ciliary profiles marking gut lumen, L. Smooth muscle cells, M, are overlain by an interrupted layer of thin coelomic epithelial cells (arrows). Scale bar, 1 μm. (**B–D**) Transverse sections of the gut in *S. elegans* showing the striking difference from that of *S. setosa*. Scale bars in each, 1 μm.

Note that (**B**) is to a higher magnification than (**A**). (**B**) and (**C**) show the two closely apposed gut walls with a single interrupted row of cilia between them. The secretory (?) vesicles are small, and there are many vacuoles of different sizes within the cells. In (**B**), membranous extensions protrude into what are probably the interior of gut cell vacuoles. In (**C**), the inner surfaces of vacuolated sacs, V, derived from adjacent gut cells are lined with electrondense lipidic (?) material, L, and are apposed to the coelomic surfaces of the gut cells. (**D**) shows the large extent of membranous vesicles within the vacuole of the gut cell and the inner cytoplasm. A single cilium is visible in the gut lumen, L. (**E**) *S. elegans*. The walls of two adjacent gut vacuolar sacs are simply two cell membranes with a few small vesicles on the inner surface of the vacuoles. Scale bar, 1 μm. (**F**) *S. elegans*. Cell with elaborate ER lying against muscle layer, M, near junction of mesentery and gut. The gut vacuolar sac, V, has a scattering of vesicle profiles in it adjacent to the ER-rich cell. Scale bar, 5 μm. (**G**) *S. elegans*. Junction of two vacuolar sacs, V, next to the muscle layer, M. Each contains vesicle and laminar profiles, as well as a few mitochondria where there is a little cytoplasm remaining. Scale bar, 5 μm.

The gut cells of *S. elegans* are much thinner than those of *S. setosa*, only some 0·5–1·0 μm across or thinner, and the agranular vesicles are much smaller than in *S. setosa* (Fig. 2B–D). Some cells are essentially much flattened versions of those in *S. setosa*, but there is no smooth muscle layer covering their 'coelomic' surfaces, and there are numerous elongate and other vesicles under this surface. Other cells have no obvious cell membrane on the 'coelomic' side e.g. Fig. 2D; in fact the cell membrane is found far from the luminal surface on the outside of an enormously expanded vacuole within the cell, so forming the sacs seen in the body cavity. Each sac is limited therefore by a gut cell membrane, and where the walls of two adjacent sacs are apposed, the two membranes are closely applied to each other (Fig. 2E, G). The sacs contain just a thin rim of cytoplasmic remains, with very occasional mitochondria, and clusters of vesicles. In some individuals, the sacs are lined with electron-dense blebs and patches of material resembling lipid droplets (Fig. 2C, but these are not seen in all, and it is not known whether the material is indeed lipid. It is only at the gut itself that the vacuolated cells have a layer of cytoplasm (albeit thin), and contain different organelles. At their outer borders, the sacs often seem to have a few fairly closely apposed membranous layers, adjacent to the coelomic epithelial cells internal to the muscle layer.

Dorsally and ventrally, the gut cells are thicker, and have either small or no vacuoles, resembling therefore to some extent those of *S. setosa*. At these positions, the gut is attached to the muscle layer not only by mesenteries in which run a small bundle of nerve fibres (as in *S. setosa*), but also by partitions that are derived from large cells lining the outer border of the body cavity which are notable for their conspicuous ER (Fig. 2F). In the living animal, these dorsal and ventral cells form obvious 'granular' bands dorsally and ventrally along the trunk (Fig. 1C). It will be seen by examination of Fig. 3, that there are real differences between the structure of the gut in the two species considered: the differences in composition of the fluids filling the body cavity are no less striking.

The composition of the coelomic and vacuolar fluids

Our analyses of the coelomic fluid in *S. setosa* and the fluid within the gut vacuoles of *S. elegans* have been made in a variety of ways (see Methods and Table 1) with varying precision; the chief difficulty however, being that the collection of the small volumes of fluid available from these small animals is attended by problems of desiccation and hydration: it is this that was probably the main cause of analytical variations on the fluid samples. It is nevertheless evident that the fluids of the two species are entirely different.

The coelomic fluid of *S. setosa* is similar in composition to sea water (Table 1). The muscle layer is separated from the coelomic cavity by a thin epithelium which is apparently incomplete; the muscle cells are therefore exposed to the coelomic fluid (Fig. 3). The outer border of the muscle layer is bounded by a thick basement membrane containing collagen fibres, and is covered by an outer multilayered epithelium. However, it is evident that these layers are freely

permeable, since immediate block of muscle activity is brought about by placing animals in Ca^{2+}-free solutions or by adding such Ca^{2+}-blockers as Mn^{2+}; Co^{2+}; and Cd^{2+} (Savineau & Duvert, 1986; Bone *et al.* 1987). It seems very probable then, that extracellular space in *S. setosa* (including the coelomic space in the trunk), is freely permeable to the surrounding sea water; hence that the

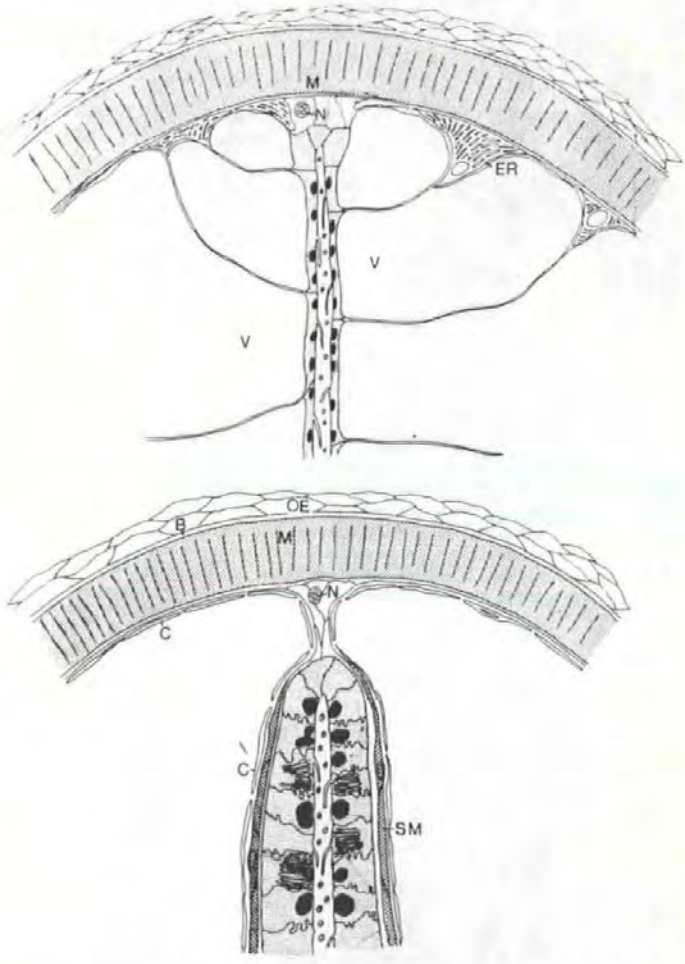

Fig. 3. Schematic diagrams showing arrangement of the dorsal part of the body in the mid-trunk region of the two species, *S. elegans* above. The gut has been drawn with a lumen for clarity, and its thickness has been exaggerated. B, Basement membrane; C, coelomic epithelium; M, locomotor muscle of body wall; N, nerve bundle; OE, outer epithelium; SM, smooth muscle of gut; V, vacuoles of gut cells.

extracellular fluid is similar to sea water. Chaetognaths do not have excretory organs and Mg^{2+} levels in the coelomic fluid are similar to sea water. There are low levels of some free amino acids (Table 1), and there is little or no NH_4^+. In *S. elegans*, however, the fluid within the sacs that fill the greater part of the body cavity in the trunk region is very different to sea water, for Na^+ is much lower, and the major anion is NH_4^+ (Table 1). Indeed NH_4^+ was at 500 mM in some

Table 1. *Some features of the composition of the fluid within the body cavity of* Sagitta elegans *and* Sagitta setosa

Method of analysis	Ion	*S. elegans* (mM)	*S. setosa* (mM)
EDS X-ray	Na^+ (1)	59 ± 26 ($n = 5$)	475 ± 63 ($n = 6$)
	Cl^- (1)	502 ± 71 ($n = 5$)	570 ± 74 ($n = 6$)
	S (as SO_4^{2-})	8 ± 0 ($n = 5$)	21 ± 0 ($n = 6$)
	Mg^{2+}	20 ($n = 5$)	64 ($n = 6$)
Ion-sensitive electrode	Na^+ (2)	17 ± 6 ($n = 6$)	—
	Cl^-	463 ± 105 ($n = 5$)	—
Flame emission and potentiometry	Cl^-	546 ± 25 ($n = 6$)	—
	Na^+	—	—
Colorimetric	NH_4^+	236 ± 78 ($n = 22$)	77 ± 5 ($n = 8$)
Ion-sensitive electrode	NH_4^+ (large sacs)	410 ± 50 ($n = 9$)	
	NH_4^+ (intermediate sacs)	175 ($n = 2$)	
	NH_4^+ (small sacs)	*ca.*10	
Analyses of whole animals			
Flame emission and potentiometry	Na^+	182 ± 24 ($n = 5$)	397 ± 22 ($n = 10$)
	Cl^-	380 ± 14 ($n = 5$)	464 ± 26 ($n = 10$)

Free amino acids in fluids and whole animals (**) by HPLC (3)	*S. elegans* **				*S. setosa* **	
	(1)	(2)	(3)	(4)	(1)	(2)
Aspartate	2·49	0·17	0·32	0·11	0·14	0·26
Glutamate	2·23	0·16	0·35	0·13	0·22	0·48
Serine	3·48	0·26	0·45	0·22	0·26	0·63
Glutamine	0·58	0·80	0·63	0·39	0·21	0·31
Histidine	4·20	0·21	0·30	0·22	—	0·21
Glycine	5·23	0·79	4·03	0·73	2·60	2·50
Threonine	4·13	0·57	0·76	0·42	0·22	0·26
Alanine	4·30	0·90	1·76	0·54	1·69	4·54
Tyrosine	2·68	0·50	0·60	0·45	0·06	0·21
Methionine	—	0·80	0·84	0·87	0·02	—
Valine	5·28	2·34	2·61	2·20	0·38	0·83
Tryptophan	3·04	0·25	0·29	0·30	—	0·11
Phenylalanine	3·06	1·06	1·26	1·08	0·18	0·38
Isoleucine	1·95	1·53	1·87	1·38	0·21	0·41
Leucine	2·89	3·18	3·62	2·78	0·41	0·55
Total (mM)	50·23	14·04	20·71	12·41	6·79	11·68

Notes. Sea water samples analysed by EDS X-ray gave Na^+, 444 mM/kg; Cl^-, 538 mM/kg; S, 28 mM/kg; and Mg^{2+}, 53 mM/kg. These are close to the theoretical values for the sea water analysed (Na^+, 455 mM/kg; Cl^-, 532 mM/kg; S, 28 mM/kg; and Mg^{2+}, 53 mM/kg.

(1) Values for *S. elegans* were obtained using an ice matrix in the ZAF/PB programme (as for *S. setosa*); inclusion of 250 mM-NH_4^+ in the matrix does not produce any significant change in the values given.

(2) The variation in NH_4^+ content of the gut sacs in *S. elegans* related to their size is probably reflected in variations in Na^+ content. Values for Na^+ obtained using ion-sensitive electrodes were from the larger sacs only, containing most NH_4^+. The values obtained by X-ray analysis of cryospecimens were from sacs of different sizes and hence include those from sacs containing less NH_4^+.

(3) Note that in the fluid samples from *S. elegans* between 45 and 60% of the free amino acids are valine, phenylalanine, isoleucine and leucine; whilst in *S. setosa* 60% are glycine and alanine. In the whole animals (**) the amino acid content is increased by cellular free amino acids, presumably mainly from muscle cells.

of the gut sacs tested with an NH_4^+-sensitive electrode; since the sacs are presumably isosmotic with sea water they can have contained very little Na^+.

Our surveys of ion content in transversely fractured *S. elegans* examined on the cryostage of the scanning microscope (as in Fig. 1D) showed that almost all

spaces between the gut and the inner border of the muscle layer were low in Na^+, and in S (presumably SO_4^{2-}) compared to sea water. There were however small areas close to the border of the muscle layer where Na^+ and S levels were similar to sea water. We interpret these as the remnants of the original coelomic cavity, virtually obliterated by the expansion of the gut sacs. Within the sacs themselves, the fluid is acidic (pH 6–6·5), and levels of free amino acids are around twice those for *S. setosa* (Table 1).

We have not carried out sufficient analyses of the NH_4^+ content of the gut sacs to assert definitely that the smaller sacs contain lower levels of NH_4^+ than the larger. The preliminary results shown in Table 1 certainly suggest that this may be the case, and may reflect the way in which the system develops; the sacs increasing their NH_4^+ content as they increase in size. The largest gut sacs are near the hinder end of the body cavity in the trunk, the smallest near the end of the oesophagus and beginning of the intestine proper, though there are some smaller sacs in the hinder region.

Unfortunately, we have not been able to examine very small animals, and have only had the opportunity to examine those after the monoserial arrangement of the gut sacs (Dallot, 1970) has become multiserial.

Density

Freshly collected specimens of both species were denser than the sea water in which they were brought to the laboratory, and sank to the bottom of the vessel in which they were placed, occasionally rising in the water during brief bursts of rapid movements. *S. setosa* seems less fragile than *S. elegans* (or perhaps better, it resists capture more successfully) for in mixed samples, most *S. setosa* are active and undamaged, whereas a high proportion of *S. elegans* are either inactive, or may even be showing signs of the lack of transparency which signals their approaching death. Fraser (1969) has previously noted that *S. elegans* is a delicate species. In good condition it is evidently quite close to neutral buoyancy in the sea water in which it was examined, for it sinks very slowly; if placed near the top of the container, it gradually sinks obliquely head downwards, since the head is the densest part of the body. *S. elegans* is very close to neutral buoyancy in mixtures of sea water and CsCl of specific gravity 1·0305 at 9 °C; the sea water alone had a specific gravity of 1·0247 at the same temperature. In such a CsCl–seawater mixture, *S. setosa* sinks, and it is not until mixtures are used whose specific gravity is 1·0357, that *S. setosa* is near neutral buoyancy. In such mixtures *S. elegans* in good condition floats, and this is a simple method of distinguishing the two. Our method of estimating density by placing animals in mixtures of CsCl and sea water is not free from objection if the fluid within the coelom has free access to the external medium, for if so it would be expected that *S. setosa* would soon sink in *any* such mixture. The measurements were made immediately on transfer, and the animals did not sink for 15 min or so. The situation with *S. elegans* is more complex, for the coelomic space is greatly reduced by the gut sacs, and these must be relatively impermeable if they are to retain NH_4^+. In fact,

specimens of *S. elegans* in appropriate mixtures in which they initially just floated never sank after much longer times. We conclude that there may have been a slight underestimate of the density of *S. setosa* by the method used, but that it is unlikely that any of the specimens of *S. elegans* examined were closer to neutral buoyancy than estimated.

If the gut is carefully removed from a specimen of *S. elegans* in sea water, the body sinks to the bottom whilst the gut and its associated sacs floats to the surface. When *S. elegans* dies, NH_4^+ diffuses out of the gut sacs and the animals increase in density; analyses of fluid extracted from specimens kept for 12 hr in sea water after death gave values very close to sea water. Similarly, we tested 15 specimens of *S. elegans* in a sea water–CsCl mixture in which those which were in good condition and transparent just floated, whilst those which were moribund and becoming opaque sank. The mean value for NH_4^+ in those which floated was 174·6 mm/kg ($\pm$27·5; $n = 8$); for those that sank 121·6 mM/kg ($\pm$25·7; $n = 7$).

It is clear from these observations that in life, the gut sacs are providing lift because they contain a fluid in which NH_4^+ has partly replaced Na^+, and that this accounts for the lower density of *S. elegans* compared to *S. setosa*.

Physiological observations

When impaled by conventional microelectrodes filled with 3 M-KCl, the sacs of the gut cells show resting potentials up to 55 mV or so. Many, however, have resting potentials very much lower than this and some do not even show a transient deflection when penetrated (since the sacs are so large it is easy to see when the tip of the electrode is lying within the sac). It seems probable that the smaller sacs have higher resting potentials than the larger, (as it is also likely that they have a lower concentration of NH_4^+); the mean resting potential of small sacs was 50 mV, that of larger sacs was 15 mV ($n = 24$). As pointed out above, however, we have not had the opportunity of examining the young stages to see if all sacs in them have high resting potentials.

The pH of the largest sacs in *S. elegans* as measured by a pH microelectrode, was around 6·4, the same pH as recorded by the electrode in a freshly made up 500 mM-NH_4Cl solution. We were unable to measure the pH in the gut lumen in the same way, in either species, since the lumen is virtual only, but injection of indicator solutions via the oesophagus gave values between 5·6 and 6·0, in reasonable accord with Parry's (1944) finding in *S. setosa* that the optimal pH for the gut enzymes was 6·4.

S. elegans is less active when collected from the sea in plankton tows than is *S. setosa*, but specimens in the best condition (as judged by their perfect transparency and rapid reaction to touch), show short bursts of locomotor muscle activity at intervals. In most animals, these are rather regular, whilst in others, the interburst intervals may vary much. In both species, whether activity is recorded in free-swimming animals or in animals attached to electrodes, two types of pattern are found: either the interburst intervals are around 30 s or much shorter, around 5–10 s (Fig. 4). We do not know why some animals should show

one rhythmic pattern, and others the other, but it seems that the interburst interval decreases as preparations age, hence that 30 s intervals are those of animals in the sea.

In *S. elegans* these more or less regular bursts of activity are rather ineffective, just moving the animal a small distance forwards on the bottom of the dish, but in the case of *S. setosa* the animals dart forwards and may rise in the water.

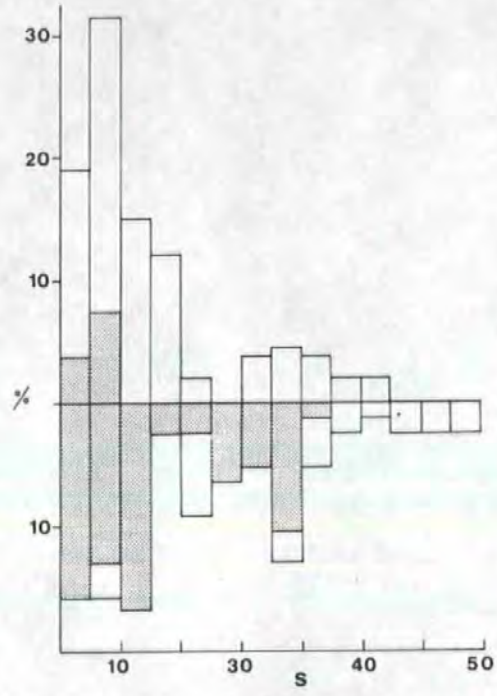

Fig. 4. Intervals between the more or less regular swimming bursts of a number of different individuals; *S. elegans* above, *S. setosa* below. Ordinate, % of total number of interburst intervals measured; abscissa: intervals between bursts grouped in 5 s blocks. Filled blocks, data from animals either attached to suction electrodes, or intracellular records from animals pinned out on Sylgard. Open blocks, data from animals free-swimming in small containers.

Perhaps this difference simply indicates that the specimens of *S. elegans* were in poor condition when examined, but it seems most probable that there is a real difference between the two species in their locomotor activity. Our expectation was that the interburst interval between the two species would be different, since *S. elegans* is less dense than *S. setosa*, and that the interval would be much longer in the former. However, this was not the case, no consistent differences in the interburst interval between the two species were found. Nor were there any obvious differences between small and larger individuals, although very few large individuals of *S. elegans* were found in good condition. The general impression gained from observing many animals in small dishes, either free-swimming, or attached to electrodes in some way, is that free-swimming animals in the best condition and fresh animals attached to electrodes both show more regular and

longer interburst intervals than free-swimming animals in poor condition. The observations of Feigenbaum & Reeve (1977) on *S. hispida* in culture have shown that in that species, the same regular rhythmic activity serves to maintain position in the water column, and increases the area searched for prey. Probably in the sea the same would be true for *S. setosa*, but it is not clear whether this is necessarily correct for *S. elegans*, since the rhythmic movements of the specimens we have examined have not been sufficient to produce the kind of hop and sink pattern found in *S. hispida*.

DISCUSSION

Our observation that the two *Sagitta* species examined differ in density and do so because one stores a fluid in which the less dense NH_4^+ in part replaces Na^+ raises a number of points that have not so far been considered. It seems that S (as SO_4^{2-}) is partly replaced by Cl^-, as in some other gelatinous macroplankton (Denton & Shaw, 1962), but this is of lesser significance insofar as density differences are concerned.

Can NH_4^+ storage by *S. elegans* suffice to account for its density difference from *S. setosa*? For animals 1·35 cm long, with a total volume of some 3·7 mm^3 the 'lift' required to change the buoyancy of *S. setosa* to that of *S. elegans* in sea water of density 1·0247 is around 19 μg. Since the density of 500 mM-NH_4Cl is 1·0068, this would be provided by 1·061 mm^3 of 500 mM-NH_4Cl. If we assume that the gut sacs in *S. elegans* occupy some 80% of the total volume of the body cavity in the trunk and that the mean thickness of the muscle layer is 10 μm, then their total volume in an animal of this size would be around 2·2 mm^3. There are differences in NH_4^+ content of the sacs; the mean results of analyses of the fluid in the body cavity, and the results from NH_4^+ micro-electrodes give approximately 250 mM-NH_4^+ so that it seems reasonable to suppose that the storage of NH_4^+ in the gut sacs of *S. elegans* accounts for the density differences between the species without requiring differences in other components such as muscle (for example) between the two. Further, *S. elegans* should be able to achieve neutral buoyancy, or make itself very close to neutral buoyancy, by increasing the NH_4^+ content of the gut sacs. If it is correct to suppose that the smaller sacs contain less NH_4^+ than the larger, then it may be that the larger individuals have larger sacs with more NH_4^+ and are thus less dense than the smaller. To judge from Kotori's (1975) figures, the early larval stages do not have gut sacs, and hence are presumably denser than sea water.

Secondly, how does *S. elegans* secrete NH_4^+ in to the gut sacs and how is it retained there? At present we cannot answer either of these questions.

NH_4^+ must presumably be derived from the food within the gut, which consists largely of copepods (Feigenbaum & Maris, 1984), but the mechanism of accumulation in the sacs is unclear. In cranchid squid, which store NH_4^+ within a large coelomic buoyancy tank (Denton, Gilpin-Brown, & Shaw, 1969) the pH of the coelomic fluid is around 5, whereas that of the blood is between 7·0 and

7·9, so that as these authors point out, the ratio of NH_4^+ in the blood (a few mM) to that in the coelom (up to 500 mM) is roughly the same as that of hydrogen ions in each compartment. By secreting an acid fluid into the coelom to trap unionised NH_3 diffusing into it by converting the NH_3 into relatively indiffusible NH_4^+, cranchid squid could accumulate high concentrations of NH_4^+ within the coelom. Manifestly, such a scheme does not apply to *S. elegans*, for the pH of the gut and gut sacs seem to be similar, around 6·0–6·4. A striking feature of the gut cells is the numerous small vesicles on the inner cytoplasmic surface facing the sac vacuole, and it is possible that the secretion process involves the formation of vesicles loaded with NH_4^+ which are then released into the sacs to add to their volume.

The NH_4^+ within the gut sacs is not free to diffuse out of them when the animal is in good condition, for equivalent NH_4Cl solutions at once block locomotor muscle activity.

The significance of the higher levels of free amino acids in *S. elegans* than in *S. setosa* (with the exception of glycine, higher in *S. setosa*) is not known, but it does not seem to be linked with NH_4^+ secretion or storage since in *S. hispida* there are no significant amounts of NH_4^+, but considerable amounts of non-protein nitrogen, partly as free amino acids (Reeve, Raymont & Raymont, 1970).

S. elegans is probably not the only species that reduces its density by accumulating NH_4^+, for in a comparative study of 40 chaetognath species, Dallot (1970) found that 9 (all belonging to the genus *Sagitta*) possessed sacculated gut cells more or less resembling those of *S. elegans*.

Although he did not ascribe a function to the curious gut sacs, (his aim was to see whether the gut structure might be useful in chaetognath classification), he concluded that the group of species sharing this character were amongst the most primitive members of the genus, most being meso- or bathypelagic, living under relatively cold and stable conditions. Whilst this may be true, there are many other chaetognaths living in such conditions that do not have the sacculated type of gut cell linked in *S. elegans* with NH_4 storage.

Nevertheless, Dallot's conclusion raises the most interesting aspect of density reduction in *S. elegans* (and possibly in the other species of the genus that share a vacuolated gut), namely whether it underlies a particular ecological strategy adoped by such species, contrasting with that adopted by denser species, and better adapted to the conditions of a particular water mass? For example, species close to neutral buoyancy might hang in the water (only requiring small movements to maintain their horizontal position), and capture their copepod prey as ambush predators. On the other hand those that are denser and sink more rapidly, presumably adopt the hop and sink technique to search up and down for their prey, and are obliged to make more energetic movements in so doing. Low-density species may therefore be better adapted to colder, higher salinity water (in which they are closer to neutral buoyancy), whilst higher-density species could better tolerate variations in sea water density resulting from varying temperature and salinity.

It is easier to suggest such an hypothesis than to disprove it. Although we know of no previous measurements of the density of any chaetognath species, most appear to be denser than the sea water in which they live. Feigenbaum & Reeve (1977) state that *S. hispida* is negatively buoyant, and Kuhl (1928) mentions that *S. setosa* sinks quite slowly in the short period of complete rest between its rapid movements, being just slightly denser than the water. However, he was careful to add that this might not be correct for all species, and Feigenbaum (1977) stated that in the laboratory, the curiously flaccid oceanic species *S. enflata* appeared to be neutrally buoyant. Feigenbaum's feeding experiments on this species indeed suggested that it was an ambush predator. It is particularly unfortunate that we do not know the density or behaviour of any of the species Dallot (1970) found to have vacuolated gut cells similar to *S. elegans*.

Two difficulties at once confront any assessment of the hypothesis that differences in density involving different methods of prey capture account for the different distributions of *S. elegans* and *S. setosa*.

First, *S. elegans* is a widespread Arctic–Boreal species that is neritic and sometimes euryhaline in the northern part of its extensive range, but stenohaline and stenothermal in the southern part as for example in the Channel and N. Biscay. *S. setosa* differs in being a temperate coastal form, which tolerates changing salinities (see Southward, 1984). The difficulty here is that although *S. elegans* is a predominantly cold-water form it may occupy somewhat different waters at different stages in the life-cycle. For instance, in the winter at Plymouth, *S. elegans* may be found inshore close to the bottom, even though there is no thermocline and vertical mixing is complete. Near the surface, juveniles of the two species may occur mixed together (see Southward, 1984). It does not seem therefore that in different places and different stages in the life-cycle, *S. elegans* behaves in the same manner.

Secondly, although the results reported in the present account make it very probable that *S. elegans* is near neutral buoyancy in the sea; so far as we are aware, there are no direct observations (from any part of its range) of its behaviour. Our observations on animals collected in a conventional plankton net suggest that adults may be very close to neutral buoyancy, and sink very slowly, their rhythmic movements serving simply to drive them only a short distance obliquely upwards. In other words, adults of *S. elegans* may be ambush predators instead of seeking up and down in the water column as their young stages perhaps do, and as all stages of *S. setosa* probably do.

Obviously, it would be interesting to pursue this idea, and we hope to take the opportunity to make observations on *S. elegans* that have been collected by the least damaging methods. Alternatively, it would be valuable to have underwater observations where *S. elegans* is known to be the only chaetognath present, as for example from the W. Atlantic (King, 1979). Since the density difference between these two 'indicator' species is, as yet, the only ecologically significant difference between them that might explain their distribution, further information about their behaviour patterns has a certain interest.

This work has proceeded intermittently over a number of years, being linked directly to the seasonal and intermittent occurrence of *S. elegans*. We owe an obvious debt to the skilful and devoted collection of plankton samples by Mr F. Hutchins and Mr C. Knott. We are also indebted to Dr A. J. Southward for identification of material, and for patient sharing of his unrivalled knowledge of the two species considered. Link Systems Ltd have very kindly permitted us to have the ZAF P/B programme on extended loan.

REFERENCES

BONE, Q., GRIMMELIKHUIJZEN, C. J. P., PULSFORD, A. & RYAN, K. P., 1987. Possible transmitter functions of acetylcholine and an RFamide-like substance in *Sagitta* (Chaetognatha). *Proceedings of the Royal Society* (B), **230**, 1–14.

BURFIELD, S. T., 1927. *Sagitta. L.M.B.C. Memoirs on Typical British Marine Plants and Animals*, no. 28, 104 pp.

CUSHING, D. H. & DICKSON, R. R., 1976. The biological response in the sea to climatic change. *Advances in Marine Biology*, **14**, 1–22.

DALLOT, S., 1970. L'anatomie du tube digestif dans la phylogenie et la systematique des chaetognathes. *Bulletin du Museum national d'histoire naturelle*, **42**, 549–565.

DANDO, P., SOUTHWARD, A. J., SOUTHWARD, E. C. & BARRETT, R. L., 1987. Possible energy sources for chemoautotrophic prokaryotes symbiotic with invertebrates from a Norwegian fjord. *Ophelia*, **26**, 135–150.

DENTON, E. J., GILPIN-BROWN, J. B. & SHAW, T. I., 1969. A buoyancy mechanism found in cranchid squid. *Proceedings of the Royal Society* (B), **174**, 271–279.

DENTON, E. J. & SHAW, T. I., 1962. The buoyancy of gelatinous marine animals. *Journal of Physiology*, **161**, 14–15*P*.

DONCASTER, L., 1902. On the development of *Sagitta*, with notes on the anatomy of the adult. *Quarterly Journal of Microscopical Science*, **46**, 351–398.

DUVERT, M., GROS, D. & SALAT, C., 1980. The junctional complex in the intestine of *Sagitta setosa* (Chaetognatha): the paired septate junction. *Journal of Cell Science*, **42**, 227–246.

FEIGENBAUM, D. L., 1977. *Nutritional Ecology of the Chaetognatha with Particular Reference to External Hair Patterns, Prey Detection, and Feeding*. Ph.D. dissertation, University of Miami, Coral Gables, Florida.

FEIGENBAUM, D. L. & MARIS, R. C., 1984. Feeding in the Chaetognatha. *Oceanography and Marine Biology, an Annual Review*, **22**, 343–392.

FEIGENBAUM, D. L. & REEVE, M. R., 1977. Prey detection in the Chaetognatha: response to a vibrating probe and experimental determination of attack distance in large aquaria. *Limnology and Oceanography*, **22**, 1052–1058.

FRASER, J. H., 1952. The Chaetognatha and other zooplankton of the Scottish area and their value as biological indicators of hydrographical conditions. *Marine Research*, no. 2, 52 pp.

FRASER, J. H., 1957. Chaetognatha. *Fiches d'identification du zooplancton*, no. 1, 6 pp.

FRASER, J. H., 1969. Experimental feeding of some medusae and chaetognatha. *Journal of the Fisheries Research Board of Canada*, **26**, 1743–1762.

GRASSI, G. B., 1883. I Chetognathi. *Fauna und Flora des Golfes von Neapel*, **5**, 126 pp.

KING, K. R., 1979. The life history and vertical distribution of the chaetognath *Sagitta elegans*, in Dabob Bay, Washington. *Journal of Plankton Research*, **1**, 153–167.

KOTORI, M., 1975. Morphology of *Sagitta elegans* (Chaetognatha) in early larval stages. *Journal of the Oceanographical Society of Japan*, **31**, 139–144.

KUHL, W., 1928. Chaetognatha. *Tierwelt der Nord- und Ostsee*, **11**(VIIb), 24 pp.

LIDDICOAT, M., BUTLER, E. I. & KNOX, S., 1975. The determination of ammonia in sea water. *Limnology and Oceanography*, **20**, 131–132.

MEEK, A., 1928. On *Sagitta elegans* and *Sagitta setosa* from the Northumbrian plankton, with a note on a trematode parasite. *Proceedings of the Zoological Soceity of London*, **30**, 743–776.

PARRY, D. A., 1944. Structure and function of the gut in *Spadella* and *Sagitta*. *Journal of the Marine Biological Association of the United Kingdom*, **26**, 16–38.

REEVE, M. R., RAYMONT, J. E. G. & RAYMONT, J. K. B., 1970. Seasonal biochemical composition and energy sources of *Sagitta hispida*. *Marine Biology*, **6**, 357–364.

RUSSELL, F. S., 1933. The seasonal distribution of macroplankton as shown by catches in the 2-metre stramin ring-trawl in off-shore waters off Plymouth. *Journal of the Marine Biological Association of the United Kingdom*, **19**, 73–82.

RUSSELL, F. S., 1935. On the value of certain animals as indicators of water movements in the English Channel and North Sea. *Journal of the Marine Biological Association of the United Kingdom*, **20**, 309–332.

RUSSELL, F. S., 1939. Hydrographical and biological conditions in the North Sea as indicated by plankton organisms. *Journal du Conseil*, **14**, 171–192.

RYAN, K. P., & PURSE, D. H., 1985. A simple plunge-cooling device for preparing biological specimens for cryotechniques. *Mikroskopie*, **42**, 247–251.

RYAN, K. P., PURSE, D. H. & WOOD, J. R., 1985. A transmission cryo-stage with a heater and integral anti-contaminator for a scanning electron microscope. *Mikroskopie*, **42**, 225–229.

SAVINEAU, J.-P. & DUVERT, M., 1986. Physiological and cytochemical studies of Ca in the primary musculature of the trunk of *Sagitta setosa* (Chaetognath). *Tissue and Cell*, **18**, 953–956.

SOUTHWARD, A. J., 1984. Fluctuations in the 'indicator' chaetognaths *Sagitta elegans* and *Sagitta setosa* in the Western Channel. *Oceanologica acta*, **7**, 229–239.

SOUTHWARD, A. J. & BARRETT, R. L., 1983. Observations on the vertical distribution of zooplankton, including post-larval teleosts, off Plymouth in the presence of a thermocline and a chlorophyll-dense layer. *Journal of Plankton Research*, **5**, 599–618.

THOMAS, R. C., 1978. *Ion-sensitive Intracellular Microelectrodes. How to Make and Use Them.* London: Academic Press.

WELSCH, U. & STORCH, V., 1983. Enzymhistochemische und elektronenmikroskopische Beobachtungen am Darmepithel von *Sagitta elegans*. *Zoologische Jahrbücher* (Abteilung für Anatomie und Ontogenie der Tiere), **109**, 23–33.